AFML-TR-78-153

LEVEL II

AD A068396

DDC FILE COPY

RESIDUAL SURFACE STRAIN DISTRIBUTIONS NEAR HOLES WHICH ARE COLDWORKED TO VARIOUS DEGREES

Metals Behavior Branch
Metals and Ceramics Division

DDC
RECEIVED
MAY 8 1979
C

November 1978

TECHNICAL REPORT AFML-TR-78-153

Final Report

Approved for public release; distribution unlimited

AIR FORCE MATERIALS LABORATORY
AIR FORCE WRIGHT AERONAUTICAL LABORATORIES
AIR FORCE SYSTEMS COMMAND
WRIGHT-PATTERSON AIR FORCE BASE, OHIO 45433

NOTICE

When Government drawings, specifications, or other data are used for any purpose other than in connection with a definitely related Government procurement operation, the United States Government thereby incurs no responsibility nor any obligation whatsoever; and the fact that the government may have formulated, furnished, or in any way supplied the said drawings, specifications, or other data, is not to be regarded by implication or otherwise as in any manner licensing the holder or any other person or corporation, or conveying any rights or permission to manufacture, use, or sell any patented invention that may in any way be related thereto.

This report has been reviewed by the Information Office (IO) and is releasable to the National Technical Information Service (NTIS). At NTIS, it will be available to the general public, including foreign nations.

This technical report has been reviewed and is approved for publication.

T. NICHOLAS
Materials Research Engineer

FOR THE COMMANDER

WALTER H. REIMANN
Asst. Chief, Metals Behavior Branch
Metals and Ceramics Division
Air Force Materials Laboratory

Copies of this report should not be returned unless return is required by security considerations, contractual obligations, or notice on a specific document.

AIR FORCE/56780/23 April 1979 — 200

SECURITY CLASSIFICATION OF THIS PAGE (When Data Entered)

REPORT DOCUMENTATION PAGE

READ INSTRUCTIONS BEFORE COMPLETING FORM

1. REPORT NUMBER: AFML-TR-78-153	2. GOVT ACCESSION NO.
3. RECIPIENT'S CATALOG NUMBER	
4. TITLE (and Subtitle): RESIDUAL SURFACE STRAIN DISTRIBUTIONS NEAR HOLES COLDWORKED TO VARIOUS DEGREES.	5. TYPE OF REPORT & PERIOD COVERED: Final Report, Oct 75 - Sep 76
	6. PERFORMING ORG. REPORT NUMBER
7. AUTHOR(s): Gary Cloud*	8. CONTRACT OR GRANT NUMBER(s): PL
9. PERFORMING ORGANIZATION NAME AND ADDRESS: Air Force Materials Laboratory (LLN), Air Force Wright Aeronautical Laboratories, AFSC, Wright-Patterson Air Force Base, Ohio 45433	10. PROGRAM ELEMENT, PROJECT, TASK AREA & WORK UNIT NUMBERS: Project No. 2307, Task No. 2307P1, Work Unit No. 2307P101
11. CONTROLLING OFFICE NAME AND ADDRESS: Air Force Materials Laboratory (LL), Air Force Wright Aeronautical Laboratories, AFSC, Wright-Patterson Air Force Base, Ohio 45433	12. REPORT DATE: November 1978
	13. NUMBER OF PAGES: 231
14. MONITORING AGENCY NAME & ADDRESS (if different from Controlling Office)	15. SECURITY CLASS. (of this report): Unclassified
	15a. DECLASSIFICATION/DOWNGRADING SCHEDULE

16. DISTRIBUTION STATEMENT (of this Report)

Approved for public release; distribution unlimited.

17. DISTRIBUTION STATEMENT (of the abstract entered in Block 20, if different from Report)

18. SUPPLEMENTARY NOTES

*National Research Council Senior Resident Associate at Air Force Materials Laboratory while conducting this research. Author is associated with Michigan State University, East Lansing, Michigan 48824.

19. KEY WORDS (Continue on reverse side if necessary and identify by block number)

Moire
Optical data processing
Photography
Strain measurement
Coldworked holes
Fatigue life improvement
Plastic deformation

20. ABSTRACT (Continue on reverse side if necessary and identify by block number)

Residual surface strain distributions were measured in the vicinity of holes in 1/4" aluminum alloy plate which had been coldworked to various degrees by a commercial process. Seven levels of coldworking between 3.8 mils and 7.8 mils radial interference were studied. Attention focused mainly on radial strains, but hoop strains were measured for two coldwork levels. A sophisticated moire technique was developed for this investigation, and refined computer routines were utilized for reduction of data and plotting of results.

DD FORM 1 JAN 73 1473 EDITION OF 1 NOV 68 IS OBSOLETE

SECURITY CLASSIFICATION OF THIS PAGE (When Data Entered)

012320 2B

The moire method involved high-resolution photography of a specimen grating before and after coldworking and subsequent generation of fringe patterns in a coherent optical processor. This report contains considerable tutorial detail about these techniques. The results are quite straight forward, and they are shown to agree reasonably well with the limited available data. The plastic deformation process appears to be quite complex, and minor changes of cold-working parameters can cause large changes in the residual strain--a factor which must be considered by designer and manufacturer.

FOREWORD

This technical report was prepared by the Metals Behavior Branch, Metals and Ceramics Division, Air Force Materials Laboratory, Wright-Patterson Air Force Base, Ohio. The research was conducted by Dr. Gary Cloud under work unit directive 22790101 during the period Oct 75 - Sep 76.

This research was conducted while the author was a senior resident associate of the National Research Council. The support of the NRC and the Air Force Materials Laboratory is deeply appreciated.

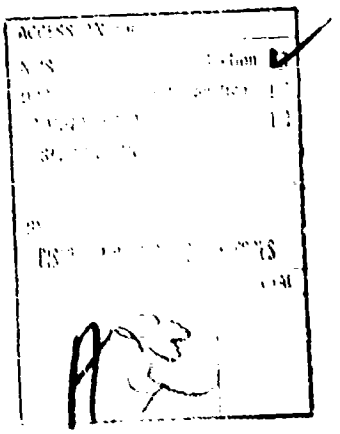

TABLE OF CONTENTS

SECTION		PAGE
I	INTRODUCTION	1
	1. Summary Statement of Problem	1
	2. Organization and Purposes of This Report	1
	3. Background of Problem	2
II	SCOPE OF STUDY	6
	1. Summary of Parameters	6
	2. Short Description of Approach	7
III	CHOICE OF METHOD OF INVESTIGATION	8
	1. Requirements and Conditions	8
	2. Chosen Approach	8
	3. Procedure Outline	9
IV	SPECIMENS	10
	1. Material	10
	2. Configuration	10
	3. Specimen Preparation	12
	4. Coldworking Process	15
V	MOIRE MEASUREMENT OF STRAIN	21
	1. Short Summary of Procedure	21
	2. Master and Submaster Gratings	22
	2.1. Master Grating	22
	2.2. Producing Submaster Gratings-Contact Copies	23
	2.3. Producing High-Frequency Submaster Gratings	25
	3. Specimen Gratings	31
	3.1. Choice of Technique	31
	3.2. Photoresist and its Application	31
	3.3. Printing Grating Onto Specimen	36
	4. Photographing Specimen Gratings	37
	4.1. Comments on Method	37
	4.2. Grating Photography	40
VI	CREATION OF MOIRE FRINGE PATTERNS	45
	1. Introduction	45
	2. Important Basic Concepts	46
	2.1. Diffraction by Superimposed Gratings	46
	2.2. Optical Fourier Transforms and Spatial Filtering	56
	3. Formation of Moire Fringe Photographs	65

TABLE OF CONTENTS (Cont'd)

SECTION		PAGE
VII	REDUCTION OF MOIRE FRINGE DATA	74
	1. General Remarks	74
	2. Digitzing Moire Fringe Data-Radial Strain	77
	3. Digitizing Moire Fringe Data-Tangential Strain	81
	4. Data Reduction and Plotting-Radial Displacement and Strain	85
	4.1. Introductory Comments	85
	4.2. Detailed Analysis and Plotting of Single Data Sets.	85
	4.3. Analysis and Summary Plotting of Multiple Data Sets.	87
	4.4. Statistical Analysis and Plotting and Composite Plots.	91
	5. Data Reduction and Plotting-Tangential Strain	96
VIII	STRAIN MEASUREMENT RESULTS	100
	1. Introductory Remarks	100
	2. Results - Radial Strain	100
	3. Results - Tangential Strain	123
IX	DISCUSSION OF RESULTS	129
	1. Purpose and Plan	129
	2. Comparison with Results of Previous Investigations	129
	3. Some Interesting Aspects of the Data	133
X	SUGGESTIONS RELATED TO FUTURE FASTENERS RESEARCH AND APPLICATIONS OF MOIRE METHOD	146
	1. Introduction	146
	2. Suggested Future Research	146
	3. Apparatus and Procedural Refinements	147
REFERENCES		150
APPENDICES		153
A	MOIRE PATTERN DIGITIZING	153
	A-1. Digitizer Program with Notations	154
	A-2. Typical Output for Radial Strain Measurement	155
	A-3. Typical Output for Hoop Strain Measurement	156
B	DETAILED DATA ANALYSES	163
	B-1. Computer Program	164
	B-2. Typical Input Deck	184
	B-3. Typical Printed Output	188

TABLE OF CONTENTS (Cont'd)

		PAGE
APPENDICES (Cont'd)		
C	SUMMARY DATA ANALYSIS	189
	C-1. Computer Program	190
	C-2. Comments on Input Required	208
D	STATISTICAL SUMMARY PLOTS	209
	D-1. Computer Program	210
	D-2. Typical Input Deck	215
	D-3. Typical Printed Output	216

LIST OF ILLUSTRATIONS

FIGURE		PAGE
4.1	Specimens Used for Measurement of Strain Near Coldworked Holes; Typical Fiducial Marking Shown.	11
4.2	Schematic of Coldworking Using Mandrel and Sleeve.	14
4.3	Typical Record of Mandrel Pulling Force Versus Mandrel Displacement During Coldworking	19
5.1	Schematic of Setup for Contact Printing of Submaster Grating.	24
5.2	Sketch of Setup for Photographically Producing Submaster Grating of High Spatial Frequency.	26
5.3	Photographs of Apparatus for Producing Reduced Submaster Gratings.	
	7a. Side View.	27
	7b. 3/4 View.	28
5.4	Sketches of Typical Cross Sections of Specimen Grating in Photoresist for Various Degrees of Exposure.	38
5.5	Sketch of Apparatus for Photographing Specimen Grating.	41
6.1	Diffraction of Narrow Collimated Light Beam by Sine Grating.	47
6.2	Diffraction of Light by Two Superimposed Sine Gratings Having Slightly Different Spatial Frequencies.	48
6.3	Formation of Two-Beam Interference Fringe Pattern by Light Diffracted Through 2 Sine Gratings Having Slightly Different Spatial Frequencies.	50
6.4	Diffraction of Wide Collimated Beam by Two Sine Gratings to Form Whole-Field Interference Patterns.	51
6.5	Diffraction of Narrow Beam by Two Bar and Space Gratings to Form Ray Groups Containing Higher Diffraction Orders.	53
6.6	Diffraction by Two Superimposed Gratings, One Having Spatial Frequency Three Times that of the Other.	55
6.7	Optical Creation of Fourier Transform of Input Signal in Form of Transparency.	57
6.8	Two Simple Space Signals and Their Optical Fourier Transforms.	58

LIST OF ILLUSTRATIONS (Cont'd)

FIGURE		PAGE
6.9	Optical System for Spatial Filtering in Fourier Transform Plane and Creation of Inverse Transform of Filtered Image.	59
6.10	Example of Optical Spatial Filtering to Create Bar Grating from a Grid of Dots or Crossed Lines.	61
6.11	Example of Optical Spatial Filtering for Image Modification.	63
6.12	Schematic of Optical Processing System used for Obtaining Moire Fringe Photographs from Specimen Grating Photoplate.	66
6.13	Photograph of Moire Optical Data Processor (early version).	67
6.14	Sample Moire Fringe Photograph (reduced)	71
6.15	Sample Moire Fringe Photograph (reduced)	72
6.16	Sample Moire Fringe Photograph (reduced).	73
7.1	Diagram of Steps Involved in Reducing Moire Fringe Photographs to Obtain Displacement and Strain.	75
7.2	Steps in Reduction of Moire Data Related to Determination of Radial Strain Distribution Near Coldworked Hole.	78
7.3	Typical Fringe Photograph Prepared for Digitizing and Computation of Radial Strain.	79
7.4	Reduction of Moire Data for Determination of Hoop Strain Distributation Near Coldworked Hole.	83
7.5	Typical Fringe Photograph Prepared for Digitizing and Computation of Hoop Strain.	84
7.6	Typical Graphs Generated by Detailed Data Reduction Program (Hole C3, Leftside, Submaster 1481 lines/inch).	
	7.6a. Plot of Baseline and Coldworked Input Data Obtained from Fringe Photographs.	88
	7.6b. Radial Displacement Plot.	89
	7.6c. Radial Strain Plot.	90
7.7	Typical Summary Individual Radial Strain Distributions Measured for One Hole.	92
7.8	Typical Statistical Summary Plot of all Radial Strain Data For One Hole (Hole C3).	93

LIST OF ILLUSTRATIONS (Cont'd)

FIGURE		PAGE
7.9	Typical Composite Statistical Summary Plot Showing Average Radial Strains.	94
7.10	Typical Plot of Hoop Strain Distributions Along Several Y-Axes at Different Radial Distances.	97
7.11	Typical Distribution of Tangential Strain as a Function of Radial Distance from Hole.	99
8.1	Measured Distributions of Residual Surface Strain Near Cold-worked Hole for 3.8 mils Radial Interference (Hole C6).	102
8.2	Measured Distributions of Residual Surface Strain Near Cold-worked Hole for 4.1 mils Radial Interference (Hole C5).	103
8.3	Measured Distributions of Residual Surface Strain Near Cold-worked Hole for 5.6 mils Radial Interference (Hole C9).	104
8.4	Measured Distributions of Residual Surface Strain Near Cold-worked Hole for 6.0 mils Radial Interference (Hole C2).	105
8.5	Measured Distributions of Residual Surface Strain Near Cold-worked Hole for 6.6 mils Radial Interference (Hole C3).	106
8.6	Measured Distributions of Redisual Surface Strain Near Cold-worked Hole for 6.6 mils Radial Interference (Hole C7).	107
8.7	Measured Distributions of Residual Surface Strain Near Cold-worked Hole for 7.2 mils Radial Interference (Hole C10).	108
8.8	Measured Distributions of Residual Surface Strain Near Cold-worked Hole for 7.8 mils Radial Interference (Hole C1).	109
8.9	Average and Standard Deviation of Radial Strain Near Cold-worked Hole for 3.8 mils Radial Interference. All Data for Hole C6.	110
8.10	Average and Standard Deviation of Radial Strain Near Cold-worked Hole for 4.1 mils Radial Interference. All Data for Hole C5.	111
8.11	Average and Standard Deviation of Radial Strain Near Cold-worked Hole for 5.6 mils Radial Interference. Opposite Sides of Hole C9 Separate.	112
8.12	Average and Standard Deviation of Radial Strain Near Cold-worked Hole for 5.6 mils Radial Interference. All Data for Hole C9.	113

LIST OF ILLUSTRATIONS (Cont'd)

FIGURE		PAGE
8.13	Average and Standard Deviation of Radial Strain Near Cold-worked Hole for 6.0 mils Radial Interference. All Data for Hole C2.	114
8.14	Average and Standard Deviation of Radial Strain Near Cold-worked Hole for 6.6 mils Radial Interference. Opposite Sides of Hole C3 separate.	115
8.15	Average and Standard Deviation of Radial Strain Near Cold-worked Hole for 6.6 mils Radial Interference. All data for Hole C7.	116
8.16	Average and Standard Deviation of Radial Strain Near Cold-worked Hole for 6.6 mils Radial Interference. All Data for Hole C3 and All Data for Hole C7 Separate.	117
8.17	Average and Standard Deviation of Radial Strain Near Cold-worked Hole for 6.6 mils Radial Interference. All Data form Holes C3 and C7 Combined.	118
8.18	Average and Standard Deviation of Radial Strain Near Cold-worked Hole for 7.2 mils Radial Interference. All Data for Hole C10.	119
8.19	Average and Standard Deviation of Radial Strain Near Cold-worked Hole for 7.8 mils Radial Interference. Opposite Sides for Hole C1 Separate.	120
8.20	Average and Standard Deviation of Radial Strain Near Cold-worked Hole for 7.8 mils Radial Interference. All Data for Hole C1.	121
8.21	Composite Summary of Average Strains Measured for All Cold-working Levels Plus Error Summary.	122
8.22	Composite Summary of Average Strains Measured for Several Cold-worked Levels. Data for 3.8 mils and 4.1 mils Radial Interference Combined.	124
8.23	Measured Hoop Strain Distributions Along Several Axes at Different Radial Distances for 5.6 mils Radial Interference (Hole C9).	125
8.24	Measured Hoop Strain Distributions along Several Axes at Different Radial Distances for 7.2 mils Radial Interference (Hole C10).	126
8.25	Radial Distribution of Hoop Strain for 5.6 mils Radial Interference (Hole C9).	127

LIST OF ILLUSTRATIONS (Cont'd)

FIGURE		PAGE
8.26	Radial Distribution of Hoop Strain for 7.2 mils Radial Interference (Hole C10).	128
9.1	Summary Plot Showing Comparison of Data with Those Obtained in Previous Investigations.	130
9.2	Detailed Summary Plot of Measured Discrepancies in Digitized Data.	141
9.3	Statistical Summary of Digitization Errors.	142

LIST OF TABLES

TABLE NO.		PAGE
4.1	Summary of Specimen Measurements and Coldworking Parameters Investigated.	17

SECTION I

INTRODUCTION

1. SUMMARY STATEMENT OF PROBLEM

The purpose of the investigation described in this report was to measure residual surface strains in the region near fastener holes in aluminum alloy plate which had been coldworked to various degrees by the process which is marketed by J.O. King, Inc.

A sophisticated moire technique was developed for the investigation. Since moire methods had not been previously used to any extent at AFML, a preliminary related objective was to devise procedures and apparatus for the measurement scheme within the limits of available equipment and funds.

2. ORGANIZATION AND PURPOSES OF THIS REPORT

Given the objectives of the investigation and the fact that the investigator was a temporary member of staff at AFML, it seems necessary that this report should serve several different but related functions. Its main technical purpose is to report on the background, procedure followed, and the results obtained in measuring strains around coldworked fastener holes. It also serves as a repository of the technical details, many of which are peculiar to the system at AFML, that develop in the course of setting up new apparatus and procedures using nonstandard techniques. Finally, it is intended to be used as a tutorial source for engineers and technicians who want to understand or utilize the apparatus and methods or, in particular, to duplicate part of the experiments discussed herein.

It is not practicable to delineate sections of this report which serve each of its functions; a report so written would be ungainly. Instead, the report is

organized along the lines of a dissertation. It is a fairly formal description of the origins of the problem; the thinking that went into choosing an approach; the procedure used from start to finish with rather more detail than one ordinarily expects in a technical report; a presentation of the results; and a discussion of the findings, measurement errors, and possible courses of future investigation. A danger of this type of reporting is that the reader may be led to think that the progress of the investigation passed logically and systematically from conception of the problem to final solution. Such a conclusion is wrong; false starts, dead ends, poor logic, mistakes, irregular progress, and confusion were present in this study to a degree at least equal to the average. On the other hand, certain self-checks and redundancies were incorporated, and possible errors were analyzed with some care; so the results are reported with reasonable confidence of their dependability.

Design people and program managers who also are mainly interested in the results are advised to skip most of Sections IV through VII, and to give Section III, IX and X only cursory reading. Technical people who are faced with similar measurement problems will want to study Sections IV through VII in detail and also to utilize the appendices.

3. BACKGROUND OF PROBLEM

Crack initiation and growth is a major cause of failure of high performance structural components and a major source of difficulty to the designer. Given the obvious seriousness of the fatigue cracking problem, the Air Force has directed designers to demonstrate that service lives of critical components will tolerate the presence of cracks of specified sizes and shapes.[1-1] A 1971 review of aircraft structural failure showed that cracks which began at fastener holes were the primary causes of one-third of early failures.[1-2] The structural designer faces

a situation where an essential component of design--the fastener--might be responsible for the failure of his design. It is desirable, obviously, to lessen, through overall design improvement and also in the specific development of fastener systems, the tendency for failures to begin at the fasteners. The designer will gain freedom, confidence, and reputation; costs will be reduced; and higher performance standards for structures will be established.

One class of techniques for improving the fatigue performance of fasteners is to plastically deform the hole prior to or during installation of the fastener. Several proprietary schemes have been invented for accomplishing this coldworking of the hole in an efficient way.[1-3] While evidence supports the assertation that coldworking improves fatigue lives,[1-2,1-5] the degree of improvement for a given degree and mode of coldworking is still not settled.

From the designer's point of view, the problem is to establish that the fatigue life of his design is not influenced by certain flaws at the coldworked hole. Experimental justification in every design situation is far from feasible. The preferred approach, as usual, is to develop analytical tools which can be used universally and to show that these tools give correct results in many different situations which can be modelled by experiments or verified by extensive service testing under controlled conditions. Indeed, most such analytical approaches will use empirical factors which are derived from experiments on known cases to get around problems caused by incomplete solutions, questionable mathematical modeling, or intractable mathematics. Thus are gained the benefits of optimum joining of theory, computation, and experiment.

Such design procedures for coldworked holes are still in the early stages of development. It is not within the scope of this investigation to discuss existing work in detail, but mention of certain aspects of analytical models will serve as partial justification of the current effort. Grandt[1-6] and Grandt and Gallagher,[1-7]

for example, have adapted the methods of fracture mechanics to develop procedures to account for the effects of coldworking at fastener holes. Their approach has been tested to a limited degree by Cathey[1-8] and by Grandt and Hinnerichs.[1-9] The fracture mechanics calculation, and probably any other analysis scheme which could be devised, requires knowledge of the stress field around the nonflawed hole after coldworking.

Little information exists about stress fields induced by the inelastic radial expansion of holes. Several applicable theories have been formulated, but they remain relatively untested. Noteworthy in this respect is the work of Sharpe[1-10] who has drawn together existing theoretical models and performed experiments to test them. Chandawanich and Sharpe[1-11] and Poosok and Sharpe[1-12] have extended this program in various aspects. Among other theoretical approaches, they checked the simple solution devised by Potter and Grandt[1-13] as well as the measurements and finite difference solution of Adler and Dupree.[1-14] A simple experimental and analytical study of interference-fit fatigue-rated fasteners has been reported by Ford and coworkers.[1-15]

The studies mentioned above are limited in one aspect that seems important. They cover only a very limited range of levels of coldworking. The values used center around the value (6 mils total radial interference) which in the industry is believed optimum, although only minimum evidence exists to show that this value gives the best fatigue improvement.[1-4,1-5] Existing information about the stress-strain field is not sufficient, then, to adequately test the relevant theories. Neither can one assess the effects of normal industrial dimensional tolerances upon either the fatigue performance or the design procedures.

The experimental investigation described in this report was undertaken to close, to a degree, this gap in our knowledge. It is, of course, not possible to measure stress directly. Given knowledge of the mechanical properties of the

material, it is possible to derive a picture of the stress field from a map of the strain field. In fact, such an approach is probably most meaningful since, owing to the imposition of displacement boundary conditions (radial interference minus springback) on the hole boundary, the strain field can be expected to be less dependent upon material properties. That is, it should be possible, within reasonable limits of accuracy, to assume that the strain field measured for one aluminum alloy is valid for a similar but different alloy; whereas the stress fields might be quite different.

SECTION II

SCOPE OF STUDY

1. SUMMARY OF PARAMETERS

As stated in Section I-1, the objective of this investigation was to measure residual surface strain fields created by coldworking fastener holes to various degrees which might be appropriate for industrial applications.

The coldworking process and apparatus marketed by J.O. King, Inc., 711 Trabert Avenue, N.W., Atlanta, Georgia, 30318, U.S.A., was the only one considered. The restriction to commercially available sizes of reamers, fastener sleeves, and coldworking mandrels limited the spectrum of coldworking levels to the following magnitudes of radial interference (mandrel radius plus sleeve thickness minus hole radius):

3.8 mils = .097 mm
4.1 mils = .10 mm
5.6 mils = .14 mm
6.0 mils = .15 mm
6.6 mils = .17 mm (2 specimens)
7.2 mils = .18 mm
7.8 mils = .20 mm

Attention was focussed mainly on the radial strain component, but tangential strain maps are reported for two levels of radial interference (5.6 mils and 7.2 mils). The effects of remote loads upon the strain fields are not considered here. A study of the effects of large compression in-plane loads was undertaken as a part of the larger project. The results are described in another report.[1-16]

Although some measurements were performed upon both sides of some specimens, the results for the side containing the sleeve anvil were not conclusive because the presence of the anvil made it impossible to do measurements close enough to the hole. These results are, therefore, ignored in this report.

All measurements were done on specimens of ¼ inch (6.3 mm) thickness using holes of ¼ inch nominal size. The only material used was 7075 T-6 aluminum alloy plate manufactured by Alcoa Corp.

Care was taken to select fasteners having uniform wall thickness, and holes and mandrels were measured carefully; otherwise the machining and coldworking procedures approximate those which might be found in a typical industrial facility. Mandrels and holes showed some degree of eccentricity, and the holes showed the slight eccentricity which is typical of hand reaming. Average values of sizes were used, and the eccentricity and taper effects were expected to enlarge the scatter.

2. SHORT DESCRIPTION OF APPROACH

A sophisticated moire technique was devised and used. Coatings were applied to each specimen with photoresist and photographed using high-resolution techniques before and after coldworking. The developed photo plates were superimposed with previously prepared submaster gratings of various spatial frequencies in a coherent optical data processor so as to gain sensitivity multiplication and useful pitch mismatch. The resulting fringe photographs were enlarged, and the fringe positions recorded in digital form using a computer-digitizer unit. The digital data was processed by computer to obtain surface displacement and strains. These results were summarized in various plotted modes through use of digital computer graphical facilities.

SECTION III

CHOICE OF METHOD OF INVESTIGATION

1. REQUIREMENTS TO BE MET

The problem of measuring strains in the vicinity of a coldworked hole is one which severely taxes any of the common techniques of experimental strain analysis. Characteristics of the strain field which must be considered when planning an approach to this measurement problem include:

a. The strain magnitudes range from about 10% compression to about 3% tension.

b. There is considerable out of plane displacement and rumpling of the surface in the plastic zone.

c. The strain gradient is large in the region of interest near the hole.

d. The area of prime interest is close to a boundary.

e. The fastener sleeve protudes slightly from the surface.

In addition, the method should give a whole-field mapping of the two principal strain components. The principal directions can be established from the symmetry (near-symmetry in the physical problem) of the strain field.

2. CHOSEN APPROACH

One of several possible variations of the moire technique appeared to satisfy best the conditions of the measurement problem. The method is whole-field and noncontacting in the variation chosen; it offers the possibility of changing sensitivity after the raw data has been recorded and examined and it can yield correct results in regions of high strain gradient and near boundaries. The moire method has been studied, refined, and used for a long time; its procedures and

pitfalls have been well explored. Important disadvantages include the general low sensitivity of basic simple moire techniques for problems involving metals, the problems and errors associated with the necessity to differentiate the moire displacement data to determine strains, and the general difficulty and tediousness of the method in comparison with, for example, resistance strain gages.

3. PROCEDURE OUTLINE

The decision was to utilize the moire technique with gratings of 1000 lines per inch (lpi) or 39.4 lines per millimeter (lines/mm) applied to the specimen using a photoresist coating. Because the specimen surface does not remain flat, a noncontacting procedure was developed which called for photographing a magnified image of the specimen grating before and after the coldworking process. These grating photographs were superimposed with one or more master gratings in an optical Fourier processor in order to form separate baseline and data moire fringe patterns. Fringe multiplication and pitch mismatch were introduced during this processing stage in order to obtain increased sensitivity and to simplify the interpolation required in subsequent data processing. The moire fringe orders and positions along the chosen axes were obtained from the photographs in digital form. Displacement and strain distributions were generated and plotted using a digital computer. Several trials of the digitizing and analysis processes were made for each fringe pattern, and, usually, several different fringe patterns were created for each specimen. The results of the various trials were studied separately for errors and consistency, after which they were averaged to obtain final strain plots.

SECTION IV

SPECIMENS

1. MATERIAL

All the specimens used in this study were cut from a single plate of 7075-T6 aluminum alloy in ¼ inch (6.4 mm) thickness. This sheet is the same stock as that used by Adler and Dupree[1-14] and Sharpe,[1-10] and it was not believed necessary to check their measurements of material properties. Also, direct comparisons with their data may be made without allowance for material variation.

2. CONFIGURATION

Two types of specimens were used; both are pictured in Figure 4.1. The design with two holes was adopted as a means of saving material. Data from previous analytical and experimental studies suggested that the strain fields in the important region within 2 hole diameters of the hole would not be affected by the other hole or the edges of the specimen. The data from this study seem to support this idea. The outside dimensions of the specimens were fixed by the facilities available for loading the specimens in the parallel study of the effects of various remote loading conditions upon the strain field.

In moire work where several stages of photographic processing are used, it is very important to have adequate fiducial marks and identity labels on the specimen surface. Typical marking patterns employed in this investigation are shown on the specimen drawings of Figure 4.1. The methods used to apply them are described at the end of the next section.

Since there were some inconsistencies in the preparation of the several specimens, it was mandatory that actual hole sizes and fiducial locations be measured. These values were obtained by ordinary gaging and with a toolmakers microscope, and the

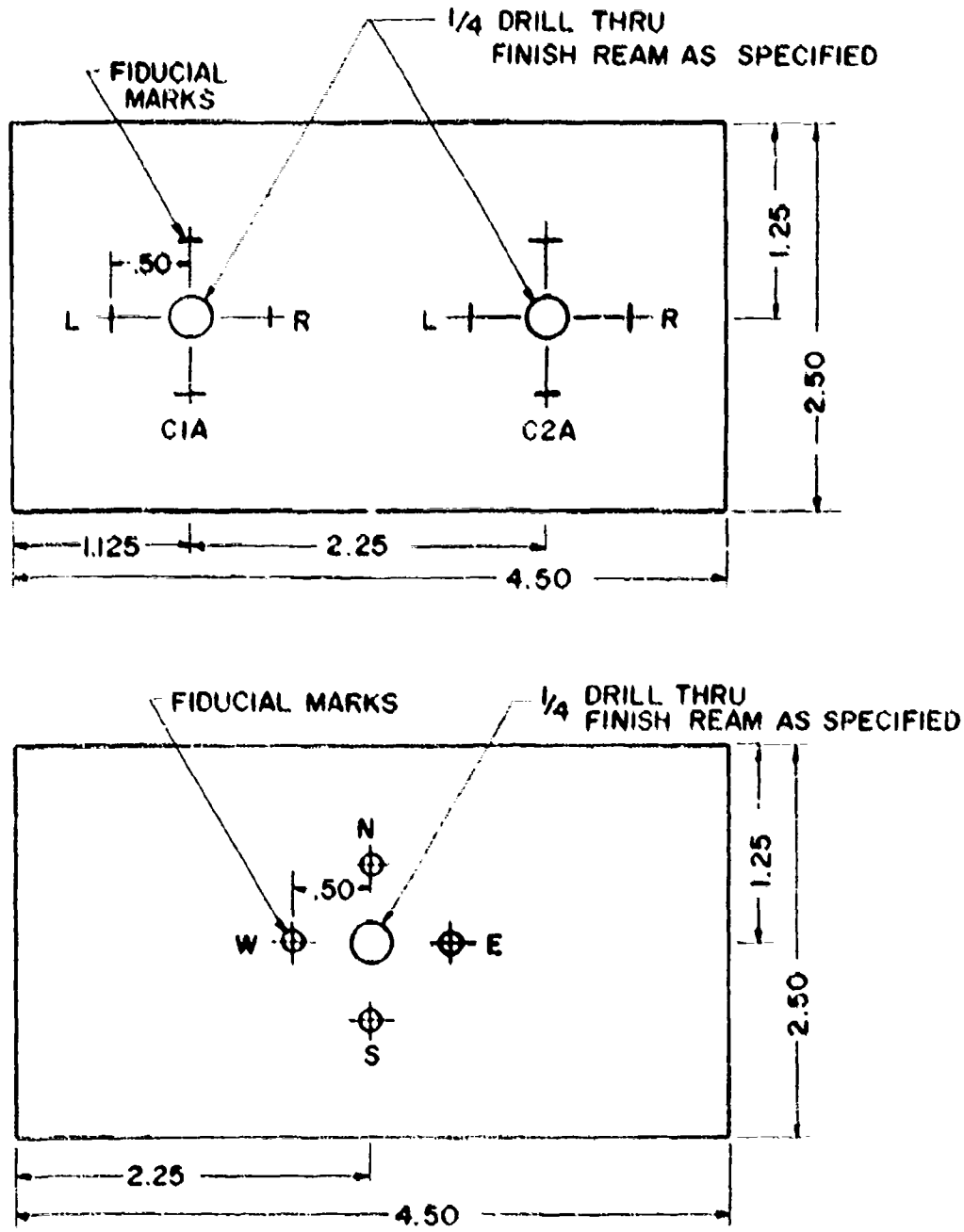

Figure 4.1. Specimens used for measurement of strain near coldworked holes; typical fiducial marking shown.

values were recorded for later use in calculating scaling factors for the data processing procedures.

3. SPECIMEN PREPARATION

The specimens were rough sawn from the stock sheet and the edges milled to size. External corners were chamfered lightly. In most cases, the hole centerlines were then marked and the holes centerpunched and then drilled on a press to a size large enough to accept the reamer pilots. In some cases, the remaining fiducial marks were then scribed and the holes reamed before rough and final polish. Other specimens had the final reaming done before polishing, with the scribing and labelling of fiducial marks performed after polish. Completion of the scribing before drilling and reaming was not entirely satisfactory because the holes tend to drift from center; and it seems better to locate the fiducial marks from the final hole edge using toolmakers gaging equipment. These differences were not serious, however, as the final locations of important features were always measured in the final stages of preparation. Reaming after polishing proved entirely unsatisfactory as it tended to raise a troublesome burr around the finished hole. On the other hand, polishing after reaming tended to round the edges of the hole slightly. This condition was observed to exist in a small degree in several of the specimens used, and it might contribute to scatter of the strain measured in the near vicinity of each hole. Lapping of the specimen surfaces instead of metallurgical polishing should eliminate the problem. Otherwise, very careful polishing technique must be observed.

In this study, specimens were rough-polished through several grades of emery cloth and metallurgical preparation paper. They were then polished with successively finer grades of diamond emery on cloth polishing wheels. Given the size of the specimens in relation to thickness and relative to the size of the polishing discs, it proved impossible to obtain a surface having uniform "grain" over the whole extent of the important areas of the specimen. As a result, light scattering and

reflection properties varied from point to point. These surface variations caused great trouble in obtaining uniformly exposed photographs of the specimen moire gratings, as may be seen in the moire fringe photographs displayed later in this report. This effect was serious in view of the stringent nature of the high-resolution photography. A worthwhile simplification and improvement in overall efficiency of the moire procedure would be effected by adoption of a lapping technique which would produce a truly flat surface with a uniform fine matte finish.

The fiducial marks were applied in various ways. In the early stages of the program, they were scribed by the usual machinist's technique of gaging and scribing with a vernier height gage resting on a surface plate. Markings so produced tended to be fairly deep and were found to either disturb the strain field or to make fringe counting and locating difficult. So, the later specimens had the fiducial marks lightly scratched into the surface with a sharp pocketknife guided by a steel rule. Some of these fine scratches were found to vanish in one or another of the photographic stages. They were, therefore, usually highlighted and identified with "presstype" lettering to facilitate locating them on the fringe photographs. This procedure was not uniformly successful, and a better method of establishing fiducial locations should be sought before future work of this sort is undertaken.

After final polishing and scribing of the fiducial marks, the moire gratings were printed onto the specimen using photoresist. The procedure is described along with the rest of the moire techniques in the next section of this report.

Subsequent to application of the gratings, the fiducial marks were touched up if needed, and identifiers and code marks were applied with presstype lettering. The precoldwork hole size was determined by several replications of measurement with a hole gage and micrometer. In most cases, a map of the fiducial marks in relation to the hole was established at this point by utilization of a Zeiss toolmaker's microscope. The specimen was then ready for recording a baseline moire grating photograph and subsequent coldworking of the hole.

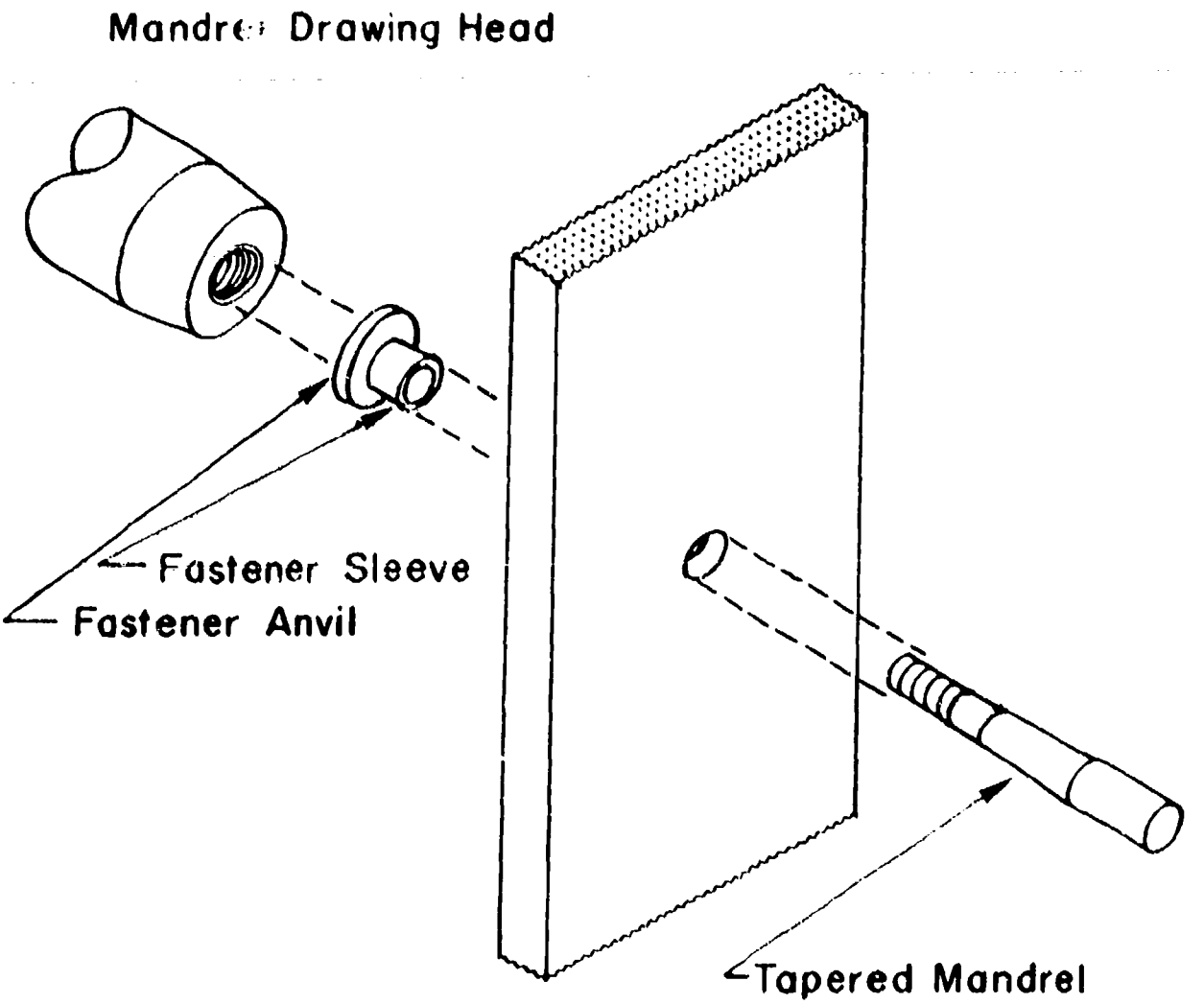

Figure 4.2 Schematic of coldworking using mandrel and sleeve.

4. COLDWORKING PROCESS

The coldworking apparatus and procedure studied in this investigation are shown which have been developed and marketed by J. O. King, Inc., 711 Trabert Avenue, N. W., Atlanta, Georgia, 30318. In this process, which is the same one studied by Sharpe[1-10] and Adler and Dupree,[1-14] a lubricant-coated stainless steel sleeve which carries an anvil on one end is inserted into the hole. A tapered mandrel is placed inside the sleeve and pulled through while the sleeve is supported on the anvil. The mandrel enlarges the sleeve and expands the hole enought to cause plastic deformation of the adjacent material. The sleeve remains in the hole, but the anvil drops off. Figure 4.2 shows details of the mandrelizing process.

While it was desired that a close approximation to the industrial process be the subject of these experiments, it was also necessary that a reasonable degree of replication of procedure and coldworking parameters be utilized in order to gain understanding of the fundamental process. In particular, the degree of coldworking should be known with good accuracy and the plastic deformation should be symmetrical with respect to the hole axis. These conditions are not trivial, as the actual degree of coldworking cannot be measured directly owing to the presence of the sleeve and the three-dimensional nature of the mandrelizing process. It is convenient and customary, therefore, to report results in terms of the radial interference between the hole and the sleeve thickness plus mandrel diameter. The calculation is based upon measurements of hole size, sleeve thickness and maximum mandrel diameter. The sleeve thickness, in turn, is computed from separate measurements of the outer and inner diameters. Clearly, the problem of establishing radial interference is not well-conditioned owing to the buildup of uncertainity involved in determining the small differences between several large measured quantities. A further uncertainty in the degree of coldworking is caused by the elastic springback of the material after the mandrel has passed through. The springback would seem to be a function of material,

mandrel taper profile, and, perhaps, the rate of drawing of the mandrel. The final inner diameter of the sleeve gives some indication of the actual coldworking which has been imposed, and it serves as a check on the other measurements if it is assumed that the sleeve thickness is not reduced by the heavy pressures involved.

The first step in the coldworking process, then, was to measure each reamed hole, sleeve inner and outer diameters, and mandrel sizes. It was found that sleeve thickness varied from sleeve to sleeve, and sometimes within a sleeve; this last mentioned characteristic being manifested as a taper in thickness from one end to the other. The measuring process was complicated by the lack of roundness of most of the sleeves, which appear mainly in the portion farthest from the anvil end and which should not affect performance of the sleeve. Because of these variations, a number of sleeves were measured to obtain approximate average values of the inner and outer diameters. The sleeves required for the experiment were then selected from an entire box of 100 pieces based upon the requirement that their diameters had to be within a few tenths of a mil of the average values established. The average sleeve thickness was found to be .00845 inches (.215 mm), which essentially equals the optimum value of .0085 in. specified by the J.O. King, Inc., literature, and which is approximately .001 thicker than the sleeves used by Sharpe[1-10] and by Adler and Dupree.[1-14]

The mandrels provided were found to have different profiles in the tapered portion, which might have led to consistent variation of data between specimens because of differing relative influences of three-dimensional effects during the coldworking process. There was also up to one mil eccentricity in the cross section of the various mandrels. These two sources of variability were ignored except to look for qualitative effects, such a lack of symmetry of the strain field, in the results.

The assortment of reamers and mandrels on hand allowed the use of only a limited number of interference levels and degrees of coldwork between 3.8 mils (.097 mm) and 7.8 mils (.20 mm) radial interference. Table 4.1 summarizes the measurements taken, the calculated values of resultant radial interference, and the residual radial expansion for the samples used. Given the methods of measurement, the variabilities

TABLE 4.1

HOLE SPECIMEN NUMBER	HOLE DIA. IN.	HOLE DIA. MINUS TWICE SLEEVE THICKNESS (NOTE A)	MANDREL DIA. IN.	DIA. INTERFERENCE IN.	RADIAL INTERFERENCE IN.	INNER DIA. OF SLEEVE AFTER COLDWORK	RESIDUAL RADIAL DISPLACEMENT	RADIAL SPRINGBACK	NO. OF FAILURE IN MANDRELIZING	COMMENTS
C1b	.2578	.2409	.2564	.0155	.0074	.2516	.0053	.0024	0	Sleeve Deburred First
C2	.2578	.2409	.2530	.0121	.0060	.2495	.0043	.0017	0	
C3	.2578	.2409	.2542	.0133	.0066	.2496	.0043	.0023	0	
~~C4~~	~~.2616~~	~~.2447~~	~~.2553~~	~~.0108~~	~~.0054~~				~~3~~	Specimen Not Completed After 3rd Failure
C5	.2617	.2448	.2530	.0082	.0041	.2496	.0024	.0017	0	
C6	.2617	.2448	.2523	.0075	.0038	.2489	.0020	.0017	1	
C7b	.2578	.2409	.2542	.0133	.0066	.2498	.0044	.0022	0	Sleeve Deburred First
~~C8a~~	~~.2578~~	~~.2409~~	~~.2523~~	~~.0114~~	~~.0057~~	~~.2464~~			~~3~~	Specimen Not Completed After 3rd Failure
C9b	.2577	.2412	.2523	.0111	.0056	.2477	.0033	.0023	2	Sleeve Slightly Extruded--1/64 below surface
C10a	.2577	.2412	.2555	.0143	.0072	.2508	.0048	.0024	1	½" Long Sleeve used 2nd time.

Notes: A. Sleeves for C1-C8 were .00845 Wall Thickness.
Sleeves for C9, C10 were .00825 Wall Thickness.

mentioned above, and the apparent consistency of the final results, one is led to conclude that the uncertainty in the reported radial interference would be about ±.0005 inches (.01 mm). Since sleeves of ¼ inch (6.35 mm) nominal shank length were not in stock at the time, ½ inch (12.7 mm) ones were cut off on a lathe to 17/64 inches (6.75 mm) length and the inside corner lightly chamfered.

The mandrelizing of each hole was accomplished by use of a frame and mandrel mounted in an Instron testing machine. Crosshead speed of the Instron during pulling of the mandrel was 0.2 inches/minute (5 mm/minute). The time-load history of the mandrel-pulling process was recorded on the Instron chart. Figure 4.3 is a typical record. The maximum mandrelizing load for each sample is shown in Table 4.1. Pathological behavior, such as slipping of the sleeve in the hole, was signaled by unusual serration in the load recorded by the Instron machine.

Slippage of the sleeve in the hole and subsequent splitting and extrusion of the sleeve from beneath the anvil was very much a problem in this study. Two specimens had to be discarded completely as a result of this behavior. In 3 specimens, failure of the process began early on, which meant that, since the sleeve was withdrawn from the hole with the mandrel, little coldworking was accomplished. In such cases, a new sleeve was installed and the expansion process restarted. Table 4.1 indicates all these deviations from normal coldworking procedure. Note that in Specimen C9 there were two failures before a successful coldwork, and this final coldworking was unusual in that the sleeve slipped about 1/32 inch, ending with the tip of the sleeve about 1/64 inch below the specimen surface. It seemed that such a failure would result in a smaller degree of coldwork, especially in the surface where strains were being measured. The decision was to complete the study of this specimen to see if it gave reasonable results. They turned out to be entirely consistent with the results from the other specimens, and the results are included in this report without any special flagging. A tentative conclusion is that a small amount of chamfering of the hole, such as was blamed by Adler and Dupree[1-14] for results which they thought questionable, would not seriously affect the strain field except, perhaps, within 10 mils or so from the hole boundary.

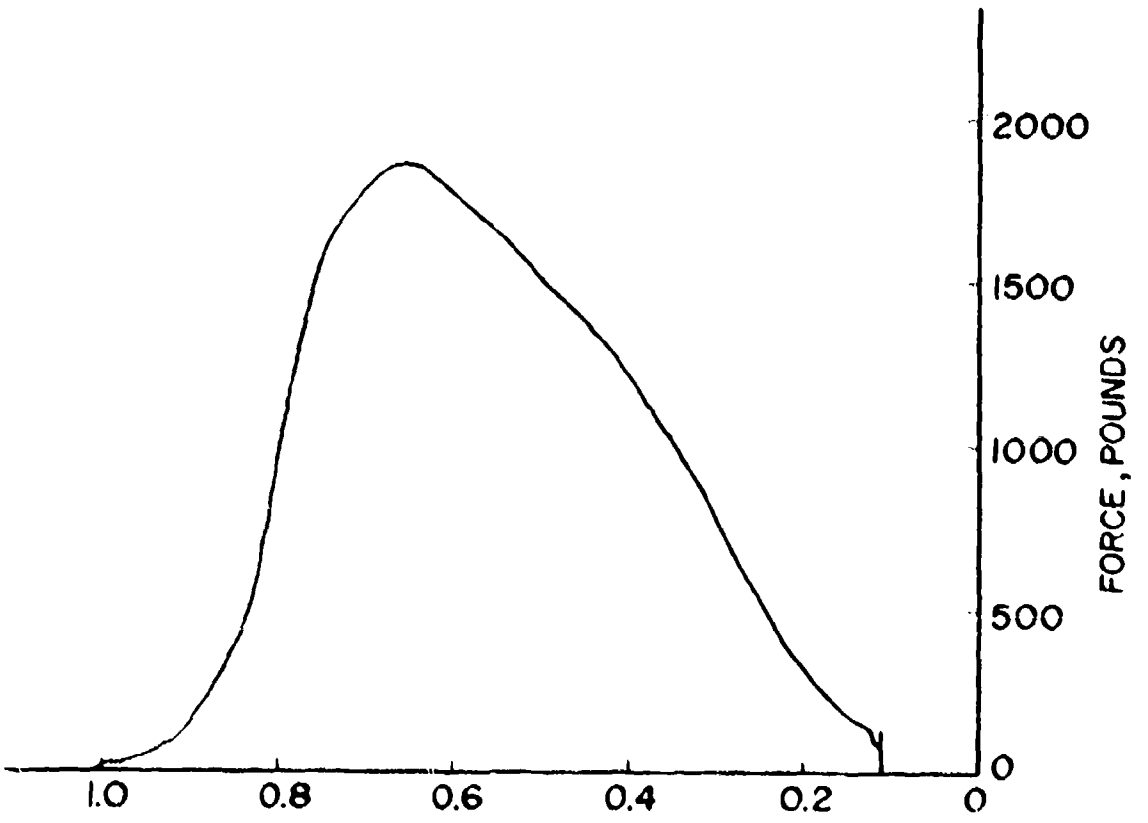

Figure 4.3. Typical record of mandrel pulling force versus mandrel displacement during cold-working.

The many failures of the mandrelizing process lead one to question the effectiveness of the procedure. There appeared to be three contributing factors. The first and most important is that the mandrels supplied were quite soft. The sleeve edge seemed to bit into the mandrel surface, and the surface of used mandrels did show evidence of scuffing and galling. Another factor might be that much of the lubricant installed by the manufacturer was removed as the sleeve was measured. Related to this is the fact that the protective coating on the sleeves was removed at the inside entering corner when the sleeves were trimmed to length. These last two factors did not seem important in that informal experiments with lubricants and polishing to reduce friction between sleeve and mandrel caused no discernible improvement. Properly hardened and polished mandrels would probably solve the problem.

SECTION V

MOIRE MEASUREMENT OF STRAIN

This section discusses the moire measurement procedure through the stage of creating the moire fringe patterns. The reduction and analysis of the fringe data is described in Section VI.

Section V.1 is a short summary of the procedure; the remaining sections describe each step in detail.

1. SHORT SUMMARY OF PROCEDURE

The measurement by the moire technique of the displacement and strain fields near coldworked holes entailed the following steps:

a. Master gratings of 1000 lines per inch (1pi) (39.4 lines/mm) were obtained and reduced photographically to create a set of working submasters of various grating frequencies including the fundamental frequency.

b. The specimen surface was cleaned thoroughly.

c. A thin coating of photoresist lacquer was sprayed onto the specimen with an airbrush and the coating dried in low heat.

d. A submaster graing was clamped to the coated specimen and the assembly exposed to unfiltered radiation from a mercury lamp in order to produce a contact image of the grating in the resist.

e. The exposed photoresist was developed.

f. The fiducial marks were touched up, highlighted, and identity labels applied.

g. The specimen was placed in a holder and the grating photographed at low magnification (1.3X)

h. The hole in the specimen was coldworked.

i. The specimen was returned to the holder and the graing, now deformed by the coldworking, was photographed again.

j. The photographic plate of the undeformed grid was superimposed with a submaster grating having a spatial frequency of 3 (sometimes 2) times the frequency of the magnified specimen grating plus or minus a small frequency mismatch.

k. The assembly was placed in a coherent optical processor and adjusted to produce the correct baseline (zero strain) fringe pattern at the processor output. This fringe pattern was photographed.

l. Steps j and k were repeated with the deformed grating photoplate.

m. Steps j-l were repeated with other submaster gratings to produce fringe patterns having different pitch mismatch, and, in some cases, different sensitivity multiplication factors. On the average about 3 such sets of baseline and data fringe patterns were produced for each coldworked specimen.

n. The fringe patterns were enlarged and printed in 8x10 inch size with medium-high contrast processing.

o. The prints of the fringe patterns were sorted and coded for identification during the data analysis procedure.

2. MASTER AND SUBMASTER GRATINGS

2.1 Master Grating

A grating having a spatial frequency of 1000 lpi (39.4 lines/mm) on a 4 inch by 4 inch glass substrate was obtained from Photolastic Inc. of Malvern, Pa., for use as a master grating. This grating, which comes mounted in an aluminum frame, is designed for use in a moire camera for real-time fringe observation, and it is not meant to serve as a master copy. Indeed, the grating proved to be of marginal quality for such a purpose. It contained many pinholes and both local and gross variations of density which were similar in appearance to fogging of photographic films. These transmittance variations, in particular, made it difficult to obtain good submaster

copies and, subsequently, affected the quality of the gratings printed onto the specimens. For lack of any other master grating, submasters made from it were used for most of this study. Also utilized were two high-quality submaster copies in 1000 lpi obtained from Nopporn Chandewanich, a Ph.D. student at Michigan State University. These copies had been taken from another Photolastic, Inc. master of better, but still marginal, quality. The final stages of the investigation were carried out with 2 inch by 2 inch submasters in 1000 lpi made by Mr. Chandawanich from a metallic film master grating of superb quality provided by Graticules Ltd., Tonbridge, TN91RN, Kent, England. These two additional 1000 lpi gratings were used only for exposing the photoresist on specimens C9 and C10. They were not utilized in the grating superposition-optical data processing stages, since gratings of higher spatial frequench are required for that purpose. The high frequency submasters had already been made by photographing the original master. It is reasonable to expect that better fringe patterns could have been obtained had submaster copies in the higher frequencies been made from a master grating which was more uniform and of higher contrast.

2.2 Producing Submaster Gratings-Contact Copies

The making of 1:1 copies of moire gratings for submasters and for printing on the specimen has been thoroughly explored and explained by Luxmoore, Holister, and Hermann,[5-1,5-2,5-3] and by Straka and Pindera[5-4] among others. The techniques described in these references have been used in this study with certain modifications. Contact copies of the Photolastic master were made by a method similar to that used by Chaing[5-5] on Kodak High Resolution Plate (HRP) using a Durst enlarger head with a 150 mm Schneider lens at f 5.6. A sketch of this setup is shown in Figure 5.1. There are several noteworthy features in this arrangement. First, the light rays falling on the master and photo plate are not collimated as is often thought necessary. It is not a source of error here because of the small equivalent source size and the intimacy of the contact between the master and the photoemulsion.

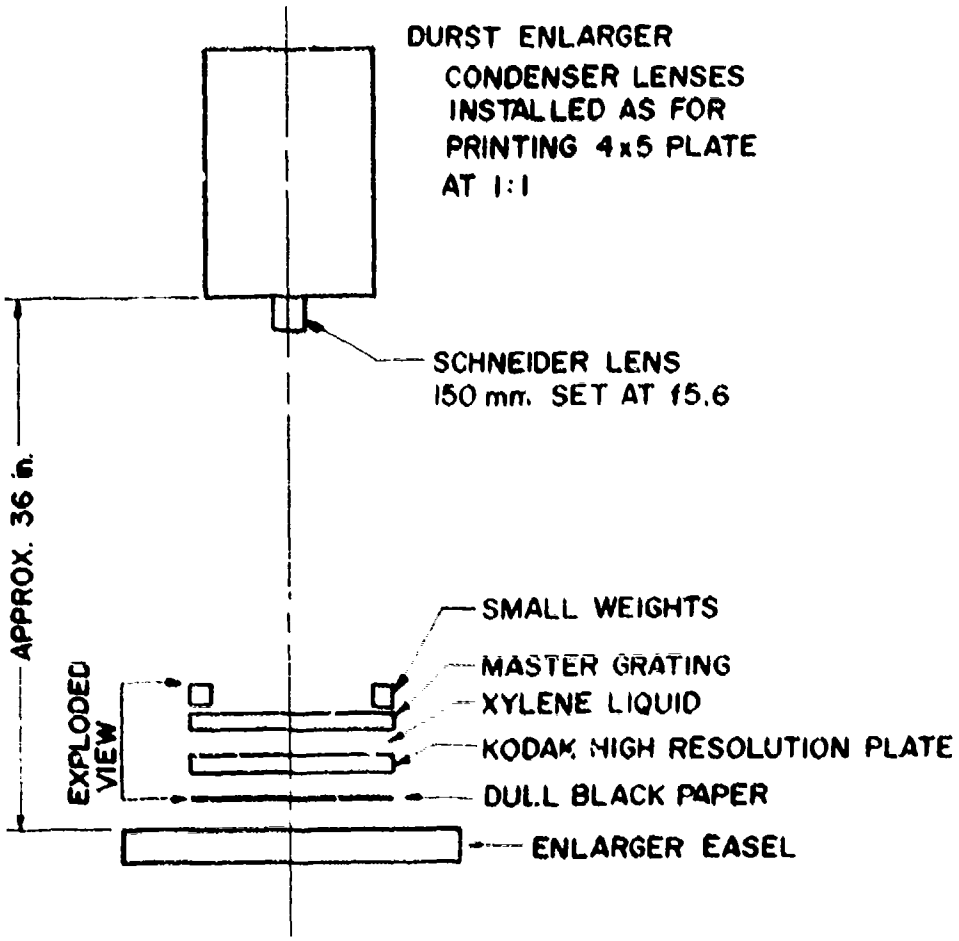

NOTE: HRP PLATES ARE NOT BACKED. BLACK PAPER ELIMINATES FOGGING BY REFLECTED LIGHT.

EXPOSURE: APP. 6-8 min. DEVELOP 12 min. IN D-19

Figure 5.1. Schematic of setup for contact printing of submaster grating.

No spacer was used between the two to eliminate the diffraction lines which appear if monochromatic light is used. The emulsion of the HRP was placed in contact with the emulsion side of the master and held by small weights on the enlarger easel. Only a thin film of index-matching fluid (xylene) was placed between the two to reduce the effects of possible lenticulation in the master. Diffraction lines did not appear because white light from the enlarger head was used. This procedure was originated as a means of reducing exposure times, which still amounted to 8 minutes with a lengthy 12 minute development of the HRP in D-19 (HRP developer being unavailable at the time). The resultant ratio of line width to space width in the grating copies was about 0.7, which is a bit on the low side for the best moire work. The submasters so obtained were quite good within the limitations imposed by the master grating.

2.3 Producing High-Frequency Submaster Gratings

Direct photographic reproduction was employed for manufacture of the several submaster gratings having various spatial frequencies required for optical data processing of the specimen photographs. Several each of gratings having spatial frequencies of 743, 783, 797, 1488, 1492, 1535, 2200, 2225, 2256, 2288, 2999 and 3049 lines per inch were produced. These values are 1, 2, and 3 times the fundamental spatial frequency of the specimen grating photographs (1000 lpi divided by magnification used) plus or minus various frequency mismatches. Figure 5.2 shows a sketch of the apparatus used and Figures 5.3 are photographs of the same.

The 1000 lpi master grating was held in a laboratory clamp base and backlit with light from a Kodak carousel slide projector. A ground glass plate was placed about 3 inches behind the grating to scatter the incident light. The lens and camera were the ones used in photographing the specimen grating. The lens was a Goerz Red Dot Artar of 9½ inches focal length and f9 maximum aperture. The lens was mounted in a Burke and James 4x5 "Orbit" monorail view camera which was stiffened with angle iron and weighted. The whole setup rested upon a Gaertner holography table which uses airbag suspension for vibration isolation.

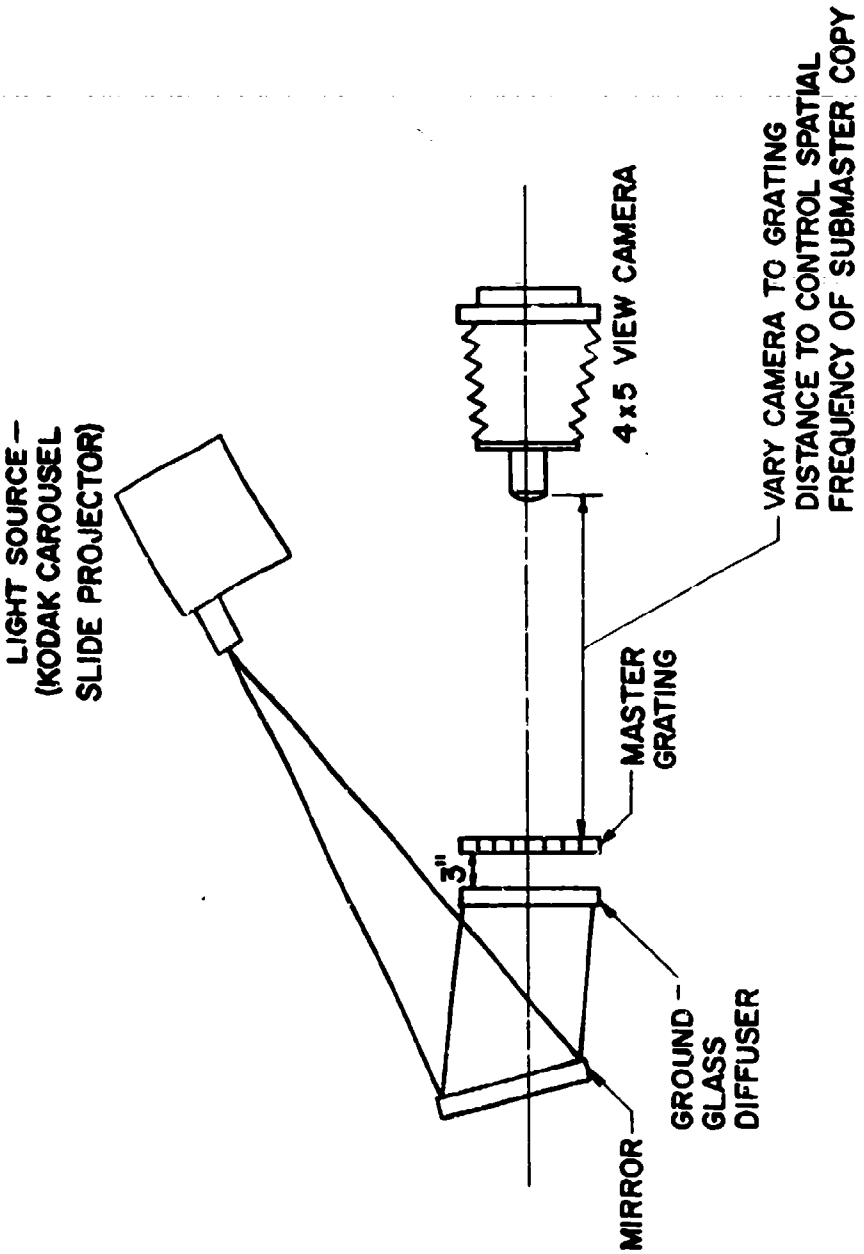

Figure 5.2. Sketch of setup for photographically producing submaster grating of high spatial frequency.

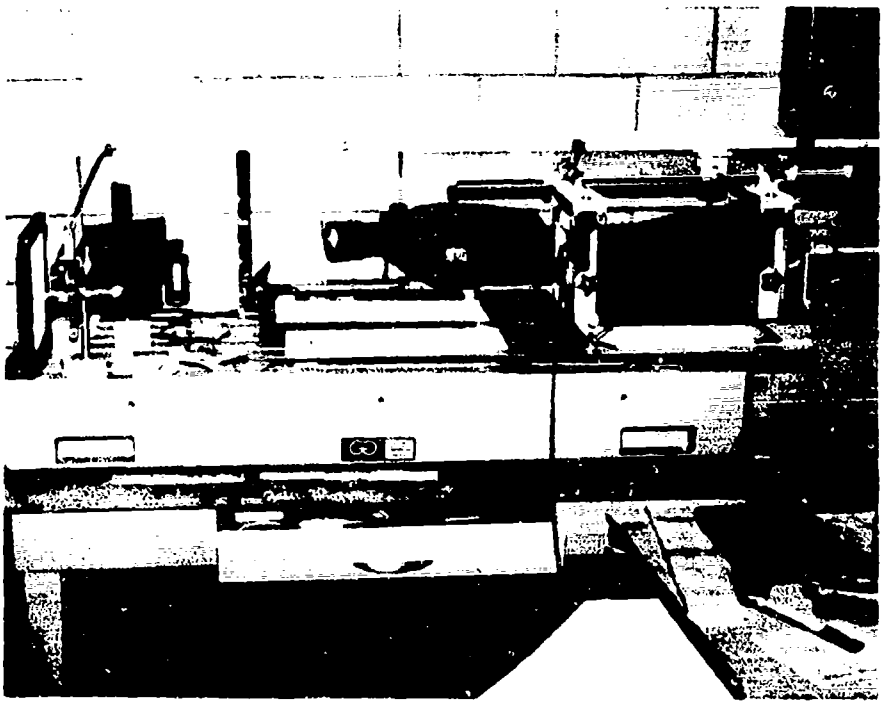

Figure 5.3. Photograph of apparatus for producing reduced submaster.

(a) Sideview.

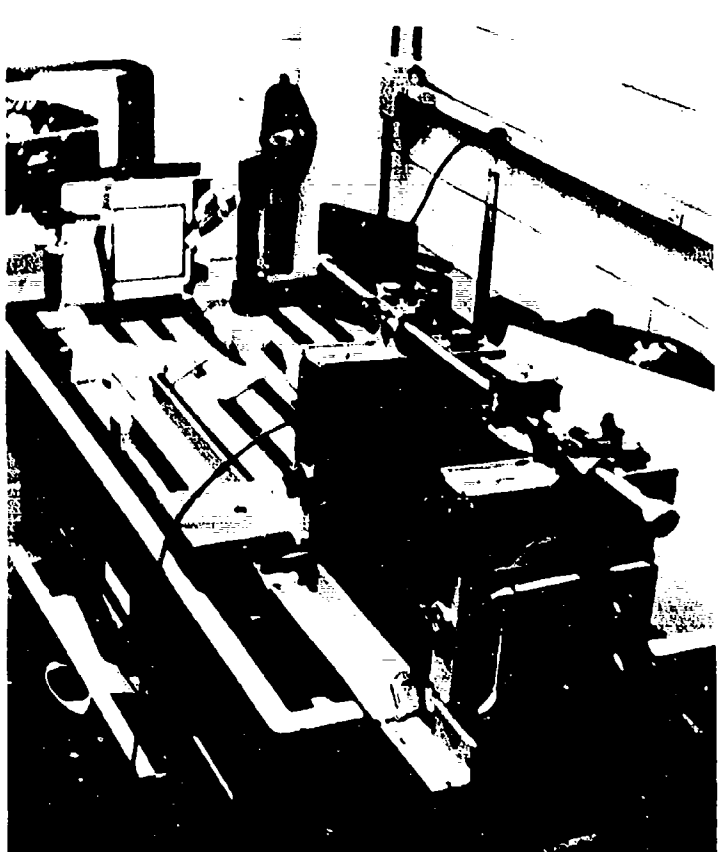

Figure 5.3. Photograph of apparatus for producing reduced submaster.

(b) 3/4 view.

Camera to subject grating distances were estimated by calculation and finalized by trial and error to give the sought-for submaster grating frequency on the photographic plate. Focus of the grating image is very critical in such a situation because of the extreme resolution and contrast required of the system. An ordinary camera ground glass is much too coarse and may not be exactly in the film plane. For this work, the ground glass was replaced by a developed and fixed unexposed film plate of the same types as were to be used in the photography. This focus plate was held in an ordinary 4x5 plate holder with the separator removed and the assembly placed in the camera back and carefully seated. All the plateholders which were used were checked to see that their critical dimensions were uniform. Critical focussing was accomplished with a handheld 50X magnifier obtained from Edmund Scientific Co. The magnifier was adjusted so that the emulsion of the focus plate was in focus when the magnifier was held against the back side of the plate. Image sharpness and parallax observations were both used as focus criteria, dye (magic marker) marks having been put into the emulsion of the focus plate for the purpose. In some cases, a previously produced contact copy of the grating was placed in the plateholder and the sharpness of the moire fringes produced on this plate was used as the focus indicator as well as an indicator of magnification.

In theory, it is best to use the maximum lens opening for greatest sharpness and resolution in such a demanding situation, and this was done for most of the grating copies. Vignetting and light falloff in the extremes of the field proved serious enough, however, that it was difficult to obtain a completely satisfactory exposure at maximum aperture. For this reason aperture settings of f11 and up to f16 were utilized for some of the copies. The slight softening of the grating was compensated by the more uniform illumination of the image. Some dodging was used in almost all the grating photography in this investigation to reduce gross gradiations in image density.

Monochromatic light is usually preferred for high-resolution photography such as this. Experiments along these lines showed image degradation because of the very long exposures with the illumination available, and this approach was abandoned. The Gorerz lens is an apochromatic type which is well-corrected for color, and white light proved best in this application.

Both Kodak High Resolution Plate (HRP) and Kodak 649-F Spectroscopic plate (often used for holography) were used for the photoreduced submasters. Grain effects were noticeable with the 649-F emulsion, but the gratings were sharp and of good contrast. Because of its higher speed, easy development and ready availability at the time, the 649-F material was used for about 90% of the submasters.

For the setup described, typical exposures were about 20-30 seconds at f9 for 649-F with a heavy 7-8 minute development in D-19. HRP exposures were about one minute, suggesting some reciprocity failure occurred at the illumination levels used.

Late in the course of the investigation, experiments were conducted to show that a slotted aperture technique devised by Forno[5-6] and Burch and Forno[5-7] could be extended to achieve improved photography of moire gratings. This improved technique is described in an Air Force Technical Report[5-8] and a technical paper.[5-9] One would expect that utilization of this slotted aperture photographic technique would yield superior reproductions of both master and specimen gratings.

Performance of the submaster gratings were checked by observing their diffraction efficiencies as they were produced. It is important to realize that both the gross transmittance and the diffraction performance of the submaster must be "complementary" to those characteristics of the specimen grating photographs in the optical data processing stage. For this reason, several different photoplates of each submaster spatial frequency were produced. Exposure and development times were varied in order to produce submasters having different properties. In general, the denser submasters proved more useful with the specimen photos subsequently produced.

To some extent, the variation of density over the extent of the submaster plate which resulted from $\cos^4$ light falloff proved useful in optical data processing. It tended to counteract the normal Gaussian distribution of light in the expanded laser beam to give a near-uniform field in the fringe photographs. This effect was exploited to the maximum.

3. SPECIMEN GRATINGS

3.1 Choice of Technique

The photoresist approach to creating gratings on the specimens was chosen because it is fairly simple, requires minimal special equipment, and offers the possibility of baking or etching the grating to make it resistant to damage. Given the severity of plastic deformation and the attendant rumpling of the specimen surface near the hole and the potential for mechanical damage to the specimen during the various stages of the experiment, the etching capability seemed important. Etching the grating also offers the possibility of examining the strain field underneath the flange end of the sleeve after sleeve withdrawal. A further potential is that the etched gratings could be used for studies at temperatures above which the photoresists vaporize or burn away. The etching capability was not needed within the eventual scope of this study, and so it was not pursued.

3.2 Photoresist and Its Application

Photoresists for moire applications have been studied and described in remarkable detail by Luxmoore, Holister and Hermann,[5-1,5-2,5-3] and their findings and techniques have been freely adapted and adopted for this coldworked hole investigation.

The photoresist chosen was Shipley AZ1350J provided by Shipley Co., Newton, Mass., 02.62, U.S.A. This particular resist is formulated for applying acid resist coatings to aluminum substrates, and its solids content is comparitively high at 30%. The companion dye, thinner, cleaner and developer were purchased with the resist.

It is desirable for moire work, as with most other photoresist usage, that the resist coating be thin and uniform. Common application methods include spinning, dipping, spraying, wiping, and roller coating. The dipping and wiping techniques were found deficient in that they always left some buildup and sagging near the hole boundary, that is, in the region of greatest interest. Attention settled, therefore, upon the spraying method. An artists' airbrush was obtained and a spraying technique which gave satisfactory uniformity and coating thickness was worked out by trial and error. Further refinement and simplification of this procedure are highly recommended if similar investigations are pursued at AFML. One definite conclusion of this research was that good specimen preparation and coating application simplify and shorten the moire analysis while yielding superior results.

In order that the photoresist wet the surface and spread to a uniform coating, it is essential that the specimen surface be chemically clean. Several different cleaning procedures were tried and all were found lacking in some small way. Part of the trouble might have originated with the material used in the final polishing stage. This possibility was not appreciated early enough for any definite action. Proper lapping should give a surface which is easier to clean.

The chemically neutral solvent "Neutra-Clean 68" provided by the Shipley Company did not work well in removing a surface film. The specimen appeared clean after initial solvent washing and then being immersed in heated Neutra-clean solution. However, bare patches tended to appear as the resist dried, indicating that the surface was not wetted in these areas.

A procedure almost exactly the same as the one which is commonly used for cleaning aluminum surfaces in preparation for the bonding of electrical resistance strain gages served quite well. Initial brisk solvent cleaning was followed by treatment with the two strain gage applications materials "M-Prep 1" and "M-Prep 2", which, evidently,

are weak solutions of phosphoric acid and sodium hydroxide, respectively. The specimen was rinsed in a spray of distilled water following this cleaning in order to assure the removal of any surface deposit of NaOH which would affect the resist. (Resist developers are essentially weak solutions of NaOH.)

Cleaning only with solvents was also utilized and worked well if care was taken. This approach was most useful for recleaning specimens after removal of a faulty sprayed resist coating. In practice, the specimen was rough cleaned by immersion in a dish of methyl ketone or acetone. The surface was rubbed with cotton while immersed in the solvent. This process was repeated with fresh solvent, after which the specimen was rinsed in a heavy spray of fresh acetone. The surface was allowed to dry and then washed in a heavy spray of distilled water, rubbed lightly with clean cotton while wet, and rinsed again in water. Finally, the wet specimens were rinsed in a copious spray of fresh reagent grade anhydrous methyl alcohol and allowed to air dry. This whole procedure was quickly, and easily completed, and the specimen was dry for coating very soon. Furthermore, the specimen is left slightly chilled which helped retard drying of the sprayed photoresist until it had had a chance to smooth and flatten. Shipley photoresist thinner was substituted for the acetone on occasion, and it seemed satisfactory. It is also easier to handle.

It is noteworthy that cleaning subsequent to removal of a poorly sprayed coating preparatory to recoating did not need to be very well done unless the poor coating resulted from initial poor cleaning. If it had been cleaned properly the first time, a few treatments with thinner and wiping tissue was adequate for subsequent cleaning. This peculiarity probably derives from the basic compatibility of the thinner, old resist residue, and new resist.

One point deserves special emphasis. It was imperative that no thinner, solvent, moisture, or dirt be left inside the hole near the corner joining the surface to be coated. If contamination was present, distortion of the coating in the form of thinning

or buildup at the hole boundary could occur. A workable technique was to clean the hole with a swab at each washing stage and to be certain that the hole was well rinsed in the final stages of cleaning.

It was permissable to eliminate the final washing in methyl alcohol and rely on flushing with distilled water for the final cleaning. In this case, drying of the specimen was carefully done in a laboratory oven, after which the specimen was cooled in a dessicator.

Testing was conducted to establish a balance of resist-thinner-dye proportions, air pressure, airbrush nozzle opening, spraying distance, and brush motion. The values arrived at represent a workable combination, but probably not the best one.

In order to produce coatings as thin as at first seemed necessary (later, thicker coatings were found better for certain situations), the photoresist required thinning considerably in excess of the degree suggested by the manufacturer. The proportions arrived at through trial were, by volume, 30 parts AZ1350J, 20 parts AZ thinner and 1 part dye. Best air pressure was about 40 psi, and it was very important that the air be dried and the pressure regulated. The "canned air" sold in art supply shops was unsatisfactory. The best nozzle setting for the airbrush used was between 1½ to 2 full turns open from the closed position.

The spraying procedure which was developed called for laying the clean and dry specimen horizontally or inclined at about 10°. The airbrush containing the resist was held about 18 inches (45 cm) from the specimen and pointing to one side of it. Flow of the atomized resist was begun and allowed to stabilize for about ½ to 1 second, after which the spray is quickly shifted onto the specimen. At the range and the air flow used, coverage was wide enough so that it was not necessary to sweep the brush; although small oscillations seemed to aid in giving good covereage while helping the settle the operator's nerves. This procedure eliminated problems connected with trying to overlap airbrush strokes. Another acceptable technique

involved holding the brush about 6 inches from the specimen with about 25 psi pressure and covering the specimen with about 3 sweeping strokes, starting closest to the operator. An overlap of 1/3 to 1/2 the fan width was used. This method gave coatings which looked good, but proved to have some large-scale thickness variations. With either approach, it was absolutely necessary to start the spray well before bringing it to beam on the specimen, as some coarse droplets are expelled at the beginning of flow.

Coating thickness was controlled by spraying time once the nozzle opening was set. The thinnest coatings used in this study (specimens C9 and C10) had coatings about 0.0001 inches (2 to 3 microns) thick, which resulted from about 3 seconds spraying time. Such a thick coating does not stay wet long enough for surface tension to have much effect, so some fine stipple in the coating was visible. Also, surface character of the specimen (the grain caused by polishing) tended to affect photographability of the grating with such thin coatings. Better grating photographs were obtained with coatings which were in the area of 0.0005 inches (13 microns) thick.

If the coating did not appear satisfactory at this point, it was removed using either thinner or acetone and recleaned by the abbreviated procedure described above. When dry, it was sprayed again. Five or six trials were sometimes required to obtain a coating which seemed adequate. Often, a bad result was traceable to poor cleaning or some other obvious source.

Because of the volatile and mildly toxic nature of the solvents and cleaners employed (with the exception of "Neutra-Clean"), all the cleaning and coating procedures were conducted in a laboratory fume hood.

After the coatings dried to touch, a process requiring only a minute or so, they were placed in a small laboratory oven for drying at a temperature of about 25C for 20-30 minutes.

The coated specimens were then placed inside padded light-tight boxes to await exposure and development of the grating image.

3.3 Printing Grating onto Specimen

The moire grating was printed into the photoresist coating on the specimen by a simple contact printing procedure in which a grating submaster was clamped to the specimen and the assembly exposed to ultraviolet light from a Mercury lamp. The procedure closely followed that described by Luxmoore, et. al.[5-1,5-2] except that a much smaller lamp was used and several improvisions were necessary. Additional useful information on producing fine periodic structures is contained in the recent paper by Austin and Stone.[5-10]

Clamping of the submaster to the specimen was accomplished with orinary spring-type clothespins; two of the clothespins also acted as legs to support the grating-specimen assembly in a vertical plane. Lenticular effects in the submaster were reduced by using a 50% aqueous glycerin solution between the submaster emulsion and the photoresist. Later, it was found that the fluid could be eliminated, probably because lenticulation of the thin submaster emulsion was not great and/or the data processing procedure was forgiving of poor gratings.

The Mercury lamp was one contained in a "Visicorder" optical strip chart recorder. This lamp has a power of only 100 watts, but its arc is so small (½ mm x ½ mm) that it was possible to bring the specimen to within 5½ inches of the lamp without losing resolution or changing the grating pitch. Still, exposures of about 6 minutes were required with the thicker coatings and fairly dense submasters used With the thinner coating on specimens C9 and C10, and with the less dense and sharper submasters available then, exposures shortened to about 3 minutes. The newly exposed photoresist was developed according to manufacturer's instructions in the standard Shipley AZ developer diluted with water.

A variation of the procedure was used with specimen C10, as both radial and tangential strains were to be measured throughout the field. A two-dimensional grid pattern of dots (as contrasted with the usual array of continuous parallel lines) was created by a two step exposure. The submaster was arranged as usual for a two minute exposure, and then rotated 90°, reclamped and the resist exposed for another 2 minutes.

One aspect of the behavior of photoresist deserves further comment. It is possible to balance exposure time and coating thickness to produce specimen gratings which will photograph more sharply than those one ordinarily thinks of as "good" gratings. The phenomenon utilized is that incomplete exposure and development leaves "debris" between the unexposed grating lines.[5-1] Figure 5.4 illustrates varying degrees of this behavior. It turns out that the debris tends to scatter and absorb the incident light, giving high contrast dark lines against the smooth unexposed lines. It seems wiser, therefore, to use a thick coating (½ to 1 mil) and not try to cut through to base metal in the exposure and development. This conclusion may not apply if more uniform surfaces are produced, especially if the finish has a matte structure from lapping.

The green dye used in the photoresist was useful only in indicating coating uniformity and in checking the exposure. It bleached rapidly when exposed to the light required for grating photography. It could be eliminated without ill effect.

4. PHOTOGRAPHING SPECIMEN GRATING

4.1 Comments on Method

This section of the report describes the procedure for photographing the photoresist specimen grating. While the description is quite complete, useful additional information is contained in a Technical Report[5-8,5-9] which describes improvements in the technique.

As mentioned in Section III, the presence of out-of-plane displacement and the protrusion of the sleeve from the surface precluded direct superposition of specimen grating and master or submaster grating to create the moire fringe pattern. Some form of optical superposition was called for.

In general, there are two ways of performing an optical superposition of gratings; and there are several variations of each of the basic approaches. In the first method,

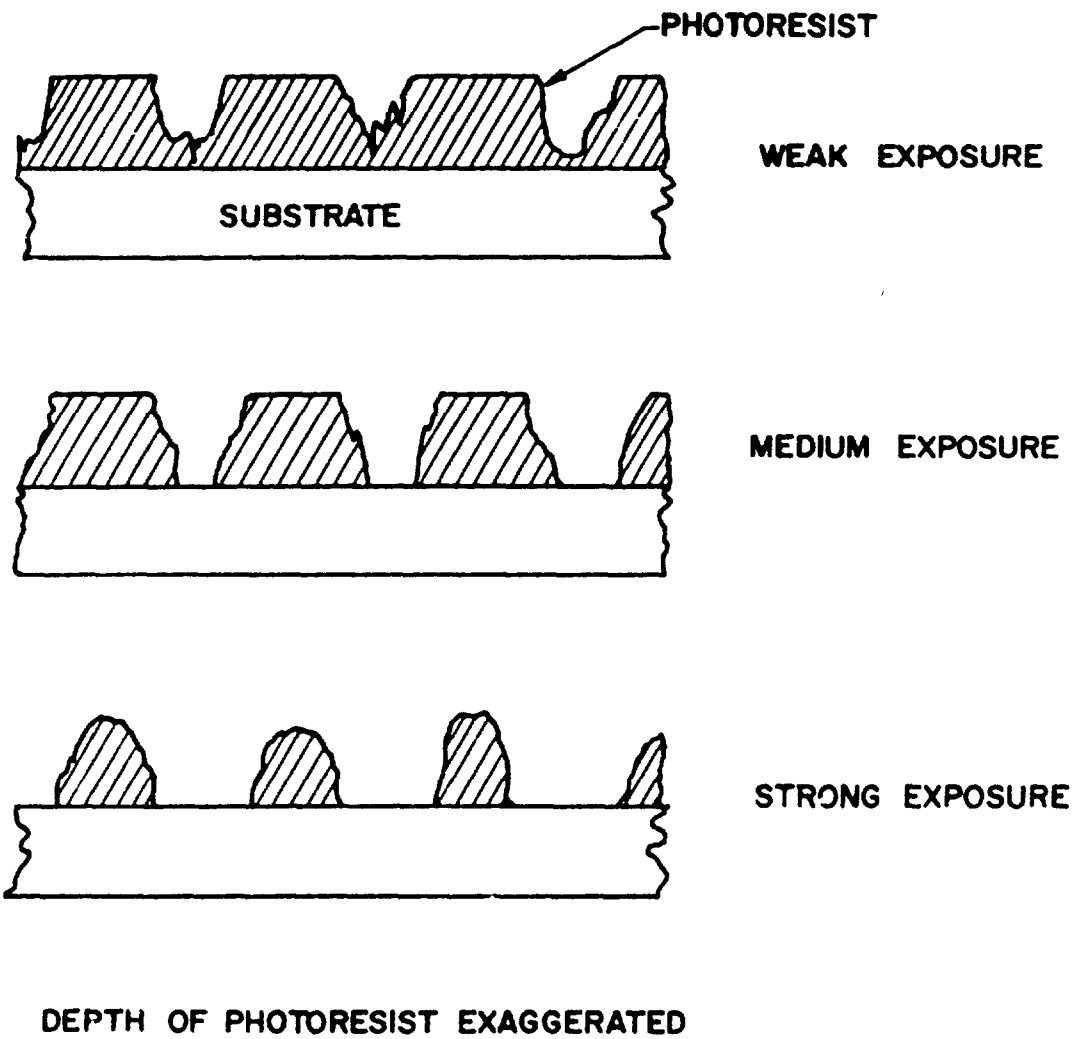

Figure 5.4. Sketches of typical cross sections of specimen grating in photoresist for various degrees of exposure.

the superposition is in real time. That is, the specimen grating is imaged by a lens and/or partial mirror system onto the master grating or its image. The resulting fringe pattern is photographed after appropriate adjustment of alignment and mismatch of the two grating images. This technique is simple in concept, but it is not so simple to use. It was tried and found wanting in fringe contrast and stability with the equipment available. Proper utilization of the slotted aperture technique referred to above[5-8,5-9] might have made this approach more attractive. However, the flexibility and control offered by the second method were a distinct advantage in this study.

In the second method, which was used exclusively, the specimen grating is photographed in one or more states, and the superposition carried out later with these gratings which have been stored on glass photo plates. It is possible to photograph the specimen in its virgin and strained states and to superimpose these two gratings. A procedure which is more flexible and more powerful is to utilize the potentials of coherent optical data processing by superimposing the specimen grating plates in turn with previously prepared submaster gratings of various spatial frequencies. Sensitivity of the measurement process can be multiplied several fold in this way, and the benefits of grating pitch mismatch may be exploited. Although it would be most usual to use the unstrained specimen grating photograph for constructing a baseline moire pattern, it is possible to use other specimen conditions as the baseline, thereby examining through the moire process the change between any two specimen states. Finally, this moire process may be undertaken in a leisurely and thoughtful way, without the hurry which attends real-time interferometry, and the original data is retrievable for further study since it is permanently stored on glass plates.

There is a price to be paid for these advantages. First there are the added complications in theory and in laboratory exercise. There is the time required to create and study twice as many fringe photos (baseline and data). Finally, there is

the critical problem of photographing the specimen grating with enough resolution and contrast so that the potentials of the optical data processing are exploited to full gain.

The technique described for the grating photography are discussed in the next section. The optical data processing of the grating photographs to form moire patterns is described in Section VI.

4.2 Grating Photography

Several different setups for accomplishing the high resolution photography of the specimen grating were tried. The best results came from the arrangement which is sketched in Figure 5.5. The apparatus used was very similar to that shown in the photographs of Figure 5.3, so additional photos are not included here. Useful descriptive data which supplements the following description are contained in Section V.2.3 of this report and also in the references cited above.[5-8,5-9]

The camera used was a 4x5 Burke and James "Orbit" monorail which was stiffened with angle iron and weighted with lead blocks and some steel plate. The lens was a Goerz Red Dot Artar apochromat having focal length of 9½ inches (2.4 cm) and maximum aperture f9. The camera was set at full extension to give an image of the specimen which was magnified by a factor of about 1.3. The specimen in its specially designed holder, the illuminating souce--a Kodak Carousel Slide projector--and the camera rested upon a Gaertner Optical table which rested upon air bags for vibration isolation.

Focus of the specimen image was very critical in this high resolution situation. The ground glass of the camera was not satisfactory for this critical work because it was too coarse and because such focus plates are often not exactly in the photo-emulsion plane. For focussing, a blank plate of the thickness and type used in the photography was developed and fixed and mounted in a 4x5 plateholder which had the separator removed. The image of the specimen in the emulsion was examined with a 50X

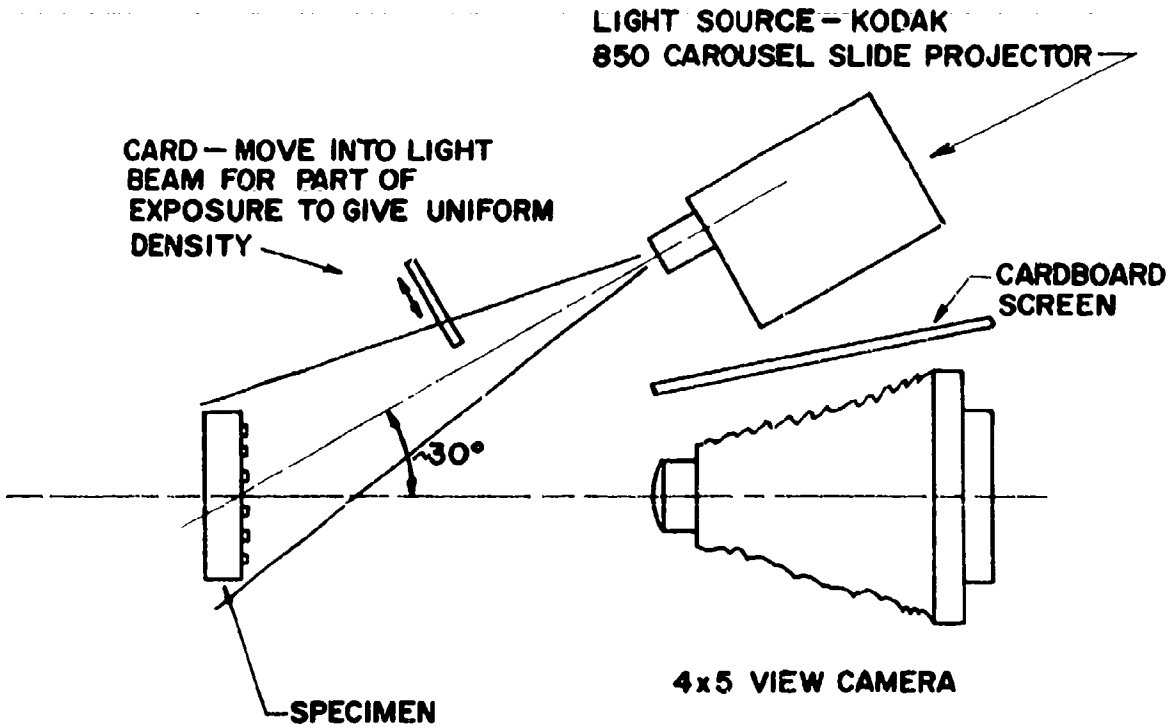

Figure 5.5. Sketch of apparatus for photographing specimen grating.

magnifier obtained from Edmund Scientific Co. which had been adjusted to focus in the emulsion plane while the magnifier base rested on the opposite of the film plate. The image of the specimen grating could be checked over the whole area of interest for maximum sharpness and contrast. As a check on focus, parallax between the grating image and marks (scratches and magic marker lines) were studied. Zero parallax meant correct focus. This focus procedure was rather tedious, but it did not need to be repeated as long as the photographic system was not distrubed.

Although a monochromatic filter is usually specified for this type of high resolution photography, it did not prove practicable here. Available light was so low that contrast and definition were lost with filtered light and the films used. White light gave better results. The Goerz lens, which is a four element symmetrical apochromat, is well corrected for transverse and longitudinal chromatic aberrations. A small amount of lateral color was noticed at the extreme edge of the focus plate when examined with the magnifier, but the aberration was far from large enough to affect definition on the grating photos.

Both Kodak High Resolution plate and backed Kodak Spectroscopic 649-F plates were utilized. The HRP material proved somewhat too slow for the illumination available, so most of this work was done with 649-F. The glass photoplates were placed in regular 4x5 plateholders which had been checked for matching critical dimensions. Exposures typically were about 20 to 30 seconds at f11 with these plates, although it depended to a degree upon the nature of the specimen surface and the thickness, expsoure, and development of the specimen photoresist coating.

The lens was used mostly at apertures of f9 and f11. Higher f-numbers gave reduced light fall-off and exposure reduction in the extremes of the field. But, the frequency response of the lens was below the limit required for photography of the 1000 lpi grating at apertures approaching f16. The lower f-numbers had to be used for proper resolution and the exposure adjusted for the best compromise over the area of interest. Dodging was utilized to even up the unequal exposure of the plate

caused by the oblique illumination. Typically, the light falling on the most brightly illuminated portion of the specimen was blocked up to about 25% of the total exposure time. Dodging was accomplished by moving a card into the light beam from the slide projector.

Exposure determination was largely by trial and error. Minor correction was possible during plate development. Crude measurements of light intensities at the camera back were obtained with an ordinary light meter. Much time and film would be saved if a sensitive photometer probe was obtained for measuring light level at the film plane during focus. It would help in adjusting illumination and in calculating exposure.

It is worth noting here that the angle of incident illumination was chosen by trial to give the best contrast in the grating image. Shadows in the three-dimensional grating structure eveidently play an important role in visibility of the grating.

The exposed 649-F plates were individually developed in Kodak D-8 developer for about 3 minutes. (See Ref. 5.11 for additional information.) D-8 is an energetic high-contrast developer. The development was monitored by very short examination under red safelight; 649-F is red sensitive. Development was stopped when plate density reached about 50%, the value which seemed to give best fringe visibility in the optical data processor. The HRP plates were developed by similar techniques in Kodak HRP developer diluted according to instructions.[5-12,5-13] Fixing, washing, and drying were normal for both types.

Considerable trouble was experienced with the polishing marks on some specimens. The brightness of any portion of the image depended very much upon the direction of the polishing marks in relation to the illumination beam. Large specimen size had made it impossible to polish the whole specimen at once, and, as a result, polishing "grain" ran in different directions in different areas. The photography problem was

most serious where thin coatings were applied over a surface having extensive surface marking. In specimens C9 and C10, for example, it was not possible to photograph the grating over the whole area of interest at one time. The specimen had to be rotated 180° in its plane and a second photograph made. This was necessary for both baseline and data photographs. Also, the specimen had to be tilted 45° in its plane to the plane of the optical axis to image with maximum clarity the regions of interest. Even so, the resulting grating photos and the eventual fringe photography were of marginal quality. A more uniform surface structure, as would result from lapping the specimens, should eliminate this problem.

In most of the other specimens, the photography of the strained grating had to be duplicated with 180° in-plane rotation for quite another reason. Under the oblique illumination required for contrast, the protruding end of the sleeve caused a shadow in the important area near the hole, and moire data as close as possible on both sides of the hole was sought.

After completion, each grating plate was inspected for diffraction efficiency to assure that the photography had been successful. It was then labelled with the specimen number and a photograph number which matched a detailed entry in the laboratory log book. It was (and is) possible, therefore, to identify any one of the large number of grating photographs at a future time and to obtain complete knowledge of its history. The plates were then stored in racks to await optical construction of moire fringe patterns.

SECTION VI

CREATION OF MOIRE GRATING PHOTOGRAPHS

1. INTRODUCTION

Although useful moire fringe patterns can be obtained by direct superposition of the grating photographs with one another or with a submaster grating, such a simple procedure does not yield the best results, nor does it exploit the full potential of the information which is stored in a photoplate. Increased sensitivity and control of the measurement process can be had by utilizing some of the basic procedures of optical data processing.

There are two related physical phenomena which are important in developing an understanding of moire fringe formation and multiplication by superimposing grating photographs in a coherent optical analyzer. The first of these phenomena is the diffraction of light by a grating, or, more accurately, by superimposed pairs of gratings having slightly different spatial frequencies, and the related phenomenon of multiple beam interference patterns produced in the diffraction orders. The second important concept is that a simple lens acts as a Fourier transformer or spectrum analyzer and offers the possibility of performing filtering operations on space frequency components in a manner analogous to the treatment of vibration and electrical signals. Actually, either concept is sufficient by itself for understanding moire phenomena from slight different points of view.

A detailed explanation and discussion of Fourier optics and diffraction phenomena are outside the scope of this report. Only the basic concepts are presented in the next section. Application of these principals to the specific measurement problem at hand are then described.

2. IMPORTANT BASIC CONCEPTS

2.1 Diffraction by Superimposed Gratings

The theory of moire fringe formation by superimposing two diffraction gratings of nearly equal pitch and orientation has been presented in elegant detail in a book by Guild[6-1] His ideas were extended, refined, and demonstrated within the context of moire strain analysis in a series of definitive papers by Post[6-2,6-3,6-4] and by Post and McLaughlin.[6-5] The following short discussion draws heavily from Post's fine explanations.

If a single narrow beam of light is made to pass normally (normal incidence is chosen for simplicity, oblique incidence may be used) through (or reflect from) a sinusoidal amplitude or phase grating, the beam will be divided into 3 parts at the grating. Figure 6.1 shows this behavior schematically. The first part, called the zero order, is an undisturbed portion of the beam which passes directly through the grating. The other two parts, called first orders, deviate symmetrically on either side of the zero order at an inclination which depends upon the spatial frequency of the grating and the wavelength of light as well as the incidence angle, which has been taken to be zero for this discussion.

Now, consider what happens when a narrow collimated beam passes through 2 sinusoidal gratings of slightly different spatial frequencies, as illustrated in Figure 6.2. Five distinct ray groups will appear in this case. The center group is a single attenuated version of the incident beam. The extreme orders, shown as +2 and -2 on the sketch each contain a single ray which has been diffracted by each of the two gratings in succession. The intermediate ray groups numbered +1 and -1 are the ones of interest in moire work. They each contain 2 rays, one of which has been diffracted at the first grating only, and the second having been diffracted at the second grating. These two rays in the group are nearly parallel because the spatial frequencies of the two gratings are nearly equal. Now, if the two rays can be made

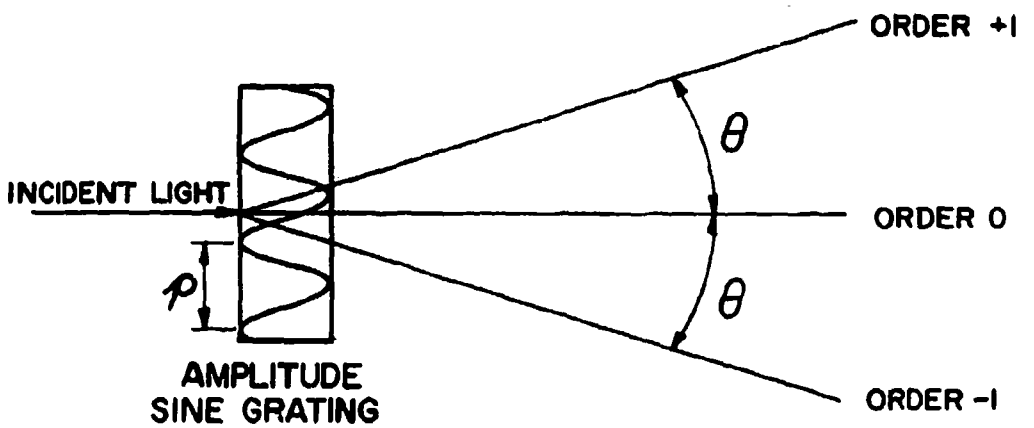

ρ = GRATING PERIOD OR PITCH

f = GRATING SPATIAL FREQUENCY = $1/\rho$

λ = WAVELENGTH OF LIGHT

T = TRANSMITTANCE OF GRATING

$T = T_o(1 - K \sin 2\pi X/\rho)$

$= T_o(1 - K \sin 2\pi f)$

$\theta = \arcsin \lambda/\rho$

Figure 6.1. Diffraction of narrow collimated light beam by sine grating.

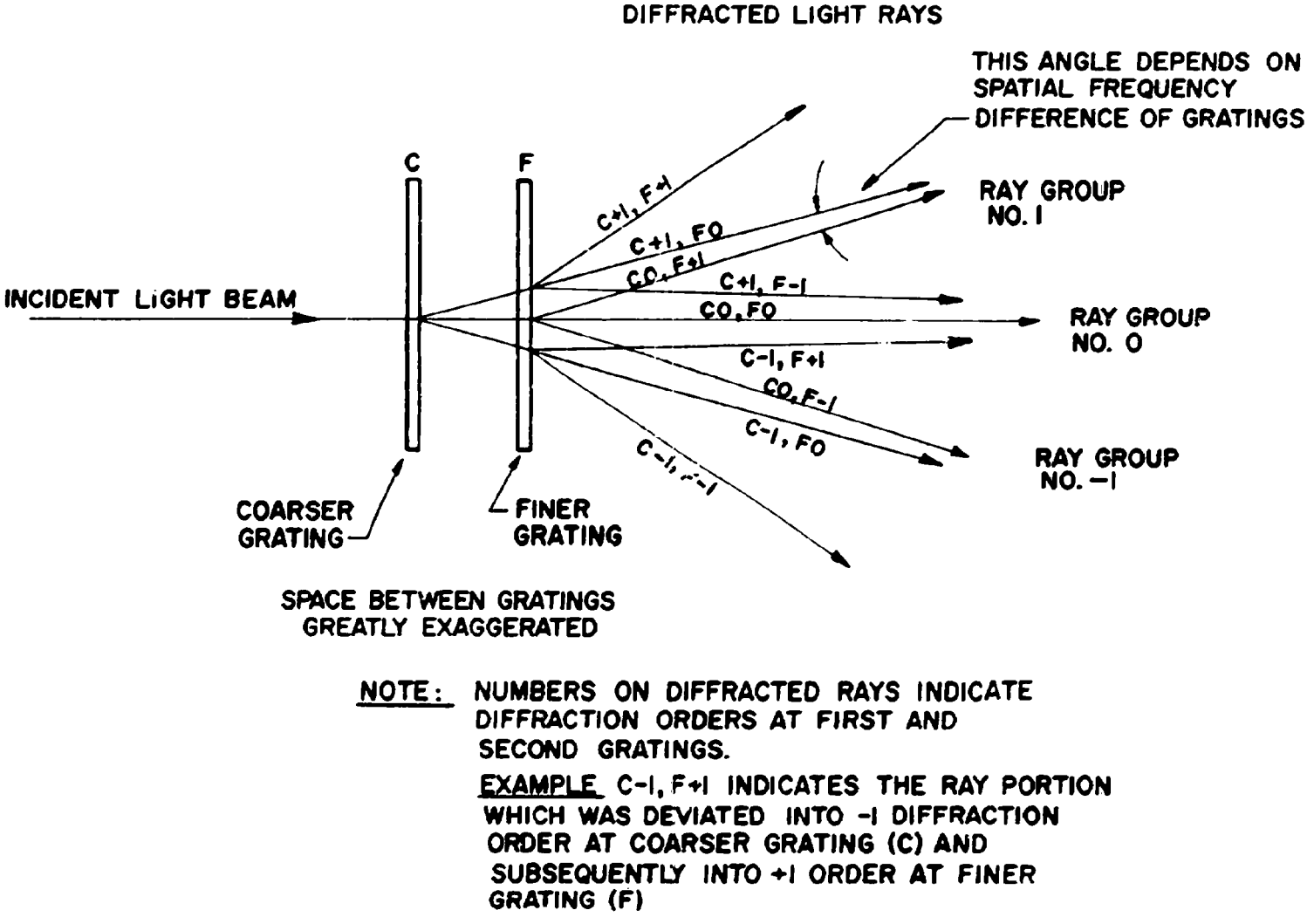

NOTE: NUMBERS ON DIFFRACTED RAYS INDICATE DIFFRACTION ORDERS AT FIRST AND SECOND GRATINGS.

EXAMPLE C-1, F+1 INDICATES THE RAY PORTION WHICH WAS DEVIATED INTO -1 DIFFRACTION ORDER AT COARSER GRATING (C) AND SUBSEQUENTLY INTO +1 ORDER AT FINER GRATING (F)

Figure 6.2. Diffraction of light by two superimposed sine gratings having slightly different spatial frequencies.

to overlap, as by a lens or imaging system, and if they both came from the same light source which has a coherence length great enough for interference to be possible, then the two rays forming a group will interfere with one another. (see Figure 6.3) The interference is that of two coherent beams impinging on a surface with a small difference of incidence angle. It is a classic example of two-beam interferometry. For a given wavelength of light, the small angular difference between the two beams is a measure of the spatial frequency difference between the two gratings. The interference fringe pattern is a function of the angular difference. The result is an interference pattern indicative of pitch and orientational differences of the two diffraction gratings. In short, it is the moire pattern of the two gratings for the area subtended by the incident beam.

For moire strain measurement, it is necessary to illuminate the whole field of the two gratings by coherent collimated (usually) light. In this case, there will be a whole field of rays being diffracted by the first grating, and a second field diffracted by the second grating, as pictured in Figure 6.4. A field lens is placed in the diffracted beams to decollimate the rays and converge them at a focus. In general, the rays diffracted at the first grating will focus at a point slightly displaced from the focus of the rays diffracted at the second grating. If they are close enough to overlap, then an interference pattern is produced. A more useful procedure is to use another lens and screen (that is, a camera) to construct images of the two grating fields with the light contained in the ray group. Essentially, two images are constructed which lie atop one another. Since coherent light was used, the two images interfere with one another, the degree of interference depending mainly upon the relative displacement of the two focal spots which, in turn, depend upon the relative inclinations of the two sets of rays coming from the diffraction gratings. The image in the camera displays, then, a pattern of interference fringes which are indicative of the local spatial frequency and orientational differences between the two gratings.

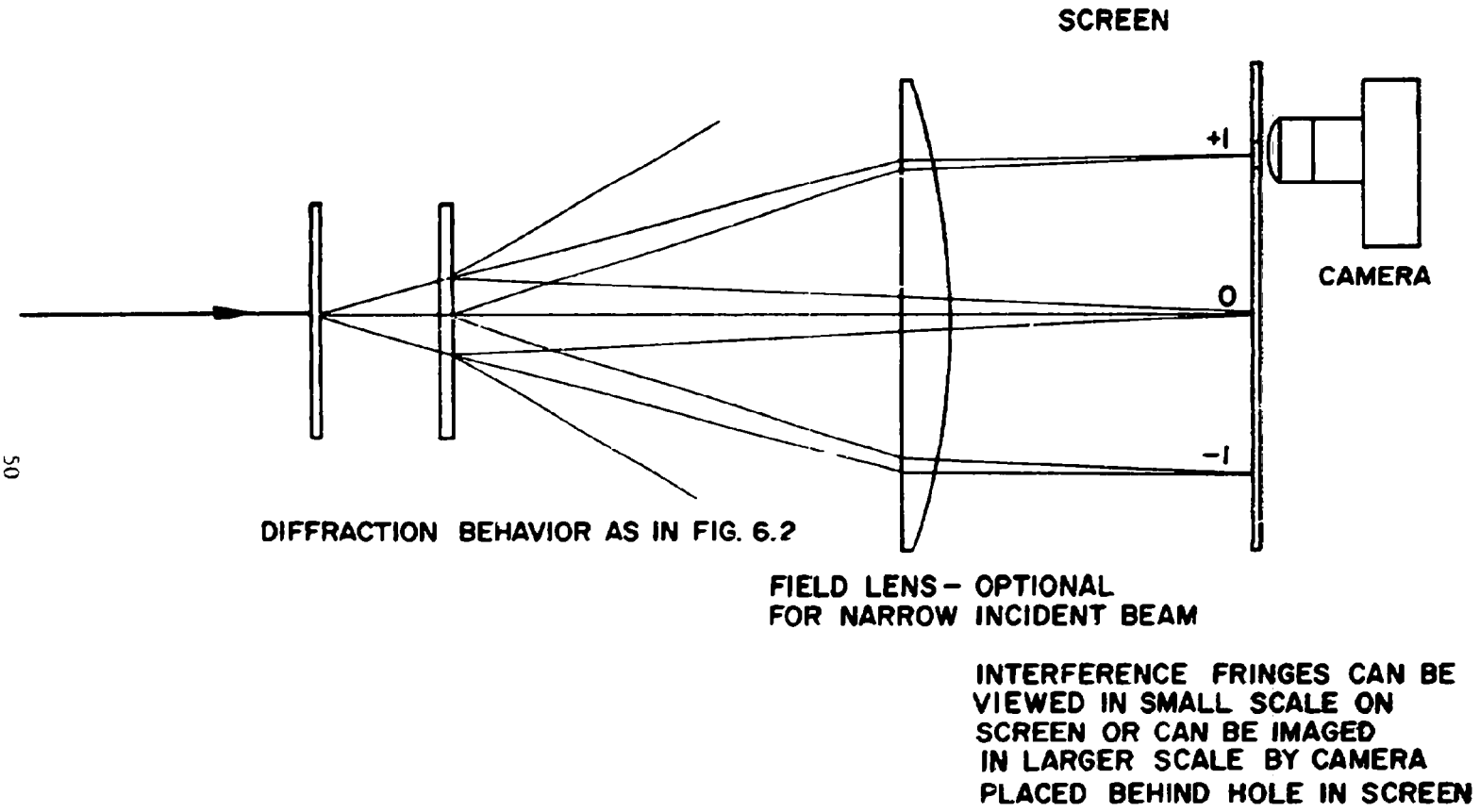

Figure 6.3. Formation of two-beam interference fringe pattern by light diffracted through 2 sine gratings having slightly different spatial frequencies.

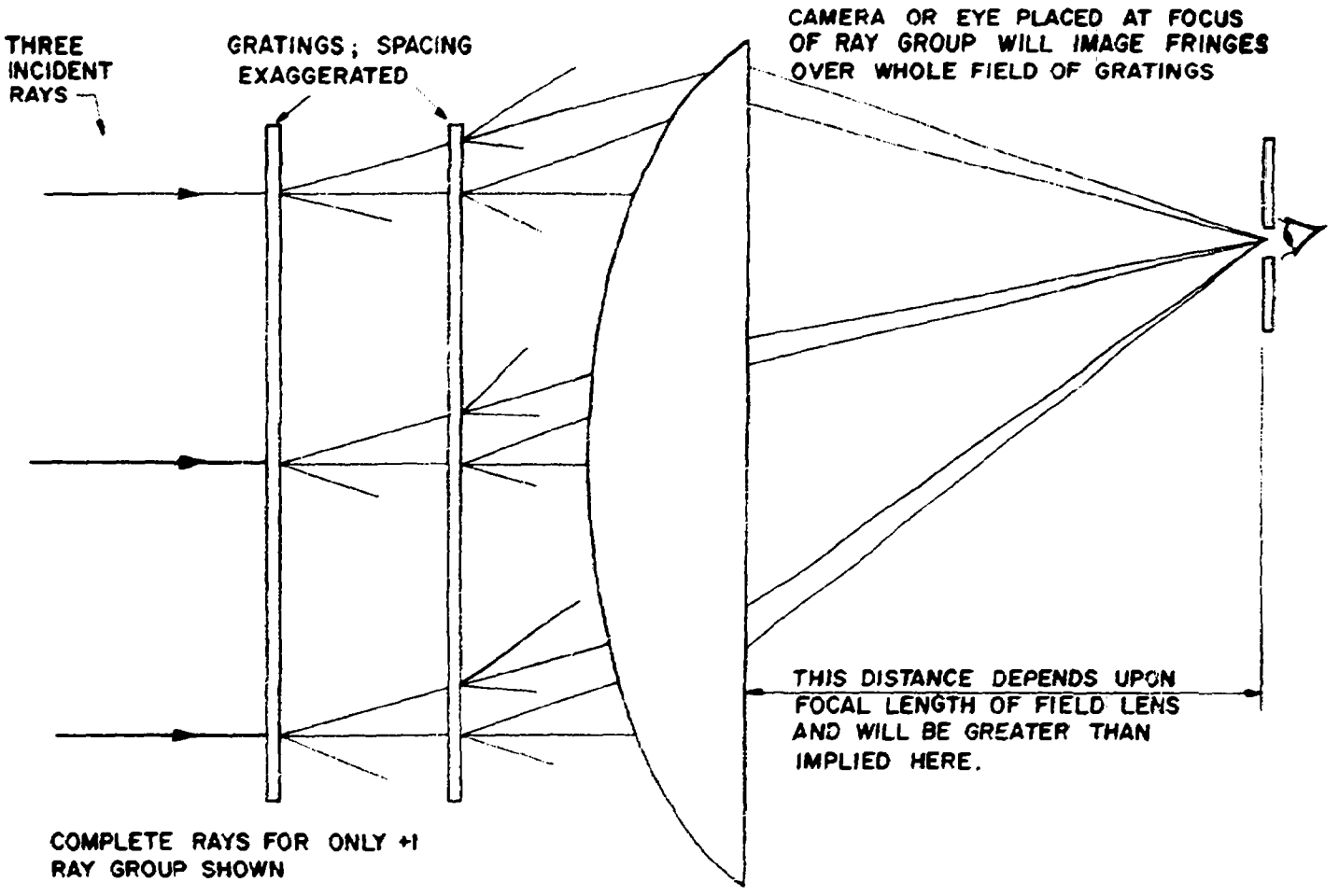

Figure 6.4. Diffraction of wide collimated beam by two sine gratings to form whole-field interference pattern.

Only minor extensions of these basic ideas suffice to understand the use of moire gratings in practical measurement situations.

The first complication is that the gratings tend to vary in pitch and orientation from point to point in any strain field of practical interest. One need only apply the reasoning outlined above to each elemental area of the whole field. The result, clearly, is a set of fringes which vary in direction and spacing from point to point in the field.

The second complication is more difficult to analyze. In general it is neither wise nor possible to work with sinusoidal gratings. There will exist, therefore, higher order diffractions at each of the two gratings. The number of orders produced from a single ray by each grating depends mainly upon the sharpness of the grating or the degree to which it approaches a rectangular wave periodic structure. One finds in such a situation that each group of near-parallel rays consists of several individual rays corresponding to different orders of diffraction at each grating. Figure 6.5 illustrates this behavior. Guild and Post, in the references cited above, consider these more complex cases in considerable detail. For this work it is sufficient to observe that the basic diffraction and interference model still applies. In general the interference at the image will involve more than two component images or beams. In practice, the higher order diffractions were attenuated to the point where only the basic two beams in each ray group were of any consequence.

There is one important related fact which holds true if the two gratings are of nearly the same spatial frequency. Each ray group in this case corresponds to a higher diffraction order which corresponds in turn to a grating frequency which is a multiple of the basic grating frequency. The image formed by any ray group contains a moire pattern corresponding to grating frequencies equal to the diffraction order or group number times the fundamental specimen grating frequency. This concept is the basis of multiplying the moire sensitivity when the two gratings must be of

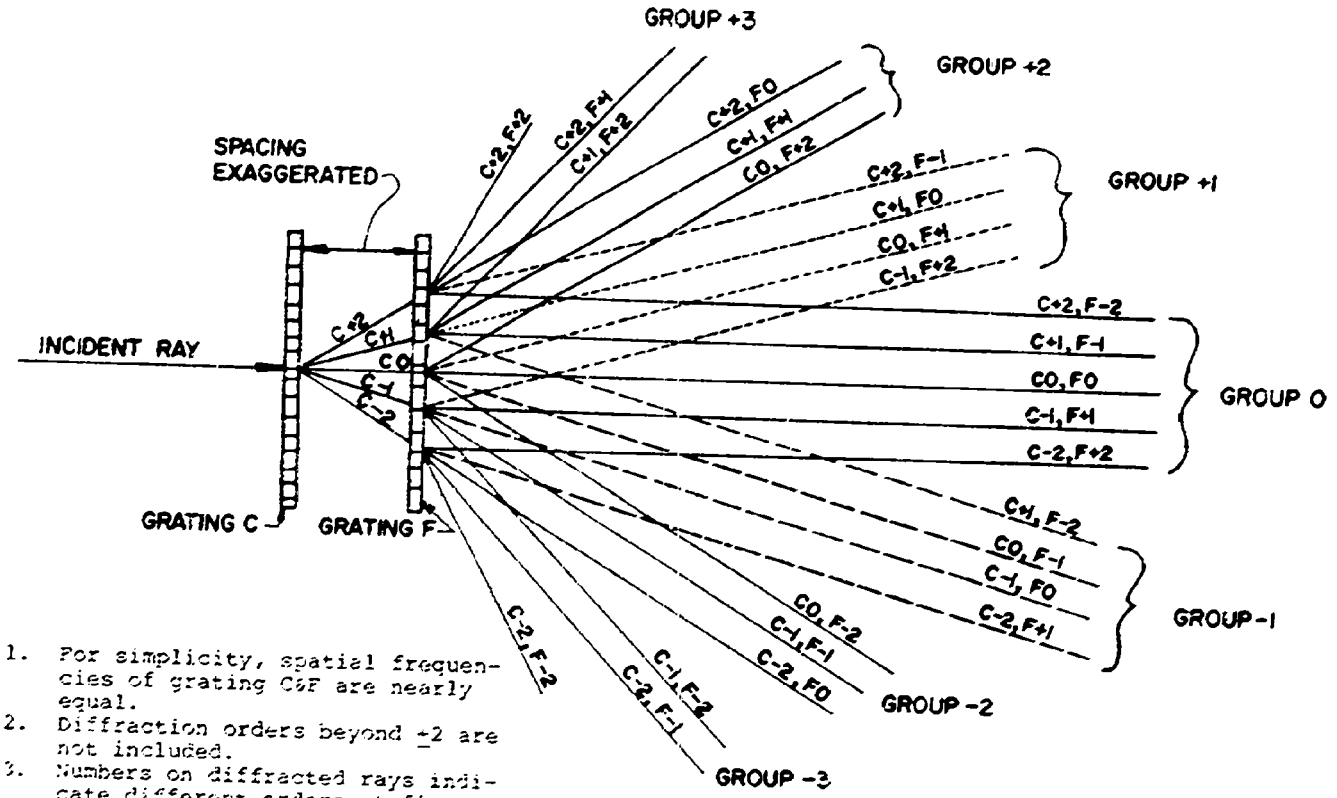

1. For simplicity, spatial frequencies of grating C&F are nearly equal.
2. Diffraction orders beyond ±2 are not included.
3. Numbers on diffracted rays indicate different orders at first and second gratings. E.g. C+2, F-1 means ray portion deviated into +2 order at grating C and then into -1 order at grating F.

Figure 6.5. Diffraction of narrow beam by two bar and space gratings to form ray groups containing higher diffraction orders.

the same base pitch. All one need do is use the light in one of the higher order ray groups to form the image and its fringe pattern. Such a multiplication technique was not utilized in this investigation, but others have used it to obtain sensitivity increases of ten-fold or more (see Ref. 6-2 for example).

A third and very important extension of the basic concepts arises when the gratings are grossly different in spatial frequency--that is, when one grating frequency is a multiple of the other plus a small additional which might be imposed deliberately and/or be the quantity which is to be determined. In such a situation, the diffractions are somewhat more complicated, as is the makeup of each of the diffracted ray groups. Figure 6.6 illustrates what happens where the second grating frequency is three times the frequency of the first. The basic idea of forming an interference pattern with the rays forming a given group still applies; the question arises as to what such an interference pattern means in terms of the frequency and orientation differences between the two gratings. A general interpretation can be very complicated. An important simplification is that, by design and because of the natural attenuation of high diffraction orders, only two of the component rays in any useful ray group will interact to form a visible fringe pattern. Examination of the two main components in, for example, ray group number 3 in the case pictured in Figure 6.6 produces the answer to the interpretation question. These two rays correspond to the first diffraction order at the fine grating and the third order at the coarse grating. The image formed with these two groups will be the same as that which would be produced by two gratings having nearly equal frequencies at three times the fundamental frequency of the coarse grating. The moire interference fringes in the image will correspond to one which would be produced by two fine gratings. This conclusion is easily supported by careful theoretical analysis. The effects of the remaining beams will be to increase the background noise in the fringe pattern, perhaps to the point of obscuring the moire fringes.

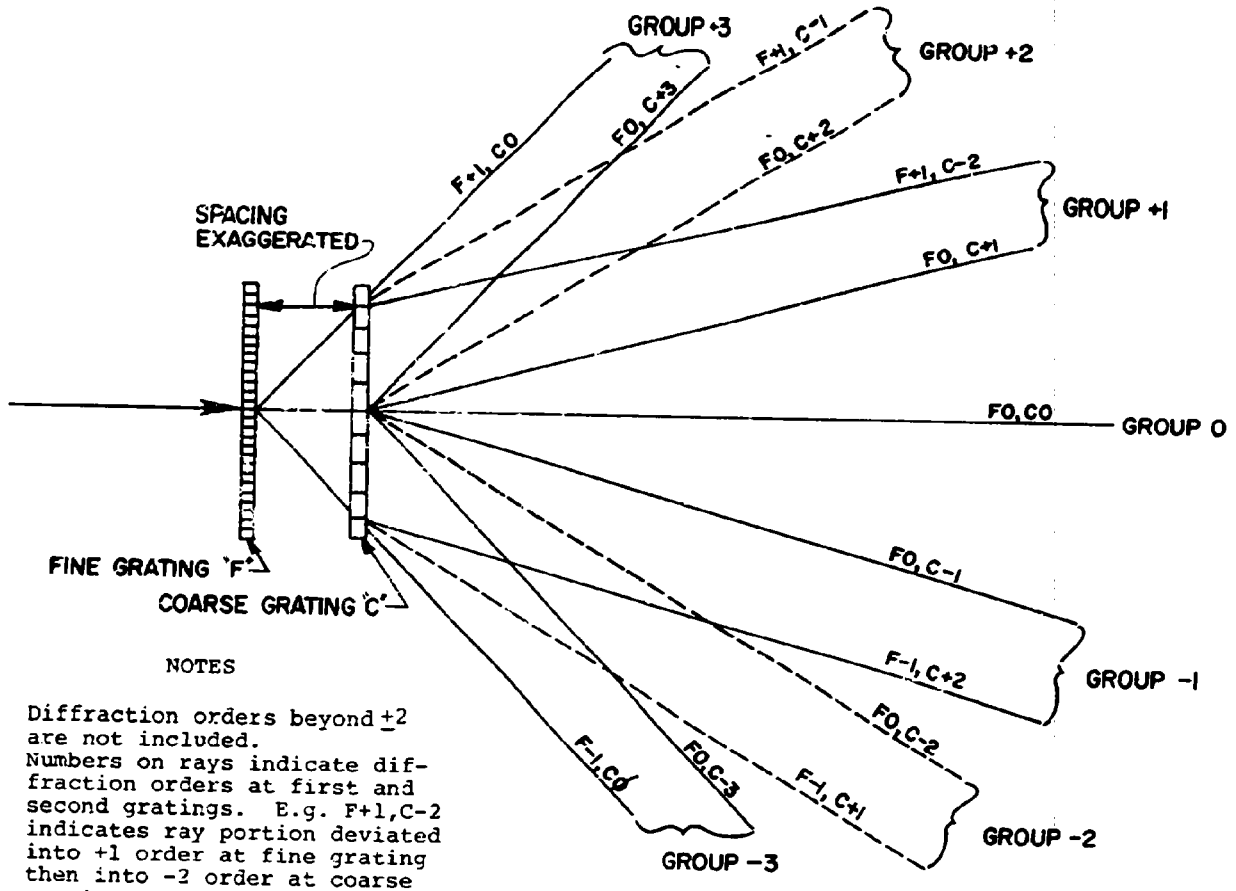

NOTES

1. Diffraction orders beyond ±2 are not included.
2. Numbers on rays indicate diffraction orders at first and second gratings. E.g. F+1,C-2 indicates ray portion deviated into +1 order at fine grating then into -2 order at coarse grating.
3. Diffraction angles shown larger than encountered in practice.

Figure 6.6. Diffraction by two superimposed gratings, one having spatial frequency three times that of the other.

A striking feature of the situation just discussed is that the moire fringe patterns in the camera image are identical, except for background noise and overall brightness, no matter which ray group is used to form the image. It is possible, and good practice, to utilize whichever group gives the best fringe visibility without further worry about the meaning of the fringes. Stated another way, the sensitivity is not increased by going to a higher diffraction order as is the case when two similar gratings are superimposed.

It is this case where one grating frequency is an integral multiple of the other that has such striking implications for moire measurement of the type used in this study. It allows the use of a coarse specimen grating which is easily applied and photographed. When superimposed with a finer grating, there appears a moire fringe pattern which is the same as that which would be created by two fine gratings. That is, a coarse specimen grating gives a measurement sensitivity which is equivalent to that of a much finer grating. Post[6-3] and others have obtained sensitivity multiplications of 20 and 30 in this way. A multiplication of 4 was the limit for this coldwork fastener investigation, and a factor of 3 was the value most commonly used because of the limited capability of the optics and the laser available.

2.2 Optical Fourier Transforms and Spatial Filtering

Another approach to understanding the creation of moire fringes by superimposing specimen and master gratings in a coherent optical system is based on the fact that a simple lens acts as a Fourier transforming device. A very basic discussion of the concepts behind this technique and simple examples of its application are contained in a paper by Cloud.[6-6] Clark, Durelli and Parks[6-7] and Nagae, Iwata, and Nagata[6-8] are only two of the fine papers which have written about using the technique in strain analysis.

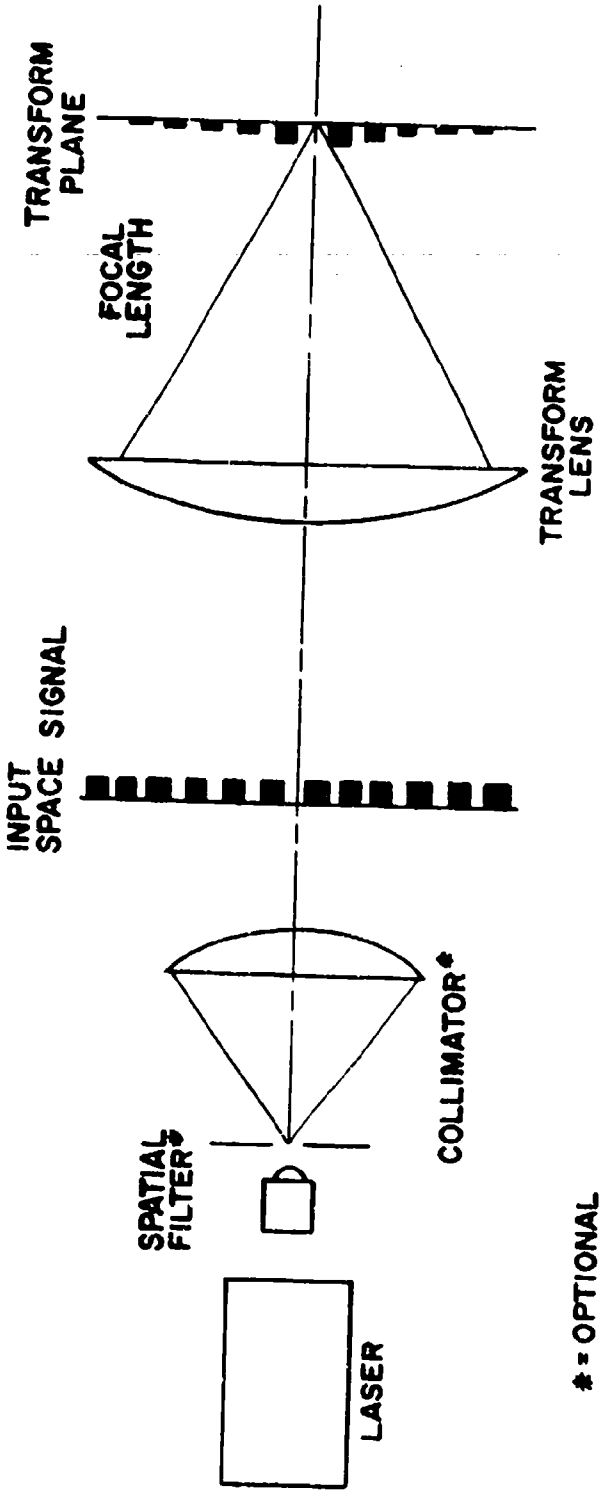

Figure 6.7. Optical creation of fourier transform of input signal in form of transparency.

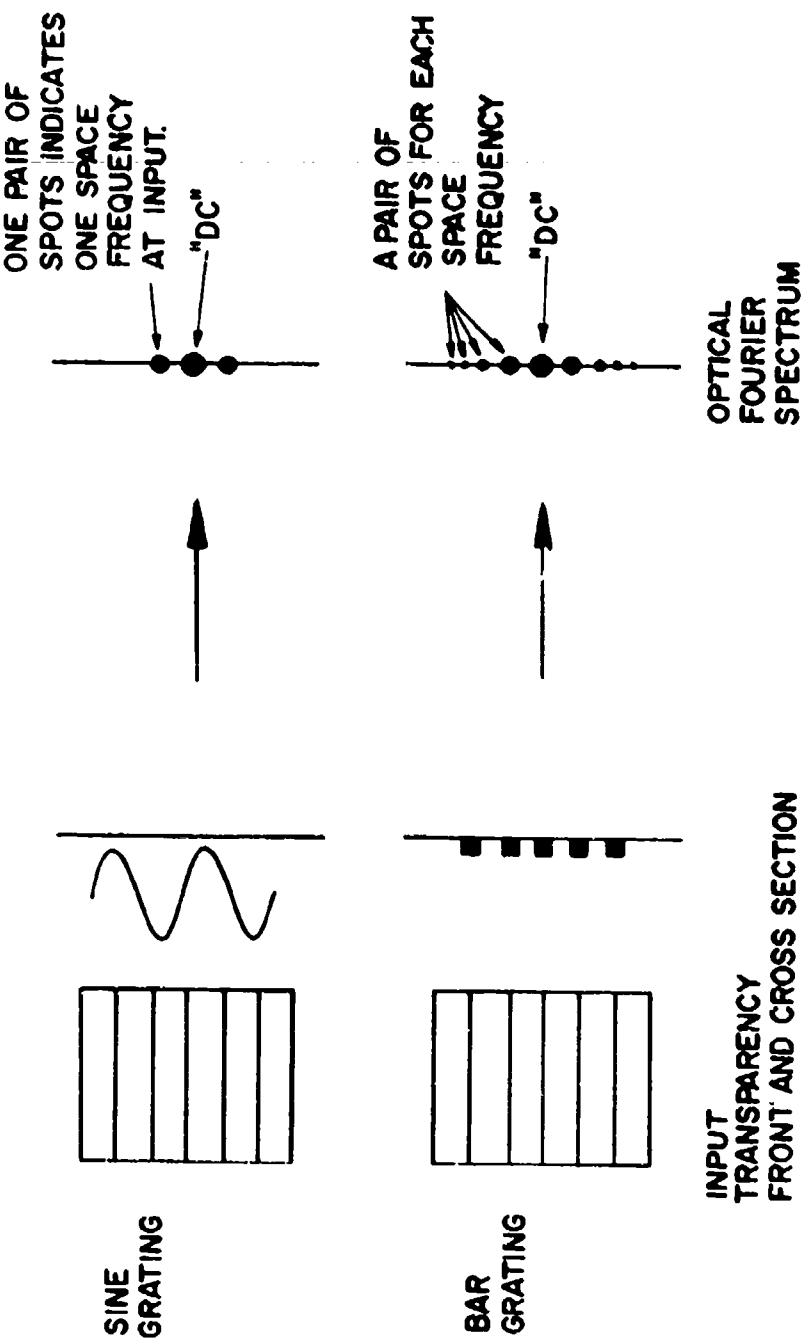

Figure 6.8. Two simple space signals and their optical fourier transforms.

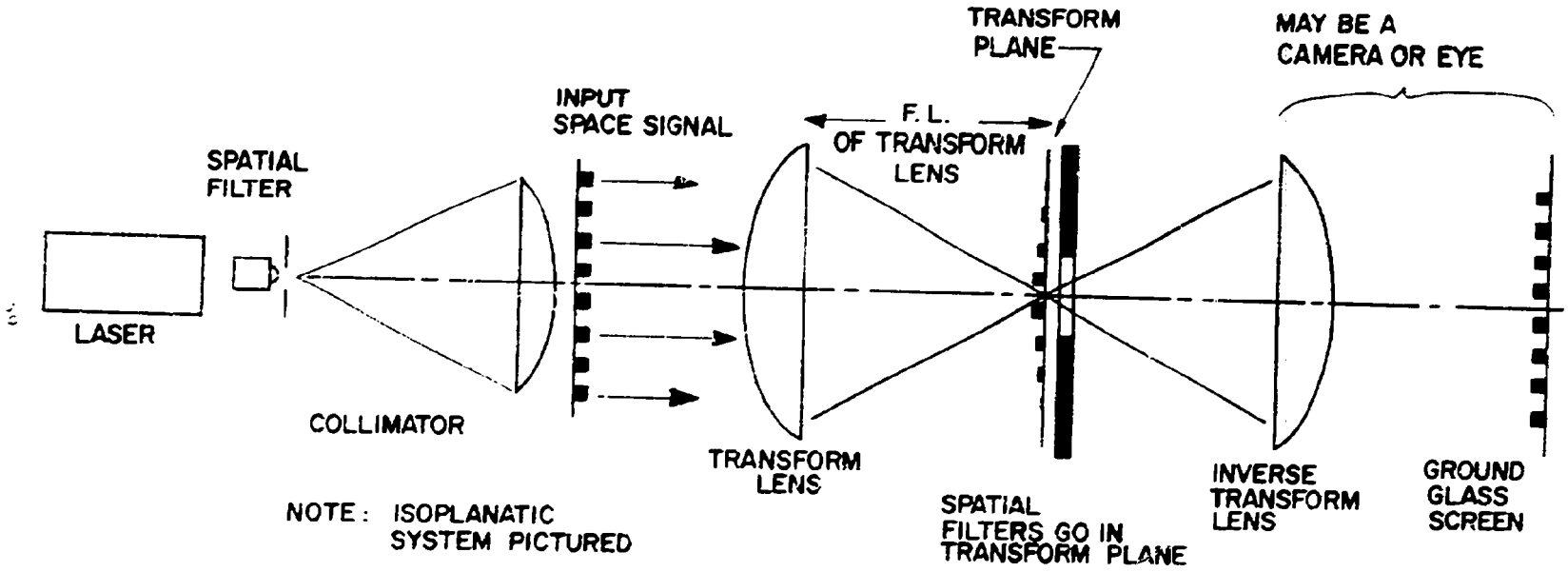

Figure 6.3. Optical system for spatial filtering in fourier transform plane and creation of inverse transform of filtered image.

Consider the situation shown in Figure 6.7 where collimated (usually) coherent light passes through some optical signal f(x,y), which often takes the form of a transparency having a transmission function which is a function of the space coordinate. The modulated light beam then passes through a simple lens. There will be produced at the back focal plane of the lens (the focus for the undisturbed light beam) a diffraction pattern which is simply related to the square of the amplitude of the Fourier transform of the input signal. If the input is a sinusoidal grating, for example, as pictured in Figure 6.8 the transform plane will exhibit three bright patches. The central dot corresponds to the uniform field or "D.C." component of the input. The other two dots indicate the spatial frequency content of the input signal, with radial distance in the transform plane representing spatial frequency in the input plane. If the input signal is a "square wave" bar and space grating (see Figure 6.8) there will be in the transform plane a row of dots whose positions and brightnesses indicate the presence and importance of various harmonics of the fundamental space frequency at the input. A two-dimensional grid input will generate a Fourier spectrum at the transform plane which is a two-dimensional array of dots corresponding to the two-dimensional Fourier transform.

Now, if another lens is placed at or near the tranform plane, the image of the original input may be cast on the screen. Such a process is shown in Figure 6.9. The second lens forms the inverse transform to recover the original input signal. It is possible and often useful, however, to modify the frequency content of the optical image at the Fourier transform plane before completing the inverse transform. This task can be accomplished by blocking or otherwise changing some portion of the light distribution at the transform plane. Such a procedure is called spatial filtering, coherent optical data processing, or optical Fourier processing.

A fundamental example of optical Fourier processing is shown in Figure 6.10. Here, the input signal is a 2-dimensional grid of crossed lines which produces a 2-dimensional array of dots at the transform plane. All the dots except the central

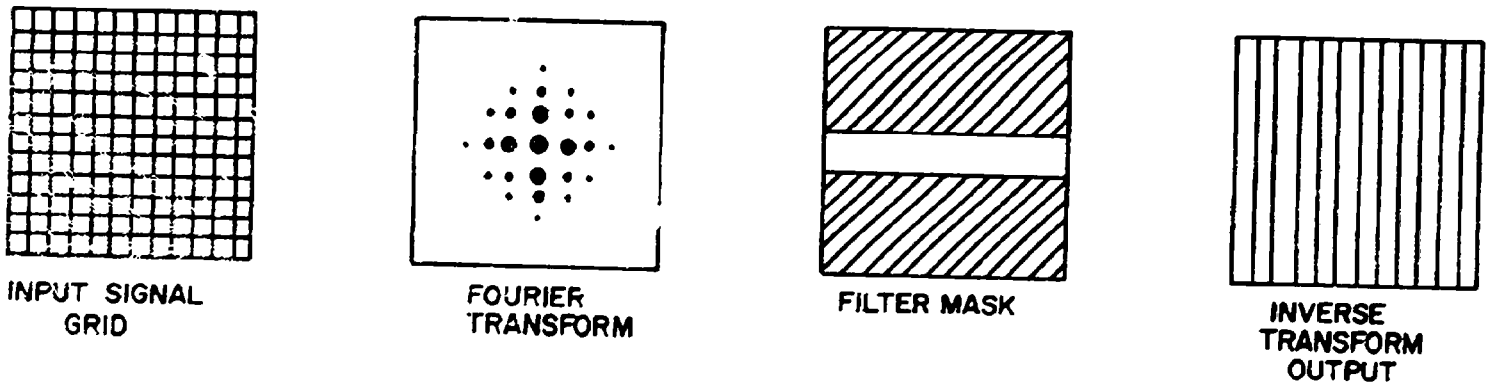

Figure 6.10. Example of optical spatial filtering to create bar grating from a grid of dots or crossed lines.

vertical row are blocked by a suitable screen with a slit which is placed in the transform. The inverse transform created by the second lens is found to be a simple grating of vertical parallel lines. The horizontal family of lines is suppressed by the optical filter which has removed all the light rays required to image the horizontal lines. The potential usefulness of such a process is very great. Figure 6.11 illustrates what can be done in modifying the appearance of a single character by blocking either the high-frequency or low-frequency components. One can imagine many applications in image enhancement, noise reduction, character recognition, and optical coding. A fundamental advantage is that the procedure is a simultaneous analog treatment of a whole optical field. The whole scene or message can be hidden in code, modified by removing portions of its frequency content, or recovered in one operation.

In the elementary situation under study here, two superimposed gratings are placed in an optical data processing system. A Fourier spectrum of the gratings is created at the transform plane. All but one of the bright dots (actually two or more bright dots close together) are eliminated by a pinhole in a dark mask. The light in this one dot is used to form an image on a screen by the second lens--this lens and screen combination being an ordinary camera. The image is constructed, then, of light which carries with it information about the periodic structure of the two gratings for whatever fundamental space frequency has been chosen by the placement of the pin hole. The only rays which get through the pin hole are those which have been modulated by the gratings at a single space frequency which may be the fundamental grating frequency or one of its harmonics.

A distinctive feature of this approach is that it considers the output image of the gratings to consist of a desirable signal plus a great deal of other information. The important signal, which is the moire pattern, is made visible by sifting it from all the extra information. We have a certain latitude in selecting the information that best suits a given purpose. Selection of higher frequency components

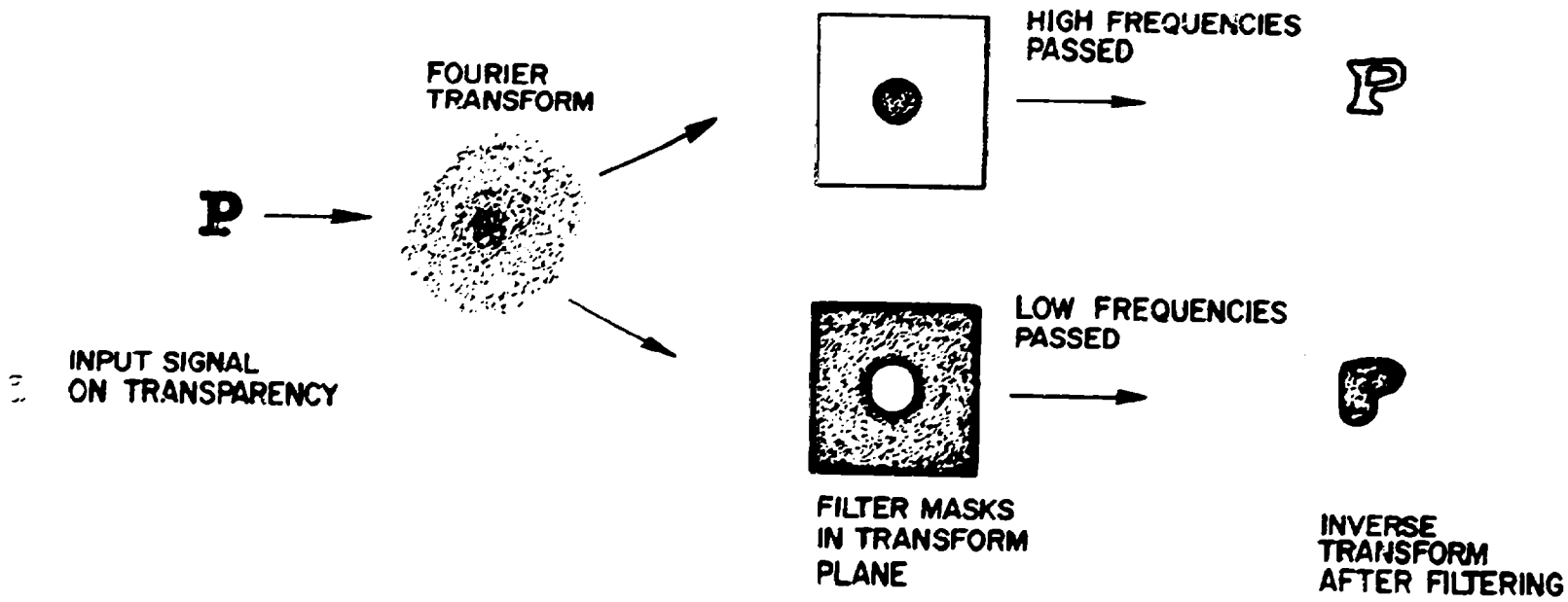

Figure 6.11. Example of optical spatial filtering for image modification.

will give moire sensitivity multiplication, for example, when the input gratings are of similar space frequencies. All the flexibility discussed in the context of the diffraction model (see Section VI-2.1) has its parallel in the Fourier filtering model.

Having two explanatory models of the same physical phenomenon raises the question of which one is correct--or are both faulty? Actually, the two explanations are not different in basic concepts. The difference is one of emphasis In the diffraction model, we look upon the diversion of portions of the incident beam of light as the important feature. With the Fourier processing approach, we are concerned with the transfer characteristics of an aperture which happens to have a lens in it, given an optical signal which is already generated by passing light through a transparency. Of course, the lens would not work correctly if the transparency did not divert portions of the incident beam by diffraction. So, the combining and rationalizing of the two approaches may be pursued to a final consistent model. The price to be paid for this nicety is a small increase of complexity. Further study of the problem will not contribut to the goals of this work, so it will be abandoned with one final observation. As so often is the case with optical processes, the uniting physical phenomenon is that of interference. This property of light is what makes visible for study those minute differences of propagation directions or wavefront shapes which are the physical manifestations of important processes such as diffraction, double refraction, and so on.

3. FORMATION OF MOIRE FRINGE PHOTOGRAPHS

The preceding two sections have outlined in general terms the function of the optical filtering system which is used to construct moire fringe photographs from a specimen grating photoplate combined with a submaster grating. The optical system devised for this purpose is pictured schematically in Figure 6.12; and a photograph of one version of the actual hardware used are presented in Figure 6.13. This apparatus was subject to a continuing process of modification and upgrading and the details discussed below differ in minor ways from what is visible in the photographs.

The light source used for most of this study was a 10 milliwatt Helium-Neon CW laser made by Jodon Corporation of Ann Arbor, Michigan. The laser beam passed through a simple and rather crude Gaertner spatial filter which converted it to a moderately clean diverging beam. This beam was directed to a spherical astronomical telescope mirror of 4 inch diameter obtained from Edmund Scientific Company. The mirror folded the beam back along the optical axis of the processor to compensate for lack of a long enough space, and it also collimated the expanded beam. The moire submaster grating and the photoplate of the specimen grating were placed emulsion sides together in the optical path normal to the light beam, and they were clamped and held to an optical mount by spring-type clothespins. Trial experimentation showed that no fluid was needed between the plates. After passing through the photoplate, the beam, now containing diffraction components, was decollimated by the simple lenses (sometimes one) acting in series. These lenses were also obtained from Edmund Scientific Co. and were 4 inches (102 mm) in diameter with focal lengths of 22 inches (559 mm). The focal plane of the system was found by trial with the data plates removed. In this plane,

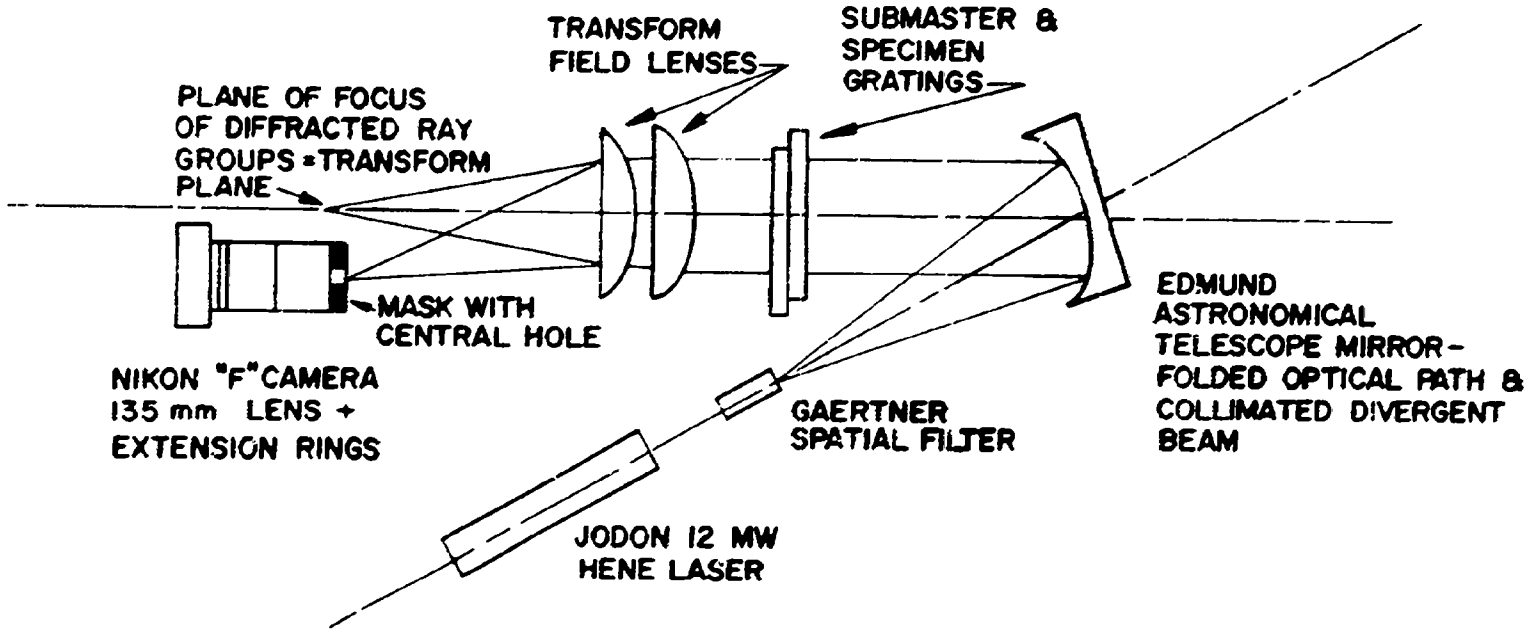

Figure 6.12. Schematic of optical processing system used for obtaining moire fringe photographs from specimen grating photoplates.

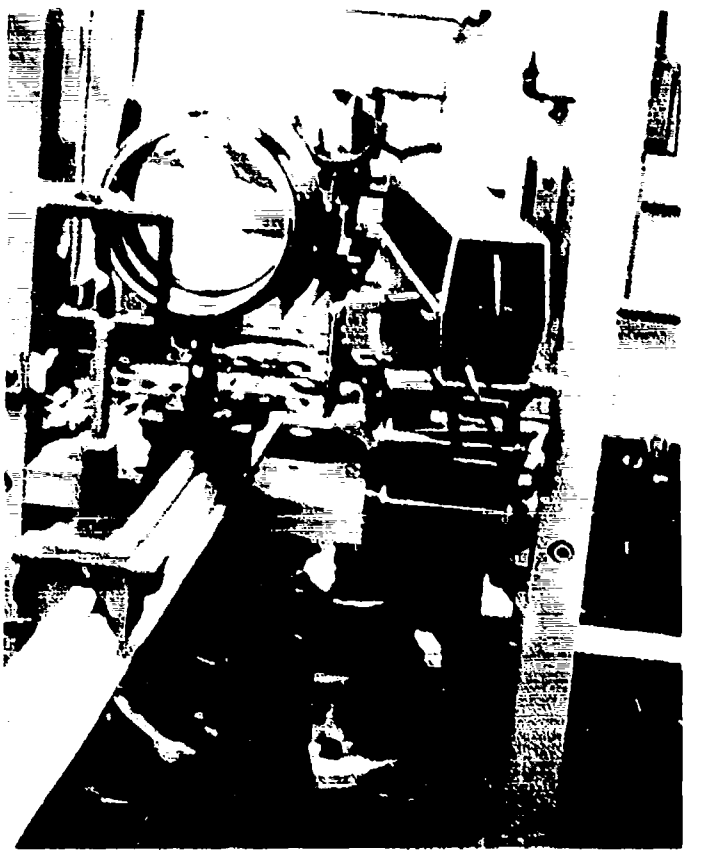

Figure 6.13. Photograph of moire optical data processor (early version).

which is the transform plane of the field lens combination, was placed a black paper screen containing a hole of approximately 3/32 inches diameter. The screen was actually contained in the filter mount of a 135 mm Nikon camera lens which was mounted along with several extension rings upon a Nikon F camera. The camera was mounted on a swinging bar so that the hole in the filter mask could be made to coincide with the chosen ray grove, a series of which appear as bright spots in the diffraction pattern. Selection of the proper bright patch must be accomplished with the camera pointed so as to focus an image of the specimen grating plate on the camera film. The whole assembly, with the exception of the laser and spatial filter which were mounted on a separate pedestal, was mounted on a simple optical bench of triangular cross-section which was obtained along with component carriers from Ealing Optical Corp.

The camera was focussed in the apparent plane of the data plates as seen through the field lens. After proper adjustment of the grating photoplates, a moire pattern was visible in the image of the specimen seen in the camera viewfinder. After final adjustment of the plates to eliminate rigid body rotation effects in the fringe pattern, the pattern was photographed. The fringe photograph negatives were made on Kodak Tri-x film, with Plus-x film being used sometimes. Exposures were worked out by trials. In practice there is a great deal of exposure latitude to be exploited in this photography of monochromatic high contrast fringe patterns.

It is at this point that the flexibility of the optical data processing procedure becomes useful. The baseline (zero strain) and deformed grating data are permanently stored on glass photographic plates. It is possible to superimpose these plates with different submaster gratings in order to gain maximum useful sensitivity multiplication and to improve subsequent fringe reading and data analysis by optimizing the spatial frequency mismatch of the superimposed gratings.

In practice, it worked out that the specimen grating photographs had a spatial frequency of 762 lpi (30 lines/mm) which results with a specimen grating of 1000 lpi magnified 1.3 times. These plates could be superimposed with submasters of around 2200 lpi to get a sensitivity multiplication of 3, or of 1542 lpi for a multiplication of 2. The various mismatches were chosen to yield the closest fringe spacing obtainable with good fringe visibility. Most grating photoplates were precessed with at least 3 mismatch levels, and sometimes with more than one sensitivity multiplication factor for checking purposes and because it was not possible to assess the quality of a dense fringe pattern through the camera viewfinder, which was used without a magnifier.

To be specific, for most of this study, each baseline photoplate and each data photoplate was superimposed in the processor with submaster grating plates of 2200, 2225, and 2256 lpi. For specimen gratings of poor quality, a sensitivity multiplication of 3 was not practicable, and submasters of 1535 and 1492 lpi were used. Some fringe patterns were made for checking purposes with submasters at 763 lpi. For several of the specimens, all or most of these several moire patterns were analyzed to give redundancy of data. This extra information was useful in gaining an appreciation of probable errors and in studying the sensitivity of the data output quality to variations in the optical data processing.

It was also possible at this stage to select by trial submasters which had density and diffraction characterisitcs which balanced with the properties of the specimen grating to produce the best fringe pattern. Also, the ray group which gave best fringe visibility could always be selected.

Following normal development of the 35 mm negatives of the fringe patterns in C-76 (Kodak D-76 plus crone additive), they were sorted, cataloged, and coded. Most of them were then enlarged and printed in 8x10 size for numerical fringe analysis.

Enlarging was done in a Durst enlarger using the second lightest contrast filter with Kodak polycontrast enlarging paper. Final printed image to specimen size ratio was approximately 7.

Samples of three of the moire fringe patterns obtained are reproduced in Figures 6.14 through 6. 16.

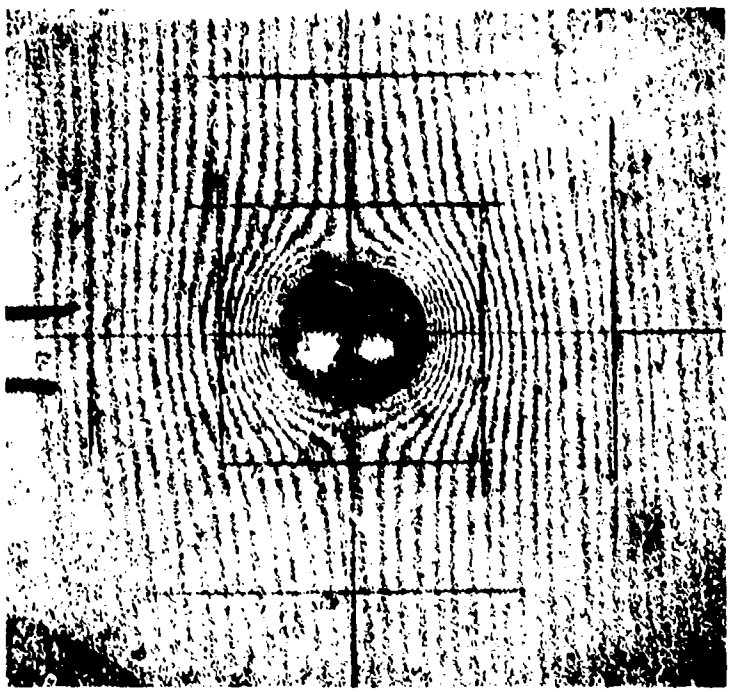

Figure 6.14. Sample moire fringe photograph (reduced).

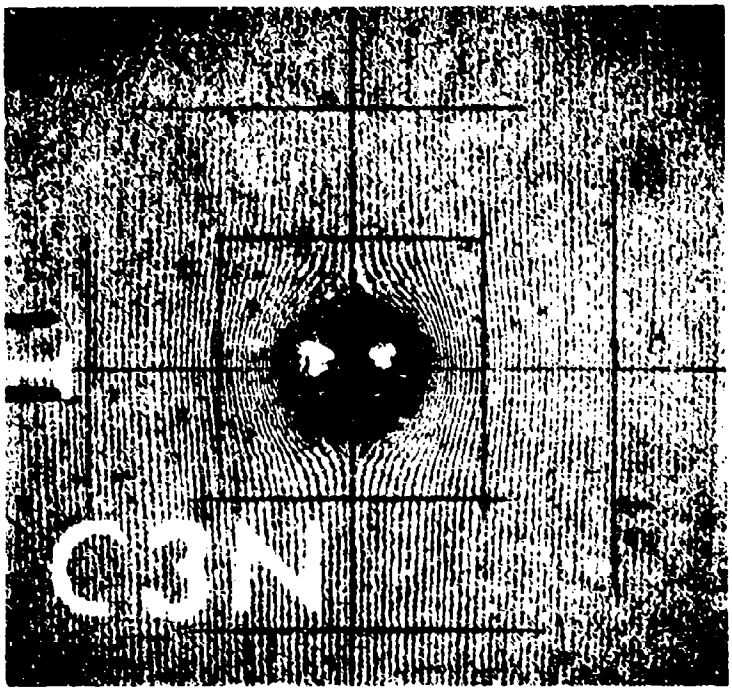

Figure 6.15. Sample moire fringe photograph (reduced)

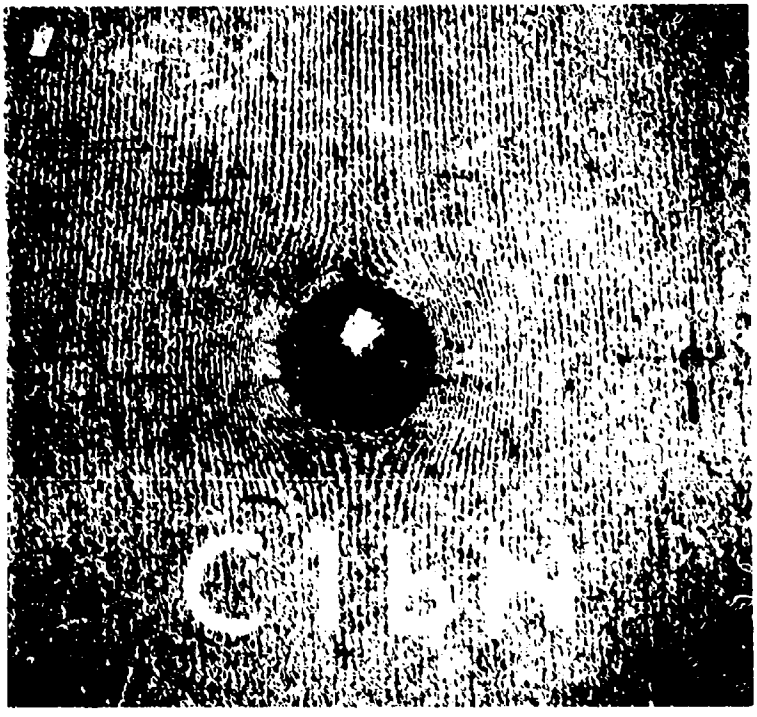

Figure 6.16. Sample moire fringe photograph (reduced)

SECTION VII

REDUCTION OF MOIRE FRINGE DATA

1. GENERAL REMARKS

A moire interference fringe is a locus of points where the in plane displacements of the specimen surface normal to the grating lines, plus pitch mismatch if it exists, is a constant multiple of the pitch (period) of the grating. Figure 7.1 shows in graphic form the process of reduction of the fringe patterns to obtain strain. The steps are outlined below.

A picture of an in-plane displacement component can be constructed by plotting moire fringe order along a given axis in the specimen, subtracting the pitch mismatch (baseline) fringe orders, and multiplying the remainder by the inverse of the grating spatial frequency and the fringe multiplication factor (sensitivity multiplication) used in the optical data processing.

Once a map of a displacement component is obtained, the corresponding strain component can be generated by calculating the derivative of displacement with respect to the appropriate space variable.

For example, if the grating lines are aligned with the y-axis in the specimen, then the x-component of displacement, u_x, is given by the moire fringe pattern. A plot of u_x along any x-axis is easily constructed. The derivative of u_x with respect to x ($\partial u_x/\partial x$) is the x component of normal strain, ε_x. Other displacement and strain components are obtained by logical extension of this idea. It is not wise, however, to develop the shear strain information by using the cross partial derivatives $\partial u_x/\partial y$ and $\partial u_y/\partial x$, as these quantities are sensitive to errors caused by relative rigid body rotations of the two gratings. If shear strain is to be measured, then the best procedure is to obtain a measurement of normal strain along

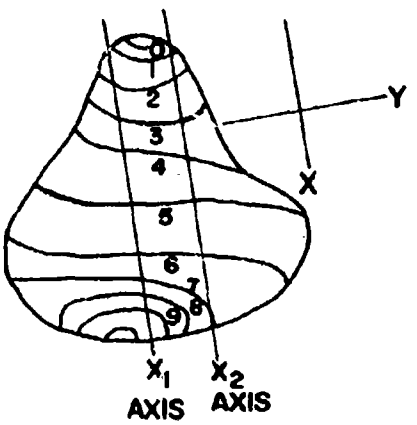

STEP 1

FRINGE PATTERN OBTAINED WITH GRILL PARALLEL TO Y-AXIS

ρ = PITCH OF GRILL
= 1/f

f = SPATIAL FREQUENCY

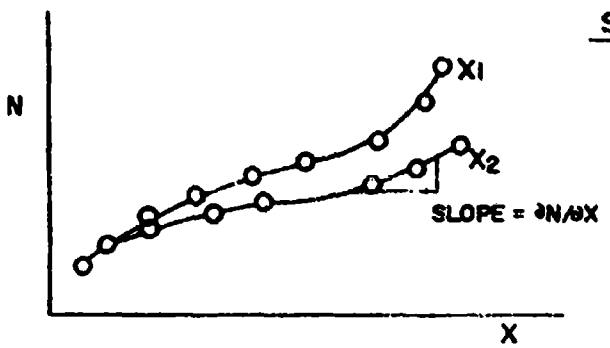

STEP 2

PLOT OF FRINGE ORDER "N" AS FUNCTION OF DISTANCE ALONG CHOSEN X-AXIS

DISPLACEMENT COMPONENT U_x IS ρN

$$\epsilon_{xx} = \rho \frac{\partial N}{\partial X}$$

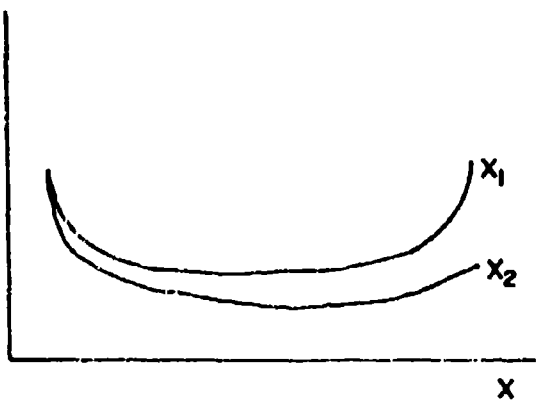

STEP 3

PLOT OF NORMAL STRAIN ϵ_{xx} AS A FUNCTION OF DISTANCE ALONG CHOSEN X-AXIS

THIS GRAPH IS DERIVED FROM THE DISPLACEMENT PLOT BY DIFFERENTIATION

Figure 7.1. Diagram of steps involved in reducing moire fringe photographs to obtain displacement and strain.

a third axis inclined to the x and y system. The strain rosette equations may then be used with the 3 normal strain components to find shear strain ε_{xy}. That the normal strain is not affected by moderate relative rotation of the gratings is easy to prove.

In this investigation the results sought were plots of normal strain in the radial direction along radial axes. Tangential strains along radial axes were desired for some of the specimens. These two determinations complete the surface strain analysis, because symmetry conditions demand that the shear strain in the radial-tangential coordinate system be zero; that is, the two normal strains measured are the principal strains.

The reduction of moire fringe data to obtain strains can be performed by graphical methods, numerical techniques, or a combined approach. When planning a data reduction program, it is well to remember that differentiation of experimental data is necessary. Such differentiation is an inefficient process in that it is laborious, often gives poor results if not done with extreme care, and an estimate of errors is difficult to obtain. Careful graphical processing is probably as dependable as any approach because it allows constant critical study of all intermediate results.

For this investigation, the volume of moire data made numerical processing highly attractive. A numerical reduction computer plotting scheme was developed which incorporated most of the advantages of high speed computing while retaining desirable features of the graphical approach, such as allowing examination of intermediate results and the introduction of a controlled small degree of data smoothing. The procedures followed were tailored to the digital equipment immediately at hand and they did not achieve maximum efficiency in terms of human labor or computer time. The process was quite acceptable for the given situation, but improvements would be appropriate if continued use of the moire technique is planned. Some such

modifications are mentioned where appropriate.

Certain aspects of the data reduction procedure for tangential strain differed from the scheme for determining radial strain. The radial strain measurement is described in detail in Sections 2 and 4 of this chapter, and variations incorporated for tangential strain determination are described in sections 3 and 5.

2. DIGITIZING MOIRE FRINGE DATA - RADIAL STRAIN

The steps involved in digitizing and reducing the moire fringe photos to obtain radial strain near the coldworked hole for a situation incorporating sensitivity multiplication and pitch mismatch interpolation are summarized pictorially in Figure 7.2. This figure represents the reasoning outlined in section 7.1 and Figure 7.1 applied specifically to the problem at hand.

Recall from Section VI that the results of the moire grating photography and optical data processing were 8x10 inch enlargements showing the moire fringes in the area near the hole along with various identifying labels and fiduciary marks. In order to obtain normal strain along an axis (call it the x-axis) normal to the grating lines, it is first necessary to obtain a record, in this case in digital form, of the distance along that axis from a fiduciary mark to each moire fringe. In the end, it was desirable to have the strain reported as a function of the distance from the hole boundary. The exact hole edge is not easily established in the data photos, however, so initial stages of the analysis were cast in terms of distance from a mark remote from the hole. The data was then converted by using the measured distance on the specimen itself from the fiduciary mark to the hole.

The first step was to number the moire fringes and identify the various fiduciary marks and the orientations of the specimens in the pictures. An example of a fringe photograph prepared for digitzing is reproduced in Figure 7.3. This preparation had to be done for a data photo and for its matching baseline fringe pattern. Numbering of the fringes was usually easy in this situation, because the strain increases as the hole is approached. The counting of fringe

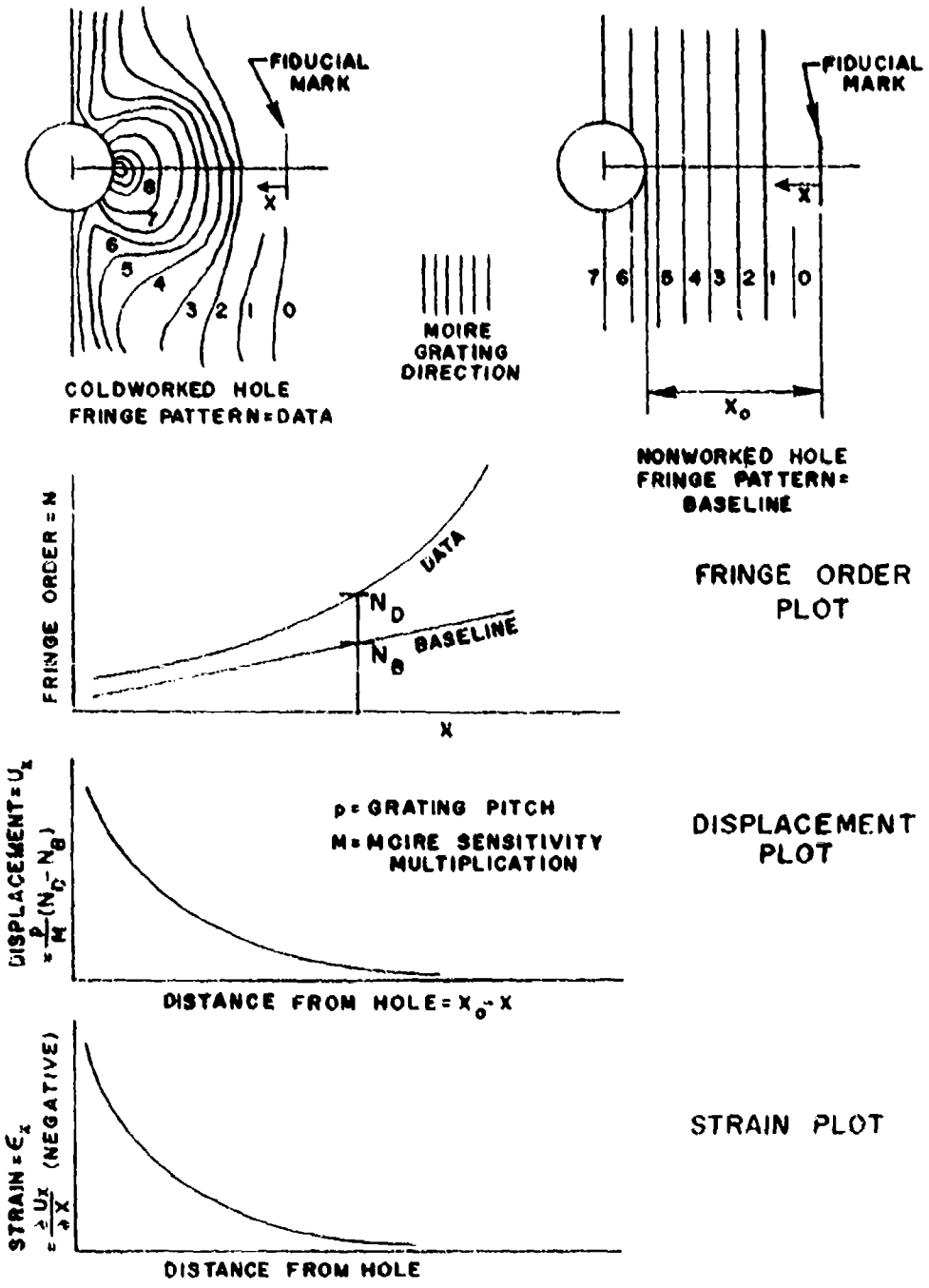

Figure 7.2. Steps in reduction of moire data related to determination of radial strain distribution near coldworked hole.

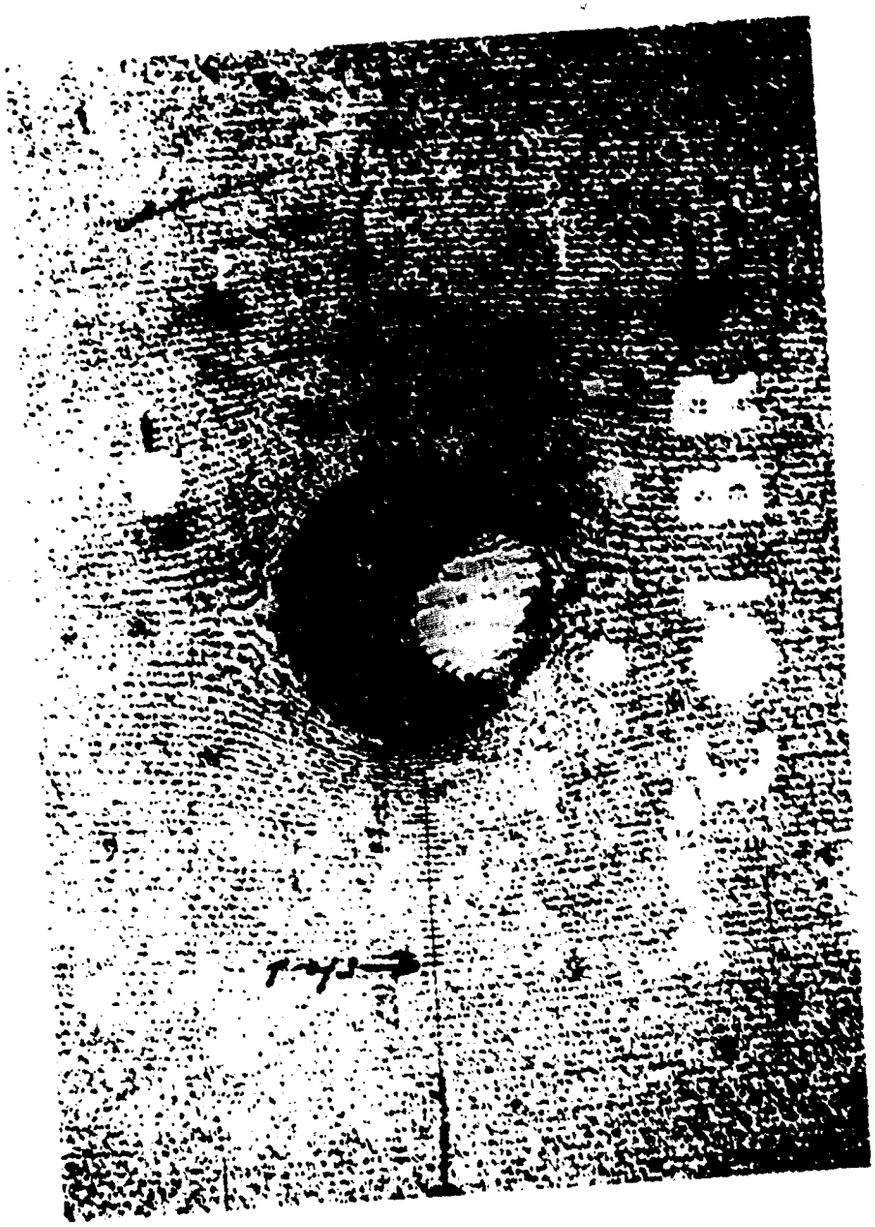

Figure 7.3. Typical fringe photograph prepared for digitizing and computation of radial strain.

orders can begin anywhere because absolute fringe number is not important; it is very important, however, that numbers or fringes be not repeated or skipped.

In all the analyses, each individual run on each side of each hole was treated separately. The results were brought together only at the end of the study when average values were calculated.

Digitizing of the fringe patterns was performed on a Hewlett-Packard Model 9820 desk top computer with a Model 9864A Digitizer Module attached. A one-dimensional digitizing program was prepared especially for moire fringe pattern analysis. An annotated copy of this program is duplicated in Appendix A along with a typical output printing. This program automatically scales the data to real specimen dimensions and incorporates a scale checking feature. It also allows for entry and printing of photograph and specimen number and the various moire parameters needed in later calculations such as grating pitch and sensitivity multiplication factor. As is typical of such programs, it is independent of position or orientation of the fringe photograph upon digitzer platform. A more unusual feature is that it is not sensitive to displacement of the cursor unit normal to the axis of interest. This characteristic allowed, for example, use of fiducial marks which were not on the axis under study for scaling and scale checking. That is, a mark at the extreme top of the picture would be used in entering scaling data when fringe locations along the horizontal centerline of the hole were being digitized.

Following initial entry of the various parameters requested by the program, the locations of fringe intersection with the axis under study are entered with the cursor. In this study, it was thought sufficient to enter only the integral order fringes (the dark bands), although the half-orders (white bands) could have been digitized also and the printed results corrected in the later computer data processing.

The digitizer program automatically counts the fringes as they are entered after being given an initial value. This convenience had its faults in that the user had to be careful when it was necessary to check an entry by digitizing the ... fringe twice. The program is constructed so that the fringe counting and digitizing can be restarted at any value, but it seemed as easy to start over on a given set of data if an error was suspected.

As mentioned, the digitizing process was applied to a moire data photograph (after coldwork) and a zero strain (before cold work) baseline photograph. These two sets of digitized fringe data form a unit for computation and plotting of displacement component and strain component with proper correction for grating pitch mismatch or other peculiarities of a given test.

Several different sets of data were obtained for each hole studied by the use of moire photos obtained with different multiplication factors and pitch mismatches. In several cases, the same photographs were digitized twice in order to analyze experimental errors derived from the digitizing process.

The data printouts from the digitizer were carefully cataloged and mounted on sheets of paper in order that they not be damaged or mixed. Digitizing was the most tedious of all the steps in the experiment and, therefore, the one least likely to be favored for repetition. The data were then read from the printed copy and punched on computer cards to fit the input format of the computer programs for data analysis and plotting.

3. DIGITIZING MOIRE FRINGE PATTERNS IN TANGENTIAL STRAIN

Digital reduction of the moire fringe photographs to obtain a mapping of tangential strain (ε_y) along a radial x-axis was somewhat more complex. To obtain ε_y the grating must be aligned with the x-axis. Plotting of fringe order and differentiation must be done along y-axes, since $\varepsilon_y = \partial u_y/\partial y$. A plot of fringe order with respect to x-distance

from a fiducial work is of no use. Rather, it is necessary to obtain and analyze a series of plots of fringe order with respect to distance in the y-direction in the vicinity of the x-axis. This procedure is carried out for as many y-axes as needed to obtain a complete picture of ε_y along the x-axis. From the values of strain obtained at the intersection of the several y-axes and the x-axis, a plot of ε_y versus $\underline{x}$ can be developed. A pictorial summary of the process is shown in Figure 7.4.

After cataloging the photographs and locating the fiducial marks, each of the data (afer coldwork) and baseline (before coldwork) photographs which were taken with the gratings oriented for determining ε_y vs x had a series of y-axes inscribed with a ballpoint pen. These axes were located or the fringe photo so that they were 0, .01, .02, .04, .1, and .2 inches from the hole edge in real specimen dimensions. A sample data photograph so prepared is reproduced in Figure 7.5.

After this preparation, the photographs were digitized by the technique, apparatus, and program described in Section 7.2, except that the locations of the moire fringe intersection with each y-axis were digitized, and the location of that y-axis from the hole was entered on the printer tape. The data from a given y-axis on a data photo was marked with the data from the corresponding y-axis on the appropriate baseline photo. A typical set of this data is reproduced in Appendix A. Each of these sets was mounted on paper sheets for filing, then punched onto computer cards for computer processing.

Although it seems to be tedious and complicated, the digitization of the fringe patterns for tangential strain calculation proved quite simple and not very time consuming. Part of the reason is that each set of data contains far fewer entries than does each batch of radial strain data. Also, the structure of the digitizing program and the HP 9820 Computer make it possible to recycle the program without reentering all the initial parameters. In fact, the moire photos proved free enough from distortion and odd shifts of moire fringes that a single set of baseline data could be used for each y-axes on the data photo. In addition, the entry of fiducial marks by the digitizer to set the zero and scale factors would only have to be done

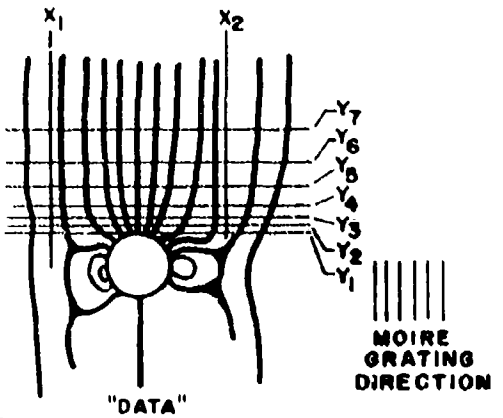

STEP 1 "DATA"

COLDWORKED HOLE FRINGE PATTERN WITH OVERLAIN FIDUCIAL NETWORK

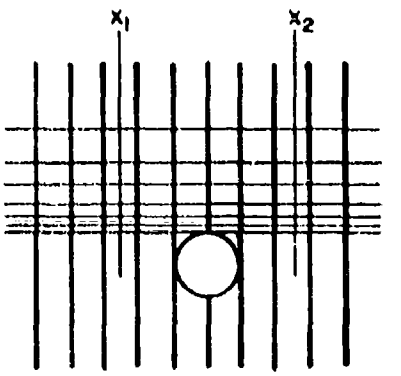

"BASELINE"

NONWORKED HOLE FRINGE PATTERN

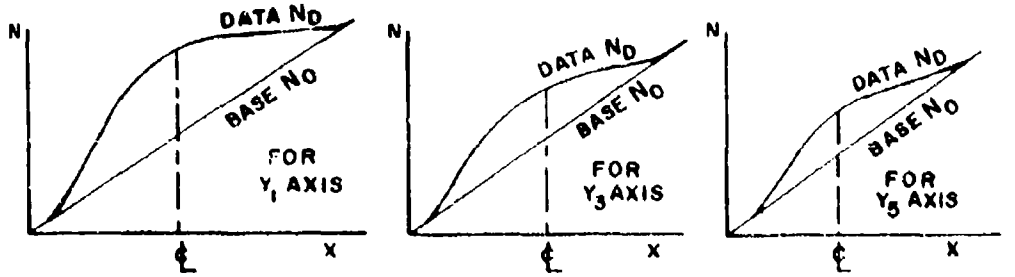

STEP 2

A PLOT OF FRINGE ORDER VERSUS DISTANCE Y FROM CONVENIENT FIDUCIAL X-AXIS (E.G. X_1-AXIS) IS CONSTRUCTED FOR EACH Y AXIS.

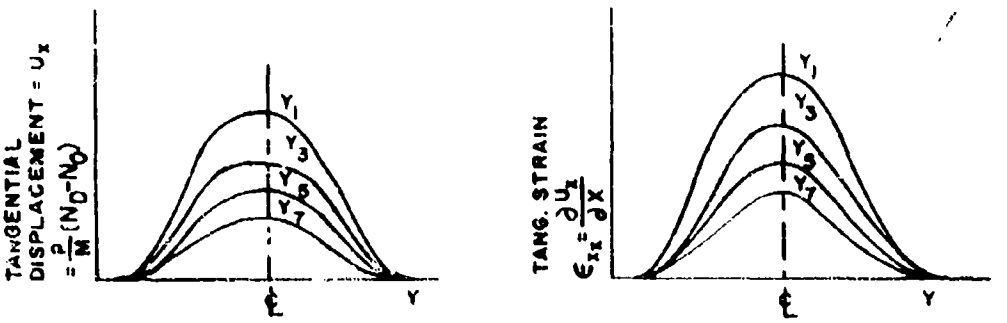

STEP 3 COMPOSITE PLOT OF DISPLACEMENT FOR EACH Y-AXIS

STEP 4 COMPOSITE PLOT OF STRAIN FOR EACH Y-AXIS

Figure 7.4. Reduction of moire data for determination of hoop strain distribution near coldworked hole.

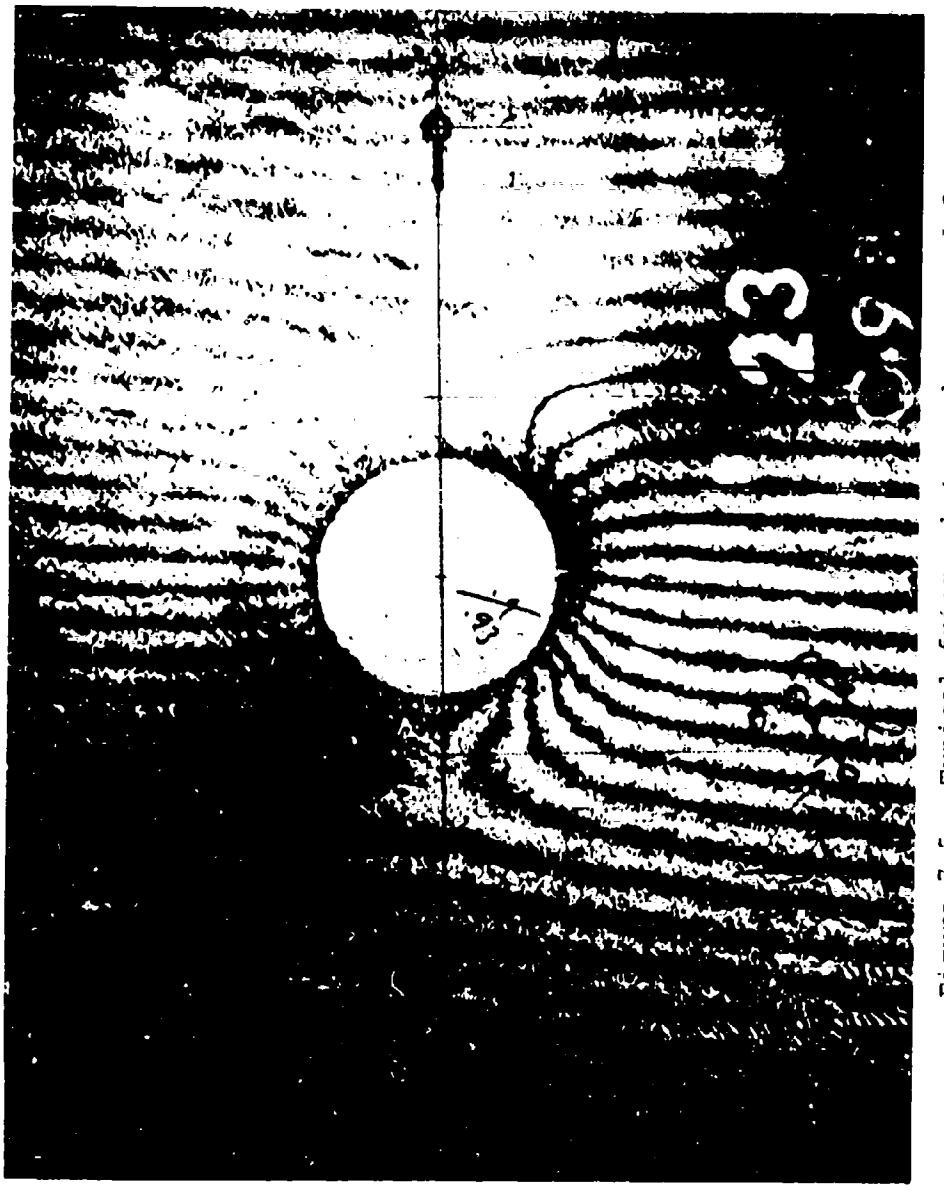

Figure 7.5. Typical fringe photograph prepared for digitizing and computation of hoop strain

once for a given photograph. These last two shortcuts were not utilized, and they are not recommended except in extremity because resultant scaling faults and errors from distortions induced by the multi-step photographic reproduction process represent errors which cannot be detected or assessed in the final results.

4. DATA REDUCTION AND PLOTTING-RADIAL DISPLACEMENT AND STRAIN

4.1 Introductory Comments

Two computer programs for reducing data and plotting results were prepared by Lt. Alan Miller of Air Force Materials Lab-Computer Activities Branch (AFML/DOC) using a spline function smoothing, curve fitting, and interpolation algorithm which had been programmed by Dr. C. P. Poirier of Aeronautical Systems Div. Computer Center (ASD/ADDS). Copies of these two programs, which are closely related to one another, are provided in Appendices B and C along with annotated sample sets of data as would be punched on cards. These two programs are described in the following two sections. A third routine was derived for generating a set of statistical summary plots for each coldworking level and for the whole experiment. That program is described in Section 7.4.4.

4.2 Detailed Analysis and Plots of Single Data Sets

The first computer program (Appendix B) was designed to give a detailed picture by printout (if desired) and graphical output which allows study of the original input, the computed displacement field, and the computed strain map. A small degree of data smoothing is contained in only the first data plotting stage. Subsequent operations are on ordinary point-by-point interpolation and finite difference schemes.

The operations performed by the detailed analysis routine (Appendix B) are as follows:

1. Read in data containing set designation (specimen number plus other identifiers), moire sensitivity multiplication factor from optical fringe data processing, moire grating spatial frequency, distance from primary fiducial mark to edge of hole, the maximum fringe order to be entered, and distances from fiducial mark to intersection of each moire fringe with the x-axis understudy. The maximum fringe order and fringe locations for the baseline fringe pattern are also read.

2. Generate fringe order numbers to match each fringe location entered as data.

3. Fit the baseline and coldwork data with two continuous smooth curves by means of a cubic spline smoothing routine. The degree of smoothing can be specified by the user; a minimum value was chosen for this study.

4. Interpolate the calculated curves to obtain fringe number as a function of distance from the fiducial mark at 100 points on the data and baseline curves. The maximum range of the curves is sorted out and divided by 100 to establish the nodes, which must be common to both data and baseline curves.

5. Subtract the baseline fringe order from the coldwork hole fringe orders for each of the 100 points and multiply this difference by the pitch (reciprocal of spatial frequency) of the grating on the specimen and divide by the sensitivity multiplication factor to obtain the radial displacement function u_x for the chosen x-axis.

6. Subtract the distance from the fiducial mark to the hole edge from each nodal x-value, which is distance to fringe order from the fiducial mark, in order to have all results reported in terms of distance from the hole.

7. Compute by finite differences the first derivative of displacement with respect to distance from the hole; this result is the radial strain at each of the 100 nodes.

8. Print, if ordered by the input control cards, all values of input fringe orders, displacements, strain, and, in addition, higher derivatives of displacement with respect to distance from the hole which have no useful meaning.

9. Scale the data and generate a plot of the input data and baseline curves. This graph shows fringe data points and the smoothed curves.

10. Plot radial displacement as a function of distance from the hole.

11. Plot radial strain as a function of distance from the hole.

12. Start over with the next complete set of date and continue for up to three sets, a limit which is imposed by computer time limits.

Samples of each of the three graphs produced by this routine are shown in Figures 7.6a-7.6c.

As mentioned above, the main purpose of this analysis program was to allow detailed study of each set of data and the results it produced. Input errors, such as faulty card punching or skipping a fringe during digitizing, were immediately evident. As proficiency and accuracy increased, this routine was used only as a last resort for data sets which seemed as if they might contain faults when processed by the less-detailed summary plotting routine.

4.3 Analysis and Summary Plotting of Multiple Data Sets

The computational scheme of the second computer routine (Appendix C) is essentially a duplicate of the one just described; it differs in the input requirements and in the output. The purpose of this program is to generate a single plot of the calculated radial strain versus distance from the hole which contains several sets of the data obtained for any one hole. Recall from the section on digitizing that several sets of data were developed for each hole because, first, it was necessary to consider the two opposite sides of the hole separately and, second,

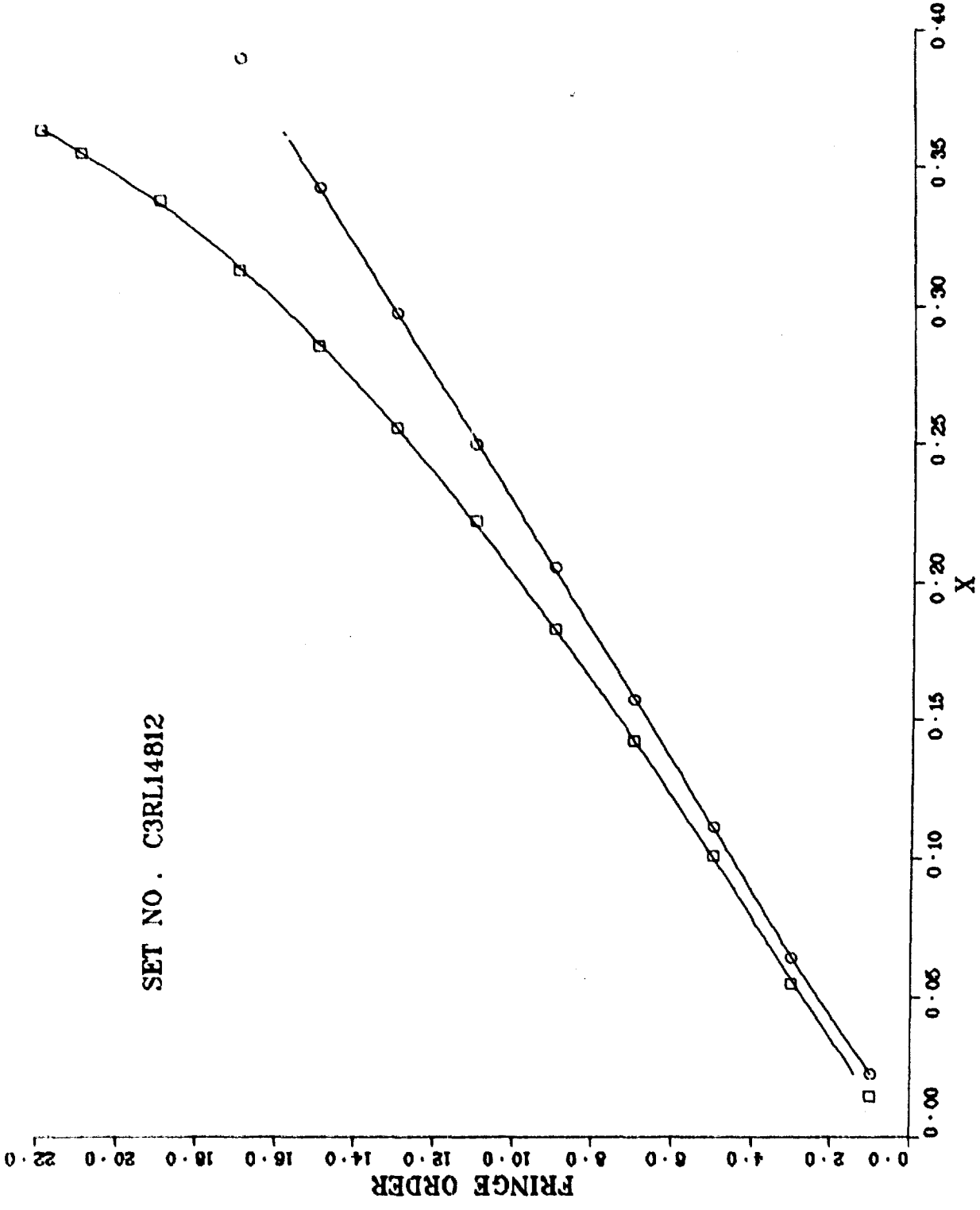

Figure 7.6 Typical graphs generated by detailed data reduction program; (a) Plot of baseline and coldworked input data obtained from fringe photographs.

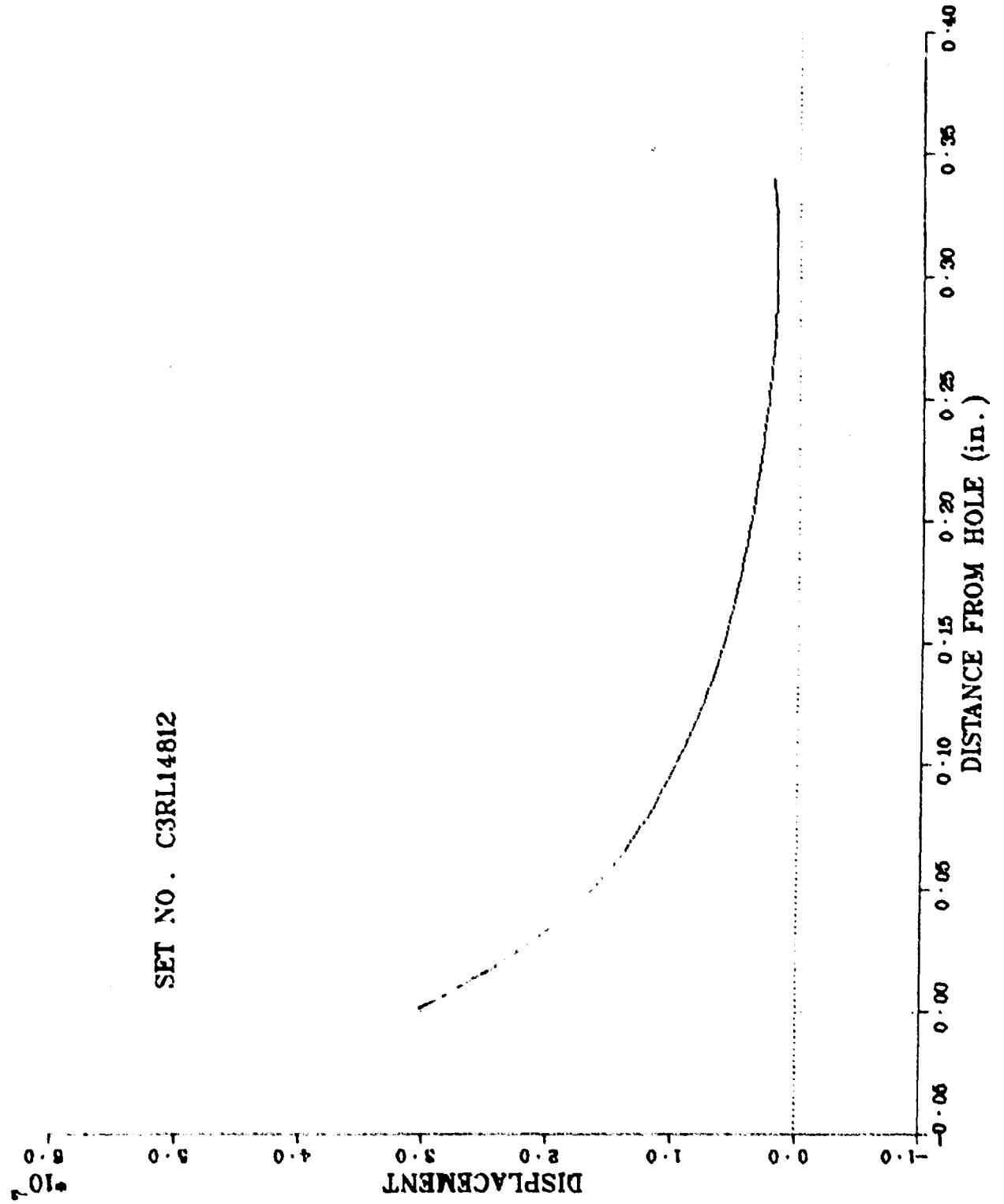

Figure 7.6 Typical graphs generated by detailed data reduction program: (b) Radial displacement plot.

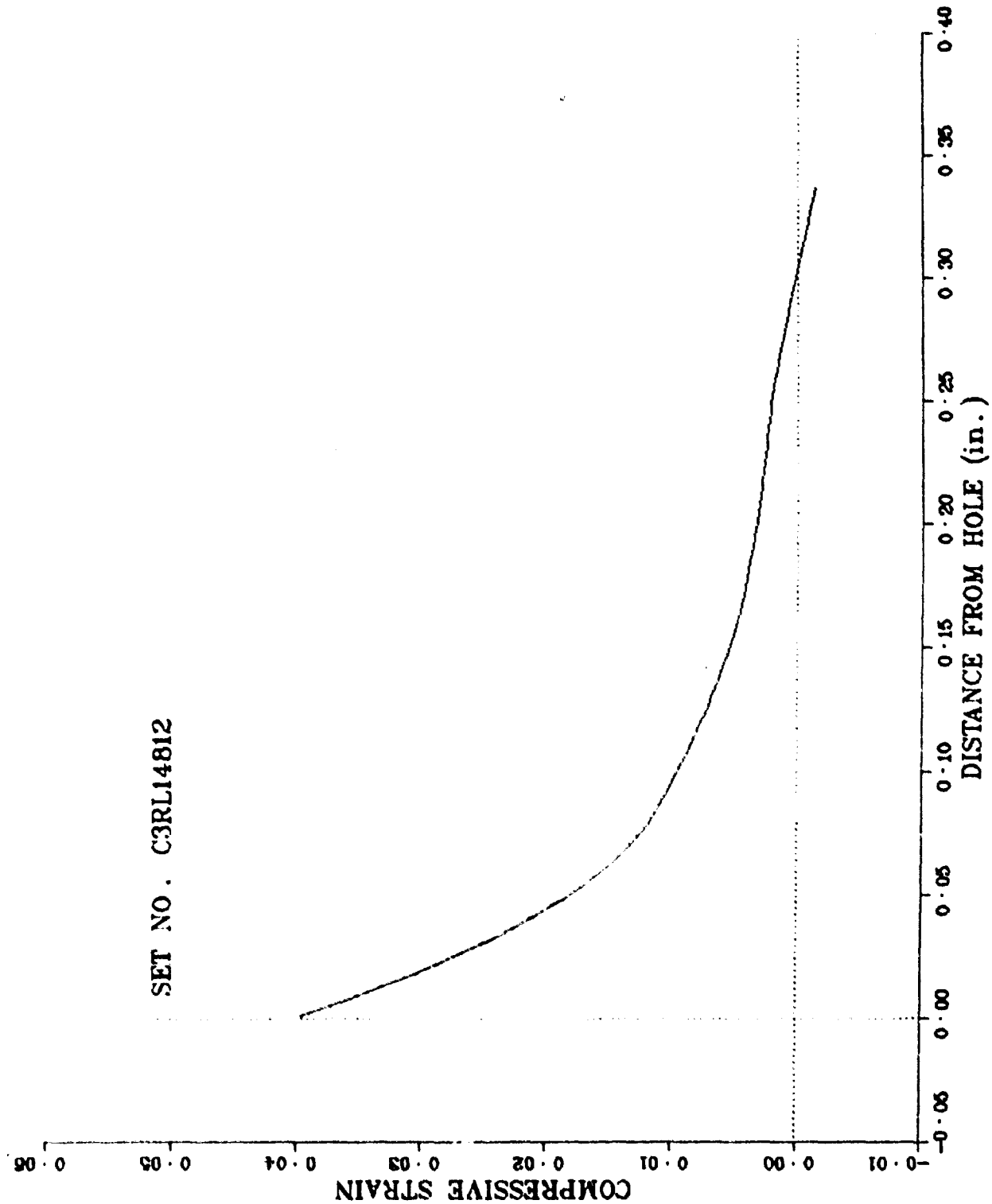

Figure 7.6 Typical graphs generated by detailed data reduction program: (c) Radial strain plot.

to give some statistical meaning to the end result and facilitate assessment of probable errors and uncertainty. This program summarized all the data for one hole on one graph. It offers an immediate indication of the repeatability of results as well as differences between opposite sides of the hole and possible effects of modification of digitizing or optical data analysis procedures.

An example of such a plot is given in Figure 7.7. Many more of these graphs are presented with the results in Section VIII. One is included here so that this section on technique can be studied by itself.

4.4 Statistical Analysis and Plotting and Composite Plots

A third computer program was devised by the author to serve two purposes in the final stages of data analysis. First, it applied simple statistics to all the data obtained for each hole (or each side of a hole) and generated printout and plots showing average strain and its standard deviation at approximately 20 points on the curve. The second function of this program was, with only very trivial modifications to create composite summary plots of the radial strain map for all degrees of cold-working which were studied.

The program listing and sample data for one hole appears in Appendix D along with a sample of the printed output. Samples of each type of graphical output from this program are reproduced in Figures 7.8 and 7.9 for study. Several more of these plots are presented as results in Section VIII.

It is important to realize that this routine was written for the computing and computer graphics facilities at Imperial College, London, England, during the author's tenure there. It cannot be used with Air Force Materials Laboratory computational facilities without modification, although the basic algorithm and graphical format are applicable.

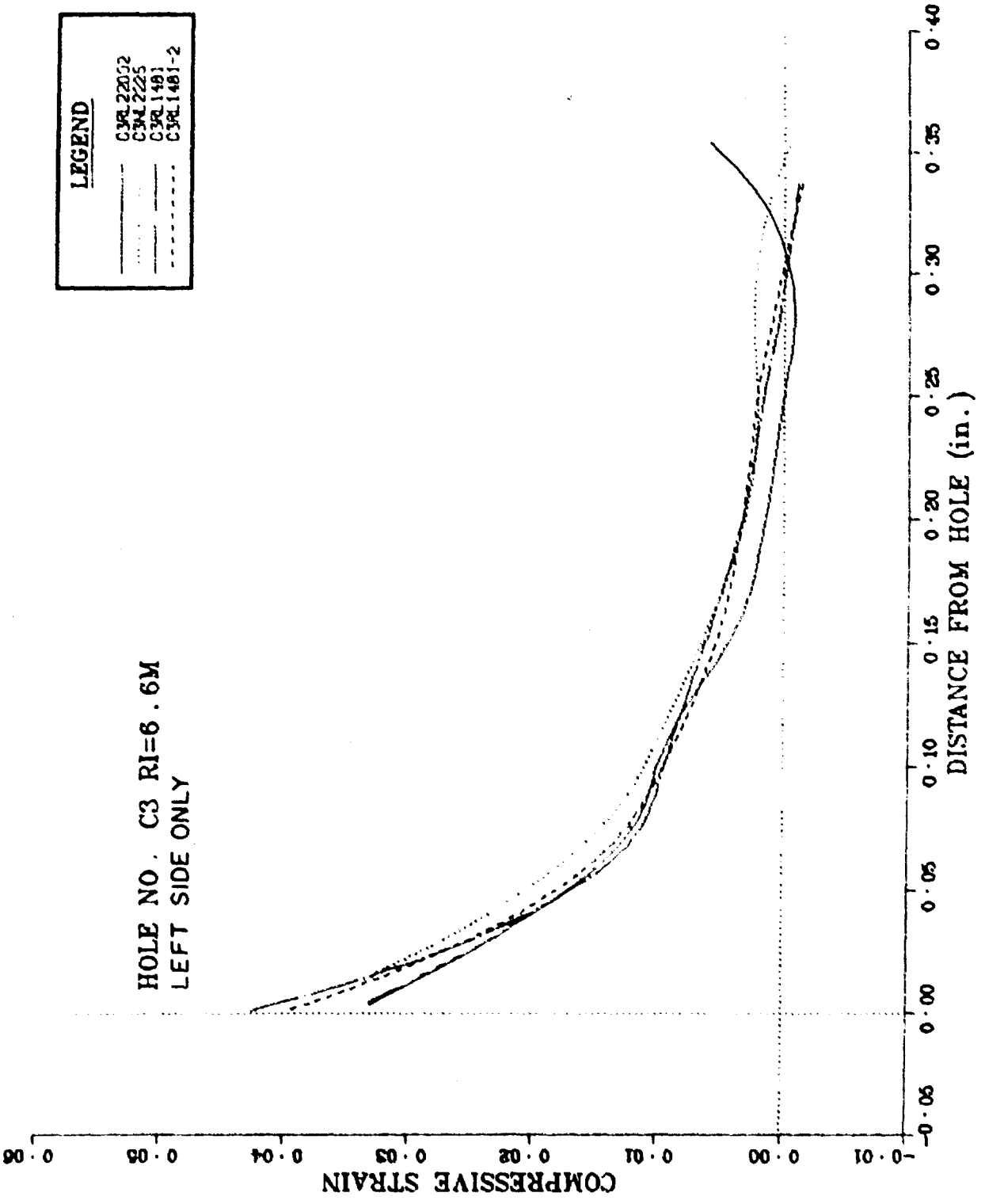

Figure 7.7 Typical summary of individual radial strain distributions measured for one hole.

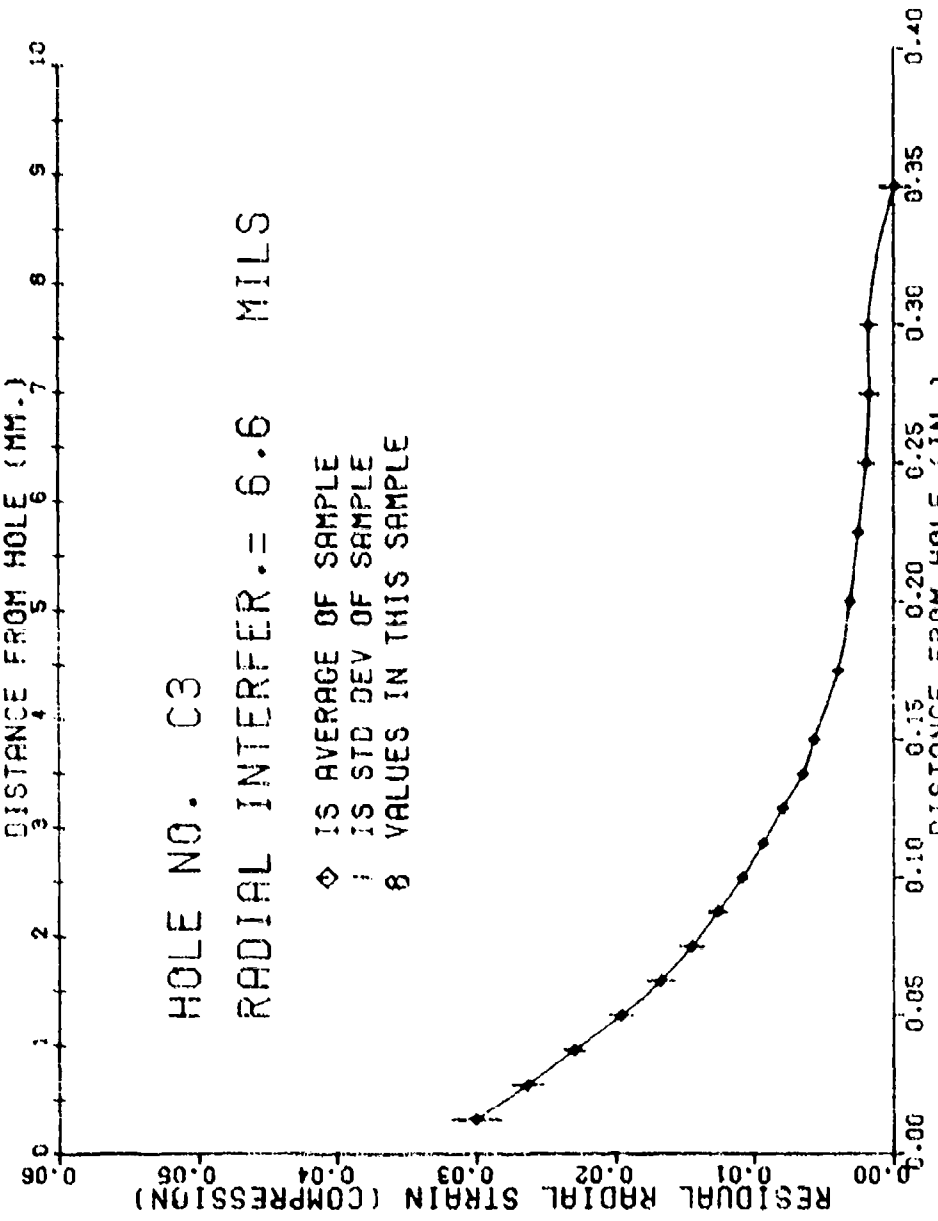

Figure 7.8 Typical statistical summary plot of all radial strain data for one hole (hole C3).

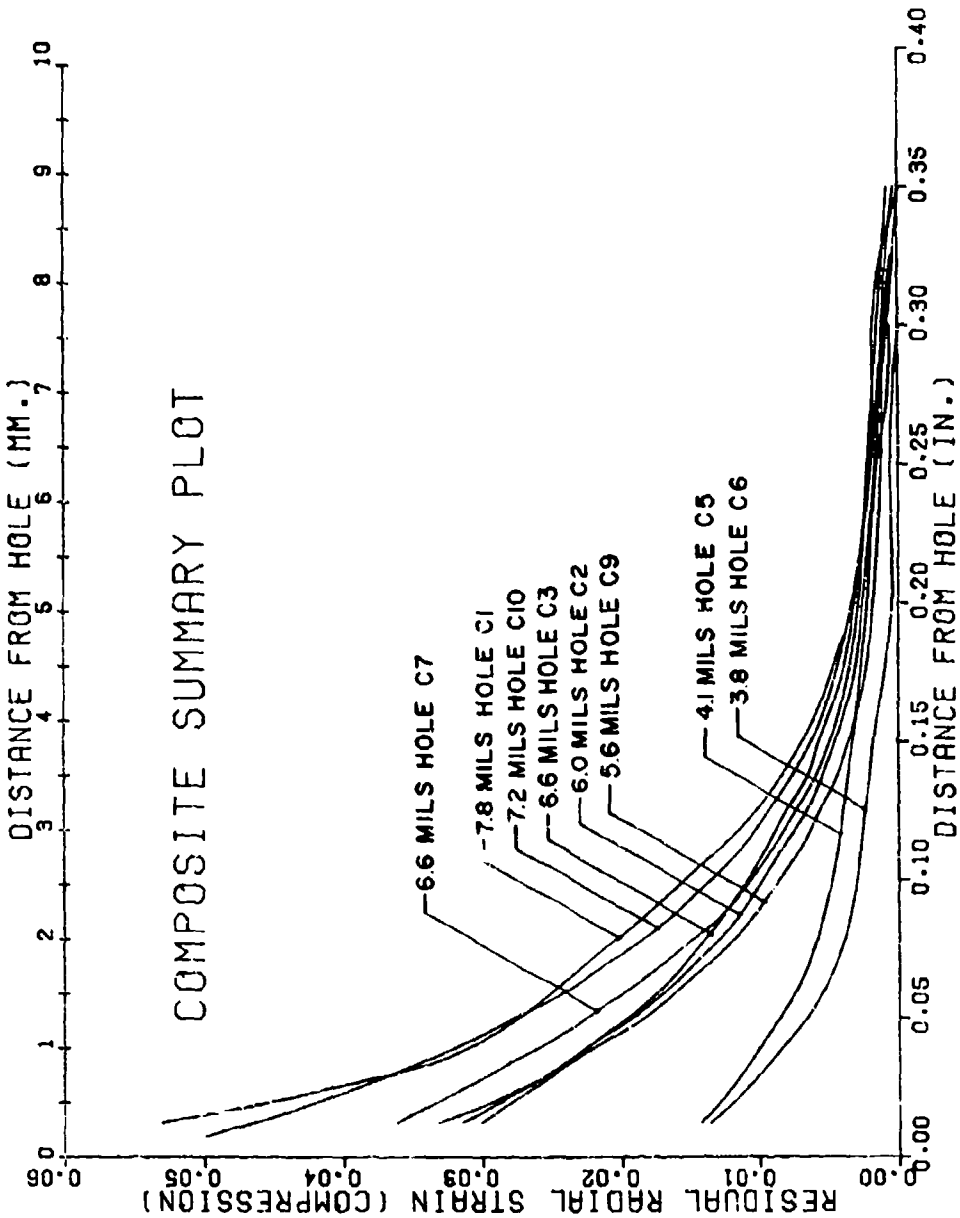

Figure 7.9 Typical composite statistical summary plot showing average radial strains for all coldworked levels.

The data for this analyses was generated by scaling strain values at several distances from the hole from all of the curves previously generated for each hole. Additional data includes hole label and interference level, number of points along the distance axis, the values of this distance scaled from the graphs in inches, the number of curves which are used as data, and the radial strain (scaled in inches) from each curve at each distance. Where appropriate, opposite sides of the hole were treated separately first and then rerun together. Also the two specimens which had identical coldwork levels were first treated separately and then combined. The flexibility of this program allowed it to be used in several different ways to fit these various situations without modification.

The specific functions of the program are:

1. Read data.

2. Scale data to correct for reading in inches from the graphs rather than in strain units and specimen dimensional units.

3. Compute average strain and standard deviation of the population of strain readings.

4. Draw, divide, and label plotting axes.

5. Plot the average strain and its standard deviation.

6. Draw a smooth curve through the plotted points. This curve-drawing algorithm uses a simple cubic spline function without smoothing. The curve passes through every data point with continuity of the function and its first two derivatives.

7. Print input data, scaled values, and computed statistical values.

8. Repeat, except for drawing axes and writing labels, for each set of data entered. That is, the statistical graphs for opposite sides of the hole can be drawn on one set of axes.

For generating composite summary graphs showing the strain distributions for several coldwork levels, the plotting of statistical values and the writing of some of the explanatory information on the graph are suppressed by making small changes in the program. The changes are printed as comments in the program listing in Appendix D.

5. DATA REDUCTION AND PLOTTING-TANGENTIAL STRAIN

The second routine, described in Section 7.4.3 served to reduce the data and plot the tangential strain distribution for a given hole. Here, the digitized data for each of the several chosen y-axes on any one fringe photo are entered as the several data sets for construction of the summary plot. The result is a plot of strain for each of these axes on one coordinate system. A sample of such a plot is shown in Figure 7.10 for study.

Because of time limitations, this program was not modified to correct axis labels and distance scales, which were left as they were for the radial strain analysis. An artificial value of the input parameter for the distance from fiducial mark to hole edge was entered to shift the x-0 axis to the center of the plot with existing scales. The "set name" data which was used to identify each curve in the radial strain summary was used to specify the location of the y-axis for each of the tangential strain plots. This procedure was not at all tidy, and it should be cleaned up if the program is used in the future for tangential strain analysis. The axis and scaling lables in Figure 7.10 have been fixed up to represent the true physical values.

The graph which is generated by the program is not in very useable form, as the desired result is a plot of the tangential strain versus distance from the hole along a radial axis. This final plot was constructed for each coldwork level for which tangential strain was studied by determining the points of intersection of the

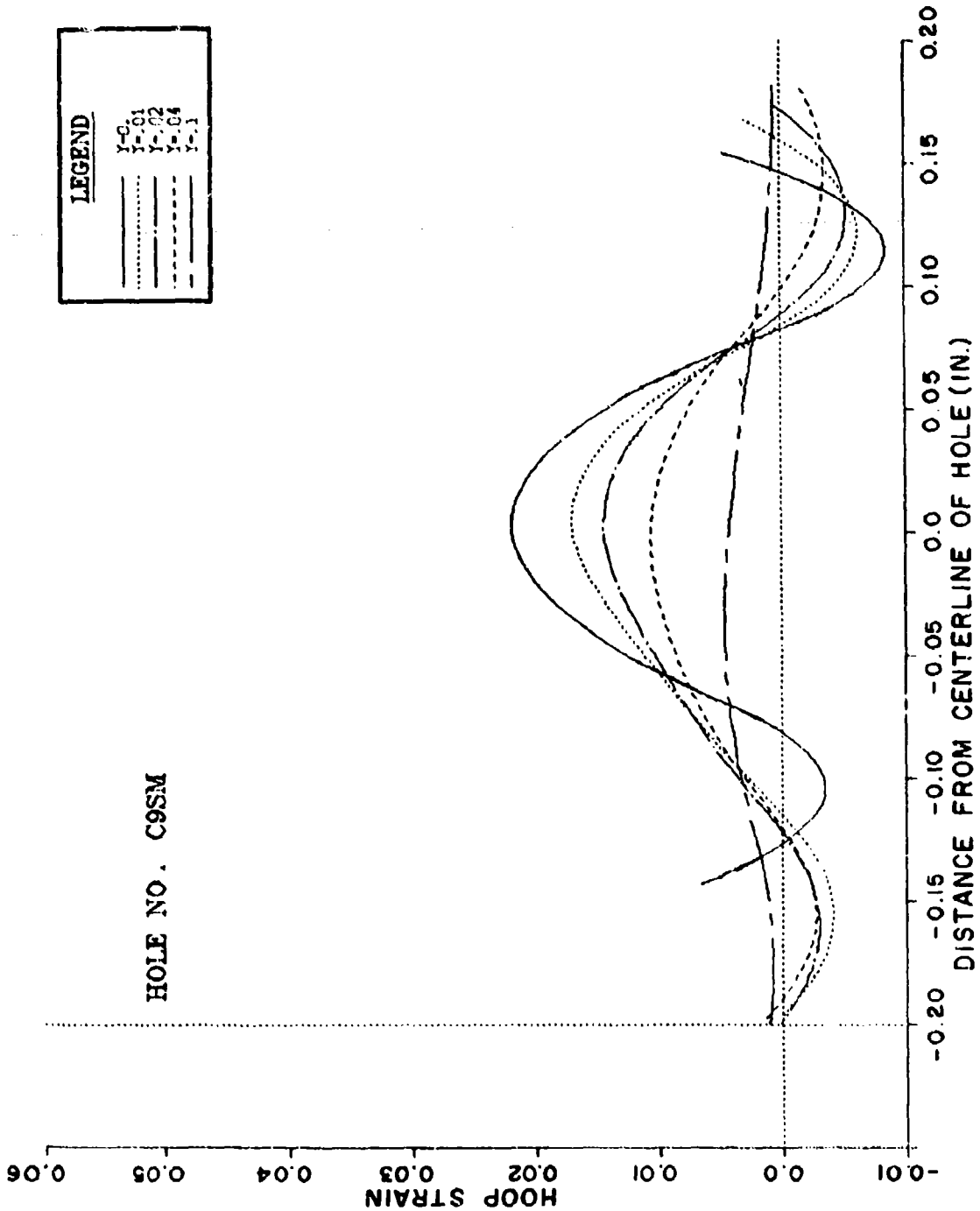

Figure 7.10 Typical plot of hoop strain distributions along several Y-axes at different radial distances.

tangential strain curves with the vertical axis, which represents the radial x-axis through the hole center. These values were replotted as a function of x-distance from the hole; the result is, for each hole, a plot of ϵ_y versus x for y = 0. A typical example of such a plot appears in Figure 7-11. A duplicate of this graph, and the remainder like it, are presented with the results in the next section.

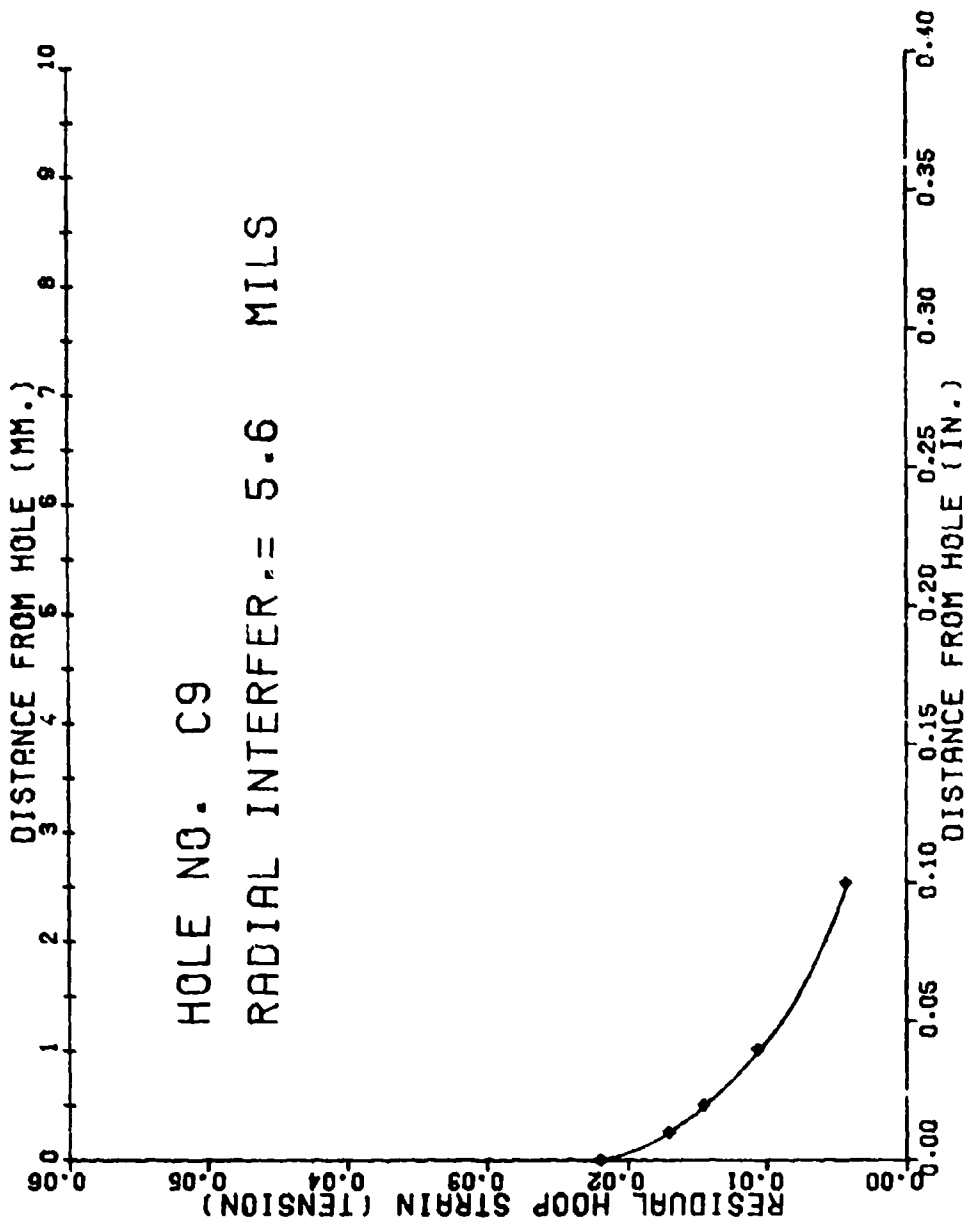

Figure 7.11 Typical distribution of tangential strain as a function of radial distance from hole.

SECTION VIII

STRAIN MEASUREMENT RESULTS

1. INTRODUCTORY COMMENTS

The purpose of this section is merely to present as a coherent unit all of the results of the moire measurement of strain near holes having various degrees of cold-work. Comparison of the results with those of other investigators, assessment of scatter and uncertainty, and discussion of several specific aspects of the data appear in Section IX.

Samples of the detailed data analysis plots showing fringe orders, displacement distribution, and strain distribution which were generated have been presented with the description of the corresponding computer routine in Section 7.4.2. There were a good many of these graphs, since there were three plots for nearly every set of moire fringe data. The graphs served their purpose in facilitating diagnosis of procedural and computational errors. All useful results, with the exception of the displacement plots which might prove valuable in the long run, are contained in the various strain summary plots which were generated as described in Sections 7.4.3 and 7.4.4. It seems unwise to include any more of the detailed plots in this report. They can be obtained through AFML/LLN or Dr. G. Cloud.

2. RESULTS-RADIAL STRAIN

The plots of radial strain are grouped according to level of coldworking. The graphs showing all individual results from each data set for each hole are in the first group. The statistical summary plots for each hole are in the second group. A composite graph of strain for all the coldworking levels and the average uncertainty is given as the final radial strain result.

Plots of radial strain versus distance from the hole boundary for each of the coldwork levels appear in Figures 8.1 through 8.8. Each of these graphs shows the strain distributions obtained from the several individual sets of data for that hole.

The statistical summaries of all the sets of data for each hole are given in Figure 8.9 through 8.20. If detailed examination of the data suggested a significant difference between opposite sides of a hole, then the sides are treated separately in the first plot for that hole, and they are lumped together in the second plot for the hole. An exception is specimen C10. The 4 extremes (North, South, East and West) of the hole were investigated, and the data shows an interesting and consistent pattern. There were only 2 sets of data for each side, however (excepting the East side which had one), which was not enough for statistical analysis of each side separately, only the overall summary plot was prepared for C10. Another exception is created by the fact that specimens C3 and C7 had the same coldworking levels, and the opposite sides of C3 were found to differ. Two summary plots (Figures 8.14 and 8.15 were prepared to show C3 East, C3 West, and C7 separately. Another graph (Figure 8.16) shows the average of all data for C3 plus the curve for C7. A third is the statistical summary for all C3 and C7 data combined (Figure 8.17).

Figure 8.21 is a composite summary of all the radial strain data. Also included is an average error analysis curve which is explained in Section 9.4. The data from C7 and C3 are combined in constructing this graph, as explained above. The peculiar tail on the curve for hole C1 in the neighborhood of r=.2 inches is believed to be an artifact of the data analysis procedure resulting from the way in which the voluminous fringe data for this hole was truncated at a fiducial mark. This tail tends to confuse the picture, so the troublesome portion was deleted on the composite summary. As mentioned in Section 7.4.4, the statistical symbols and data points have been eliminated from the composite plots for clarity.

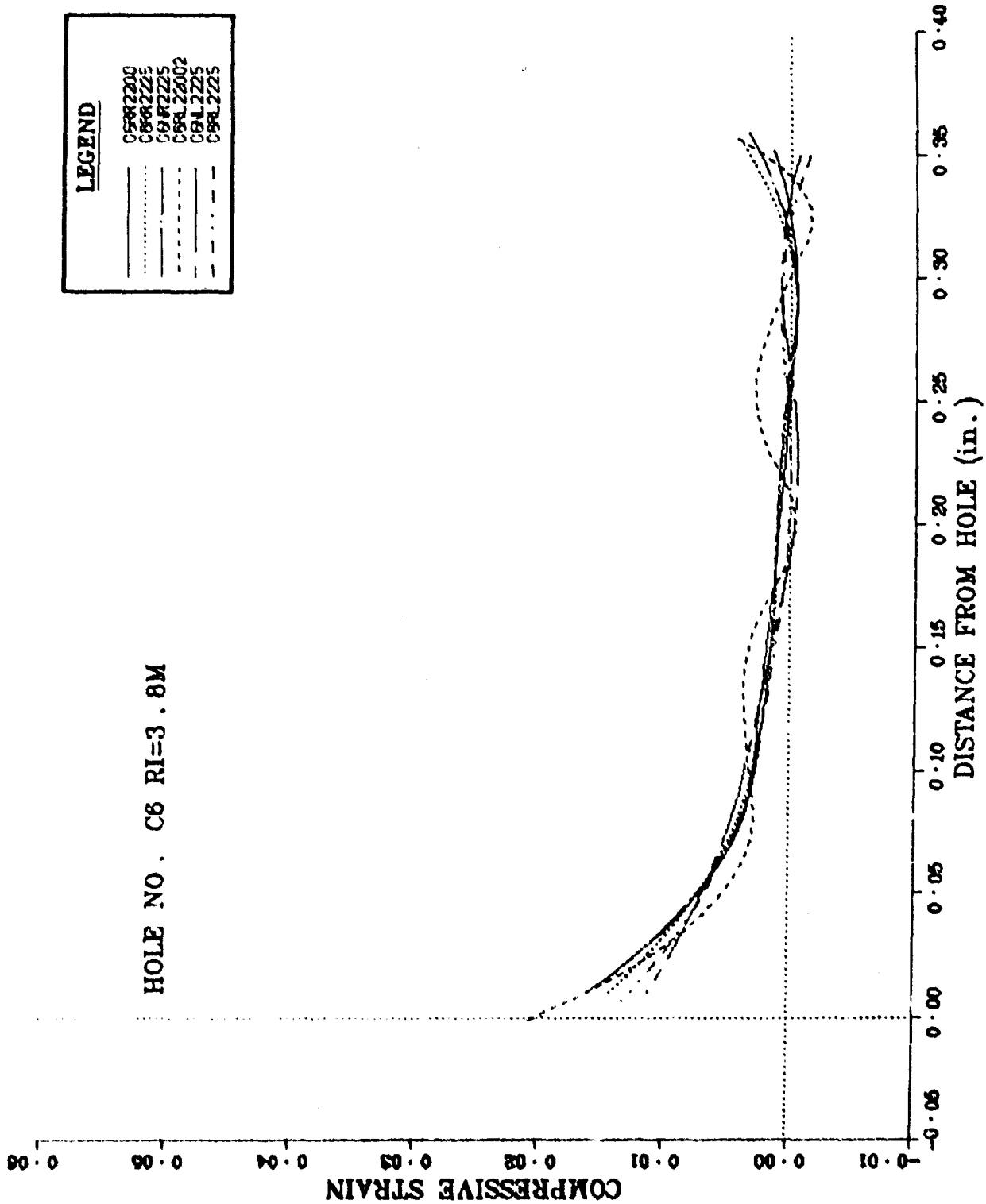

Figure 8.1 Measured distributions of residual surface strain near cold-worked hole for 3.8 mils radial interference (hole C6).

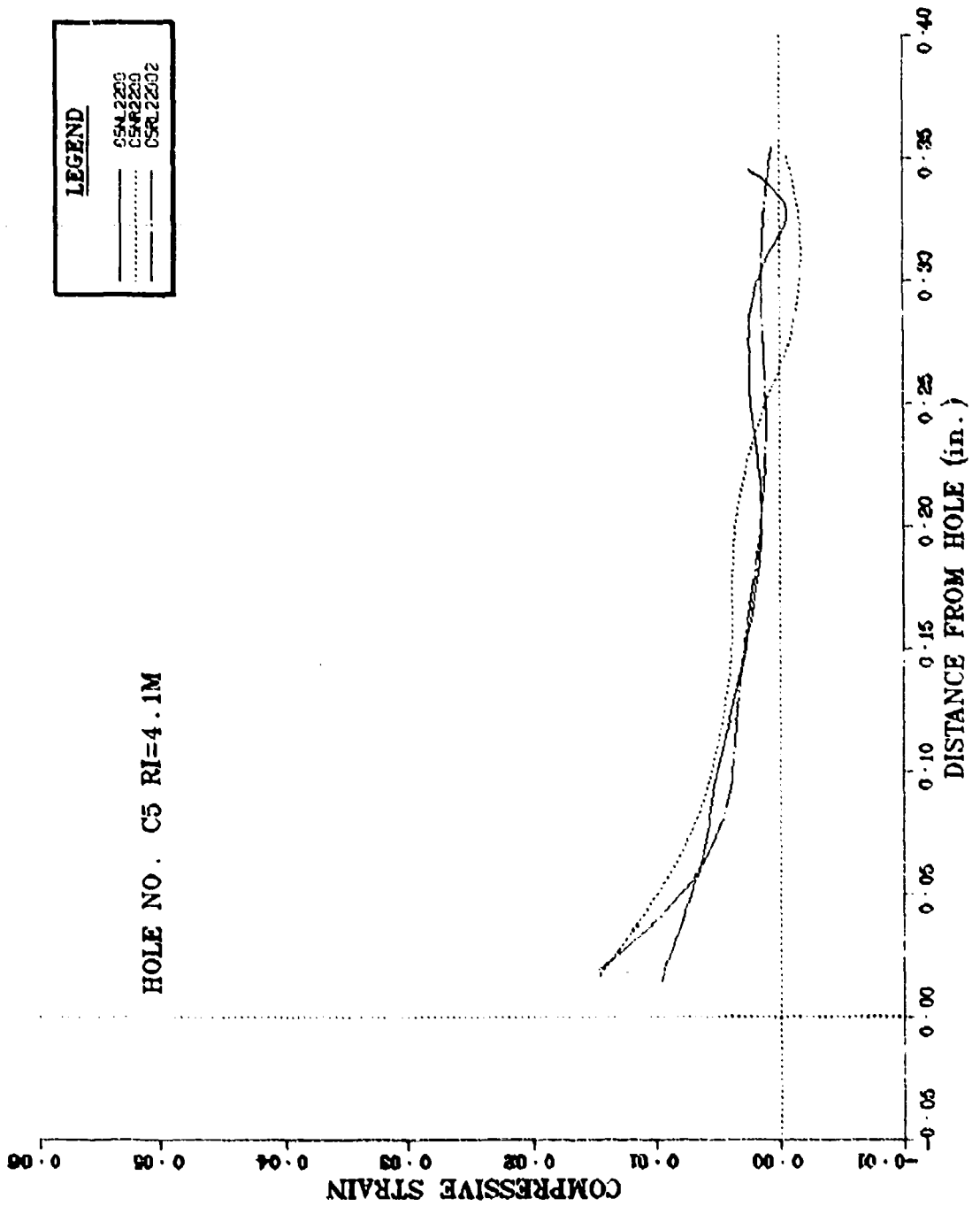

Figure 8.2 Measured distributions of residual surface strain near cold-worked hole for 4.1 mils radial interference (hole C5).

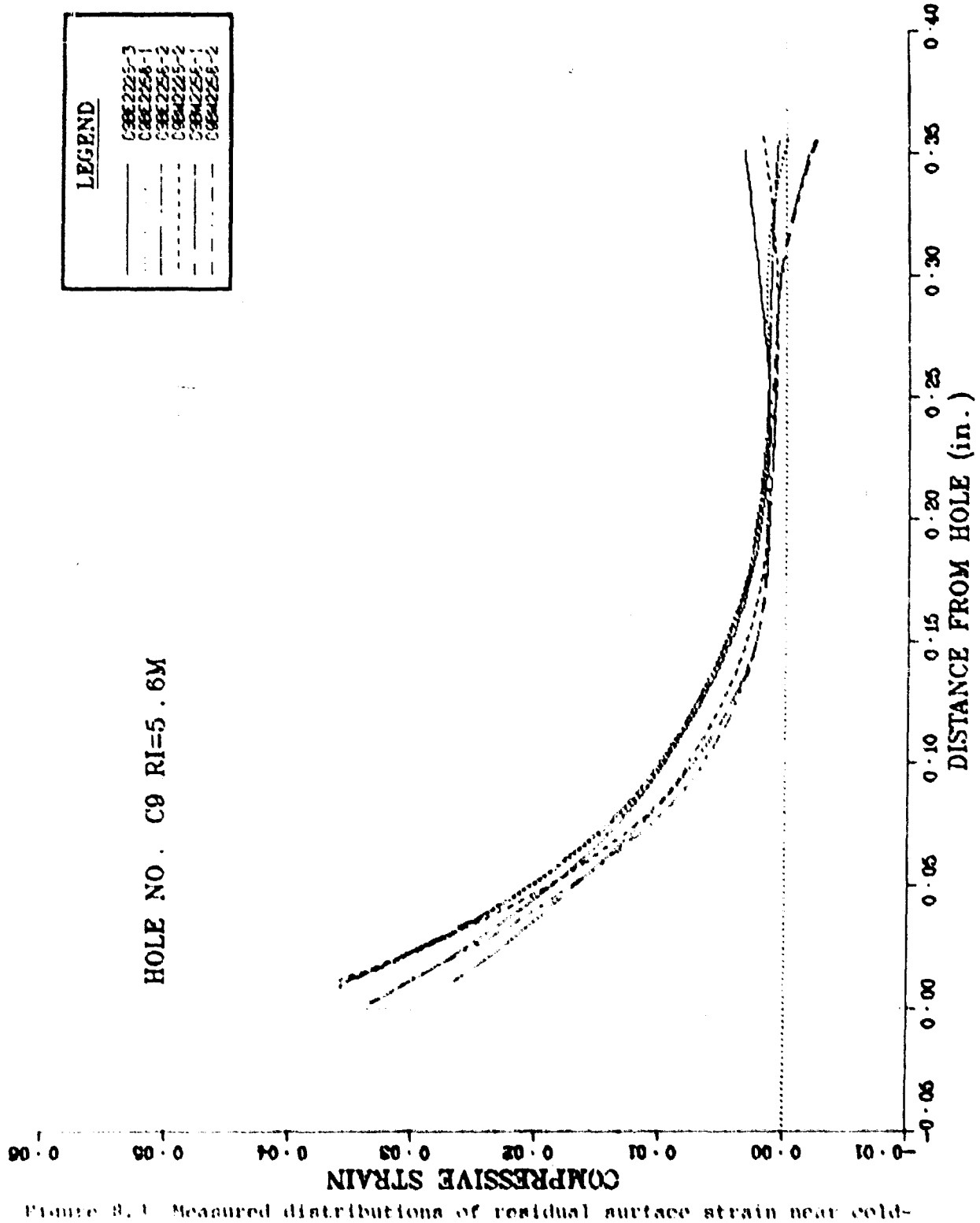

Figure 8.1 Measured distributions of residual surface strain near cold-worked hole for 5.6 mils radial interference (hole C9).

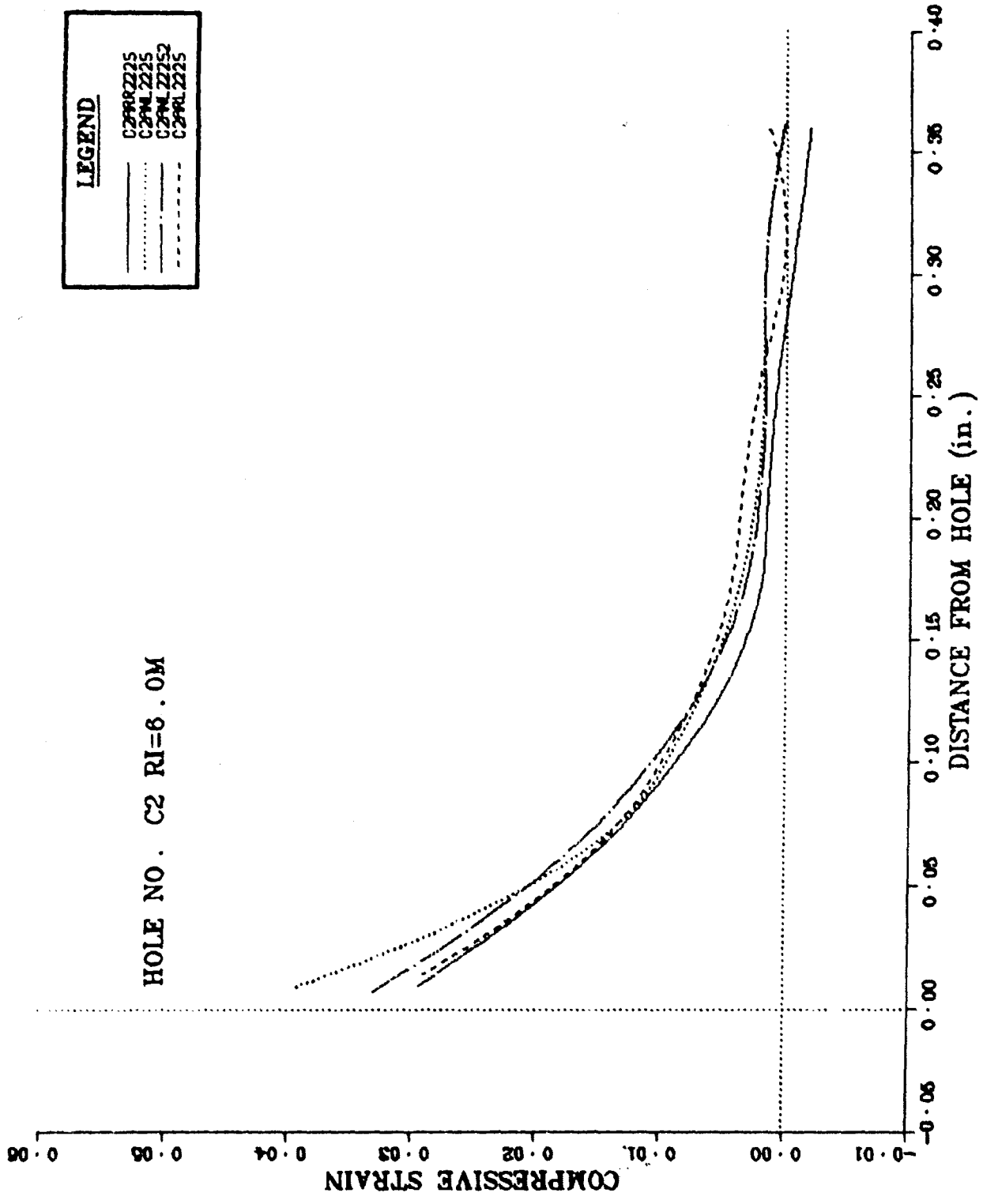

Figure 3.4 Measured distributions of residual surface strain near cold-worked hole for 6.0 mils radial interference (hole C2).

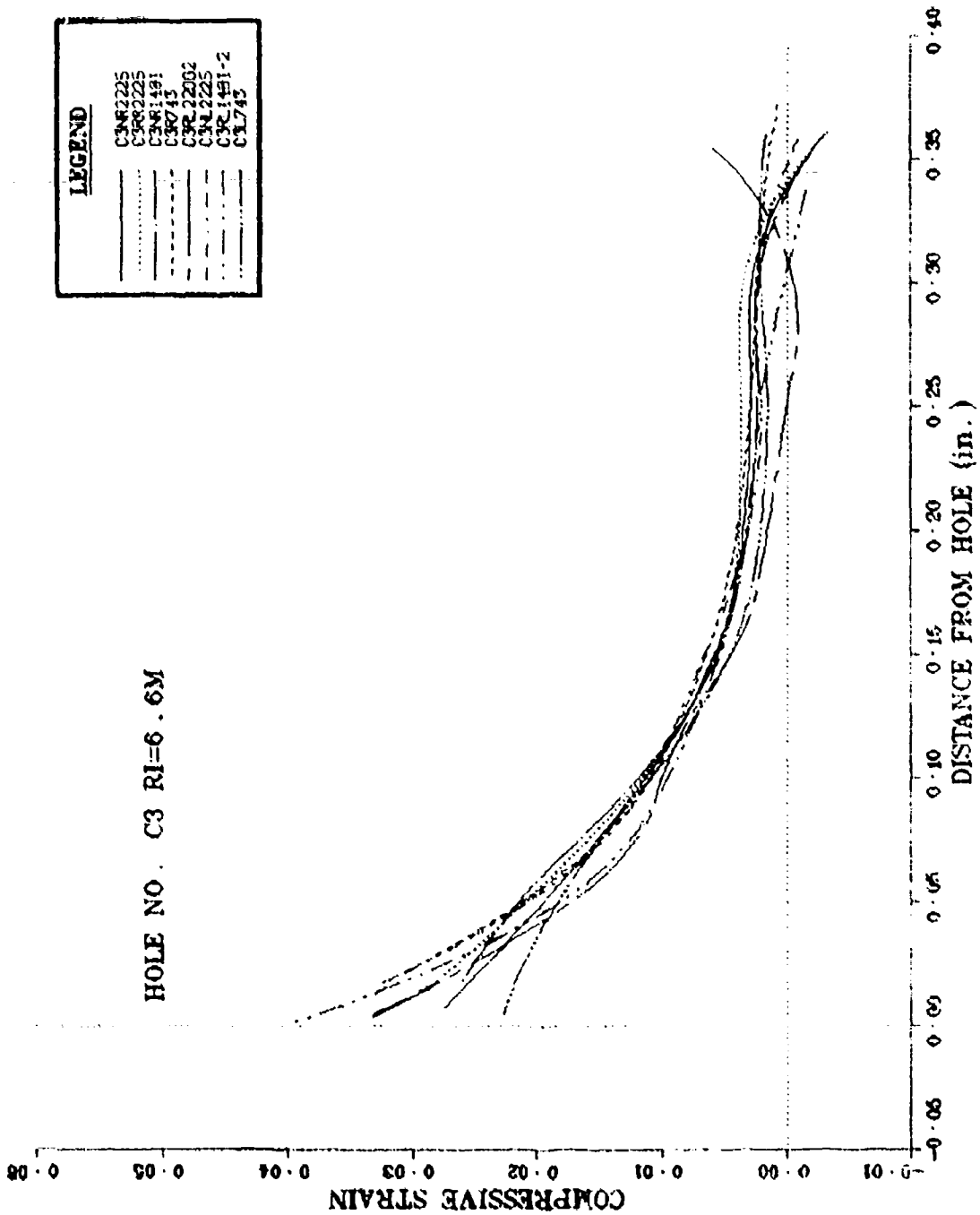

Figure 8.5 Measured distributions of residual surface strain near cold-worked hole for 6.6 mils radial interference (hole C3).

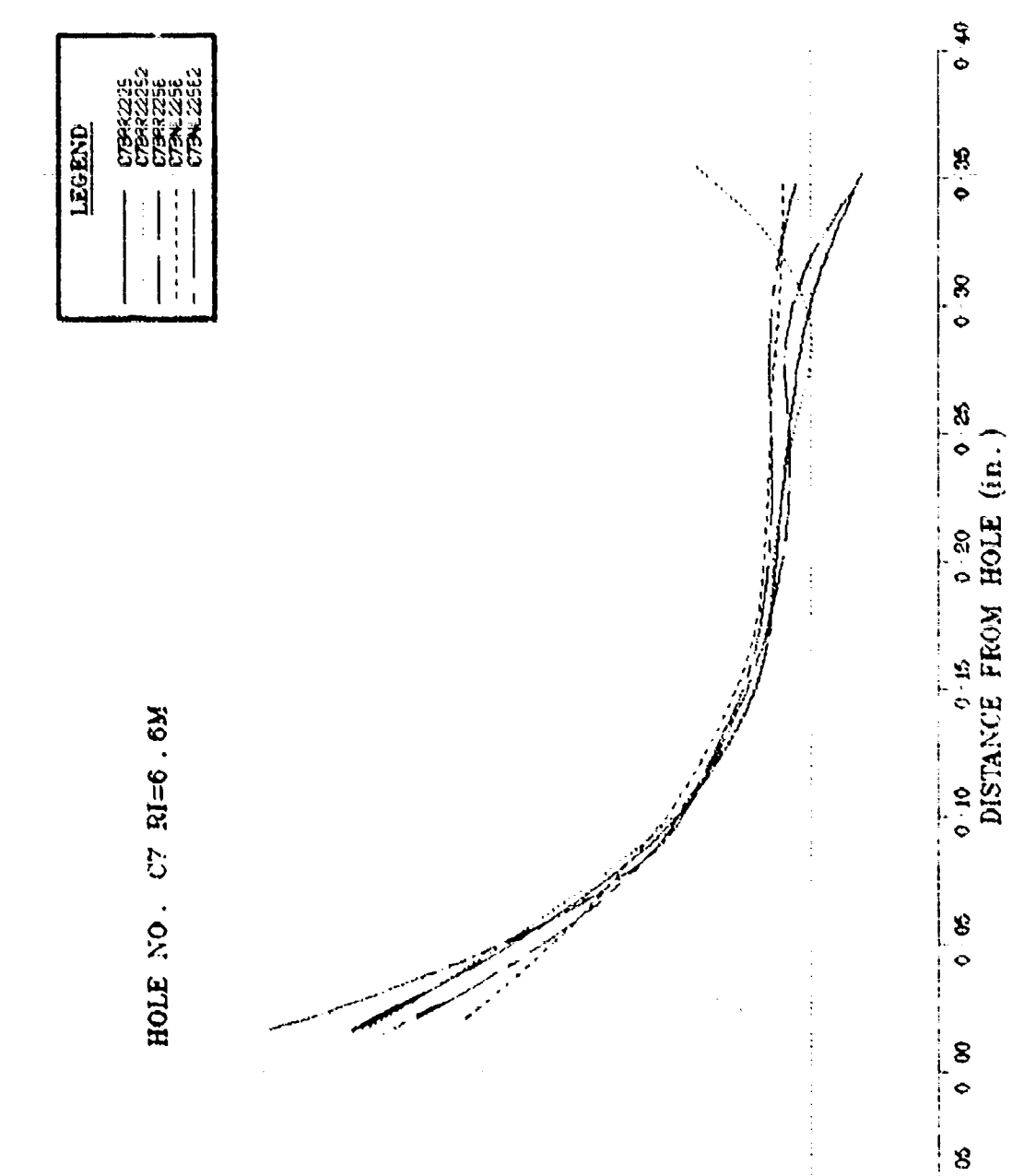

Figure 3.6 Measured distributions of residual surface strain near cold-worked hole for 6.6 mils radial interference (hole C7).

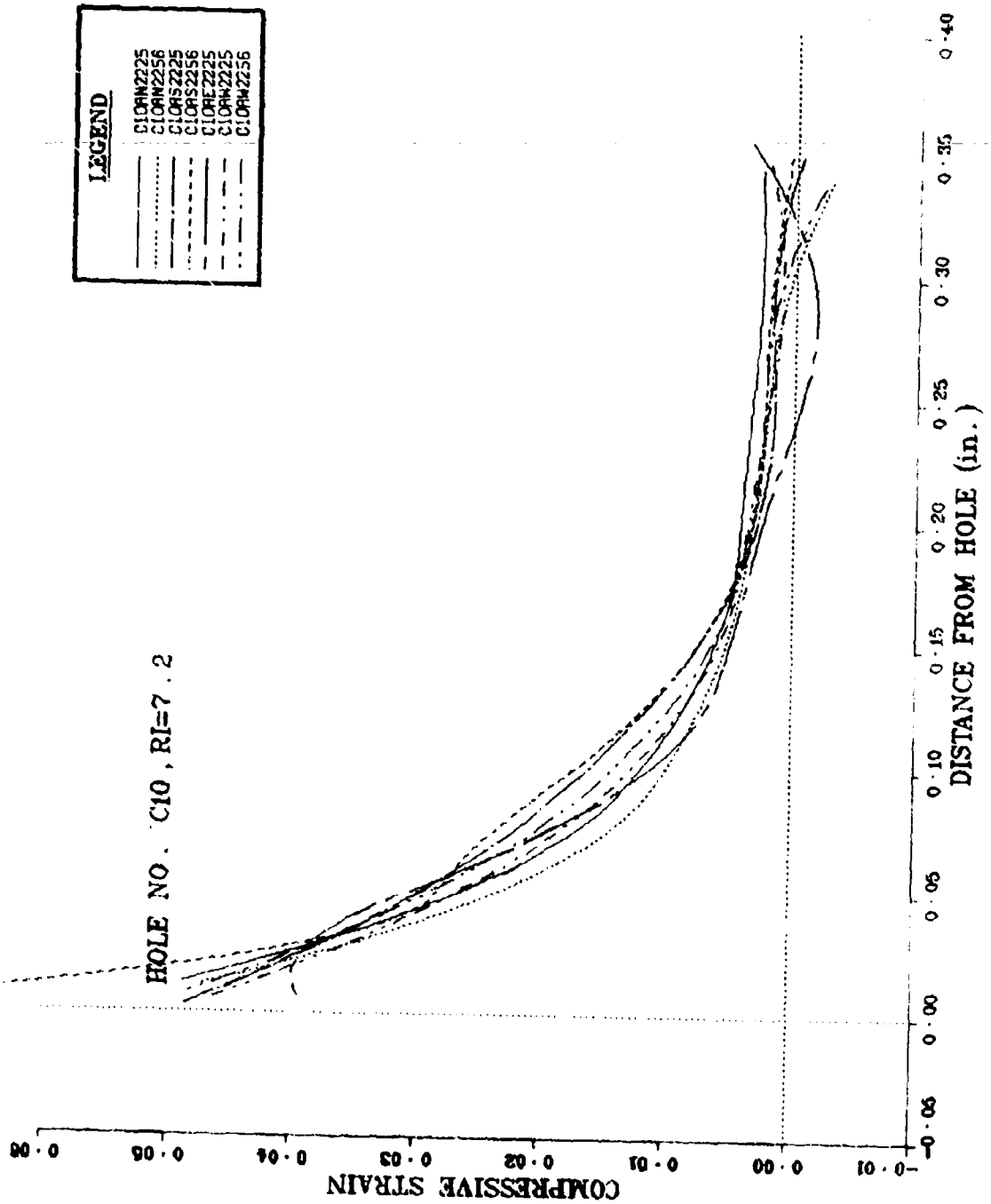

Figure 8.7 Measured distributions of residual surface strian near cold-worked hole for 7.2 mils radial interference (hole C10).

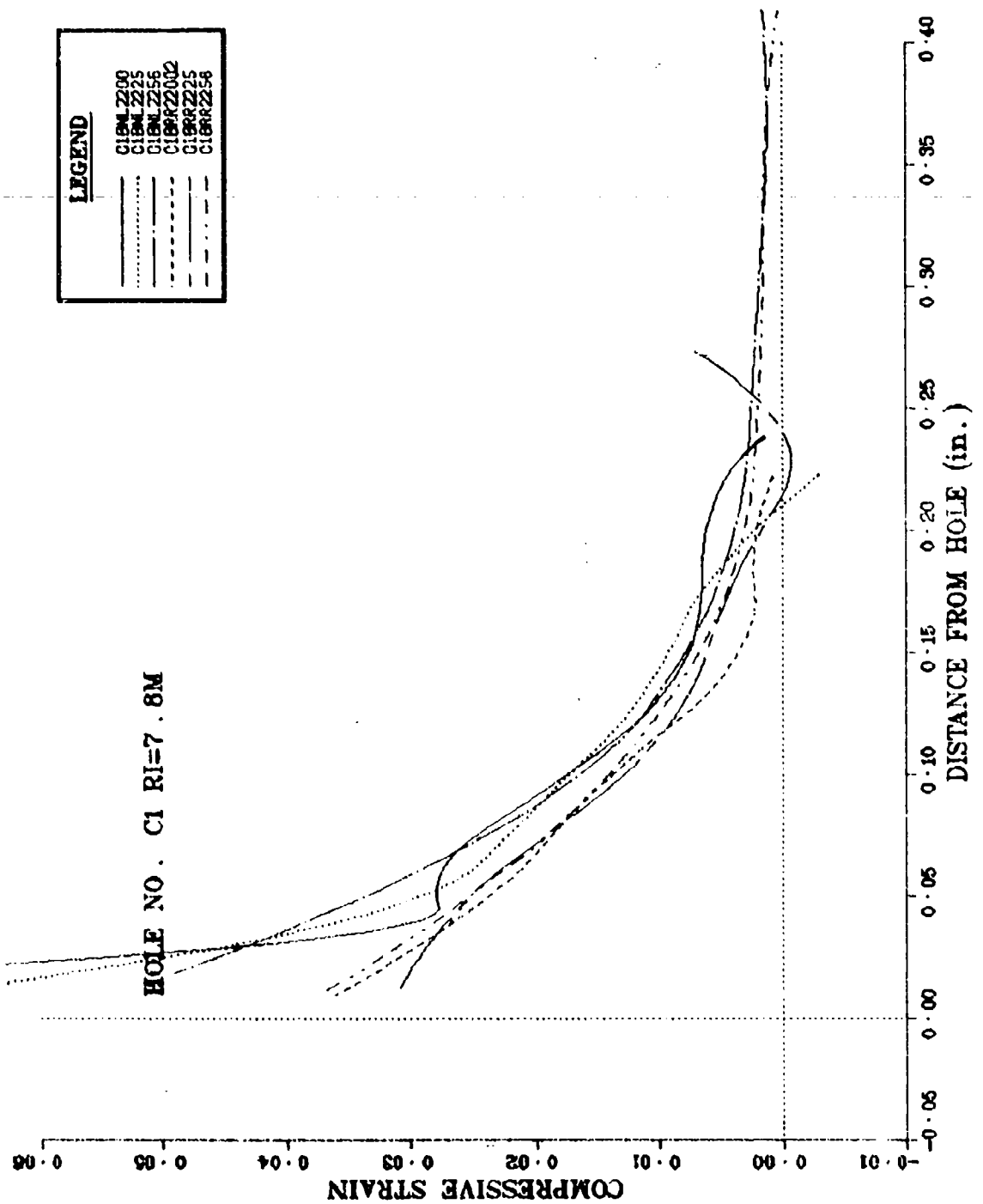

Figure 8.8 Measured distributions of residual surface strain near cold-worked hole for 7.8 mils radial interference (hole C1).

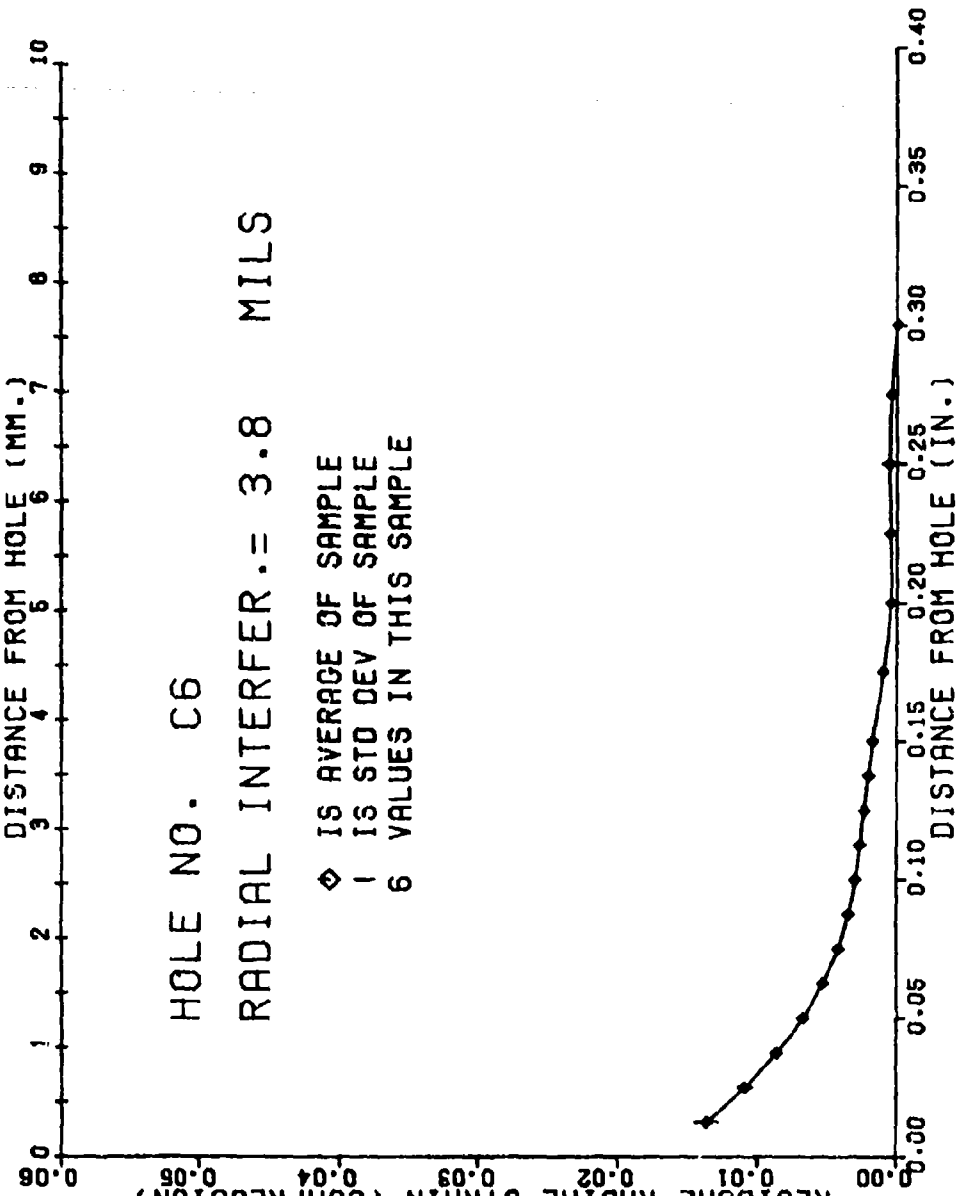

Figure 8.9 Average and standard deviation of radial strain near coldworked hole for 3.8 mils radial interference - all data for hole C6.

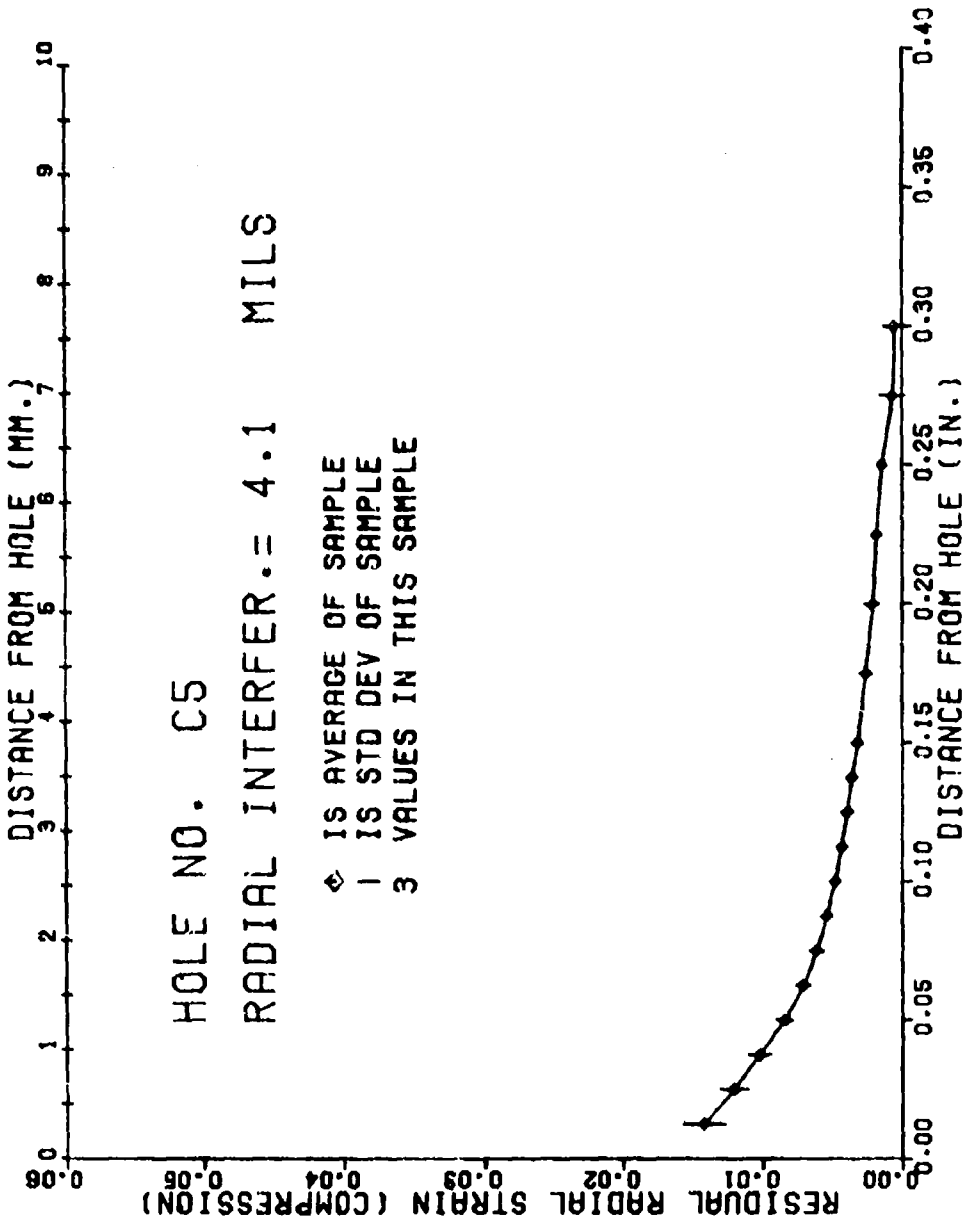

Figure 8.10 Average and standard deviation of radial strain near coldworked hole for 4.1 mils radial interference - all data for hole C5.

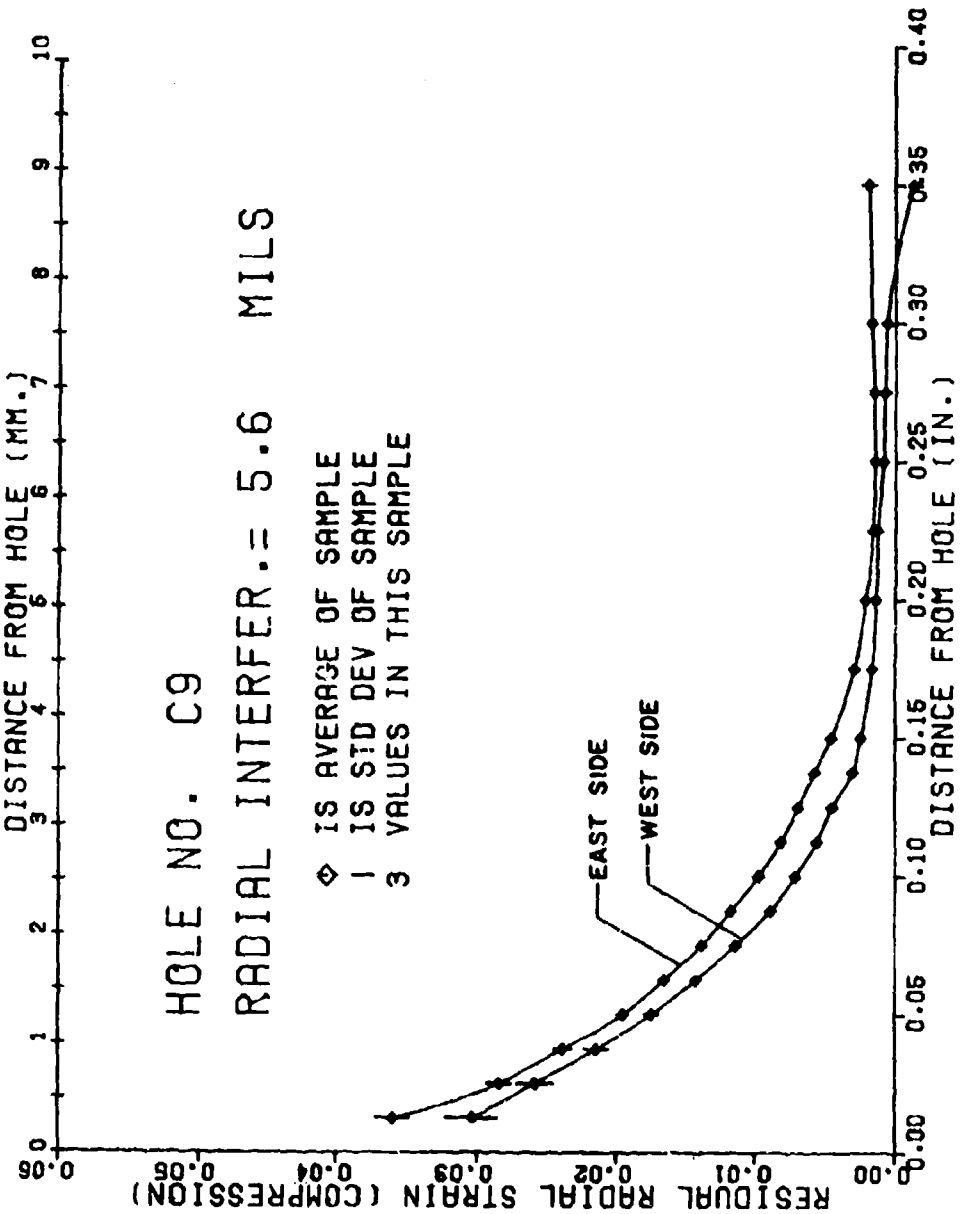

Figure 8.11 Average and standard deviation of radial strain near coldworked hole for 5.6 mils radial interference - opposite sides of hole C9 separate.

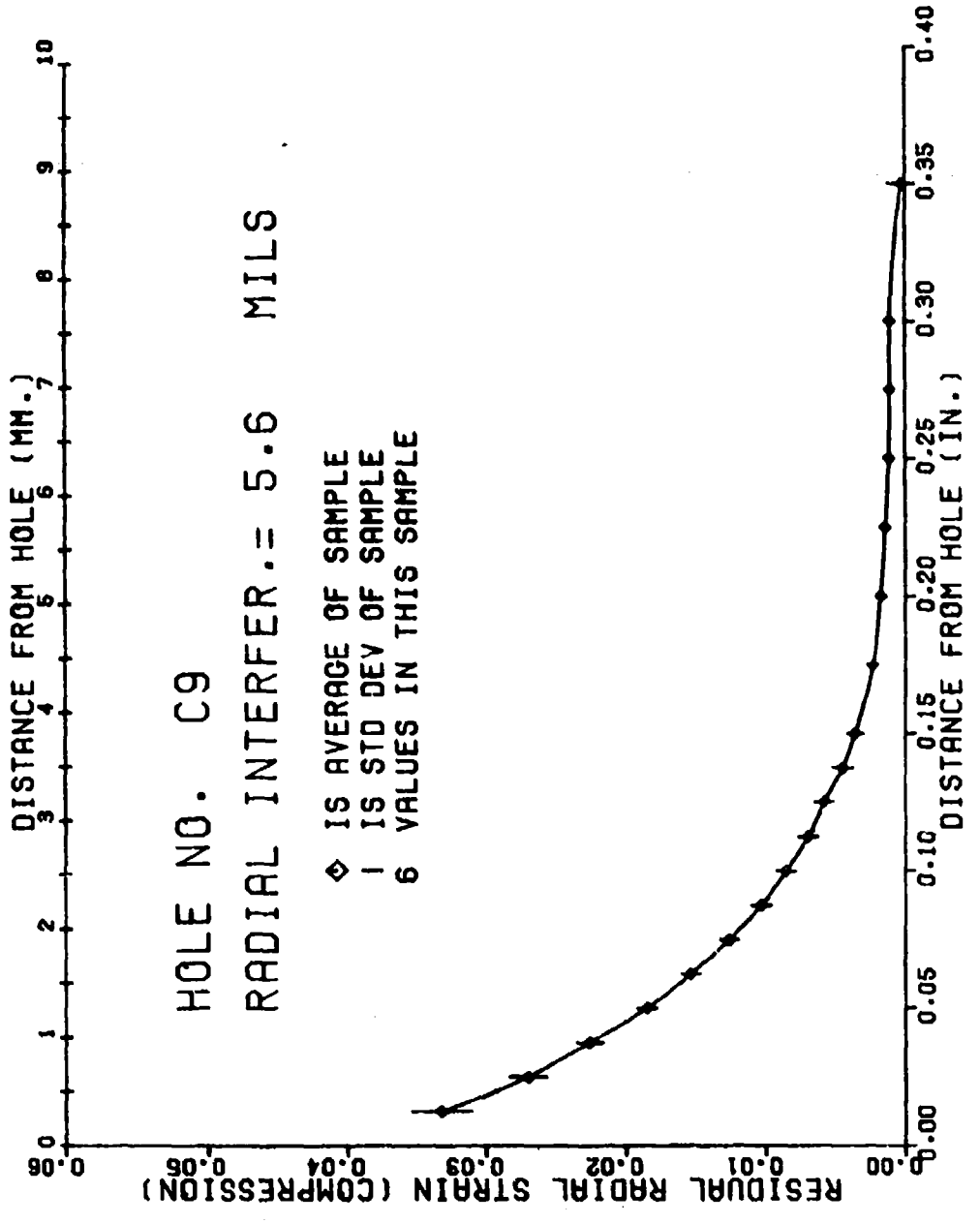

Figure 8.12 Average and standard deviation of radial strain near coldworked hole for 5.6 mils radial interference - all data for hole C9.

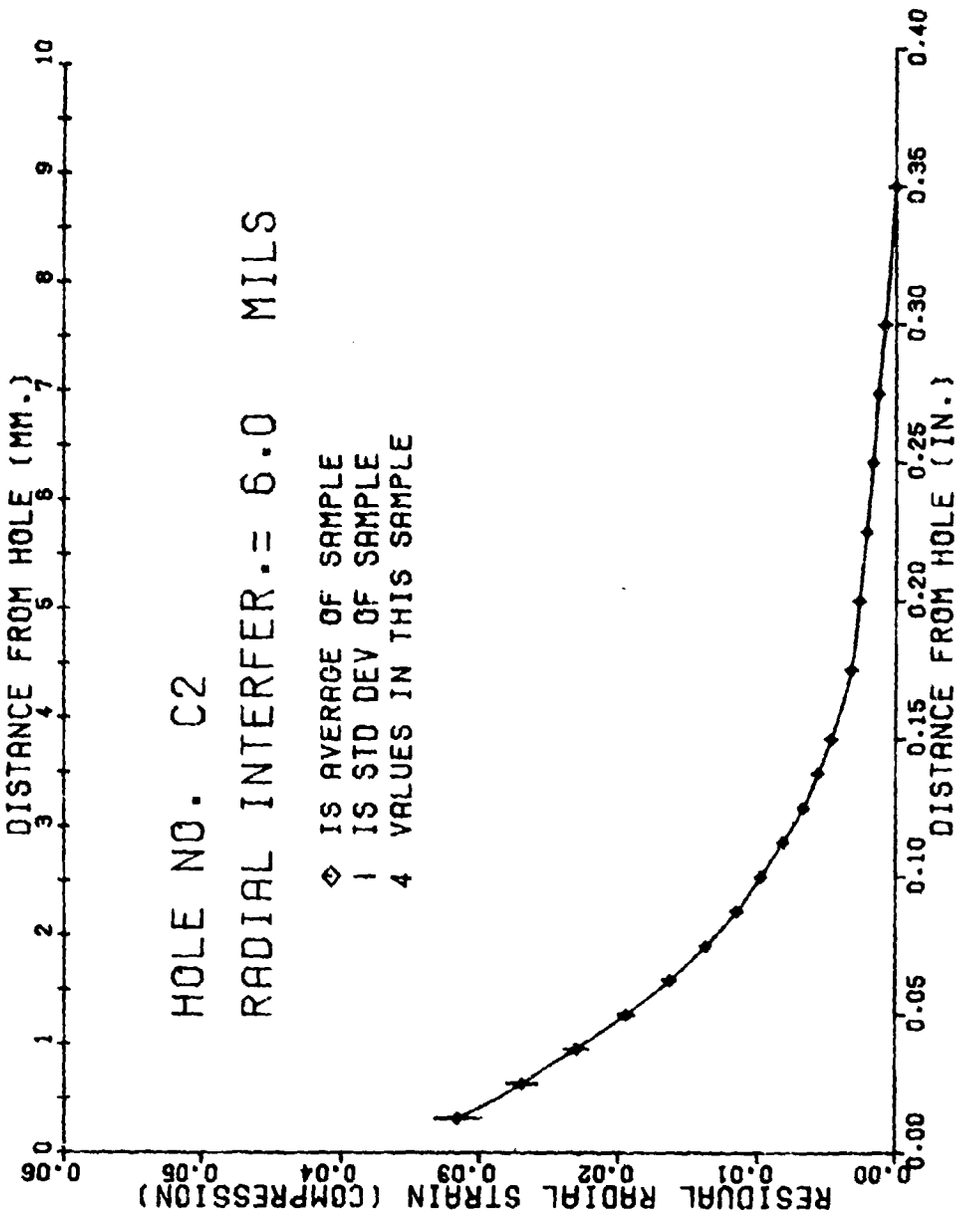

Figure 3.13 Average and standard deviation of radial strain near coldworked hole for 6.0 mils radial interference - all data for hole C2.

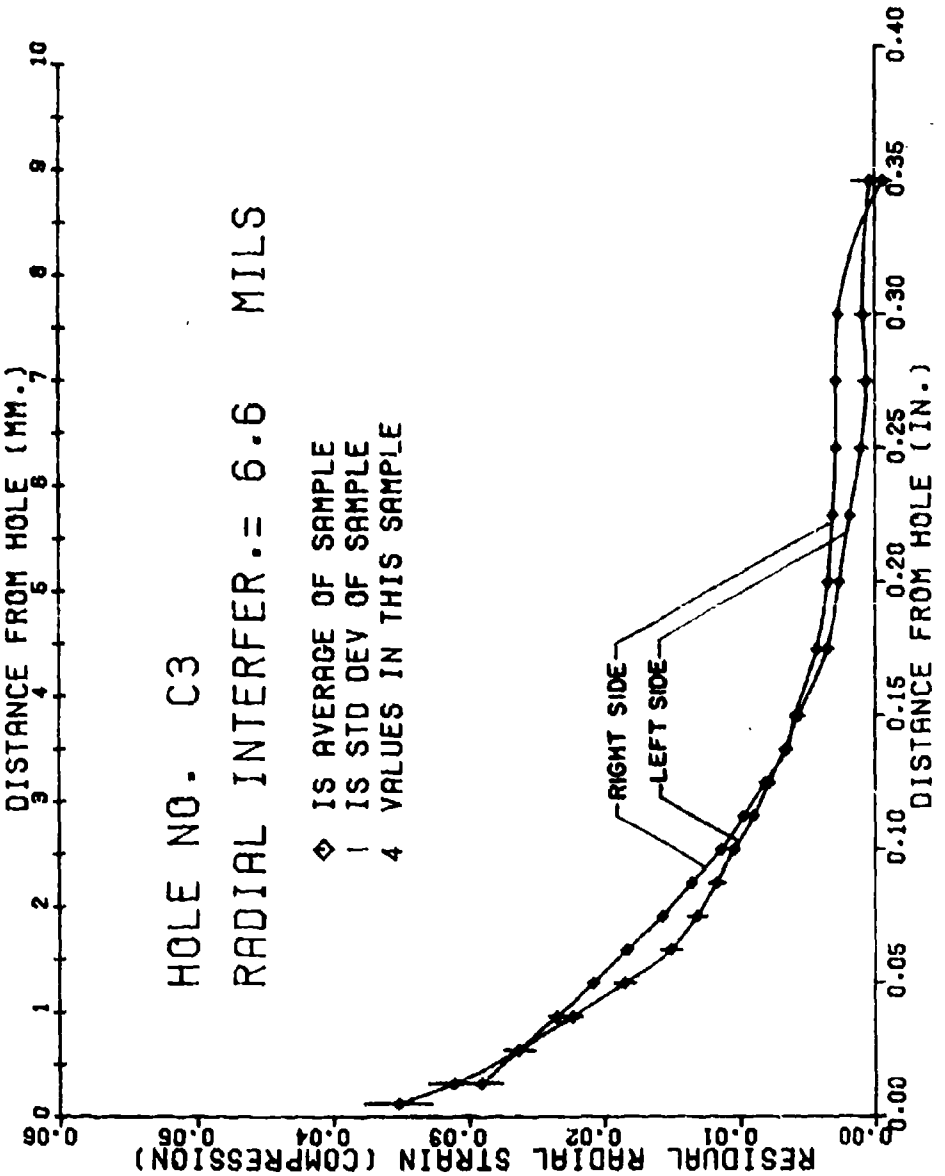

Figure 8.14 Average and standard deviation of radial strain near coldworked hole for 6.6 mils radial interference - opposite sides for hole C3 separate.

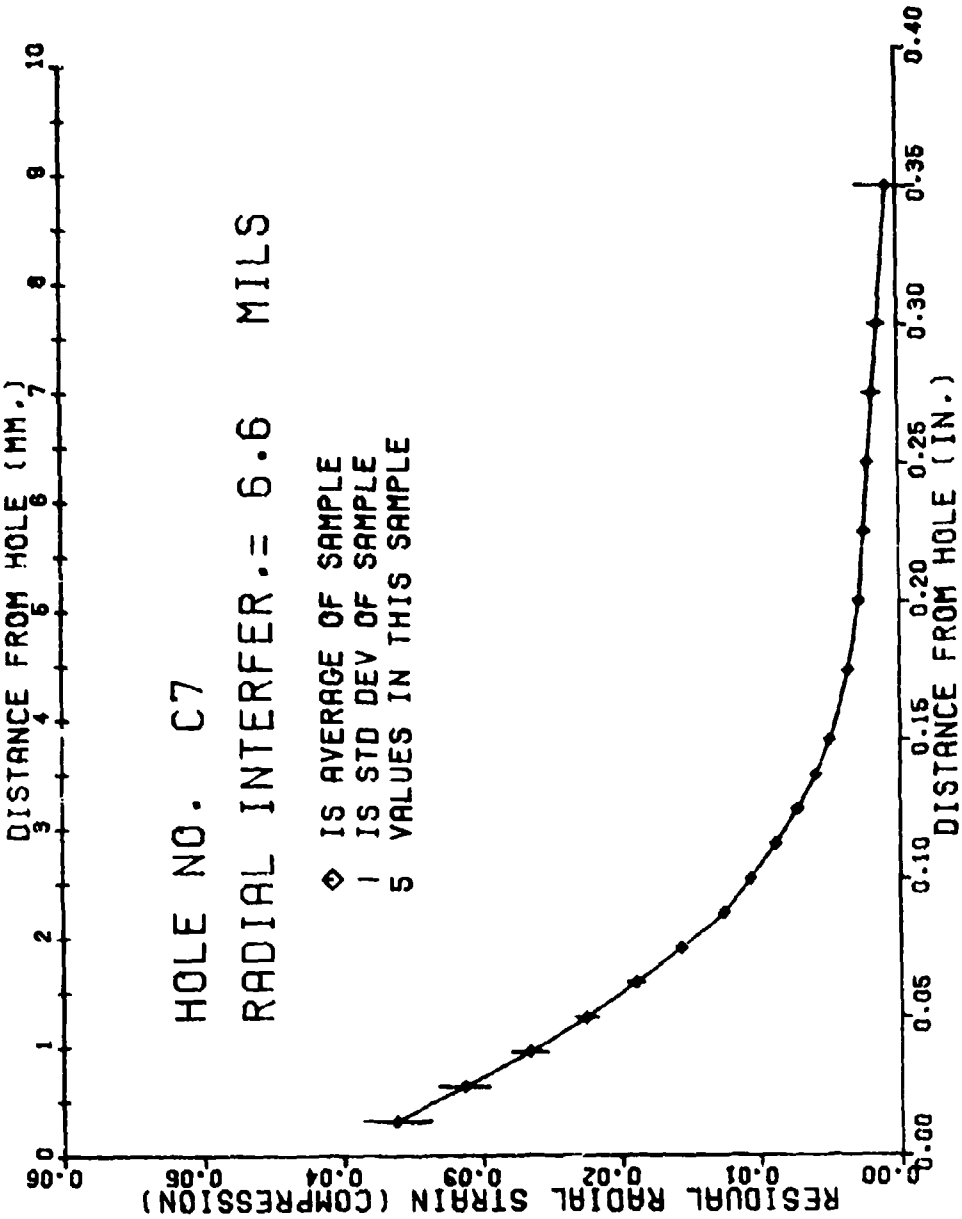

Figure 8.15 Average and standard deviation of radial strain near coldworked hole for 6.6 mils radial interference - all data for hole C7.

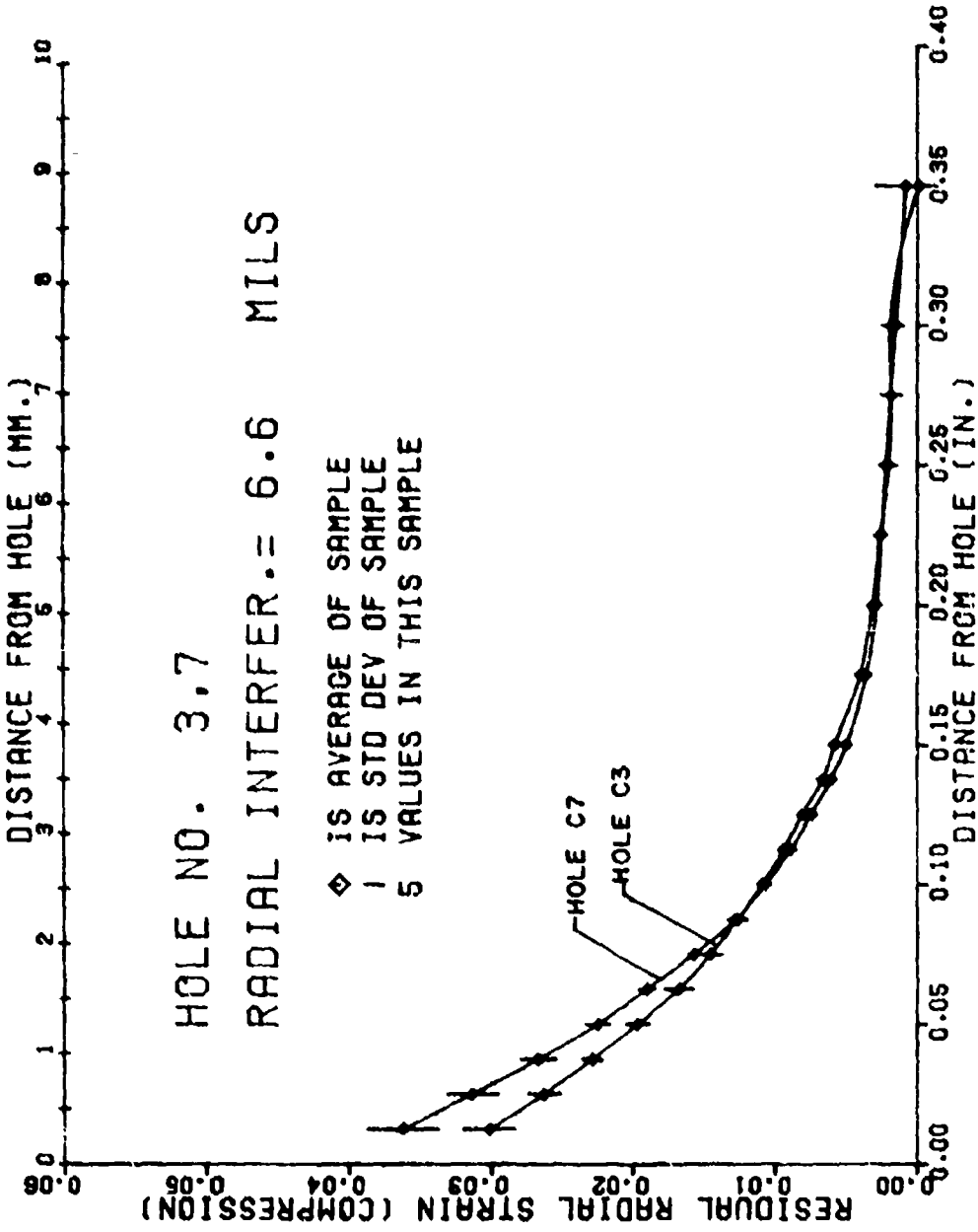

Figure 8.16 Average and standard deviation of radial strain near coldworked hole for 6.6 mils radial interference - all data for hole C3 and all data for hole C7 separate.

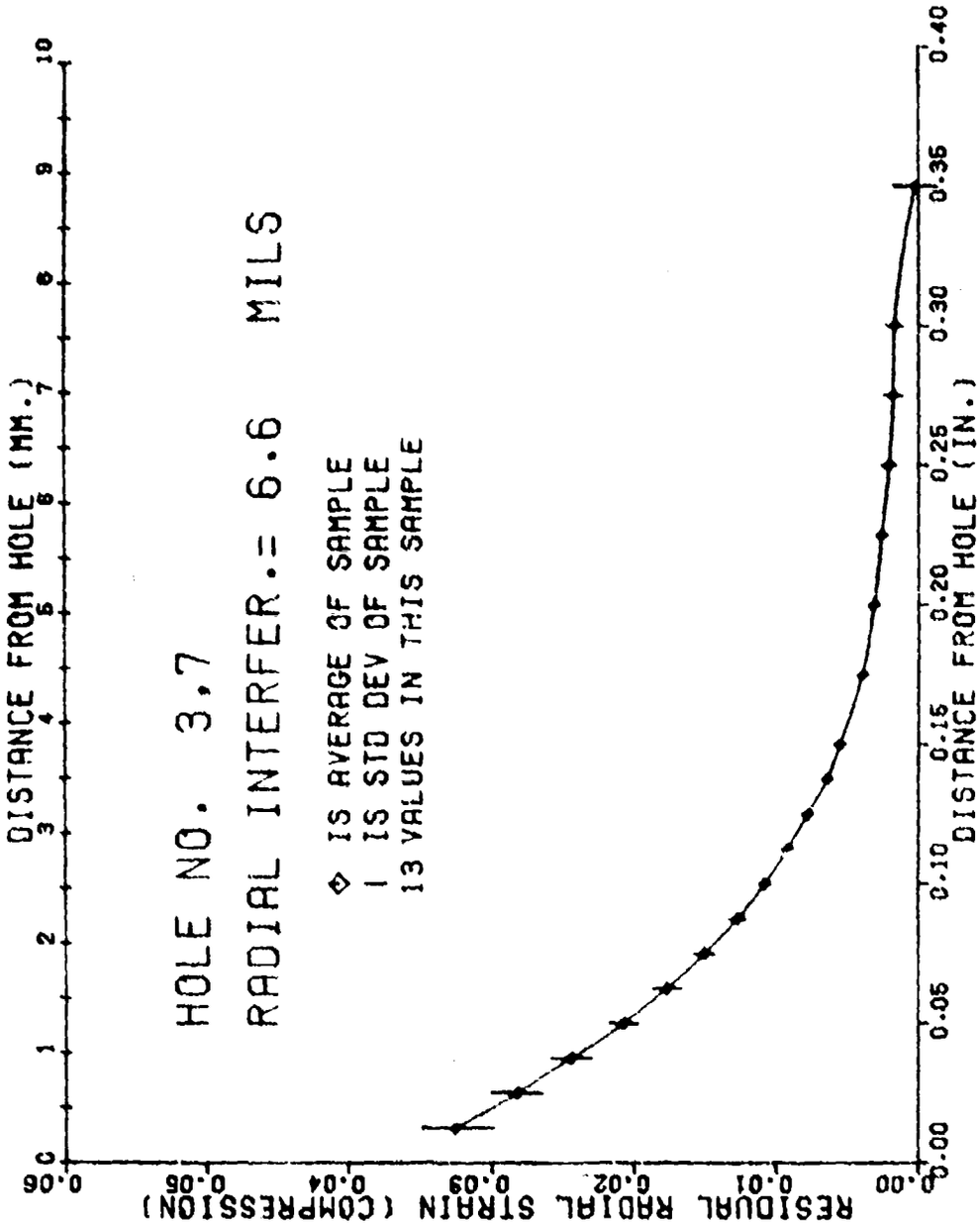

Figure 8.1 Average and standard deviation of radial strain near coldworked hole for 6.6 mils radial interference - all data from holes C3 and C7 combined.

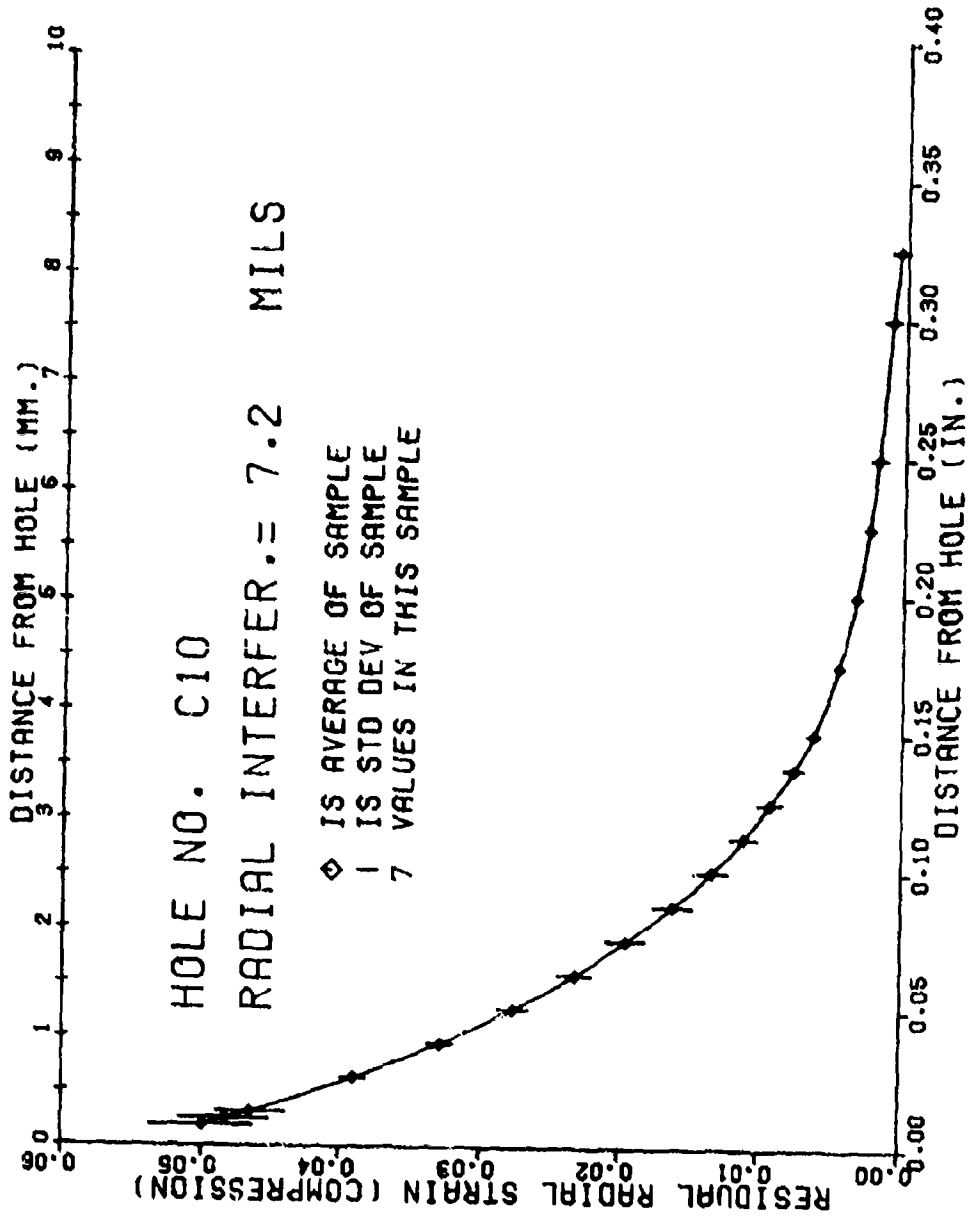

Figure 8.18 Average and standard deviation of radial strain near coldworked hole for 7.2 mils radial interference - all data for hole C10.

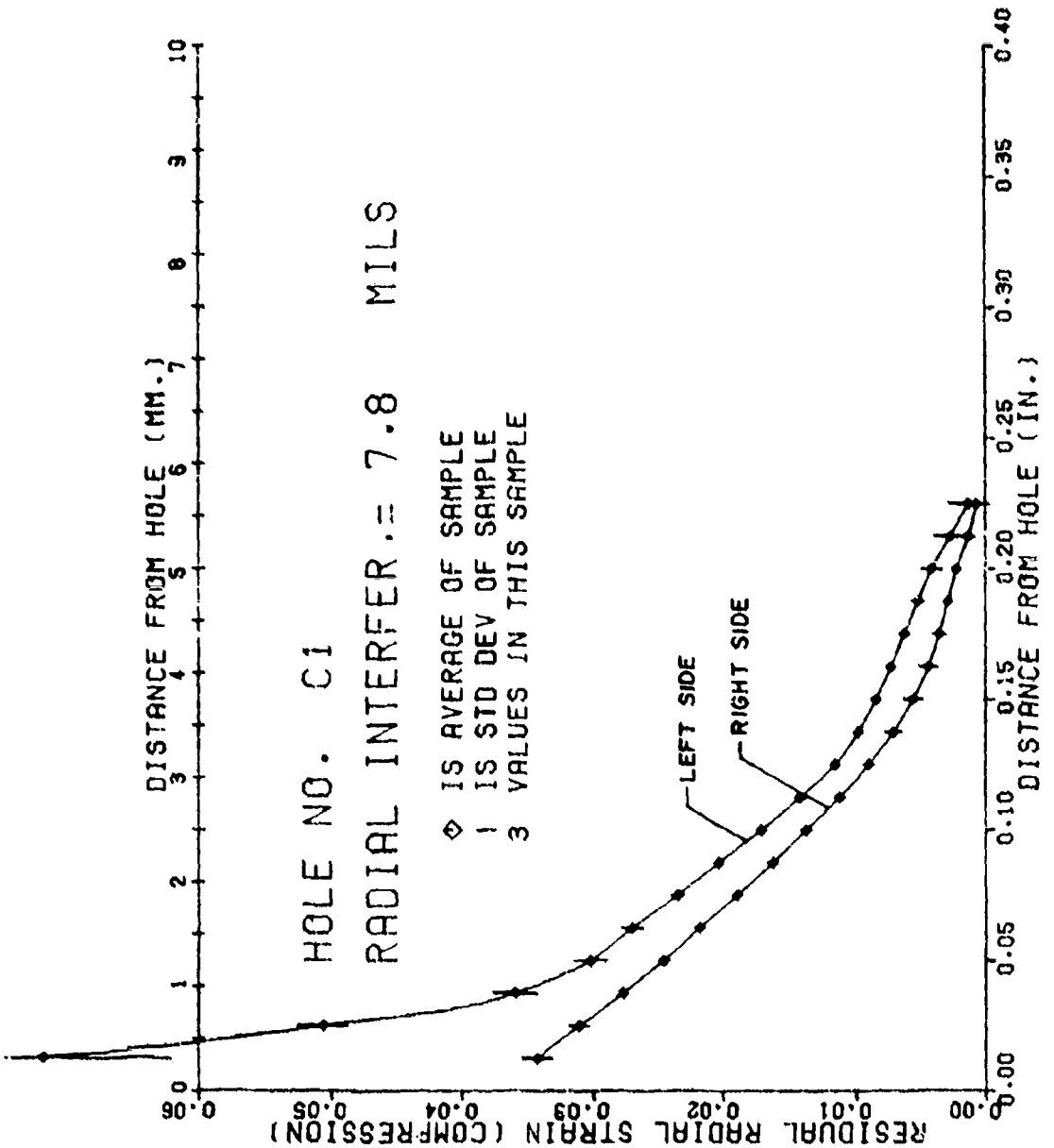

Figure 8.19 Average and standard deviation of radial strain near coldworked hole for 7.8 mils radial interference - opposite sides for hole C1 separate.

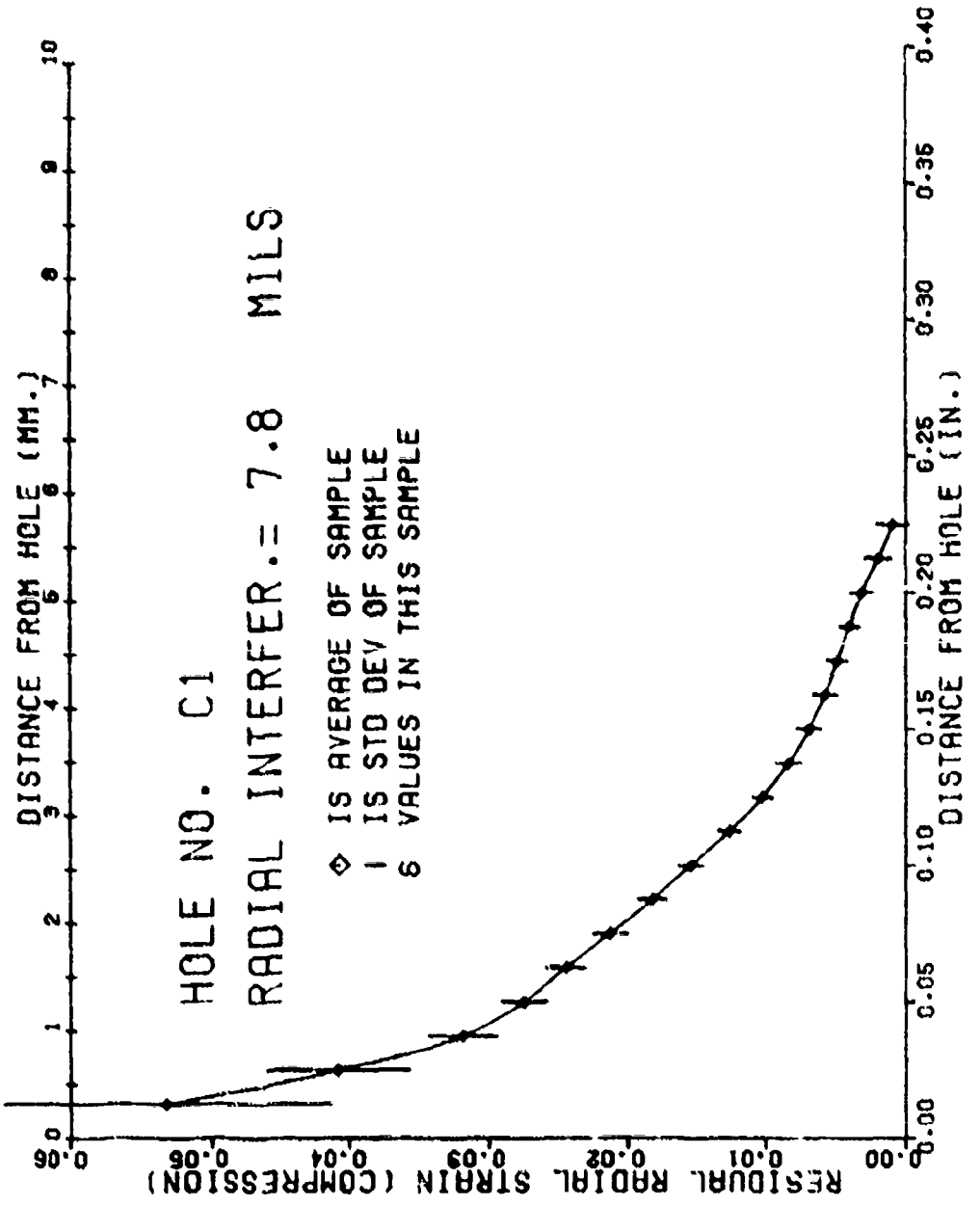

Figure 8.20 Average and standard deviation of radial strain near coldworked hole for 7.8 mils radial interference - all data for hole C1.

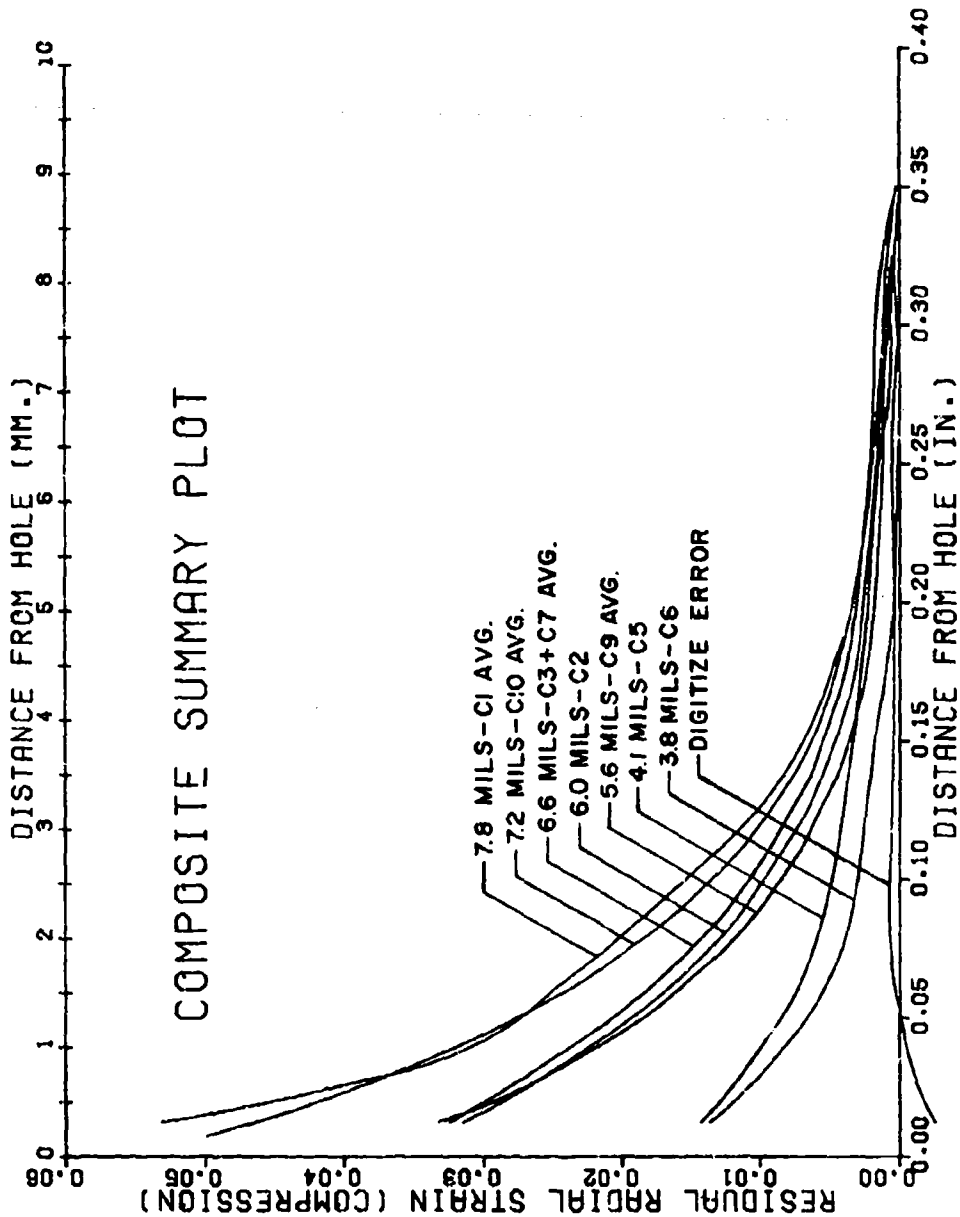

Figure 8.21 Composite summary of average strains measured for all coldworking levels plus error summary.

Examination of the general composite summary also suggests that the strain measured for hole C5 is a bit large for radial distance greater than about .15 inches, and that for hole C6 is a little bit low. The radial interference levels for these two holes differed by only 0.3 mils, which is smaller than the uncertainty. It seemed reasonable to average these two batches of data to obtain a statistical summary curve for about 4 mils of radial interference. Such a curve was plotted with the other summary curves on a second composite graph which is shown in Figure 8.22. This graph on the previous one can be taken as the final result of the radial strain investigation.

3. RESULTS - TANGENTIAL STRAIN

Figure 8.23 and 8.24 display the y-component of normal strain along several y-axes at various radial distances from the hole for specimens C9 and C10. The record of tangential strain along the radial centerline (ϵ_y at $y = 0$ as a function of x) was extracted from these graphs according to the methods outlined in Section 7.5 and plotted. The resulting graphs appear in Figures 8.25 and 8.26.

It is important to note that the tangential strain was derived for only one side of each of the two holes. The results are subject to the lack of symmetry in strain fields that is evident in the radial strain results. Specimens C9 and C10 both showed some lack of symmetry, and the tangential strain plots must be considered to be less dependable than the radial strains reported.

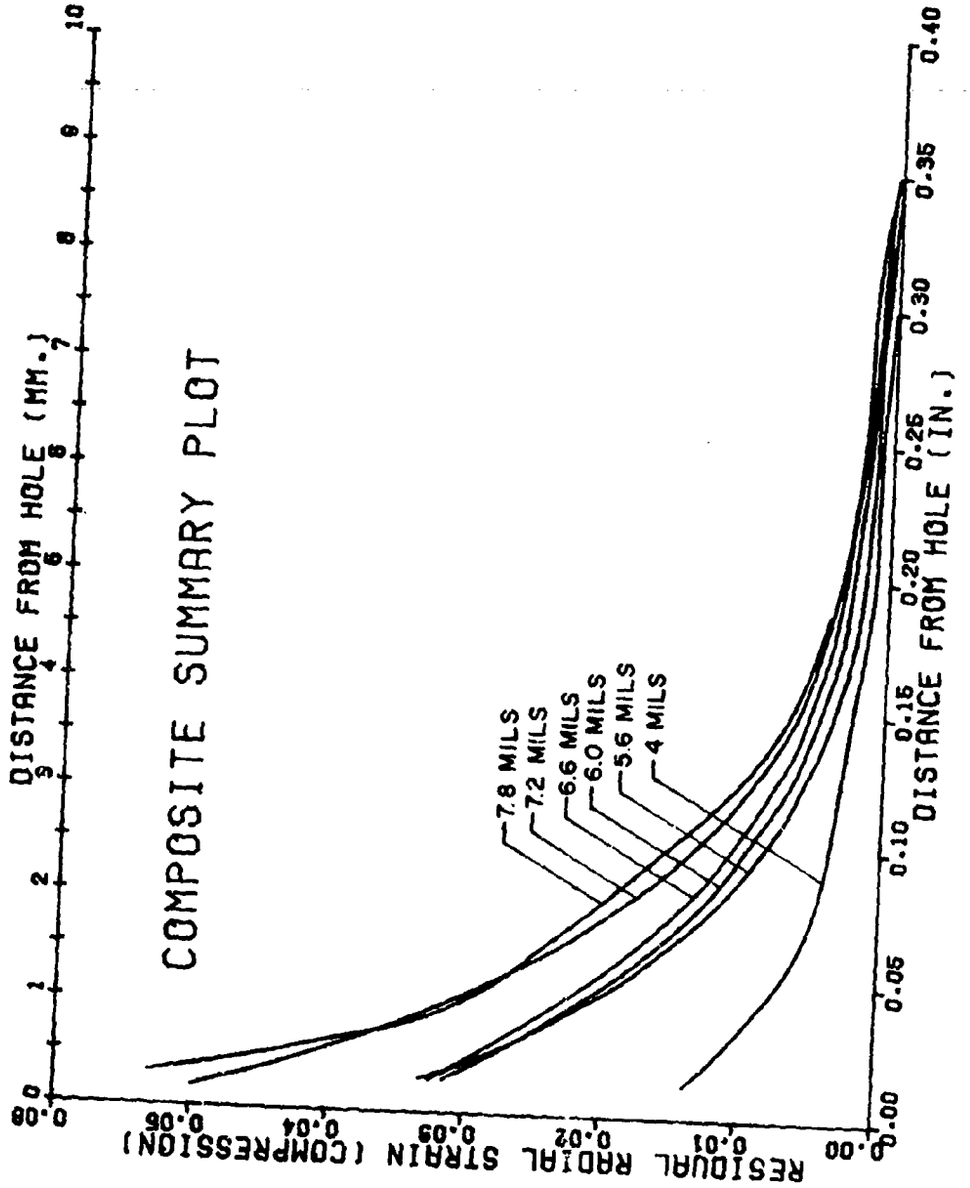

Figure 8.22 Composite summary of average strains measured for several coldworking levels - data for 3.8 mils and 4.1 mils radial interference combined.

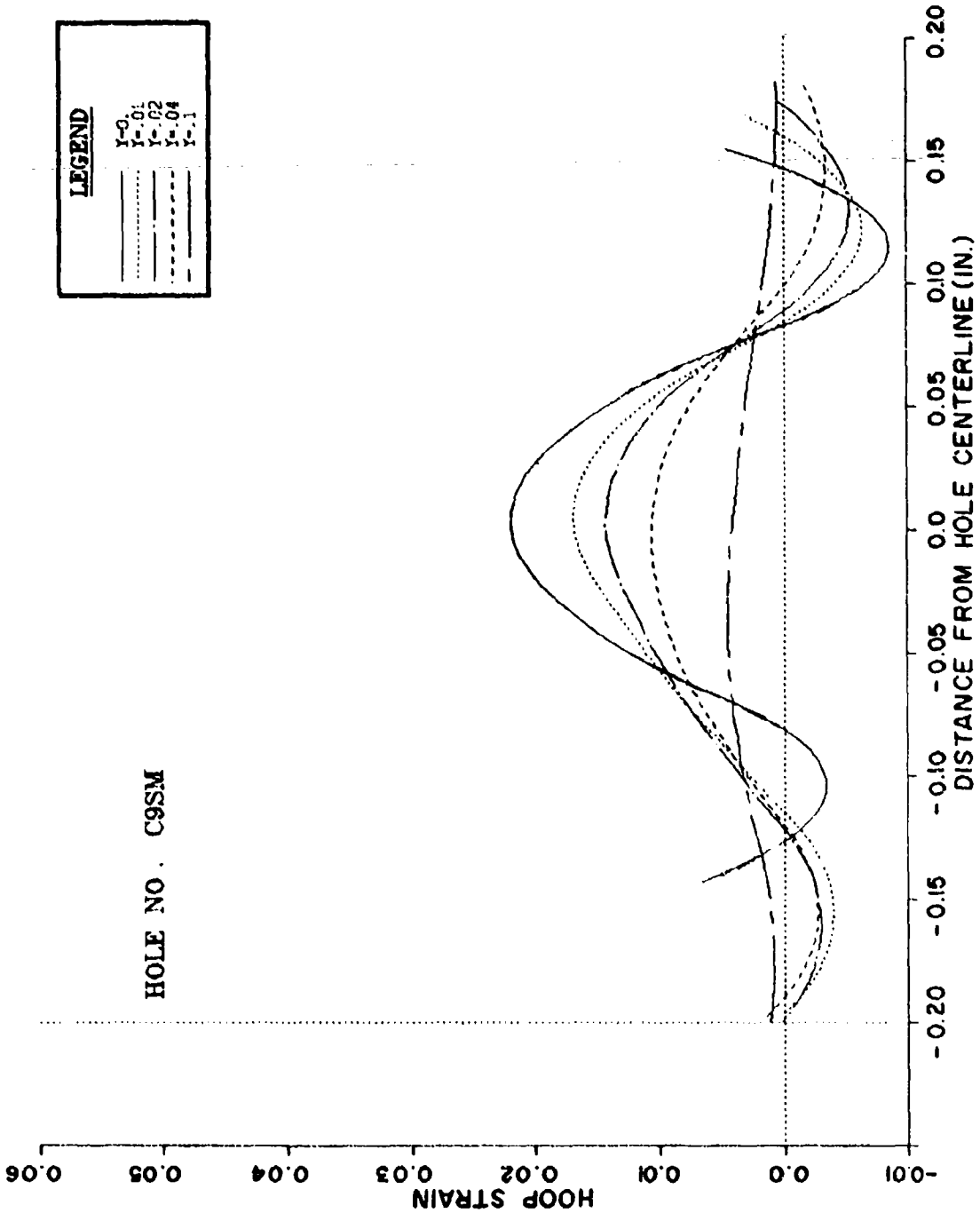

Figure 8.23 Measured hoop strain distributions along several axes at different radial distances for 5.6 mils radial interference (Hole C9).

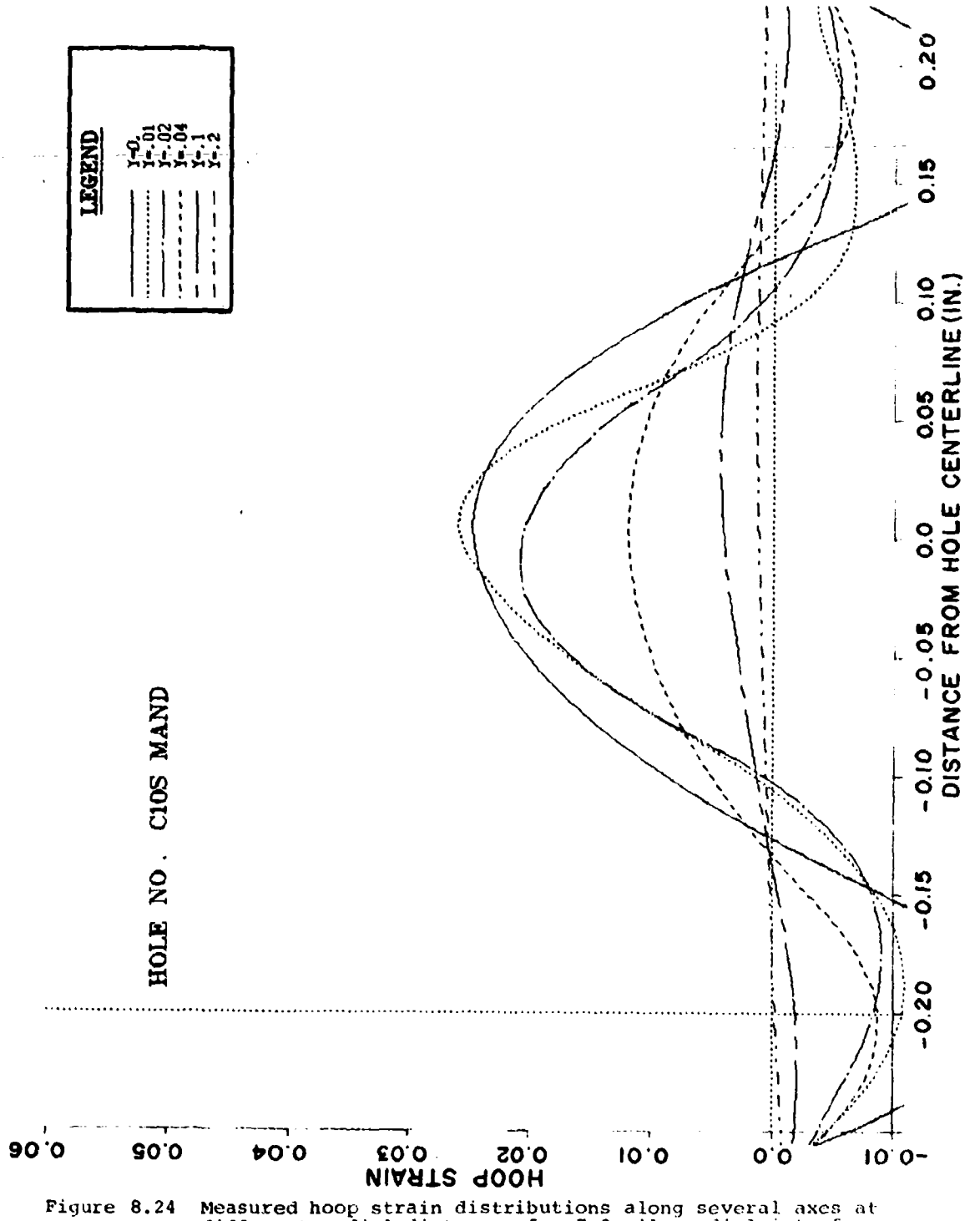

Figure 8.24 Measured hoop strain distributions along several axes at different radial distances for 7.2 mils radial interference (hole C10).

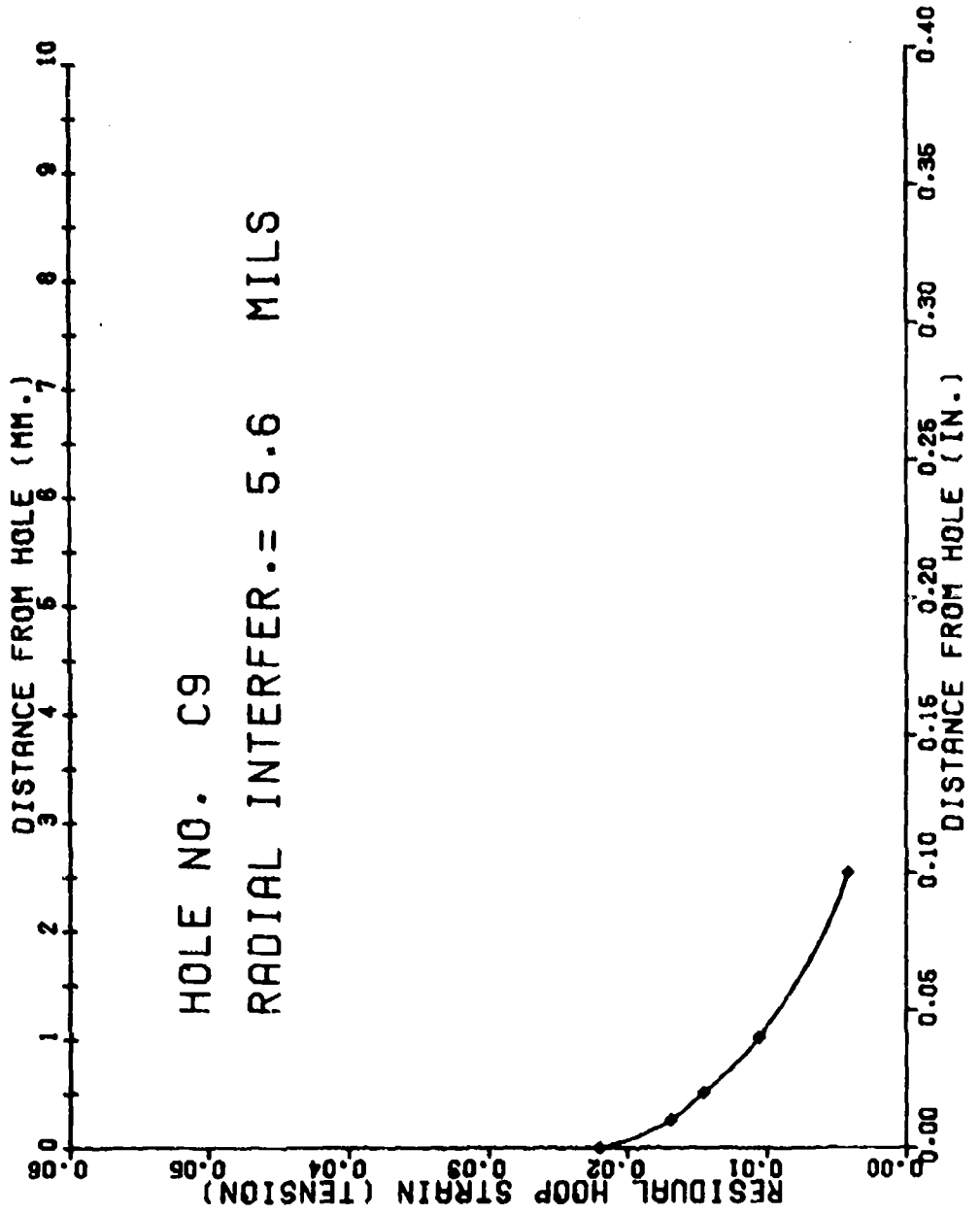

Figure 8.25 Radial distribution of hoop strain for 5.6 mils radial interference (hole C9).

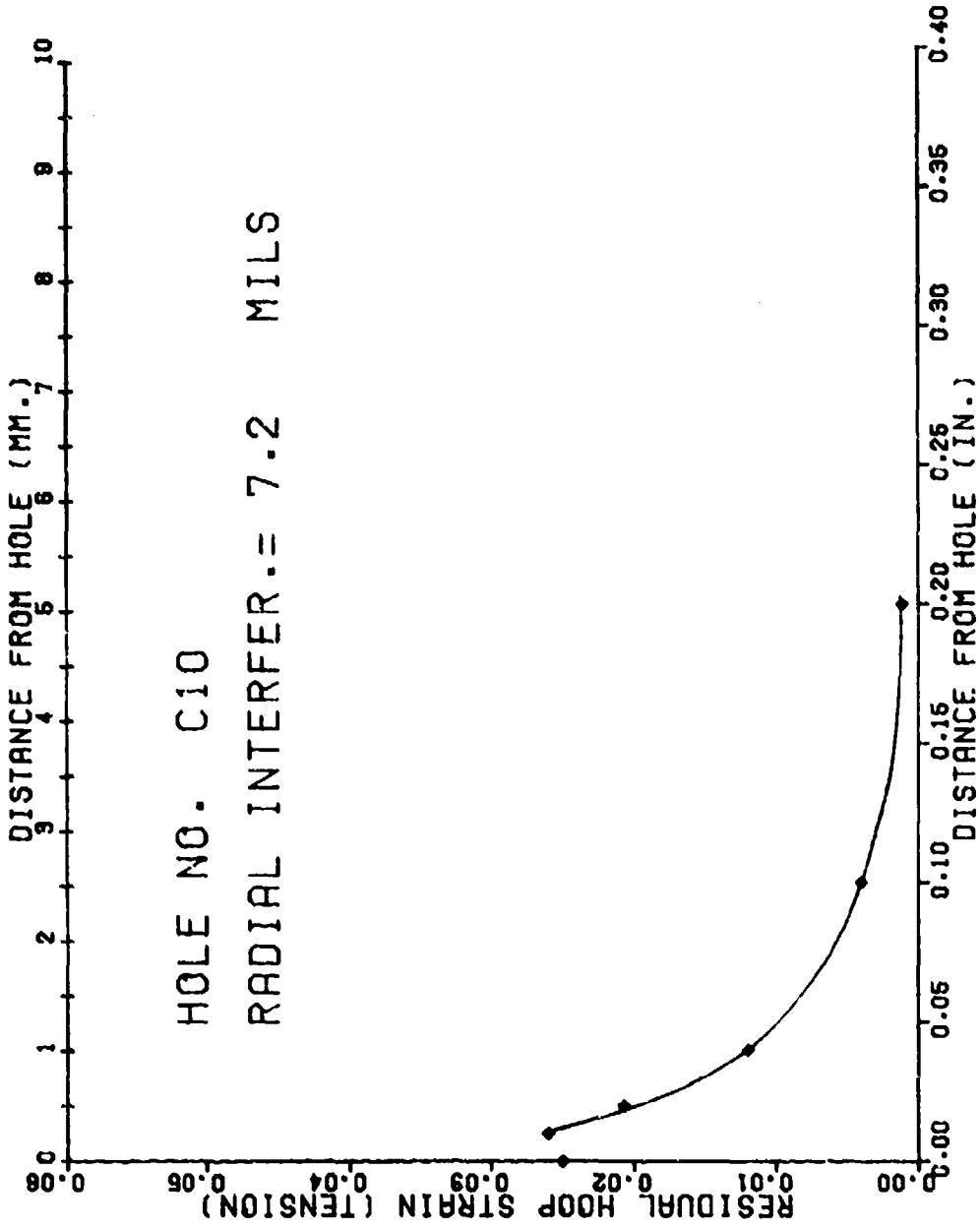

Figure 8.26 Radial distribution of hoop strain for 7.2 mils radial interference (hole C10).

SECTION IX

DISCUSSION OF RESULTS

1. PURPOSE AND PLAN

The purpose of this section is to point out several aspects of the results which might escape notice under less than detailed study, but which might be important to the designer or manufacturer. As a part of the discussion, the measurements are compared with those obtained in previous investigations, and points of agreement and discrepancy are noted and discussed. Soucres of error in the measurements are considered, and their importance established when possible.

2. COMPARISON WITH RESULTS OF PREVIOUS INVESTIGATIONS

Figure 9.1 is a duplicate of the composite plot of residual radial surface strain near coldworked holes to which has been added the data obtained by Sharpe (1-10) and Adler and Dupree (1-14). Sharpe's curve is an average from several different sides of the hole, and the Adler-Dupree result is an average from 2 opposite sides. Both groups used a coldworking level of nominal 6 mils residual interference.

Clearly, the Adler-Dupree data agree quite well with those of this study. This correlation was not expected, since Adler and Dupree themselves questioned the validity of their measurements, which did not agree with their finite-element model. They believed that the radial strain had been reduced by the small amount of chamfer which had been given to the corner where the hole intersects the surface. This conclusion was cited by Sharpe as the apparent reason for the discrepancy between his results and those of Adler and Dupree. The fact that the Adler-Dupree results agree with the measurements obtained in this investigation, wherein 4 specimens were coldworked to about the same nominal 6 mils of radial interference used by Adler and Dupree, suggests, however, that the problem may lie with their finite element analysis instead of in their measurements. The disagreement is in a direction which would result from chamfering the holes, but supports the notion that the Adler-Dupree results

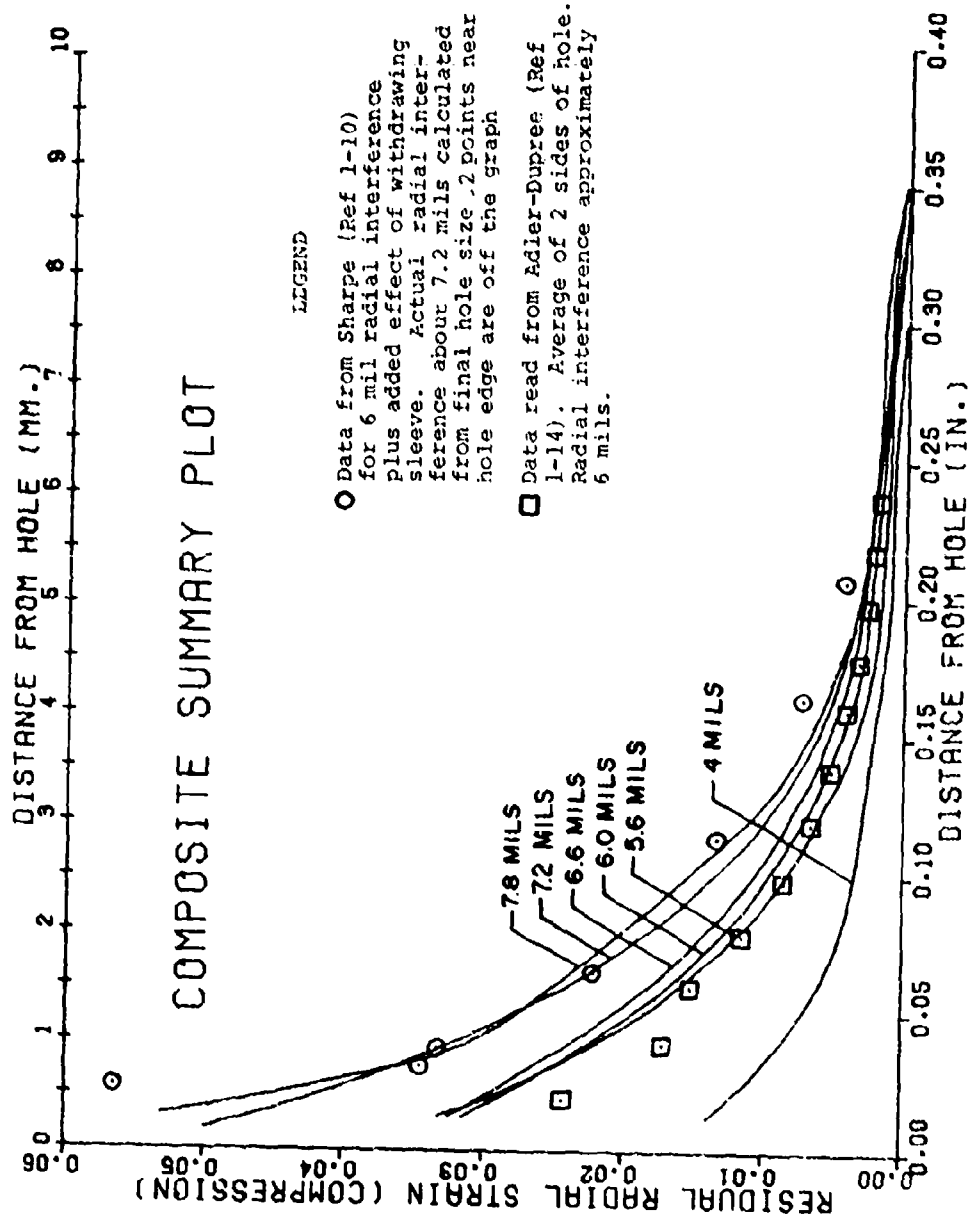

Figure 9.1 Summary plot showing comparison of data with those obtained in previous investigations.

are basically correct and were perturbed only a small amount (10% or so) by the chamfer.

A singular difficulty was experienced in trying to interpret the Adler-Dupree data. Their report (1-14) does not clearly state the coldworking level used. They mention 6 mils radial expansion, but it is not clear whether this amount is the radial interference or the residual radial deformation. If they meant to report r esidual expansion, then the descrepancy would be larger.

The obvious next question is "why do Sharpe's measurements, which evolved from a careful and well-documented experimental program, show much larger strains than those reported here?" A clue is provided by the difference between the radial expansion (radial interference) and the residual expansion (permanent deformation or residual displacement of the hole boundary) figures which are specified by Sharpe. His figures suggest an average spring back (radial interference minus residual expansion) which amounts to about 0.6 mils. Table 1-1 of this report shows an average springback for the specimens coldworked to about 6 mils radial expansion as about 2 mils. That is, the permanent radial deformation in Sharpe's study was about 1.4 m ils larger than the residual deformation found here for the same radial interference. If the comparison was made on the basis of "coldwork degree", that is, the residual expansion after coldworking, then Sharpe's curves should agree with those given here for about 7.4 mils radial interference. The closest values used in this study were 7.2 and 7.8 mils radial intereference. Figure9.1 demonstrates that Sharpe's measurements do indeed agree quite well with the strain distributions measured in this study for those levels of coldwork. The only significant difference is in the strain gradient near the hole, although each result is within the scatter bands of the other. The reason for this minor disagreement probably is the same as the reason why the residual deformations are different when the radial interference levels were about the same.

Identification of the reason for the difference of residual radial expansion between the two studies seems important because it might be an important source of scatter in industrial performance of the process. In fact, the difference seems to arise because of a necessary peculiarity on the specimen preparation procedure devised by Sharpe. He found it necessary to withdraw the sleeve after the hole was mandrelized and before the strain measurements were taken. This withdrawal was accomplished by reversing the specimen in the mandrelizing fixture, supporting it by a washer, and using the mandrel a second time to engage the sleeve and pull it free. It would appear that this treatment might add a small increment to the total coldworking level. This supposition is supported by a quotation from Reference 1-10; "The process of pulling the sleeve out, even though it took only about one-fourth the force required to pull the mandrel through, contributes significantly to the deformation in the specimen." An additional factor might be that the hydraulic mandrelizing apparatus used by Sharpe gave more of a dynamic deformation process than did the mechanical-drive Instron used in this study. At any rate, it seems that comparison is valid only if it is done on the basis of equal residual radial expansion. Such a comparison shows very good agreement between the two investigations. It is worth noting that the two studies utilized two entirely different measurement techniques, and one seems to support the other.

As a result of the discrepancy noted above, one is faced with a dilema when he tries to correlate measured strain fields and the industrial process with theoretical solutions for coldworked holes. One cannot withdraw the sleeve without upsetting the very field he is to measure, and existing theories do not account for the presence of the sleeve (Heisenberg's Principle lives). Reference 1-10 treats in detail the various applicable theories, and they are not considered herein.

3. SOME INTERESTING ASPECTS OF THE DATA

There are several aspects of the detailed results and the summary plots which are illuminating and, possibly, of some importance. These details are discussed below in no particular priority of order.

As was pointed out in Section VIII, the measured strain values from specimens C3 and C7 were averaged to produce the strain distribution shown in the composite summary plot for 6.6 mils (.17 mm) radial interference. That these two specimens had the same coldworking level was a fortuitous accident which created a severe test of the whole experimental procedure. A radial interference other than 6.6 mils had been calculated for specimen C3. The results for the false strain level were not consistent with the others obtained. Finally, a check of the carefully-maintained experiment log book brought the error to light, and there was an accidental duplication of coldworking level which, because it was not discovered until most of the data had been analyzed, served as a useful check. Figure 8.14 through 8.16 demonstrate that the agreement is very good. In fact, the difference between the average strain levels in C7 and C3 is of about the same magnitude as the difference between opposite sides of the hole in Specimen C3 (see Figures 8.14 and 8.16). This generally good agreement in an unscheduled checking procedure suggests that the results of this study are dependable.

It was mentioned also in Section VIII that comparison of the summary plots (see Figures 8.9,8.10 and 8.21) leads one to suspect that the strain measured for specimen C5 (radial intereference 4.1 mils) are generally too large, especially for distances larger than about 0.15 inches (3.8 mm). The detailed analysis plot in Figure 8.2 lends support to this idea since the sample comprises only 3 sets of data, and there is considerable disagreement and inconsistency between the sets. The strain values for specimen C6 seem more dependable although they might be a trifle small. There are 6 sets of data in the detailed graph for C6 (Figure8.1), and these data show good agreement except for one set. Even this one discrepancy seems to have evolved from fringe counting difficulties near a fiducial mark.

A logical conclusion is that the C5 data should be discarded or averaged with the results from C6. The coldwork levels for C5 and C6 differ by only 0.3 mils, which is less than the uncertainty in determining the coldwork. Such an averaging procedure was used in creating the final composite plot of Figure 8.22.

Somewhat similar remarks could be made for the whole assembly of specimen C9, C2, C3, and C7; and again for the C1 and C10 pair. On the other hand, the difference of 0.6 mils radial intereference in the first group is outside the probable measurement uncertainty, and the difference of 0.4 mils for the second group is barely less. Also, most of the observed differences in the curve for nearly equal coldwork levels are consistent with expected trends. The suggested averaging of data was, therefore, not undertaken.

Lack of symmetry of the coldworking process is apparent in many of the results, and it should be considered by the designer as a source of uncertainty in fatigue life predictions. The most significant example of unequal straining at opposite sides of the hole was offered by specimen C1, as is evident in Figures 8.8 and 8.19. Strain magnitudes in the critical few mils near the hole differ by a factor of 2. Additional significant discrepancies between opposite sides are shown in Figures 8.5 and 8.14 for C-3, in Figures 8.3 and 8.11 for C9, and in Figure 8.7 for C10. Additional comment about the behavior of C10 appears below.

The large level of coldworking in specimen C1 gave rise to a very large number of moire fringes with the pitch mismatch and sensitivity multiplication employed. Fringe counting was begun at about .22 inches from the hole rather than at the usual .35-.40 inches. There appears to be a related data fault or processing difficulty between .20 and .225 inches from the hole for C1 (see Figure8.8). This segment of the C1 strain distribution curves was merely suppressed in generating the composite summary plots, although it does appear in the more detailed ones.

The detailed analysis (Figure 8-5) and the statistical summary plots (Figures 8.14 and 8.15) for specimen C3 show a fairly large scatter of strain values, even when allowance is made for the consistent differences between opposite sides of the hole. This extra scatter is traceable to the fact that C3 was the first specimen to be analyzed. Experimental procedures, especially in the optical moire fringe processing and in the fringe pattern digitizing stages were not yet well developed. In particular, the critical importance of careful digitzing was not then fully appreciated. Also, the moire fringe photographs suggested that unusually extensive rumpling of the plastic region occurred with hole C3, and this factor may have contributed to the scatter.

Another interesting aspect of the results from specimen C3, and a partial explanation for the scatter of data, lies in the fact that this specimen was used as a test of the effects of using different sensitivity multiplication factors in the moire fringe formation process in addition to the usual various degrees of pitch mismatch. The object of this limited extra study was to optimize the optical data processing to produce the best balance of fringe visibility, displacement sensitivity, and closeness of fringe spacing. Referring to Figure 8.5, data sets marked 743 are for no sensitivity multiplication (multiplication factor = 1) and a pitch mismatch of only about 18 lpi. Those curves marked 1481 come from a sensitivity multiplication of 2 and pitch mismatch of 41 lpi. The remainder of the data curves, in common with most of the data from the other specimens, correspond to a sensitivity multiplication of 3 with pitch mismatch values of 27, 58 and 83 lpi.

In this one case studied, there was surprisingly little penalty paid for using a sensitivity multiplier of 2 rather than 3. The loss of sensitivity is, evidently, offset by the greater contrast and better definition which is characteristic of the fringe photos taken with the lower multiplication. The results for a sensitivity

multiplier of unity are more questionable--at least on the left side of the hole (data set C3L743 in Figure 8.5). Part of the problem here might be that not enough pitch mismatch was used. A tentative conclusion is that, even with high quality data processing schemes, the basic sensitivity of 1000 lines/inch of the moire gratings used without sensitivity multiplication is not great enough to give highly dependable measurements with the range of strain studied here. Moire multiplication factors of 2 or more should be incorporated unless finer gratings can be used.

Since it was necessary to discard one set of data when constructing the statistical summary for hole C3, the one showing the most discrepancy, that being the data just referred to (C3L743) was the set left out. Reading of the C3 results for purposes of constructing the summary plots was done with separate detailed plots for the left and right sides of the hole. These plots are not reproduced here. The detailed plots of Figure 8.5 which shows all the data sets for C3 is too congested to be of use in the final data reduction.

The detailed analysis plots (Figure 8.8) and the summary plots (Figures 8.19 and 8.20) for hole C1 also appear at first glance to contain excessive scatter. Closer examination shows that there is consistency of measurement for any one side of the hole. Even the discrepancies between individual curves for one side of the hole are consistent with expectations. Consider, for example, the curves labeled C1BNL2200 C1BNL2225, and C1BNL2256. These three lines are the strain fields on the left side of C1 obtained with 3 different degrees of pitch mismatch in the optical data processing. The pitch mismatch is numerically greatest for the line labeled 2200 and smallest for the 2256 value. Now, pitch mismatch essentially serves the function of inserting an interpolation scale between fringes--the greater the mismatch, the greater the interpolation capability, which implies a greater sensitivity to local strain gradients. The shapes of the 3 curves just pointed out suggest that there might be some local discontinuity, a grain boundary for example, at a radial distance from the hole of

about 0.05 inches. The data derived with the greater pitch mismatch was most sensitive to this anomaly; the interemdiate mismatch results show intermediate sensitivity; and the smaller mismatch appeared to miss tne local discontinuity entirely.

The detailed data plots for hole C10 also appear at first to be excessively scattered. Here 4 sides of the hole were studied (labeled N,S,E,W), and close examination of Figure 8.7 shows that the data sets for any one side of the hole are in very good agreement with one another. It is just that the different sides give different results, as was observed for many of the specimens. The only troublesome data set for C10 is the one (not two) set for the east side of the hole (called C10AE). This set should be viewed with some skepticism, since all the C10AE fringe photographs were difficult to read. The source of this difficulty was in the reflection problems experienced in the specimen grating photography. Section 5.3 mentions these problems and their causes in some detail. The one set of C10 data does not have discernable effect on the statistical results for hole C10, so it was not deleted.

4. ASSESSMENT OF ERROR AND SCATTER

In order that the user of the data reported can have some idea of the uncertainties which affect his design, it is desirable to identify the sources of error (consistent wrong results) and scatter (random error); to try to classify the sources as to whether they produce error or scatter; and to give an estimate or measurement if possible, of the magnitude of the possible error. An estimate of the total scatter can be derived from the statistical summaries already presented, within the limits of the experiment. The sources of this scatter have not really been identified as yet.

It is characteristic of the moire technique that the specimen grating exactly follows the surface strain, barring faulty adhesion of the photoresist. The grating photographs, then, can be accepted as an exact replica of the specimen surface displacements with possible geometrical errors (scaling and distortion) interjected by the photographic optics. These possible errors have been largely eliminated by the comparison and subtraction process used in obtaining moire fringe patterns from the grating photo plates as well as in the use of fiducial marks to establish and check the scaling during digitizing of the fringe patterns. That is, in the first instance, the specimen was always photographed in its initial and final states in identical photographic circumstances. The grating photo plates were optically analyzed with the same submasters in the same optical processor using identical procedures. The moire fringes for zero strain were then subtracted from the fringes in the final state. Barring careless technique and mistakes, such as putting a photoplate into the optical processor backwards, or bumping the camera between photographs, all errors which might be caused by improper focus, faulty alignment of the camera, erroneous measurement of grating frequency, and so on will be common to baseline and "at strain" fringe patterns and will disappear from the difference and, therefore, from the final result.

It is, then, only in the reading and analysis of the fringe data where uncompensated errors or scatter effects can arise. The displacements and strains computed depend entirely upon proper counting of the moire fringes and upon locating the cursor of the digitizer exactly on fringe center. Likewise, uncompensated scaling errors can enter if the locations of the fiducial marks are not known accurately on the specimen or are not read correctly during digitizing. There is no way in which this digitizing process, which depends upon manual alignment of a crosshair graticule with a fringe band or the image of a fiducial mark on a photograph, can be done with

complete accuracy. Certainly the digitizing procedure used in this study is subject to error and inconsistency. One can only try to insure that the errors will be random so that they can be eliminated as a source of false results by the final statistical treatment, and then he can test the results and intermediate procedures to see if this ideal is approached.

Faulty fringe counting yields, in general, an error which is not compensated or detectable. As a result of the detailed plotting procedures used in this study, all such errors should have been identified and eliminated. As shown below, it is possible that such an error might have been missed in certain situations, and it would remain undetected except as a possible lack of consistency when replications were conducted on the same specimen. That is, if a fringe counting error remains in the data, it might not be distinguishable from normal scatter.

Consistent (as opposed to random) faults in the digitizing procedure are another source of error which is not directly assessable. In general, the human eye-hand combination is extremely skillful in locating the center of a fuzzy line provided the line is well-behaved. If the line (interference fringe) curves sharply or is not symmetrical in its intensity distribution, the eye is misled because it locates the center of gravity of a segment of the line. Random mistakes of this sort merely contribute to data scatter. A consistent fault in locating fringe or fiducial mark center results in error whose presence is not self-evident. A measure of the seriousness of such error can, however, be derived by digitizing a carefully prepared known fringe pattern or comparing measured strain with calculated values for a specimen in which the strain is known.

An interesting and useful aspect of this study was the estimation of any consistent digitizing error through replication of the digitizing process with several fringe photos. Such a procedure does not meet the strict requirement outlined above for determining an overall consistent error. It can, however, yield an estimate of the average error which will appear in any one set of strain data as a result of

digitizing faults which are not of the type resulting from pathological fringe patterns. The procedure was to digitize the same photographs twice for several test cases. The two sets of data from one photograph were then entered into the data reduction program as the "zero strain" and "mandrelized" portions of the complete data input required for the computer routine. The program subtracts one set from the other and computes "displacement" and "strain" distributions as usual. The "strain" calculated represents a false strain which might result from faulty digitizing as well as error propagation in the reduction program. Zero digitizing discrepancy should give a null result. Figure 9.2 is the detailed summary plot for 3 such trials The extra fourth plot in this figure is that error which would result if the set of baseline (zero strain) data from one side of a specimen was used in place of the baseline for the other side. This substitution might create a digitizing error which is accepted to reduce digitizing time by requiring one baseline digitization for all the data sets from one hole. All four of these curves (Figure 9.2) were treated statistically in the same way as has been described for the strain data, and the resulting statistical error analysis plot is shown as Figure 9.3 as well as being included in the composite summary in Figure 8.21.

A further important source of uncertainty includes consistent and random errors in determining the radial interference, which is related to the degree of coldwork. This determination is poorly conditioned in that it can be derived only by subtraction of the hole radius from the sum of the mandrel radius plus the sleeve thickness, itself determined as one-half the difference between inside and outside diameters. Error propagation in such a process can be very serious, and there is no good way to asses such errors except by sectioning the cold worked specimen and measuring final hole size and basing all reporting on the residual deformation thus calculated. This procedure was utilized by Sharpe (1-10) but not employed here as it was thought necessary to base the experiments on the interference parameter which can be calculated from simple measurements made as part of the industrial application of the commercial coldwork process. A positive aspect of the study being reported upon

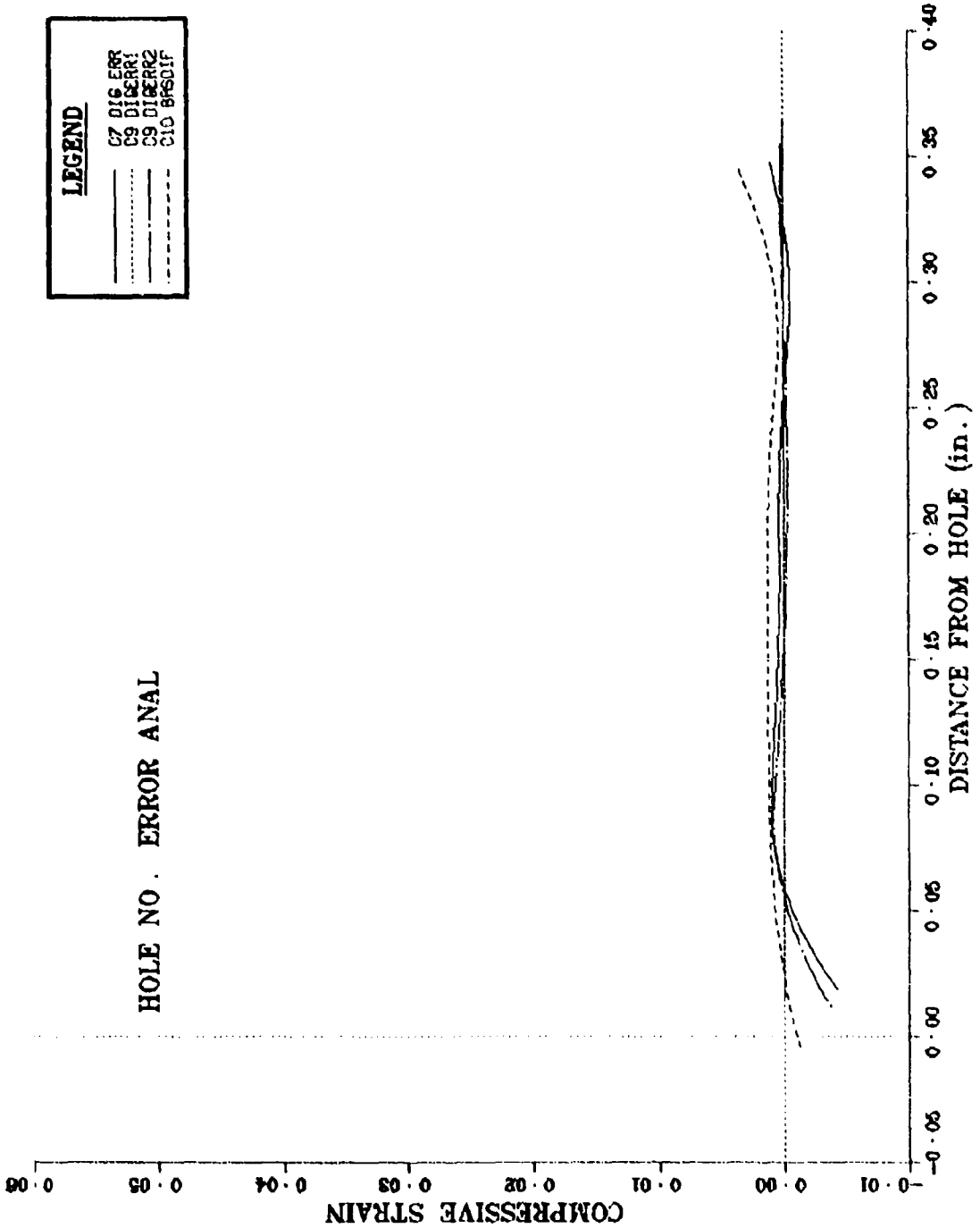

Figure 9.2 Detailed summary plot of measured discrepancies in digitized data.

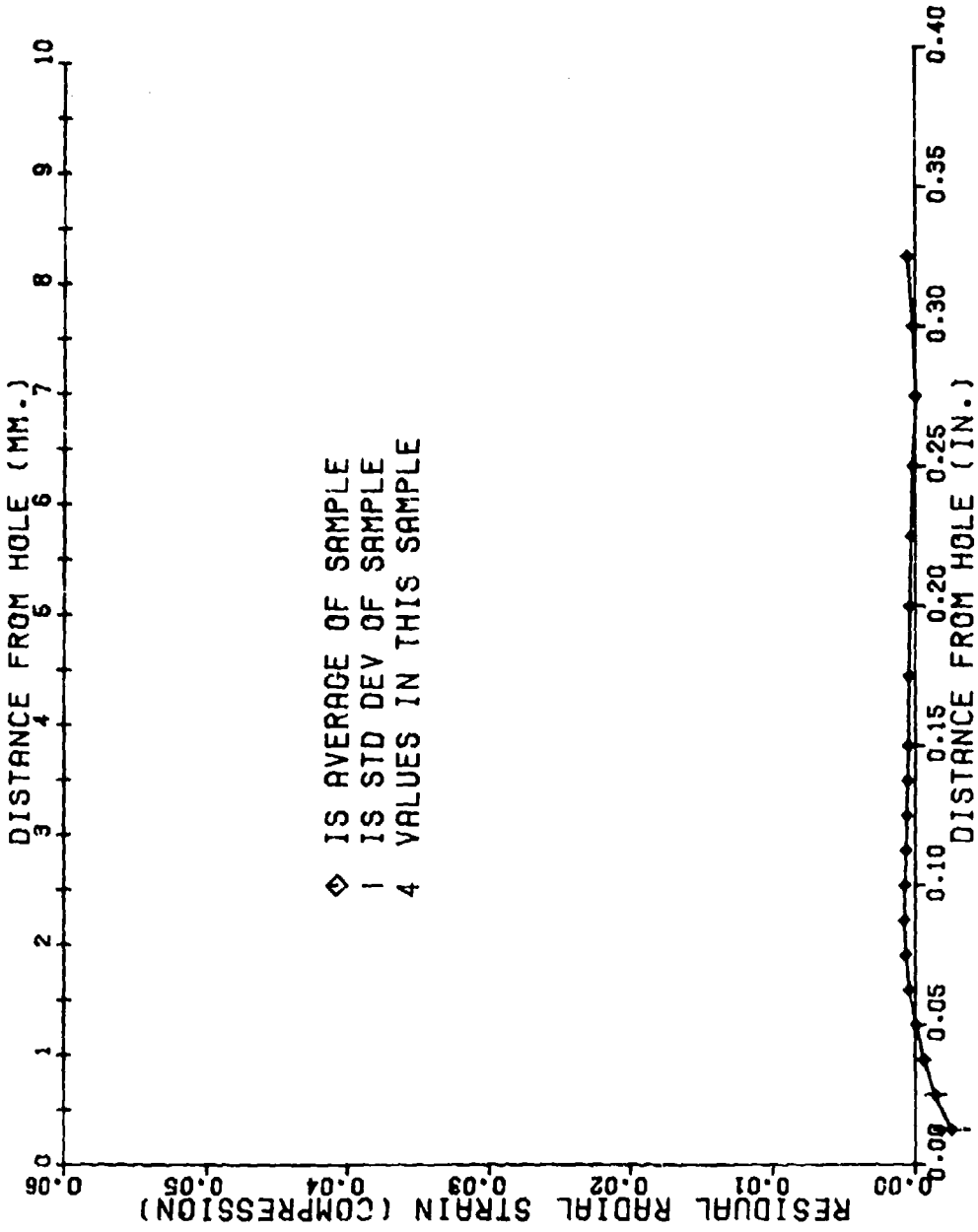

Figure 9.3 Statistial summary of digitization errors.

is that the final inner diameter of the sleeve was measured to give an indication of the residual coldwork. The detailed displacement plots were also extrapolated to the hole edge to determine the displacement at that point as given by the moire data. These two independent determinations of the residual displacement of the hole boundary agreed to within the limits of the extrapolation accuracy, which is not great because of the difficulty of accurate extrapolation in a region of high strain gradient. All factors considered, a best guess of the uncertainty of radial interference levels reported here would be about $\pm$0.5 mils (.013 mm).

Material variations are another source of uncertainty in the results, as are variations in the mandrelizing procedure. Difficulties encountered with slippage of the sleeve during mandrel pulling were mentioned in Section 4.4. No ill effects of these procedural problems were detectable in the results, so it is assumed that they are minimal. Material variations can be expected to be negligable since all specimens came from a common sheet.

The fortuitous and unplanned replication of strain measurement at one coldwork level in specimens C3 and C7 gives probably the best indication of the sum of the uncertainties which might result from material variations, oddities in the mandrelizing procedure, errors of determining radial interference, and so on. The history and results of this aspect of the study were outlined in Section 9.3. The discrepancy appears to be acceptable, and the indicated magnitude of it could probably be used as an overall uncertainty figure by a designer. The general agreement of results from the 4 specimens near the 6 mils radial interference level, the general consistency of the results for C1 and C10 near the 7.5 mils radial interference level, and the fair agreement of C5 and C6 data at the 4 mil level support the conclusion that the total uncertainties are well within an acceptable limit.

One detail remains to be examined. As suggested at various places previously in this report, there was evidence of considerable lack of smoothness in the strain fields, especially in the heavily deformed areas near the hole. Evidence of this behavior was quite striking in many of the fringe photographs made with a large pitch mismatch between specimen grating photograph and submaster; the larger pitch mismatch results, of course, in a closely packed system of narrow moire fringes. Near the hole, the fringes would often appear quite crooked, at times taking on a scalloped appearance. At other locations, the fringes would be close together (implying large strains) a short distance from the hole and then be further apart (meaning smaller strain) closer to the hole. This behavior is entirely opposite to what would normally be expected, but it might be within the limits for strain distributions in heavily deformed crystalline materials. The oddest behavior occurred when a moire fringe intersected what appeared to be a slip line or a grain boundary. Here, the fringes would appear to be discontinuous, and there would be a step-wise change in fringe order of a half-order or more. This behavior was extremely troublesome when the fringes changed by one whole order at a discontinuity, especially if it happened near the axis along which the fringe locations were being read on the digitizer, as it was very easy to obtain a faulty count of fringe order. In many cases, it was necessary to trace and count the fringes, with the aid of a marker and a magnifying glass, inward toward the hole along different radial lines to establish accurately fringe order and location. Even so, there were a few fringe photos in which the fringe count remained ambiguous in certain areas of the pattern. The experiment was designed to give enough redundancy of data so that these questionable results could be discarded when detected. Even so, there may have been a few cases of faulty fringe interpretation which slipped through and contributed scatter in the results. One should not confuse these errors of fringe interprotation with the scatter resulting from the normal ragged nature of the strain field. The latter is perfectly acceptable and must be considered by the

designer as a source of uncertainty. Faulty fringe interpretation yields an undesirable error or scatter which cannot be eliminated by examination of the results. It can only be detected and screened out by careful fringe counting and replication of the counting on the troublesome photographs. Both measures were employed here.

Many of the general and specific comments made above for the radial strain data apply equally to the tangential strain measurements, and little remains to be added. It is important to recognize that the tangential strains as plotted in Figures 8.25 and 8.26 are less dependable than the radial strain data because there was no replication and statistical processing of several sets of data for each level of radial interference. Also, the tangential strains are a fraction of the radial values, and cannot be measured as accurately with the same apparatus and techniques. The measurement sensitivities available were marginal for tangential strains.

SECTION X

SUGGESTIONS RELATED TO FUTURE FASTENERS RESEARCH AND APPLICATIONS OF MOIRE METHOD

1. INTRODUCTION

It seems appropriate to include here mention of some lines of research which would contribute to the understanding and usefulness of coldwork fasteners as well as expand the utility of the data continued in this report. Also, there is a possibility that the moire facility built for this investigation might be utilized in the future for additional research on fasteners and on other projects of interest to the Air Force. The purpose of this Section, therefore, is to assemble in one place several suggestions for improving the experimental apparatus and procedure as well as ideas for extending the usefulness of the experience and data already obtained.

2. SUGGESTED FUTURE RESEARCH

A. One fact seems to be clear from this investigation and the related research of Sharpe[1-10] and Adler and Dupree.[1-14] The strain field created through the specimen by the process of drawing a tapered mandrel through a sleeved hole is a complex three-dimensional one. It is doubtful that observation of the surface manifestation of this strain field can lead to complete understanding of the coldworking process either in a refined laboratory version or in its practical industrial form. It might be true that enough understanding, predictability and control of the process can be obtained through surface strain measurements to satisfy design requirements. On the other hand, it might be safer and wiser, and in the long run more cost-effective, to invest in a careful experimental study of the three-dimensional strain field.

B. Another aspect of the current state of knowledge is that analytical models of the strain field produced by expanding a hole are not complete and satisfactory. This is true even for an idealized process, and analysis of the practical process seems quite far off. Development and refinement of models can be pursued on two fronts. One would be continued experimental study of surface (and possibly 3-dimensional) strain fields for laboratory models which incorporate to a maximum the idealizations of tractable analytical models. Such study would show whether the analyses are on the right track. Additional continued effort should be maintained in developing analytical techniques which account more accurately for the realities of the commercial process on common work-hardening (granular if possible) materials.

C. An obvious and useful step would be to obtain an empirically-based analytical expression for the strain (and uncertainty) as a function of radial interference and distance from the hole. A reasonable beginning could be made with the data contained in this report. A brief and crude preliminary attempt suggests that the curves could be adequately fitted with a second-order polynomial, but other functions might be better.

3. APPARATUS AND PROCEDURAL REFINEMENTS

The equipment and techniques employed proved reasonably sufficient to obtain acceptable results. Considerable care and familiarity with quirks of the apparatus were required, and it is doubtful that a technician or engineer could step in and obtain good data without practice. Certain improvements in the apparatus and procedures would minimize wasted effort and enhance the probability of obtaining superior results in limited time. Several such suggestions are listed below:

1. All the optical equipment, including the grating photography setup and the optical data processing system should be remounted on a stable and accurate optical bench.

2. A new and better master grating should be obtained. Depending on improvements to the photographic system, it would be wise to change to a master grating of finer pitch, say 2000 or 3000 lines/inch. The Micro Line Division of Bausen and Lomb, Jamestown, New York, 14701, advertizes metal ronchi rulings when would be acceptable in quality and price.

3. The most useful sizes of submaster gratings should be remade using the new master grating and/or the benefits of photography with slotted apertures.

4. A better lens should be obtained for grating photography. In particular, one having larger useful aperture and, therefore, higher frequency response, the possiblity of higher magnification, and less light fall-off at field extremes would greatly simplify all the photographic portions of the moire procedure. The other steps in the experimental procedure would be made easier by reason of improved contrast, more uniform grating photos, larger image sizes, and so on. In adopting such a lens, the fine color correction of the Goerz apochromat would have to be sacrificed, and it might be necessary to use a color filter to compensate for the increased chromatic observation. A flat-field process lens is suggested.

5. The technique for applying photoresists should be further refined. The spinning technique should be considered, and it might be possible to use an ordinary metallurgical lap as the spin table. If the airbrush technique is retained, it seems probably that further thinning of the resist should give better results.

6. The photoresist should be filtered according to the manufacturer's direction.

7. A more powerful light source for exposing the photoresist should be devised. This set up could be incorporated into the specimen photography apparatus or the optical bench.

8. Depending on the amount of data to be obtained, some automation

should be incorporated into the fringe pattern digitzing and data punching procedure. The current method makes it by far the most tedious part of the whole moire technique, although it does have the advantage of allowing careful checking of the digitized information. A digitizing densitometer might be used, but it is likely that such an instrument would be confounded by optical noise in the form of coherent light speckle. An ordinary digitizer with card punch output seems most suitable.

9. If additional study of coldworked holes is to be undertaken, a new set of hardened and polished mandrels which are matched in taper profile must be obtained.

10. Etching of the specimen grating into the specimen surface and subsequent removal of the photoresist is recommended in situations where mechanical or thermal damage to the specimen surface is possible, or where flaking of the photoresist seems to take place. Photography of the specimen grating may or may not be rendered more difficult in this situation. Only a light etch which serves to roughen and discolor the surface between the photoresist lines would be necessary, and such a grating might actually improve photographic contrast.

11. In advance of any further studies of sleeved fasteners, a micrometer which can be used to measure directly the thickness of the sleeve wall should be obtained.

11. REFERENCES

1-1. Military Specification MIL-A-834444, United States Air Force, July 1974.

1-2. Gran, R.J., Orazio, F.D., Paris, P.D., Irwin, G.R., and Hertzberg, R., "Investigation and Analysis Development of Early Life Aircraft Structural Failures", Technical Report AFFDL-TR-70-149, Wright-Patterson AFB, Ohio March 1971.

1-3. Kohl, R., "Fasteners That Fatigue", Machine Design, 47, 5, 98-102, 20 February 1975.

1-4. Petrak, G.J., Stewart, R.P., "Retardation of Cracks Emanating from Fastener Holes", Eng. Fract. Mech., 6, 2, 275-282, September 1974.

1-5. Tiffany, C.F., Stewart, R.P., and Moore, T.K., "Fatigue and Stress-Corrosion Test of Selected Fastener/Hole Processes", Technical Report ASD-TR-72-111, Wright-Patterson AFB, Ohio, January 1973.

1-6. Grandt, A.F., "Stress Intensity Factors for Some Through-Cracked Fastener Holes", Internat. Jrnl, Fracture, 11, 2, 283-294, April 1975.

1-7. Grandt, A.F., Gallagher, J.P., "Proposed Fracture Mechanics Criteria to Select Mechanical Fasteners for Long Service Lives", Special Tech. Pub. 559, ASTM, 1974.

1-8. Cathey, W.H., "Determination of Stress Intensity Factor for Coldworked Fastener Holes in 7075 Aluminum Using the Crack Growth Method", Technical Report AFML-TR-74-283, Wright-Patterson AFB, Ohio, May 1975.

1-9. Grandt, A.F., and Hinnerichs, T.D., "Stress Intensity Factor Measurements for Flawed Fastener Holes", Proc. Army Symposium on Solid Mechanics, 1974, AMMRC-MS-74-8, Sept. 1974.

1-10. Sharpe, W.N., "Measurement of Residual Strains Around Coldworked Fastener Holes", Scientific Report, AFOSR Grant 75-2817, Bolling AFB, Washington D.C., April 1976.

1-11. Chandawanich, N., Sharpe, W.N.,Jr., "An Experimental Study of Crack Initiation and Growth From Coldworked Holes", Proc. 1978 SESA Spring Meeting, Wichita, Kansas, May 1978.

1-12. Poolsuk, S., Sharpe, W.N.,Jr., "Measurement of the Elastic-Plastic Boundary Around Coldworked Holes", Journal App. Mech., Paper 78-WA/APM 2, in press.

1-13. Potter, R.M., and Grandt, A.F.,Jr., "An Analysis of Residual Stresses and Displacements Due to Radial Expansion of Fastener Holes", ASME 1975 Failure prevention and Reliability Conference, Washington D.C., Sept. 1975.

1-14. Adler, W.F., and Dupree, D.M., "Stress Analysis of Coldworked Fastener Holes", Technical Report AFML-TR-74-44, Wright-Patterson AFB, Ohio July 1974.

1-15. Ford, S.C., Leis, B.N., Utah, D.A., Griffith, W., Sampath, S.G. and Mincer, P.M., "Interference Fit Fastener Investigation", Technical Report AFFDL-TR-75-93, Wright Patterson AFB, Ohio, Sept. 1975.

1-16. Cloud, G.L., and Corbly, D.M., "Effect of Large Compressive In-Plane Loads on Residual Strains Near Coldworked Fasteners", Technical Report in preparation, Wright-Patterson AFB, Ohio.

5-1. Luxmoore, A., and Hermann, R., "An Investigation of Photoresists for Use in Optical Strain Analysis", Jrnl. Strain Anal., 5, 3, 162, July 1970.

5-2. Holister, G.S., and Luxmoore, A.R., "The Production of High-Density Moire Grids", Exp. Mech., 8, 210, May 1968.

5-3. Luxmoore, A.R., and Hermann, R., "The Rapid Deposition of Moire Grids", Expl. Mech. 11, 5, 375, August 1971.

5-4. Straka, P., and Pindera, J.T., "Applications of Moire Grids for Deformation Studies in a Wide Temperature Range", Exp. Mech., 14, 5, 214, May 1974.

5-5. Chiang, F.P., "Production of High Density Moire Grids-Discussion", Exp. Mech., 9, 6, 286, June 1969.

5-6. Forno, C., "White-Light Speckle Photography For Measuring Deformation, Strain, and Shape", Optics and Laser Tech., 217, Oct. 1975.

5-7. Burch, J.M. and Forno, C., "A High Sensitivity Moire Grid Technique for Studying Deformation in Large Objects", Optical Eng. 14, 2, 178, Mar-Apr 1975.

5-8. Cloud, G.L., "Slotted Apertures for Multiplying Grating Frequencies and Sharpening Fringe Patterns in Moire Photography", Technical Report AFML-TR-76-164, WPAFB, Ohio (1977).

5-9. Cloud, G.L., "Slotted Apertures for Multiplying Grating Frequencies and Sharpening Fringe Patterns in Moire Photography", Optical Engineering 15, 6, 578-582, (Nov-Dec 1976).

5-10. Austin, S., and Stone, F.T., "Fabrication of Thin Periodic Structures in Photoresist: A Model", App. Opt. 15, 4, 1070-1074, April 1976.

5-11. Kodak Plates and Films for Scientific Photography, Kodak Publication, P-315, Eastman Kodak, Co., 1973.

5-12. Kodak High Resolution Plates, Kodak Publication P-47, Eastman Kodak Co., 1974.

5-13. Techniques of Microphotography, Kodak Publication P-52, Eastman Kodak Co., 1970.

6-1. Guild, J., The Interference Systems of Crossed Diffraction Gratings, Clarendon Press, Oxford, (1956).

6-2. Post, D., "Analysis of Moire Fringe Multiplication Phenomena", App. Opt., 6, 11, 1938, November 1967.

6-3. Post, D., "New Optical Methods of Moire Fringe Multiplication", Exp. Mech. 8, 2, 63, Feb. 1968.

6-4. Post. D., "Moire Fringe Multiplication with a Nonsymmetrical Doubly Blazed Reference Grating", App. Opt., 10, 4, 901-907, April 1971.

6-5. Post. D., and MacLaughlin, T.F., "Strain Analysis by Moire-Fringe Multiplication", Exp. Mech., 11, 9, 408, Sept. 1971.

6-6. Cloud, G.L., "Lasers in Engineering Education", Eng. Ed., 66, 8, 837, May 1976.

6-7. Clark, J.A., Durelli, A.J., and Parks, V.J., "Shear and Rotation Moire Patterns Obtained by Spatial Filtering of Diffraction Patterns", Jrnl, Strain Anal. 6, 2, 134 (1971).

6-8. Nagae, S., Iwata, K., and Nagata, R., "Measurement of Strain Distribution in a Plane Metal Plate by Optical Spatial Filtering" App. Opt., 14, 1, 115, Jan. 1975.

APPENDIX A

MOIRE PATTERN DIGITIZING

```
:
'
'
'
```

Appendix A-2

Typical Output for Radial Strain Measurement

```
MOIRE PATTERN
DIGITIZING PROG

DATA SET NO.=
        23776122
P=
            1906
M=
               3
C=
               1
X0=
            .364

DIG(XMAX,0)

COORD SET CHECK:
DIGITIZE ANY
KNOWN POINT

YOUR X WAS
      0.0000E+00

DIGITIZE DATA

(X,Y) PAIRS ARE

       2.479E-01
               1

       3.350E-01
               2

       6.080E-02
               3

       9.055E-02
               4

       1.191E-01
               5

       1.464E-01
               6

       1.711E-01
               7

       1.935E-01
               8

       2.170E-01
               9

       2.369E-01
              10

       2.543E-01
              11

       2.692E-01
              12

       2.828E-01
              13

       2.952E-01
              14

       3.076E-01
              15

       3.187E-01
              16

       3.262E-01
              17

       3.349E-01
              18

       3.411E-01
              19

       3.485E-01
              20
```

Best Available Copy

Appendix A-3

Typical Output for Hoop Strain Measurement

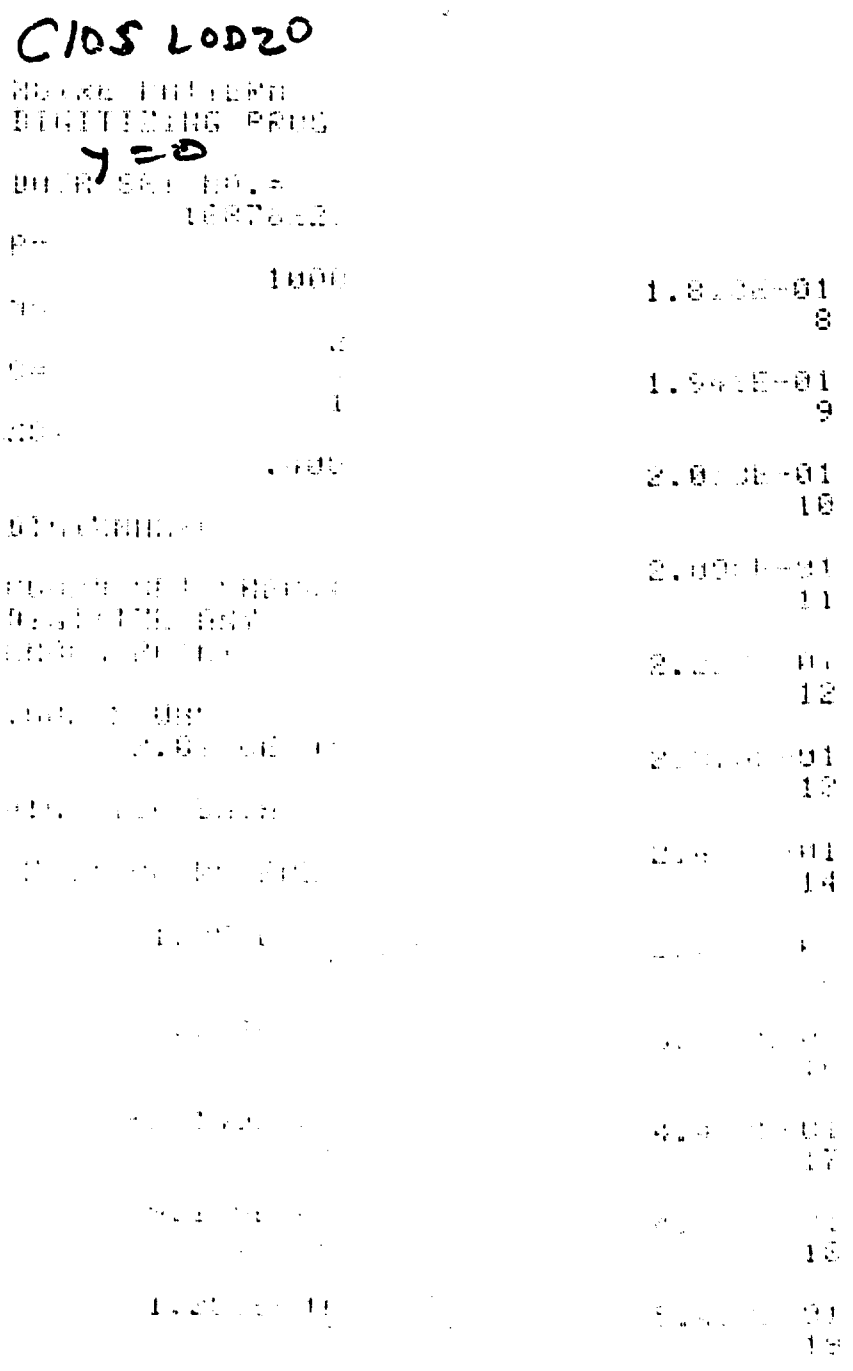

Best Available Copy

```
[illegible]
[illegible]
[illegible]
        16876[illegible]
[illegible]
            1000
M=
               2
C=
               1
[illegible]
             400
[illegible]
 [illegible] SET CHECK
 [illegible] ANY
 [illegible] POINT

 [illegible] WAS
      2.0[illegible]E-01

[illegible] DATA

[illegible] PAIRS ARE

      [illegible]E-01
               1

      [illegible]
               [illegible]

      [illegible]
               [illegible]

      [illegible]
               4

      [illegible]E-01
               5

      1.47[illegible]E-01
               6

      1.622E-01
               7

      1.750E-01
               8

      1.892E-01
               9

      2.020E-01
              10

      2.120E-01
              11

      2.2[illegible]E-01
              12

      2.4[illegible]E-01
              13

      2.5[illegible]E-01
              14

      [illegible]
               1

      3.[illegible]E-[illegible]

      4.[illegible]E-01
              17

      4.[illegible]E-01
              18

      5.4[illegible]E-01
              19
```

Best Available Copy

Best Available Copy

$\gamma = .02$

```
MOTOR PATTERN
DIGITIZING PROG
y=.04
DATA SET NO.=
        16876207
P=                                  1.352E-01
            1000                            7
M=                                  1.622E-01
               2                            8
C=                                  1.821E-01
               1                            9
X0=                                 2.007E-01
            .400                           10
DIG(XMAX,0)                         2.191E-01
                                           11
COORD SET CHECK:
DIGITIZE ANY                        2.376E-01
KNOWN POINT                                12
YOUR X WAS                          2.576E-01
        1.9812E-01                         13
DIGITIZE DATA                       2.903E-01
                                           14
(X,Y) PAIRS ARE
                                    3.[illegible]E-01
        -1.3[illegible]E-01                15
                1
                                    [illegible]E-01
        -[illegible]E-01                   16
                2
                                    [illegible]E-01
        -4.[illegible]E-01                 17
                3
                                    [illegible]E-01
        [illegible]E-01                    18
                4
                                    [illegible]E-01
        6.[illegible]E-02                  19
                5
                                    [illegible]E-01
        1.[illegible]E-01                  19
                6
```


Best Available Copy

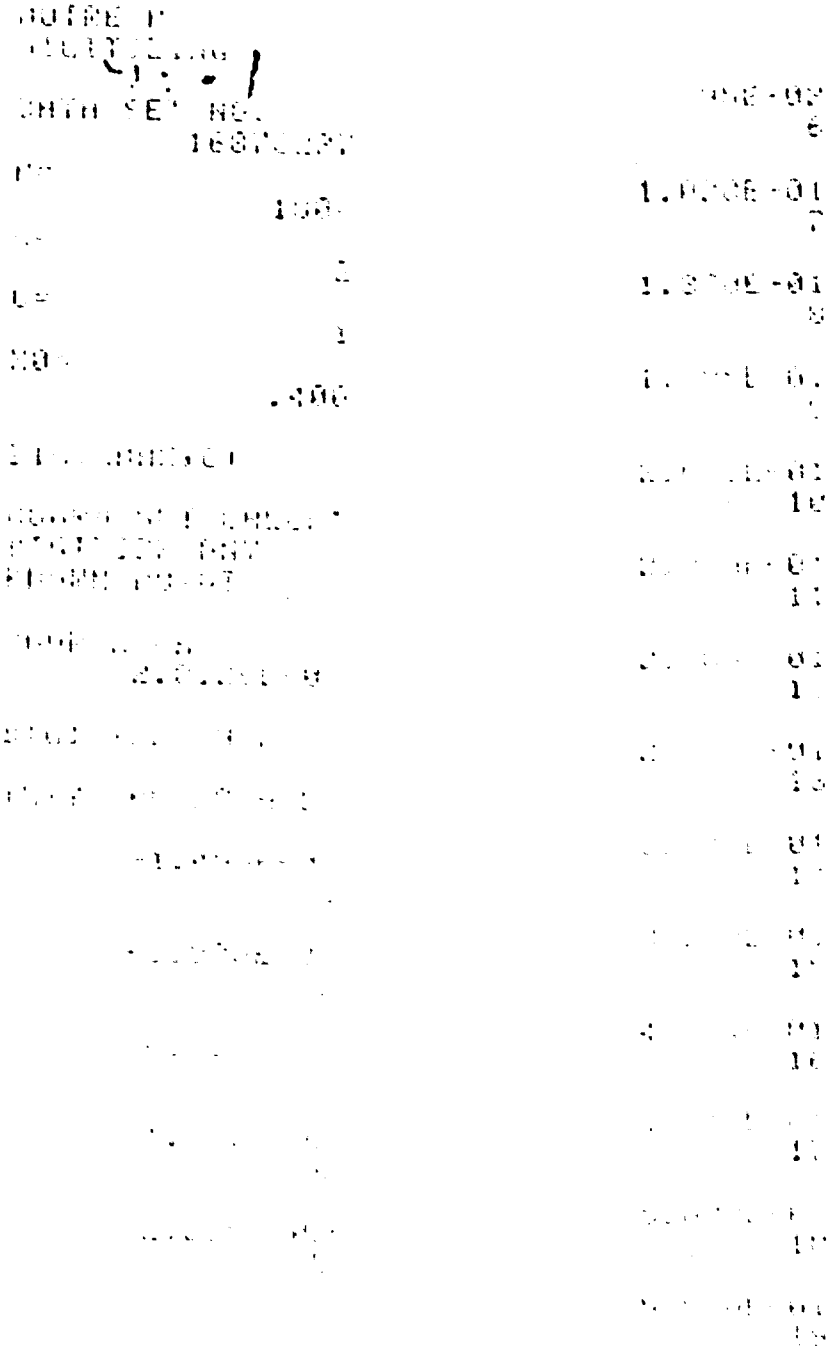

Best Available Copy

```
[illegible]
DIGITIZING [illegible]

DATA SET NO.=
        169 [illegible]
P=
            1000
M=
                2
C=
                1
X0=
            .400

DIGIXMAX=0

COORD SET CHECK:
DIGITIZE ANY
KNOWN POINT

[illegible]
      [illegible]

DIGIT[illegible]

[illegible]

      [illegible]
                1

      [illegible]

      [illegible]

      [illegible]

      [illegible]

      [illegible]

      [illegible]
```

```
1.239E-01
        8

1.622E-01
        9

1.964E-01
       10

2.[illegible]E-01
       11

2.[illegible]E-01
       12

3.[illegible]E-01
       13

3.[illegible]E-01
       14

3.[illegible]E-01
       15

4.[illegible]E-01
       16

4.[illegible]E-01
       17

5.[illegible]E-01
       18

5.[illegible]E-01
       19
```

Best Available Copy

APPENDIX B

DETAILED DATA ANALYSIS AND PLOTTING

Appendix B-1

Computer Program

```
PROGRAM MOIRE      74/74   OPT=1                          FTN 4.6+446        07/20/7
      PROGRAM MOIRE (INPUT,OUTPUT,PLFILE=0)
C
C
      COMMON /INTP/ YINT(101,2)
      COMMON /DIFY/ YDIF(101),DY(100)
      COMMON X(80,2),Y(80,2),NPTS(2),XPL(101),XL,XH,YL,YH,XMIN,XMAX,ISET
      REAL M
      LOGICAL FIN
C
      CALL COMPRS
      FIN = .FALSE.
      IC = 0
C
C ---- ENTER RUN DATA
C
  100 IC = IC+1
      CALL READIN (P,M,C,X0,IPR,FIN)
      IF (FIN) GO TO 1000
C
C --- DETERMINE X-RANGE FOR INTERPOLATION & DELTA VALUE
C
      CALL RANGE (DEL)
C
C --- COMPUTE INTERPOLATED "SMOOTH" CURVES THRU DATA & BASE SETS
C
      CALL INTERP (DEL)
C
C --- PLOT INPUT & SMOOTHED DATA
C
      CALL PLOTR (1)
C
C --- COMPUTE CURVE DIFFERENCES & DERIVATIVES
C
      PMC = P*M*C
      CALL DIFF (PMC,DEL)
C
C --- CORRECT ABCISSA ARRAY
C
      CALL CORRECT (X0)
C
C --- PLOT DIFFERENCE CURVE
C
      CALL PLOTR (2)
C
C --- PLOT STRAIN CURVE
C
      CALL PLOTR (3)
C
C --- PRINT OUTPUT IF DESIRED
C
      IF (IPR .NE. 1) GO TO 100
      CALL WRITOUT (IC,DEL)
      GO TO 100
 1000 CALL DONEPL
      STOP
      END
```

```
IROUTINE READIN     74/74   OPT=1                    FTN 4.6+446        07/20/7

      SUBROUTINE READIN (P,M,C,X0,IPR,FIN)
      COMMON X(80,2),Y(80,2),NPTS(2),XPL(101),XL,XH,YL,YH,XMIN,XMAX,ISET
      REAL M
      LOGICAL FIN
C
C --- INPUT RUN CONSTANTS
C
      READ 1, ISET
    1 FORMAT (A10)
      IF (EOF(5LINPUT)) 50,5
    5 READ *, P,M,C,X0,IPR
C
C --- INPUT DATA VALUES
C
      READ *, NPTS(1),Y(1,1)
      N = NPTS(1)
      READ *, (X(J,1),J=1,N)
C
C --- COMPUTE REMAINING DATA Y-VALUES
C
      DO 10 I=2,N
      Y(I,1) = Y(I-1,1) + 1.0
   10 CONTINUE
C
C --- INPUT BASELINE VALUES
C
      READ *, NPTS(2),Y(1,2)
      N = NPTS(2)
      READ *, (X(J,2),J=1,N)
C
C --- COMPUTE REMAINING BASE Y-VALUES
C
      DO 20 I=2,N
      Y(I,2) = Y(I-1,2) + 1.0
   20 CONTINUE
C
C
      RETURN
C
   50 FIN = .TRUE.
      RETURN
      END
```

```
ROUTINE RANGE      74/74   OPT=1                    FTN 4.6+446      07/20/7

      SUBROUTINE RANGE (DEL)
      COMMON X(80,2),Y(80,2),NPTS(2),XPL(101),XL,XH,YL,YH,XMIN,XMAX,ISET
C
      N1 = NPTS(1)
      N2 = NPTS(2)
C
      IF (X(1,1) .LE. X(1,2)) GO TO 20
      XMIN = X(1,1)
      XL = X(1,2)
      GO TO 40
C
   20 XMIN = X(1,2)
      XL = X(1,1)
C
   40 IF (X(N1,1) .GE. X(N2,2)) GO TO 60
      XMAX = X(N1,1)
      XH = X(N2,2)
      GO TO 80
C
   60 XMAX = X(N2,2)
      XH = X(N1,1)
C
   80 DEL = (XMAX-XMIN)/100.0
C
      IF (Y(1,1) .LE. Y(1,2)) YL = Y(1,1)
      IF (Y(1,2) .LE. Y(1,1)) YL = Y(1,2)
      IF (Y(N1,1) .GE. Y(N2,2)) YH = Y(N1,1)
      IF (Y(N2,2) .GE. Y(N1,1)) YH = Y(N2,2)
C
      RETURN
      END
```

```
*ROUTINE INTERP      74/74   OPT=1                    FTN 4.6+446        07/20/7
      SUBROUTINE INTERP (DEL)
      COMMON /INTP/ YINT(101,2)
      COMMON X(80,2),Y(80,2),NPTS(2),XPL(101),XL,XH,YL,YH,XMIN,XMAX,ISET
      DIMENSION WD(80),RD(80),XN(80),FN(80),GN(80),DN(80),THETA(80),
     +  W(1200)
      DATA WD/80*1.0/
C
C
      DO 10 I=1,101
      XPL(I) = XMIN + DEL*(I-1)
   10 CONTINUE
C
      DO 40 I=1,2
      CALL SPLIN1 (NPTS(I),KNOTS,X(1,I),Y(1,I),WD,RD,XN,FN,GN,DN,THETA,
     +  W,0,0)
         DO 20 K=1,101
         YINT(K,I) = SPLIN2 (XPL(K),KNOTS,XN,FN,GN,1)
   20    CONTINUE
   40 CONTINUE
C
C
      RETURN
      END
```

```
                74/74    OPT=1                          FTN 4.6+446          07/20/7

      SUBROUTINE SPLIN1(M,N,XD,YD,WD,RD,XN,FN,GN,DN,THETA,W,IPRINT,IFIT)
C
C  *  *  *  *  *  *  *  *  *  *  *  *  *  *  *  *  *  *  *  *  *  *  *
C
C
C - - A ROUTINE TO FIT THE SMOOTHEST CURVE THRU A GIVEN SET OF DATA
C     USING CUBIC SPLINES.
C
C          M = TOTAL NUMBER OF DATA POINTS.
C          N = NUMBER OF KNOTS USED (INPUT OR OUTPUT DEPENDING ON IFIT)
C         XD = X-COOR. DATA ARRAY (INPUT)
C         YD = Y-COOR. DATA ARRAY (INPUT)
C         WD = WEIGHT FOR EACH DATA POINT (GENERALLY = 1.0, IF W(I) = 0.
C              THEN THE ITH POINT WILL BE OMITTED FROM THE FIT) (INPUT)
C         RD = AN ARRAY CONTAINING YD(I)-S(XD(I)) (OUTPUT)
C         XN = AN ARRAY CONTAINING THE KNOT POSITIONS (INPUT OR OUTPUT
C              DEPENDING ON IFIT)
C         FN = AN ARRAY CONTAINING THE VALUES OF THE SPLINE AT THE KNOTS
C              (OUTPUT)
C         GN = AN ARRAY CONTAINING THE VALUES OF THE DERIVATIVE OF THE
C              SPLINE AT THE KNOTS (OUTPUT)
C         DN = AN ARRAY CONTAINING THE VALUES OF THE 3RD DERIVATIVE
C              DISCONTINUITIES OF THE SPLINE ACROSS THE KNOTS (ROUGH
C              ESTIMATE OF THE ERROR IN THE FIT) (OUTPUT)
C      THETA = WORKING ARRAY
C          W = WORKING ARRAY (MUST BE DIMENSIONED ATLEAST 7*M+8*N+6)
C     IPRINT = PRINT OPTION
C              1 PRINT RESULTS AFTER EACH ITERATION
C              0 NO PRINT PRODUCED
C             -1 PRINT RESULTS FOR BEST FIT ONLY
C       IFIT = FIT OPTION
C              0  PROGRAM WILL AUTOMATICALLY SELECT KNOT POSITIONS
C              1 CALCULATE THE SPLINE WITH THE INPUT SET OF KNOT
C                POSITIONS **CAUTION N MUST BE .GE. 5 AND XN(1)=XD(1),
C                XN(N)=XD(M) FOR CORRECT RESULTS.
C
C
C     THE NORMAL MODE OF OPERATION IS TO ALLOW THE PROGRAM TO
C     AUTOMATICALLY SELECT THE OPTIMAL KNOT POSITIONS BASED ON
C     STATISTICAL ERROR TESTS. IN THIS MODE OF OPERATION IT IS DIFFICULT
C     TO PREDICT THE REQUIRED DIMENSION FOR THE ARRAYS XN, FN, GN, DN,
C     THETA, AND W. THE PROGRAM WILL NEVER MAKE N GT M SO A SAFE
C     DIMENSIONALITY FOR THESE ARRAYS WOULD BE M. SPLIN1 CALLS SPLIN3
C     TO CALCULATE THE LEAST SQUARES SPLINE APPROXIMATION.
C
C
C  *  *  *  *  *  *  *  *  *  *  *  *  *  *  *  *  *  *  *  *  *  *  *
C
C
      DIMENSION XD(1),YD(1),WD(1),RD(1),XN(1),FN(1),GN(1),DN(1),
     1          THETA(1),W(1)
C
C     OMIT DATA WITH ZERO WEIGHTS
C
      MM=1
      J=1
      DO 1 I=2,M
```

```
IROUTINE CORRECT    74/74   OPT=1                    FTN 4.6+446        07/20/7

      SUBROUTINE CORRECT (XA)
      COMMON X(80,2),Y(80,2),NPTS(2),XPL(101),XL,XH,YL,YH,XMIN,XMAX,ISET
C
C --- THIS ROUTINE COMPUTES CORRECTION FOR DISTANCE FROM HOLE
C
      DO 10 I=1,101
      XPL(I) = XA - XPL(I)
   10 CONTINUE
C
      RETURN
      END
```

ROUTINE SPLIN1 74/74 OPT=1 FTN 4.6+446 07/20/7

```
      IF(WD(I)) 3,2,3
    2 IF(I-M) 4,3,3
    4 W(J)=XD(I)
      W(J+1)=YD(I)
      W(J+2)=FLOAT(I)
      J=J+3
      GO TO 1
    3 MM=MM+1
      XD(MM)=XD(I)
      YD(MM)=YD(I)
      WD(MM)=WD(I)
    1 CONTINUE
      J=1
      K=MM
    7 IF(K-M) 5,6,6
    5 K=K+1
      XD(K)=W(J)
      YD(K)=W(J+1)
      WD(K)=W(J+2)
      J=J+3
      GO TO 7
C
C     INITIALIZATION OF ITERATIONS
C
    6 IF(IFIT .EQ. 1) GO TO 110
      JA=1
      IF(WD(1)) 9,8,9
    8 JA=2
    9 N=5
      XN(1)=XD(1)
      XN(5)=XD(MM)
      XN(3)=0.5*(XN(1)+XN(5))
      XN(2)=0.5*(XN(1)+XN(3))
      XN(4)=0.5*(XN(3)+XN(5))
  110 IW=7*MM+3*N+6
      DO 10 I=1,N
      J=IW+I
   10 W(J)=XN(I)
      IF=-IPRINT
C
C     CALCULATE THE HISTOGRAMS FOR NEW SCALE FACTORS
C
   11 J=0
      K=1
      SA=0.
   12 SA=SA+WD(K)**2
      K=K+1
      IF(XD(K)-XD(1)) 12,12,13
   13 SA=(SA+0.5*WD(K)**2)/(XD(K)-XD(1))
   14 J=J+1
      IF(XD(K)-XN(J+1)) 15,15,16
   16 GN(J)=SA*(XN(J+1)-XN(J))
      GO TO 14
   15 GN(J)=SA*(XD(K)-XN(J))+0.5*WD(K)**2
   17 K=K+1
      IF(K-MM) 18,18,19
   18 IF(XD(K)-XN(J+1)) 20,20,21
```

```
ROUTINE SPLIN1      74/74    OPT=1                          FTN 4.5+446          07/20/7

   20 GN(J)=GN(J)+WD(K)**2
      GO TO 17
   21 SA=0.5*(WD(K-1)**2+WD(K)**2)/(XD(K)-XD(K-1))
      GN(J)=GN(J)-0.5*WD(K-1)**2+SA*(XN(J+1)-XD(K-1))
      GO TO 14
C
C     CALCULATE THE NEW SCALE FACTORS
C
   19 K=IW+2
      GN(1)=0.00025216*GN(1)*(W(K)-W(K-1))**8/(XN(2)-XN(1))
      DO 22 J=3,N
      IF(XN(J)-W(K)) 23,23,24
   24 K=K+1
   23 GN(J-1)=0.00025216*GN(J-1)*(W(K)-W(K-1))**8/(XN(J)-XN(J-1))
   22 GN(J-2)=ALOG(GN(J-2)+GN(J-1))
      NN=N-2
      HS=1.386294
      DO 97 J=2,NN
   97 GN(J)=AMIN1(GN(J),GN(J-1)+HS)
      J=NN-1
   98 GN(J)=AMIN1(GN(J),GN(J+1)+HS)
      J=J-1
      IF(J) 99,99,98
   99 DO 25 J=3,N
   25 THETA(J-1)=SQRT(EXP(GN(J-2))/(XN(J)-XN(J-2)))
C
C     CALCULATE THE SPLINE APPROXIMATION WITH CURRENT KNOTS
C
      CALL SPLIN3(NM,N,XD,YD,WD,PD,XN,FN,GN,DN,THETA,W,IP)
      IF(IFIT .EQ. 1) GO TO 41
C
C     APPLY STATISTICAL TEST FOR EXTRA KNOTS
C
      J=IW+1
      JJ=0
      K=JA
      TMAX=0.
      IIS=1
   26 KC=-1
      SW=0.
      SP=0.
      RP=0.
      J=J+1
      JJ=JJ+1
      W(JJ)=0.
   27 IF(W(J)-XD(K)) 28,29,30
   30 KC=KC+1
      SW=SW+WD(K)**2
      SP=SP+RP*RD(K)
      RP=RD(K)
      K=K+1
      GO TO 27
   29 IF(WD(K)) 31,28,31
   31 KC=KC+1
      SW=SW+WD(K)**2
      SP=SP+RP*RD(K)
   28 IF(SP) 32,32,33
```

```
ROUTINE SPLIN1      74/74    OPT=1                          FTN 4.6+446          07/20/7

      33 SW=(SW/SR)**2
         PP=SQRT(SR/FLOAT(KC))
         IF (FLOAT(KC)-SW) 32,32,34
      34 IF (IIS .EQ. 3) GO TO 37
         IF (IIS .EQ. 2) GO TO 36
         PPP=PP
         IIS=3
         IF(FLOAT(KC)-2.*SW) 38,38,39
      37 W(JJ-1)=PPP
         TMAX=AMAX1(TMAX,PPP)
      38 IIS=2
      36 W(JJ)=PP
         TMAX=AMAX1(TMAX,PP)
         GO TO 38
      32 IIS=1
      38 IF(W(J)-XN(N)) 26,40,40
C
C        TEST WHETHER ANOTHER ITERATION IS REQUIRED
C
      40 IF(TMAX) 41,41,42
C
C        CALCULATE NEW TREND ARRAY, INCLUDING LARGER TRENDS ONLY
C
      42 TMAX=0.5*TMAX
         I=0
         J=1
         JW=1
         K=IW+1
         THETA(JW)=W(K)
      43 I=I+1
         K=K+1
         IF(W(I)-TMAX) 44,44,45
      44 JW=JW+1
         THETA(JW)=W(K)
      46 FN(J)=0.
         J=J+1
         IF(W(K)-XN(J)) 47,47,46
      45 JW=JW+2
         THETA(JW-1)=0.5*(W(K-1)+W(K))
         THETA(JW)=W(K)
         IF(XN(J+1)-THETA(JW-1)) 46,46,48
      48 FN(J)=1.
         J=J+1
      47 IF(J-N) 43,49,49
C
C        MAKE KNOT SPACINGS BE USED FOUR TIMES
C
      49 IK=1
         KL=1
         FN(2)=AMAX1(FN(1),FN(2))
      50 K=KL+3
      51 IF(FN(K)) 52,52,53
      52 K=K-1
         IF(K-KL) 54,54,51
      53 K=K-1
         FN(K)=1.
         IF(K-KL) 54,54,53
```

```
ROUTINE SPLIN1     74/74   OPT=1                    FTN 4.6+446        07/20/7

      54 K=K+1
         IF(K-N) 55,56,56
      55 IF(XN(K+1)-XN(K)-1.5*(XN(K)-XN(K-1))) 54,54,56
      56 KU=K
         FN(K-2)=AMAX1(FN(K-2),FN(K-1))
      57 KKU=K
      58 K=K-1
         IF(K-KL) 59,59,60
      60 IF(XN(K)-XN(K-1)-1.5*(XN(K+1)-XN(K))) 58,58,61
      61 FN(K+1)=AMAX1(FN(K),FN(K+1))
      59 KKL=K
         KZ=4
         IF(FN(K)) 62,62,63
      63 K=K+1
         IF(K-KKU) 64,65,65
      64 IF(FN(K)) 66,66,63
      66 KZ=3
      62 KZ=KZ+1
         K=K+1
         IF(K-KKU) 67,65,65
      67 IF(FN(K)) 62,62,68
      68 IF(KZ-3) 69,69,70
      69 J=K-KZ
      71 FN(J)=1.
         J=J+1
         IF(J-K) 71,63,63
      70 IF(K+1-KKU) 72,65,65
      72 K=K+1
         FN(K)=1.
         GO TO 63
      65 IF(KL-KKL) 73,74,74
      73 FN(KKL-2)=AMAX1(FN(KKL-2),FN(KKL+1))
         FN(KKL-1)=AMAX1(FN(KKL-1),FN(KKL+3))
      75 K=KKL-4
      78 IF(FN(K)) 76,76,77
      76 K=K+1
         IF(K-KKL) 78,79,79
      77 FN(K)=1.
         K=K+1
         IF(K-KKL) 77,79,79
      79 IF (IK .EQ. 1) GO TO 57
         IF (IK .EQ. 2) GO TO 80
      74 IF(KU-N) 91,82,92
      91 KL=KU
         FN(KL+1)=AMAX1(FN(KL+1),FN(KL-2))
         FN(KL)=AMAX1(FN(KL),FN(KL-4))
         GO TO 60
      82  IK = 2
         KKL=N
         GO TO 75
C
C     INSERT EXTRA KNOTS FOR NEW APPROXIMATION
C
      80 DO 87 J=1,N
      87 GN(J)=XN(J)
         NN=1
         DO 84 J=2,N
```

```
ROUTINE SPLIN1     74/74   OPT=1                    FTN 4.6+446        07/20/7

            IF(FN(J-1)) 85,85,86
         86 NN=NN+1
            XN(NN)=0.5*(GN(J-1)+GN(J))
         85 NN=NN+1
            XN(NN)=GN(J)
         84 CONTINUE
            J=NN
            IW=7*MM+8*N+6
            DO 87 J=1,JN
            I=IW+J
         87 W(I)=THETA(J)
            GO TO 11
      C
      C     RESTORE DATA WITH ZERO WEIGHTS
      C
         41 IF(MM-M) 98,89,89
         89 IF(IPRINT) 90,90,91
         98 J=-2
            K=MM
         92 J=J+3
            K=K+1
            W(J)=XD(K)
            W(J+1)=YD(K)
            W(J+2)=WD(K)
            IF(K-M) 42,93,93
         93 I=INT(W(J+2)+0.1)
         94 IF(K-I) 95,95,96
         96 XD(K)=XD(MM)
            YD(K)=YD(MM)
            WD(K)=WD(MM)
            K=K-1
            MM=MM-1
            GO TO 94
         95 XD(K)=W(J)
            YD(K)=W(J+1)
            WD(K)=0.
            K=K-1
            J=J-3
            IF(J) 91,91,92
         91 CALL SPLIN3(M,N,XD,YD,WD,RD,XN,FN,GN,DN,THETA,W,IABS(IPRINT))
         90 RETURN
            END
```

```
UNCTION SPLIN2      74/74   OPT=1                    FTN 4.6+446        07/20/7

      FUNCTION SPLIN2(X,N,XN,FN,GN,ITYPE)
C
C  *  *  *  *  *  *  *  *  *  *  *  *  *  *  *  *  *  *  *  *  *  *  *  *  *
C
C
C  - -  A FUNCTION UTILITY TO BE USED IN CONJUNCTION WITH THE SPLINE
C       ROUTINES SPLIN4 OR SPLIN1.
C
C           X = THE VALUE OF THE INDEPENDENT VARIABLE AT WHICH THE SPLINE
C               OR ITS DERIVATIVE ARE TO BE EVALUATED. X MUST BE BETWEEN
C               XN(1) AND XN(N) FOR CORRECT RESULTS.
C           N = THE NUMBER OF KNOTS (RETURNED BY SPLINING ROUTINES)
C          XN = ARRAY OF KNOT POSITIONS (RETURNED BY SPLINE ROUTINES)
C          FN = ARRAY OF SPLINE VALUES (RETURNED BY SPLINE ROUTINES)
C          GN = ARRAY OF DERIVATIVE VALUES (RETURNED BY SPLINE ROUTINES)
C       ITYPE = 1 RETURNS SPLINE VALUE AT X
C               2 RETURNS THE DERIVATIVE VALUE AT X
C
C
C  *  *  *  *  *  *  *  *  *  *  *  *  *  *  *  *  *  *  *  *  *  *  *  *  *
C
      DIMENSION XN(1),FN(1),GN(1)
      IF(X .LT. XN(1)) GO TO 100
      IF(X .GT. XN(N)) GO TO 110
       DO 8 K=1,N
       IF(X .NE. XN(K)) GO TO 8
       KK = K
       GO TO 120
    8 CONTINUE
      DO 10 K=2,N
      IF(X .GT. XN(K)) GO TO 10
      JK=K
      GO TO 20
   10 CONTINUE
   20 HH=XN(JK)-XN(JK-1)
      HH3=HH**3
      T1=HH*GN(JK-1)+FN(JK-1)-FN(JK)
      T2=HH*GN(JK)+FN(JK-1)-FN(JK)
      T3=XN(JK)-X
      T4=X-XN(JK-1)
      IF (ITYPE .EQ. 2) GO TO 201
      SPLIN2=(T3*FN(JK-1)+T4*FN(JK))/HH+T3*T4*(T3*T1-T4*T2)/HH3
      RETURN
  201 SPLIN2=(FN(JK)-FN(JK-1))/HH-T3*T4*(HH*(GN(JK-1)+GN(JK))+2.*(FN(JK-
     1        1)-FN(JK)))/HH3+(XN(JK-1)+XN(JK)-2.*X)*(T3*T1-T4*T2)/HH3
      RETURN
  100 JK=2
      GO TO 20
  110 JK=N
      GO TO 20
  120 IF (ITYPE .EQ. 2) GO TO 701
      SPLIN2=FN(KK)
       RETURN
  701 SPLIN2=GN(KK)
      RETURN
      END
```

```
ROUTINE SPLIN3      74/74    OPT=1                          FTN 4.6+446          07/29/7

      SUBROUTINE SPLIN3(M,N,XD,YD,WD,RD,XN,FN,GN,DN,THETA,W,IPRINT)
C
      DIMENSION W(1),XD(1),YD(1),WD(1),RD(1),XN(1),FN(1),GN(1),DN(1),
     1          S(7),THETA(1)
C
C     TRANSFER KNOTS TO W, AND INSERT EXTRA KNOTS AT ENDS OF RANGE
C
      XN(N)=AMAX1(XN(N),XD(M))
      DO 1 I=1,N
    1 W(I+3)=XN(I)
      DO 2 J=1,3
      K=4-J
      W(K)=W(K+1)+W(K+1)-W(K+2)
      K=J+N
    2 W(K+3)=W(K+2)+W(K+2)-W(K+1)
C
C     SET UP THE LEAST SQUARES EQUATIONS IN W
C
      I=1
      J=2
      K=N+13
      AA=1.0/((W(3)-W(4))*(W(3)-W(5))*(W(3)-W(6))*(W(3)-W(7)))
      D=1.0/((W(5)-W(1))*(W(5)-W(2))*(W(5)-W(3))*(W(5)-W(4)))
    3 A=AA
      AA=1.0/((W(J+2)-W(J+3))*(W(J+2)-W(J+4))*(W(J+2)-W(J+5))*
     1   (W(J+2)-W(J+6)))
      B=AA*(W(J+2)-W(J+6))/(W(J+2)-W(J+1))
      DD=D
      D=1.0/((W(J+4)-W(J))*(W(J+4)-W(J+1))*(W(J+4)-W(J+2))*
     1   (W(J+4)-W(J+3)))
      C=DD*(W(J+3)-W(J-1))/(W(J+3)-W(J+4))
      FN(J-1)=K-7
      IF(J-2) 4,4,5
    4 W(K-6)=-DD
      W(K-5)=-C-D
      W(K-4)=A+B
      W(K-3)=AA
      W(K-2)=0.
      IF(I-M) 6,6,7
    6 W(K-1)=1.
      W(K)=0.
      GO TO 8
    5 W(K-4)=-AW*(W(K-4)+C+D)
      W(K-3)=AW*B
      W(K-2)=AW*AA
    8 K=K+7
      IF(I-M) 9,9,12
    9 IF(W(J+3)-XD(I)) 11,10,10
   10 W(K-6)=DD*WD(I)*(W(J+3)-XD(I))**3
      W(K-5)=WD(I)*(C*(W(J+3)-XD(I))**3+D*(W(J+4)-XD(I))**3)
      W(K-4)=WD(I)*(A*(XD(I)-W(J+1))**3+B*(XD(I)-W(J+2))**3)
      W(K-3)=WD(I)*AA*(XD(I)-W(J+2))**3
      W(K-2)=WD(I)*YD(I)
      W(K-1)=0.
      W(K)=0.
      I=I+1
      GO TO 8
```

```
   12 IF(J-N) 11,4,4
   11 J=J+1
      AW=6.*THETA(J-1)
      W(K-6)=AW*CD
      W(K-5)=AW*C
      W(K-4)=A+B
      GO TO 3
    7 W(K-1)=0.
      W(K)=1.
      FN(J)=K
C
C     APPLY HOUSEHOLDER ORTHOGONAL TRANSFORMATIONS TO OBTAIN AN UPPER
C     TRIANGULAR LEAST SQUARES MATRIX
C
      KUMAX=K
      I=1
      IPR=N-1
      NPINIT=7
   13 I=I+1
      IPR=IPR+7
      NP=NPINIT
      J=I+NP
      KL=MAX0(IPR+8,IFIX(FN(J-8)+1.5))
      KU=IFIX(FN(J-7)+0.5)
      IF(NP-7) 14,14,15
   14 W(IPR+1)=0.
      W(IPR+2)=0.
      W(IPR+3)=0.
      W(IPR+4)=0.
   15 IF(KU-KL) 25,25,17
   17 NPINIT=MAX0(3,NPINIT-1)
      GO TO 18
   16 NP=NP+1
      J=IPR+NP
      W(J)=W(J-1)
      W(J-1)=W(J-2)
      W(J-2)=W(J-3)
      W(J-3)=0.
      KL=KU+1
      J=I+NP
      KU=IFIX(FN(J-7)+0.5)
   18 DO 19 J=1,NP
      JP=IPR+J
   19 S(J)=W(IPR+1)*W(JP)
      KPIV=0
      PIVMAX=ABS(W(IPR+1))
      DO 20 K=KL,KU,7
      DO 21 J=1,NP
      JJ=K+J
   21 S(J)=S(J)+W(JJ-1)*W(K)
      IF(PIVMAX-ABS(W(K))) 70,20,20
   70 PIVMAX=ABS(W(K))
      KPIV=K
   20 CONTINUE
      IF(KPIV) 71,71,72
   72 DO 73 J=1,NP
      JJ=IPR+J
```

```
SROUTINE SPLIN3     74/74   OPT=1                    FTN 4.6+446        07/20/7

      A=W(JJ)
      W(JJ)=W(KPIV)
      W(KPIV)=A
      KPIV=KPIV+1
   23 CONTINUE
   21 AA=SIGN(SQRT(S(1)),W(IPP+1))
      B=W(IPP+1)+AA
      A=1.0/(AA*B)
      DO 22 J=2,NP
      JP=IPP+J
      S(J)=A*(S(J)+AA*W(JP))
   22 W(JP)=W(JP)-B*S(J)
      W(IPP+1)=-AA
      DO 23 K=KL,KU,7
      A=W(K)
      DO 24 J=2,NP
      JJ=K+J
      W(JJ-2)=W(JJ-1)-A*S(J)
   24 CONTINUE
   23 CONTINUE
      IF(KU-KUMAX) 25,26,26
   25 IF(NP-7) 16,27,27
   27 GN(I)=SQRT(W(IPP+1)**2+W(KU+1)**2)
      A=W(IPP+1)/GN(I)
      B=W(KU+1)/GN(I)
      C=W(KU+5)
      DO 28 J=1,3
      JP=IPP+J
      JJ=KU+J
      W(JP)=A*W(JP+1)+B*W(JJ+1)
      W(JJ)=A*W(JJ+1)-B*W(JP+1)
      W(JJ+4)=-B*W(JP+4)
   28 W(JP+4)=A*W(JP+4)
      W(IPP+4)=B*C
      W(KU+4)=A*C
      GO TO 13
   26 IF(NP-4) 29,29,17
C
C     BACK-SUBSTITUTION TO OBTAIN MULTIPLIERS OF FUNDAMENTAL SPLINES
C
   29 K=KUMAX
      DO 30 J=1,4
      K=K-7
      JJ=IPP+J
      DO 31 I=1,3
      KK=K+I
      JK=JJ+I
      W(KK)=W(JK)
      L=IPP+1
      LK=KK
   32 IF(L-JJ) 33,34,34
   33 L=L+1
      LK=LK+3
      W(KK)=W(KK)-W(LK)*W(L)
      GO TO 32
   34 W(KK)=W(KK)/W(IPP+1)
   31 CONTINUE
```

```
      IPR=IPR-7
   39 CONTINUE
      L=N
   35 IF(IPR-N) 36,36,37
   37 K=K-3
      L=L-1
      DO 38 I=1,3
      KK=K+I
      JJ=IPR+I
   38 W(KK)=(W(JJ+4)-W(IPR+1)*W(KK+3)-W(IPR+2)*W(KK+6)-W(IPR+3)*W(KK+9)
     1       -W(IPR+4)*W(KK+12))/GN(L)
      IPR=IPR-7
      GO TO 35
   36 KRES=K
C
C     CALCULATE SPLINE VALUES AT THE DATA POINTS, AND SCALAR PRODUCTS
C
      KSDATA=KRES-3*M
      I=1
      J=1
      DO 43 L=1,5
   43 S(L)=0.
      KK=KSDATA
      AA=1.0/((W(3)-W(4))*(W(3)-W(5))*(W(3)-W(6))*(W(3)-W(7)))
      D=1.0/((W(5)-W(1))*(W(5)-W(2))*(W(5)-W(3))*(W(5)-W(4)))
   39 J=J+1
      K=K+3
      A=AA
      AA=1.0/((W(J+2)-W(J+3))*(W(J+2)-W(J+4))*(W(J+2)-W(J+5))*
     1   (W(J+2)-W(J+6)))
      B=AA*(W(J+2)-W(J+6))/(W(J+2)-W(J+1))
      DD=D
      D=1.0/((W(J+4)-W(J))*(W(J+4)-W(J+1))*(W(J+4)-W(J+2))*
     1  (W(J+4)-W(J+3)))
      C=DD*(W(J+3)-W(J-1))/(W(J+3)-W(J+4))
   40 IF(XD(I)-XN(J)) 41,41,39
   41 DO 42 L=1,3
      LK=L+K
      KU=L+KK
   42 W(KU)=A*W(LK+3)*(XD(I)-W(J+1))**3+(B*W(LK+3)+AA*W(LK+5))*
     1       (XD(I)-W(J+2))**3+(C*W(LK)+DD*W(LK-3))*(W(J+3)-XD(I))**3
     2       +D*W(LK)*(W(J+4)-XD(I))**3
      RD(I)=YD(I)-W(KK+1)
      AS=WD(I)*RD(I)
      BS=WD(I)*W(KK+2)
      CS=WD(I)*W(KK+3)
      S(1)=S(1)+BS*BS
      S(2)=S(2)+BS*CS
      S(3)=S(3)+CS*CS
      S(4)=S(4)+AS*BS
      S(5)=S(5)+AS*CS
      I=I+1
      KK=KK+3
      IF(I-N) 40,40,44
C
C     CALCULATE THE RESIDUALS AND PARAMETERS OF THE REQUIRED SPLINE
C
```

```
ROUTINE SPLIN3      74/74    OPT=1                          FTN 4.6+446          07/20/7

      44 DET=S(1)*S(3)-S(2)*S(2)
         A=(S(3)*S(4)-S(2)*S(5))/DET
         B=(S(1)*S(5)-S(2)*S(4))/DET
         K=KSDATA
         DO 45 I=1,N
         K=K+3
      45 RD(I)=RD(I)-A*W(K-1)-B*W(K)
         KL=KRES+1
         DO 46 K=KL,KUMAX,3
      46 W(K)=W(K)+A*W(K+1)+B*W(K+2)
C
C        COMPUTE ELEMENTS OF FN,GN AND DN
C
         K=KRES
         AA=1.0/((W(2)-W(3))*(W(2)-W(4))*(W(2)-W(5))*(W(2)-W(6)))
         DN(1)=0.
         DO 47 J=1,N
         A=AA*W(K+4)*(XN(J)-W(J+1))**2
         AA=1.0/((W(J+2)-W(J+3))*(W(J+2)-W(J+4))*(W(J+2)-W(J+5))*
        1    (W(J+2)-W(J+6)))
         B=AA*(W(K+7)+W(K+4)*(W(J+2)-W(J+6))/(W(J+2)-W(J+1)))*
        1   (XN(J)-W(J+2))**2
         DD=W(K+1)*(W(J+4)-XN(J))/((W(J+4)-W(J))*(W(J+4)-W(J+1))*
        1    (W(J+4)-W(J+2)))
         FN(J)=A*(XN(J)-W(J+1))+B*(XN(J)-W(J+2))+DD*(W(J+4)-XN(J))
         GN(J)=3.0*(A+B-DD)
         IF(J-1) 48,48,49
      49 DN(J)=6.0*(GN(J-1)+GN(J)+2.0*(FN(J-1)-FN(J))/(XN(J)-XN(J-1)))/
        1(XN(J)-XN(J-1))**2
         DN(J-1)=DN(J)-DN(J-1)
      48 K=K+3
      47 CONTINUE
C
C        PROVIDE PRINT IF REQUESTED
C
         IF(IPRINT) 50,50,51
      50 RETURN
C
      51 PRINT 52
      52 FORMAT(1H1,35X,*SPLINE APPROXIMATION OBTAINED BY SPLIN3*//4X,1HI,
        19X,5HXN(I),18X,5HFN(I),18X,5HGN(I),13X,16H3RD DERIV CHANGE,11X,
        28HTHETA(I)//)
         I=1
         PRINT 63,I,XN(I),FN(I),GN(I)
      54 I=I+1
         IF(I-N) 55,56,56
      55 PRINT 63,I,XN(I),FN(I),GN(I),DN(I),THETA(I)
         GO TO 54
      56 PRINT 63,I,XN(I),FN(I),GN(I)
         PRINT 57
      57 FORMAT(///4X,1HI,9X,5HXD(I),18X,5HYD(I),18X,5HWD(I),19X,3HFIT,
        118X,8HRESIDUAL//)
         J=2
         DO 58 I=1,N
      59 IF(XD(I)-XN(J)) 60,60,61
      61 PRINT 62
      62 FORMAT(5X)
```

```
ROUTINE SPLIN3      74/74   OPT=1                    FTN 4.6+446        07/20/7

            J=J+1
            GO TO 59
         57  YDSD = YD(I)-RD(I)
            PRINT 63,I,XD(I),YD(I),WD(I),YDSD      ,RD(I)
         63 FORMAT(I5,5E23.14)
         59 CONTINUE
            GO TO 50
            END
```

```
ROUTINE DIFF        74/74   OPT=1                    FTN 4.6+446        07/20/7

            SUBROUTINE DIFF (PMC,DEL)
            COMMON /INTP/ YINT(101,2)
            COMMON /DIFY/ YDIF(101),DY(100)
      C
      C --- COMPUTE DIFFERENCES & DIVIDE BY PMC
      C
            DO 20 K=1,101
            YDIF(K) = (YINT(K,1) - YINT(K,2))/PMC
         20 CONTINUE
      C
      C --- COMPUTE DERIVATIVES
      C
            DO 40 K=2,101
            DY(K-1) = (YDIF(K) - YDIF(K-1))/DEL
         40 CONTINUE
            RETURN
            END
```

```
ROUTINE PLOT:        74/74    OPT=1                          FTN 4.6+446          07/20/

      SUBROUTINE PLOTR (IP)
      COMMON /INTP/ YINT(101,2)
      COMMON /DIFY/ YDIF(101),DY(100)
      COMMON X(80,2),Y(80,2),NPTS(2),XPL(101),XL,XH,YL,YH,XMIN,XMAX,ISET
C
      CALL BGNPL(IP)
      CALL PHYSOR (1.,.7)
      CALL TRIPLX
C
      IF (IP .EQ.3) GO TO 300
      IF (IP .EQ. 2) GO TO 200
C
C --- BASIC PLOT
C
      CALL TITLE (1H ,-1,"X",1,"Y",1,9.,7.)
      CALL GRAF (XL,"SCALE",XH,YL,"SCALE",YH)
      CALL CURVE (X(1,1),Y(1,1),NPTS(1),-2)
      CALL CURVE (X(1,2),Y(1,2),NPTS(2),-2)
      CALL CURVE (XPL,YINT(1,1),101,0)
      CALL CURVE (XPL,YINT(1,2),101,0)
      GO TO 500
C
C --- DIFFERENCE PLOT
C
  200 CALL TITLE (1H ,-1,"DISTANCE FROM HOLE*",100,"DISPLACEMENT",12,9.,
     *  7.)
      CALL GRAF (-.05,.05,.4,-.001,.001,.006)
      CALL CURVE (XPL,YDIF,101,0)
      CALL DOT
      CALL PLVEC (-.05,0.,.4,0.,0)
      CALL PLVEC (0.,-.001,0.,.006,0)
      GO TO 500
C
C --- STRAIN PLOT
C
  300 CALL TITLE (1H ,-1,"DISTANCE FROM HOLE*",100,"STRAIN",6,9.,7.)
      CALL GRAF (-.05,0.05,0.4,-0.01,0.01,0.06)
      CALL CURVE (XPL(2),DY,100,0)
      CALL DOT
      CALL PLVEC (-.05,0.0,0.4,0.0,0)
      CALL PLVEC (0.,-.01,0.,.06,0)
C
C
  500 CALL MESSAG ("SET NO. *",100,1.2,6.)
      CALL MESSAG (ISET,10,"ABUT","ABUT")
      CALL ENDPL(0)
      RETURN
      END
```

```
ROUTINE WRITOUT     74/74    OPT=1                          FTN 4.6+446          07/20/7

      SUBROUTINE WRITOUT (IC,DEL)
      COMMON /INTP/ YINT(101,2)
      COMMON /DIFY/ YDIF(101),DY(100)
      COMMON X(80,2),Y(80,2),NPTS(2),XPL(101),XL,XH,YL,YH,XMIN,XMAX,ISET
C
C
      PRINT 100, IC
      PRINT 105, XMIN,XMAX,DEL
      PRINT 110
      PRINT 115, XPL(1),YINT(1,1),YINT(1,2),YDIF(1)
      DO 50 K=2,101
      PRINT 115, XPL(K),YINT(K,1),YINT(K,2),YDIF(K),DY(K-1)
   50 CONTINUE
C
      PRINT 120
C
  100 FORMAT (1H1,//,5X,"OUTPUT -- MOIRE DATA ANALYSIS -- SET #",I2,//)
  105 FORMAT (5X,"COMPUTED VALUES USED -",//10X,"XMIN = ",E17.9/10X,
     +  "XMAX = ",E17.9/7X,"DELTA X = ",E17.9//)
  110 FORMAT (4X,"DISTANCE FROM HOLE",10X,"Y1",19X,"Y2",15X,
     +  "DISPLACEMENT",12X,"STRAIN",/)
  115 FORMAT (4X,5(E16.9,5X))
  120 FORMAT (1H1)
      RETURN
      END
```

Appendix B-2

Typical Input Deck

PROGRAM NAME: MOIRE

OWNER: Gary Cloud, AFML/LLN, 52624

AUTHOR: Lt. Alan R. Miller, AFML/DOC, 56890

DESCRIPTION OF INPUT REQUIREMENTS:

A. This program was designed to permit an infinite number of data sets to be entered. However, due to time constraints on the plotter, it is recommended that no more than three(3) sets be entered per run.

B. There are six(6) individual input data types necessary for each set of data. They are:

1. Card #1: Set Number - Format (A10)
   a. Program will use the first 10 characters encountered in columns 1-10. For best results, recommend beginning in column 1.

2. Card #2: P, M, C, XO, IPR - Format (FREE)
   a. Separate each parameter by a comma(,).
   b. P,M,C, and XO are REAL run constants.
   c. IPR - Output parameter (integer).
      1.) Enter 1 to obtain output; enter 0 otherwise.

DATA INPUT:

3. Card #3: NPTS, Y1- Format (FREE) - separate by comma
   a. NPTS - Integer number of data points to be processed in DATA set.
   b. Y1 - Initial y-value in DATA set.

4. Card #4: X(1) - X(NPTS) - Format (FREE)
   a. May cover as many cards as necessary to enter "NPTS" values. One value may not continue over two cards. Note: Exactly "NPTS" values must be entered. Otherwise program results are undeterminable.

BASELINE INPUT:

5. Card #5: NPTS, Y1 - The same notes apply
6. Card #6: X(1) - X(NPTS) here as for Cards 3&

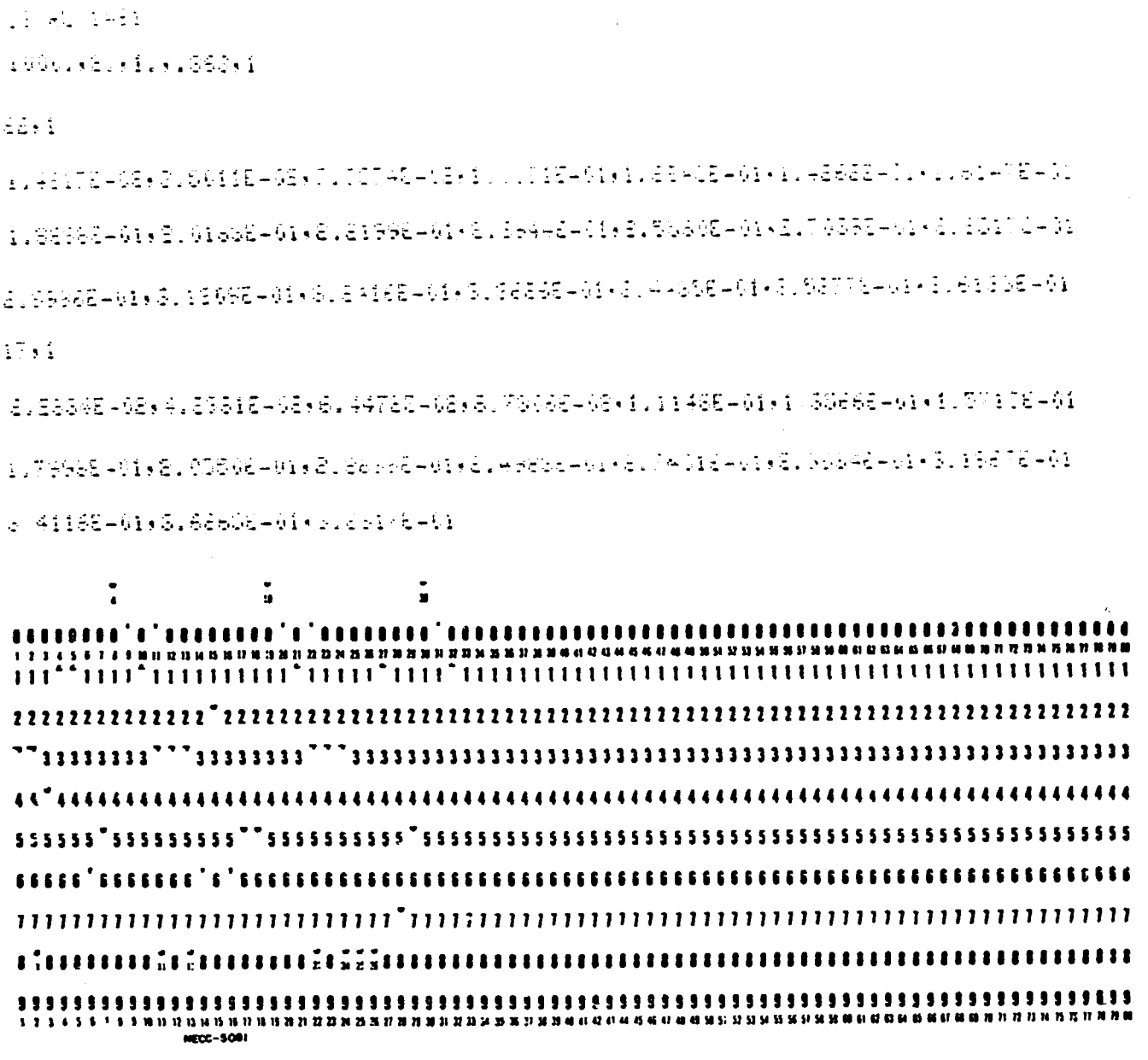

Appendix B-3

Typical Printed Output

OUTPUT -- 4CIRE DATA ANALYSIS -- SET # 1

COMPUTED VALUES USED -

XMIN = -.59257000E-02
XMAX = .33692000E+00
DELTA X = .34244570E-02

X	Y1	Y2	Y1-Y2	ΔY
-.59257000E-02	-.46243792E-01	0.	-.46243792E-04	
-.25972+00E-02	.37291021?E-01	.7451545?9E-01	-.37224437?E-04	.263073006E-05
.93121+00E-03	.11971113?E+00	.1453090?40E+00	-.2873?95?3E-04	.245787568E-05
.4?58?71?0E-02	.2?113737+E+00	.2221318?5E+00	-.2099?9?11E-04	.227621993E-05
.77?8128?0E-02	.2817027?1E+00	.2956349?5E+00	-.1383?1444E-04	.208995333E-05
.1121?585?E-01	.?0153756?E+00	.3684691?3E+00	-.7331?5669E-05	.189603589E-05
.14?4?0?2?E-01	.?407739+7E+00	.?+2295813E+00	-.1511?2?3?E-05	.1697467?7E-05
.17?7?+?9?E-01	.?195+36?1E+00	.?159?59?5E+00	.?607?65?6E-05	.1493?4?41E-05
.21?0195?0E-01	.?3737?217E+00	.?9?97?54+?E+00	.?007?7?1?E-05	.1283?7?39E-05
.2493?+13?E-01	.?762?9482E+00	.?6?4?407?5E+00	.1166?7?69E-04	.1067?5?52E-05
.2??5?+?7?1E-01	.?5+369?84E+00	.?397?7482E+00	.1457?5?26E-04	.?46?85?97E-06
.3?747?27?E-01	.?325?6?12E+00	.?159?1?35E+00	.1663?777?E-04	.619?63?20E-06
.3?21?784?E-01	.?11?00?52E+00	.?929?5126E+00	.1?0?49?6?E-04	.?97?89?89E-06
.3?6+?2+1?E-01	.?937?4?4E+00	.?711?8117E+00	.1?53?6?65E-04	.149?655?3E-06
.42?725?96E-01	.1?6?911?2E+01	.1?5?69?09E+01	.1?71492?5E-04	-.?9?460?66E-07
.45??+11?5?E-01	.1143?56?9E+01	.1131?9724E+01	.1715445?E-04	-.?5?14?06E-06
.+?9?9?12?E-01	.1?287?774E+01	.1217?8491E+01	.1562?6?3E-04	-.4?1?01423E-06
.5?5?+?69?E-01	.1?09?4?76E+01	.1?95539?8E+01	.1?6?469?5E-04	-.5?0?49?67E-06
.5?7?6?2?8E-01	.1?9?48173E+01	.1?7?54?2?E+01	.119+145?2E-04	-.543+5?6?8E-06
.5?21+?8?E-01	.1+72129+1E+01	.1+6185?69E+01	.1?6?7?7??E-04	-.49?2?734E-06
.62?+3+?5E-01	.1554?94472+01	.15+5?2?65E+01	.?9?7?1+4?E-05	-.?7?663157E-06
.6?7?+?97?E-01	.1?36?84?3E+?1	.162?62?1+E+01	.?5?+4?7??E-05	-.1?4756?07E-06
.6?5?+?5+?E-01	.172?2?757E+?1	.1711?1?71E+01	.?5?7?531+E-05	.?74?80173E-07
.72?2?11?E-01	.1+?3?71??E+?1	.1794?5?51E+01	.?911+?7?7E-05	.?6?71?15E-06
.7?357?6?E-01	.1?8?2?251E+?1	.1?7572?8?E+01	.125?4?125E-04	.77?9?7?7E-06

APPENDIX C

SUMMARY DATA ANALYSIS

Appendix C-1

Computer Program

```
PROGRAM CLOUD      74/74    OPT=1                          FTN 4.5+414        08/05/7

      PROGRAM CLOUD (INPUT,OUTPUT,PLFILE=0)
C
C
      COMMON /INTP/ YINT(101,2)
      COMMON /DIFY/ YDIF(101),DY(100)
      COMMON /PLOTER/ XPAY(900),YPAY(900),INUM
      COMMON X(10,2),Y(80,2),NPTS(2),XPL(101),XL,XH,YL,YH,XMIN,XMAX,ISET
      REAL M
      LOGICAL FIN
C
      CALL COMPRS
      FIN = .FALSE.
      IC =
      INUM = 0
C
C ---- ENTER RUN DATA
C
      READ 1,ISET
    1 FORMAT (A10)
  100 CALL READIN (P,M,C,X0,IPR,FIN)
      IF (FIN) GO TO 500
C
C --- DETERMINE X-RANGE FOR INTERPOLATION & DELTA VALUE
C
      CALL RANGE (DEL)
C
C --- COMPUTE INTERPOLATED "SMOOTH" CURVES THRU DATA & BASE SETS
C
      CALL INTERP (DEL)
C
C --- CORRECT ABSCISSA ARRAY
C
      CALL CORRECT (X0)
C
C --- COMPUTE CURVE DIFFERENCES & DERIVATIVES
C
      PMC = P*M*C
      CALL DIFF (PMC,DEL)
C
      IC = IC+1
      GO TO 100
  500 CALL PLOTR (IC,ISET)
 1000 CALL DONEPL
      STOP
      END
```

```
ROUTINE READIN      74/74    OPT=1                                  FTN 4.5+414          08/05/7

      SUBROUTINE READIN (P,M,C,X0,IPR,FIN)
      COMMON /STNAM/ ISTNM(9),IST
      COMMON X(80,2),Y(80,2),NPTS(2),XPL(101),XL,XH,YL,YH,XMIN,XMAX,ISET
      REAL M
      LOGICAL FIN
      DATA IST/0/
C
C --- INPUT RUN CONSTANTS
C
      IST = IST+1
      READ 1, ISTNM(IST)
    1 FORMAT (A10)
      IF (EOF(5LINPUT)) 50,5
    5 READ *, P,M,C,X0,IPR
C
C --- INPUT DATA VALUES
C
      READ *, NPTS(1),Y(1,1)
      N = NPTS(1)
      READ *, (X(J,1),J=1,N)
C
C --- COMPUTE REMAINING DATA Y-VALUES
C
      DO 10 I=2,N
      Y(I,1) = Y(I-1,1) + 1.0
   10 CONTINUE
C
C --- INPUT BASELINE VALUES
C
      READ *, NPTS(2),Y(1,2)
      N = NPTS(2)
      READ *, (X(J,2),J=1,N)
C
C --- COMPUTE REMAINING BASE Y-VALUES

      DO 20 I=2,N
      Y(I,2) = Y(I-1,2) + 1.0
   20 CONTINUE
C
C
      RETURN
C
   50 FIN = .TRUE.
      RETURN
      END
```

```
ROUTINE RANGE        /4/74    OPT=1                                    FTN 4.5+414          08/05/7

      SUBROUTINE RANGE (DEL)
      COMMON X(30,2),Y(80,2),NPTS(2),XPL(101),XL,XH,YL,YH,XMIN,XMAX,ISET

      N1 = NPTS(1)
      N2 = NPTS(2)

      IF (Y(1,1) .LE. X(1,2)) GO TO 20
      XMIN = X(1,1)
      XL = X(1,2)
      GO TO 40

   20 XMIN = X(1,2)
      XL = X(1,1)

   40 IF (X(N1,1) .GE. X(N2,2)) GO TO 50
      XMAX = Y(N1,1)
      XH = Y(N2,2)
      GO TO 80

   50 XMAX = X(N2,2)
      XH = Y(N1,1)

   80 DEL = (XMAX-XMIN)/100.0

      IF (Y(1,1) .LE. Y(1,2)) YL = Y(1,1)
      IF (Y(1,2) .LE. Y(1,1)) YL = Y(1,2)
      IF (Y(N1,1) .GE. Y(N2,2)) YH = Y(N1,1)
      IF (Y(N2,2) .GE. Y(N1,1)) YH = Y(N2,2)

      RETURN
      END
```

```
ROUTINE INTERP      74/74    OPT=1                          FTN 4.5+414          08/05/7

      SUBROUTINE INTERP (DEL)
      COMMON /INTP/ YINT(101,2)
      COMMON X(80,2),Y(80,2),NPTS(2),XPL(101),XL,XH,YL,YH,XMIN,XMAX,ISET
      DIMENSION WD(80),RD(80),XN(80),FN(80),GN(80),DN(80),THETA(80),
     + W(1200)
      DATA NP/80*1.0/
C
C
      DO 10 I=1,101
      XPL(I) = XMIN + DEL*(I-1)
   10 CONTINUE
C
      DO 40 I=1,2
      CALL SPLIN1 (NPTS(I),KNOTS,X(1,I),Y(1,I),WD,RD,XN,FN,GN,DN,THETA,
     + W,0,0)
         DO 20 K=1,101
         YINT(K,I) = SPLIN2 (XPL(K),KNOTS,XN,FN,GN,1)
   20    CONTINUE
   40 CONTINUE
C
      RETURN
      END
```

```
ROUTINE CORRECT     74/74    OPT=1                          FTN 4.5+414          08/05/7

      SUBROUTINE CORRECT (X0)
      COMMON X(80,2),Y(80,2),NPTS(2),XPL(101),XL,XH,YL,YH,XMIN,XMAX,ISET
C
C --- THIS ROUTINE COMPUTES CORRECTION FOR DISTANCE FROM HOLE
C
      DO 10 I=1,101
      XPL(I) = X0 - XPL(I)
   10 CONTINUE
C
      RETURN
      END
```

```
      74/74    OPT=1                                  FTN 4.5+414          08/05/7

      SUBROUTINE SPLINE(M,N,XD,YD,WD,RD,XN,FN,GN,DN,THETA,W,IPRINT,IFIT)
C
C  *  *  *  *  *  *  *  *  *  *  *  *  *  *  *  *  *  *  *  *  *  *  *  *  *  *
C
C - - A ROUTINE TO FIT THE SMOOTHEST CURVE THRU A GIVEN SET OF DATA
C     USING CUBIC SPLINES.
C
C          M = TOTAL NUMBER OF DATA POINTS.
C          N = NUMBER OF KNOTS USED (INPUT OR OUTPUT DEPENDING ON IFIT)
C         XD = X-COORD. DATA ARRAY (INPUT)
C         YD = Y-COORD. DATA ARRAY (INPUT)
C         WD = WEIGHT FOR EACH DATA POINT (GENERALLY = 1.0, IF W(I) = 0,
C              THEN THE ITH POINT WILL BE OMITTED FROM THE FIT) (INPUT)
C         RD = AN ARRAY CONTAINING YD(I)-S(XD(I)) (OUTPUT)
C         XN = AN ARRAY CONTAINING THE KNOT POSITIONS (INPUT OR OUTPUT
C              DEPENDING ON IFIT)
C         FN = AN ARRAY CONTAINING THE VALUES OF THE SPLINE AT THE KNOTS
C              (OUTPUT)
C         GN = AN ARRAY CONTAINING THE VALUES OF THE DERIVATIVE OF THE
C              SPLINE AT THE KNOTS (OUTPUT)
C         DN = AN ARRAY CONTAINING THE VALUES OF THE 3RD DERIVATIVE
C              DISCONTINUITIES OF THE SPLINE ACROSS THE KNOTS (ROUGH
C              ESTIMATE OF THE ERROR IN THE FIT) (OUTPUT)
C      THETA = WORKING ARRAY
C          W = WORKING ARRAY (MUST BE DIMENSIONED ATLEAST 7*M+8*N+6)
C     IPRINT = PRINT OPTION
C              1 PRINT RESULTS AFTER EACH ITERATION
C              0 NO PRINT PRODUCED
C             -1 PRINT RESULTS FOR BEST FIT ONLY
C       IFIT = FIT OPTION
C              0  PROGRAM WILL AUTOMATICALLY SELECT KNOT POSITIONS
C              1 CALCULATE THE SPLINE WITH THE INPUT SET OF KNOT
C                POSITIONS **CAUTION N MUST BE .GE. 5 AND XN(1)=XD(1),
C                XN(N)=XD(M) FOR CORRECT RESULTS.
C
C
C     THE NORMAL MODE OF OPERATION IS TO ALLOW THE PROGRAM TO
C     AUTOMATICALLY SELECT THE OPTIMAL KNOT POSITIONS BASED ON
C     STATISTICAL ERROR TESTS. IN THIS MODE OF OPERATION IT IS DIFFICULT
C     TO PREDICT THE REQUIRED DIMENSION FOR THE ARRAYS XN, FN, GN, DN,
C     THETA, AND W. THE PROGRAM WILL NEVER MAKE N GT M SO A SAFE
C     DIMENSIONALITY FOR THESE ARRAYS WOULD BE M. SPLINE CALLS SPLINE
C     TO CALCULATE THE LEAST SQUARES SPLINE APPROXIMATION.
C
C
C  *  *  *  *  *  *  *  *  *  *  *  *  *  *  *  *  *  *  *  *  *  *  *  *  *  *
C
C
      DIMENSION XD(1),YD(1),WD(1),RD(1),XN(1),FN(1),GN(1),DN(1),
     1          THETA(1),W(1)
C
C     OMIT DATA WITH ZERO WEIGHTS
C
      M=1
      N=1
      DO 1 I=2,M
```

```
ROUTIN. SPLIN1      74/74    OPT=1                          FTN 4.5+414          08/05/7

      IF(WD(I)) 3,2,3
    2 IF(I-M) 4,3,3
    4 W(J)=XD(I)
      W(J+1)=YD(I)
      W(J+2)=FLOAT(I)
      J=J+3
      GO TO 1
    3 MM=MM+1
      XD(MM)=XD(I)
      YD(MM)=YD(I)
      WD(MM)=WD(I)
    1 CONTINUE
      J=1
      K=MM
    2 IF(K-M) 5,6,6
    5 K=K+1
      XD(K)=W(J)
      YD(K)=W(J+1)
      WD(K)=W(J+2)
      J=J+3
      GO TO 2
C
C     INITIALIZATION OF ITERATIONS
C
    6 IF(IFIT .EQ. 1) GO TO 110
      JA=1
      IF(WD(1)) 9,8,9
    8 JA=2
    9 N=3
      XN(1)=XD(1)
      XN(5)=XD(M)
      XN(3)=0.5*(XN(1)+XN(5))
      XN(2)=0.5*(XN(1)+XN(3))
      XN(4)=0.5*(XN(3)+XN(5))
  110 IW=7*MM+8*N+6
      DO 10 I=1,N
      J=IW+I
   10 W(J)=XN(I)
      IP=-IPRINT
C
C     CALCULATE THE HISTOGRAMS FOR NEW SCALE FACTORS
C
   11 J=2
      K=1
      SA=0.
   12 SA=SA+WD(K)**2
      K=K+1
      IF(XD(K)-XD(1)) 12,12,13
   13 SA=(SA+0.5*WD(K)**2)/(XD(K)-XD(1))
   14 J=J+1
      IF(XD(K)-XN(J+1)) 15,15,16
   16 GN(J)=SA*(XN(J+1)-XN(J))
      GO TO 14
   15 GN(J)=SA*(XD(K)-XN(J))+0.5*WD(K)**2
   17 K=K+1
      IF(K-MM) 18,18,19
   18 IF(XD(K)-XN(J+1)) 20,20,21
```

```
ROUTINE SPLINE      76/7+   OPT=1                          FTN 4.5+414        08/05/7

      22 GN(J)=GN(J)+WD(K)**2
         GO TO 17
      21 SA=3.0*(W(K-1)**2+WD(K)**2)/(XD(K)-XD(K-1))
         GN(J)=GN(J)-0.5*WD(K-1)**2+SA*(XN(J+1)-XD(K-1))
         GO TO 19

C        CALCULATE THE NEW SCALE FACTORS

      11 K=IN+2
         GN(1)=0.00025216*GN(1)*(W(K)-W(K-1))**3/(XN(2)-XN(1))
         DO 23 J=2,N
         IF(XN(J)-W(K)) 23,23,24
      24 K=K+1
      23 GN(J-1)=0.00025216*GN(J-1)*(W(K)-W(K-1))**3/(XN(J)-XN(J-1))
      22 GN(J-2)=ALOG(GN(J-2)+GN(J-1))
         NN=N-2
         HS=1.3+02
         DO 97 J=2,NN
      97 GN(J)=AMIN1(GN(J),GN(J-1)+HS)
         J=NN-1
      98 GN(J)=AMIN1(GN(J),GN(J+1)+HS)
         J=J-1
         IF(J) 99,34,99
      33 DO 25 J=3,N
      25 THETA(J-1)=SQRT(EXP(GN(J-2))/(XN(J)-XN(J-2)))

C        CALCULATE THE SPLINE APPROXIMATION WITH CURRENT KNOTS

         CALL SPLIT(NM,N,XD,YD,WD,KD,XN,FN,GN,ON,THETA,W,IP)
         IF(IFIT .EQ. 1) GO TO 41

C        APPLY STATISTICAL TEST FOR EXTRA KNOTS

         J=IN+1
         JJ=0
         K=JA
         TMAX=0.
         III=1
      26 KC=-1
         SW=0.
         SR=0.
         RP=0.
         J=J+1
         JJ=JJ+1
         W(JJ)=0.
      27 IF(W(J)-XD(K)) 28,28,30
      30 KC=KC+1
         SW=SW+RD(K)**2
         SR=SR+RP*RD(K)
         RP=RD(K)
         K=K+1
         GO TO 27
      29 IF(WD(K)) 31,28,31
      31 KC=KC+1
         SW=SW+RD(K)**2
         SR=SR+RP*RD(K)
      28 IF(SR) 32,32,33
```

```
ROUTINE SPLIN1      74/74    OPT=1                          FTN 4.5+414          08/15/

   33 SW=(SW/SQ)**2
      RP=SQRT(SR/FLOAT(KP))
      IF (FLOAT(KP)-SW) 32,32,34
   34 IF (IIS .EQ. 3) GO TO 37
      IF (IIS .EQ. 2) GO TO 35
      RRP=RP
      IIS=3
      IF(FLOAT(KP)-2.*SW) 38,38,39
   37 W(JJ-1)=RRP
      TMAX=AMAX1(TMAX,RRP)
   39 IIS=2
   36 W(JJ)=RP
      TMAX=AMAX1(TMAX,RP)
      GO TO 38
   32 IIS=1
   38 IF(W(J)-XN(N)) 25,43,40
C
C     TEST WHETHER ANOTHER ITERATION IS REQUIRED
C
   40 IF(TMAX) 41,41,42
C
C     CALCULATE NEW TREND ARRAY, INCLUDING LARGER TRENDS ONLY
C
   42 TMAX=0.5*TMAX
      I=0
      J=1
      JW=1
      K=IW+1
      THETA(JW)=W(K)
   43 I=I+1
      K=K+1
      IF(W(I)-TMAX) 44,44,45
   44 JW=JW+1
      THETA(JW)=W(K)
   46 FN(J)=0.
      J=J+1
      IF(W(K)-XN(J)) 47,47,46
   45 JW=JW+2
      THETA(JW-1)=0.5*(W(K-1)+W(K))
      THETA(JW)=W(K)
      IF(XN(J+1)-THETA(JW-1)) 46,46,48
   48 FN(J)=1.
      J=J+1
   47 IF(J-N) 43,49,49
C
C     MAKE KNOT SPACINGS BE USED FOUR TIMES
C
   49 IK=1
      KL=1
      FN(2)=AMAX1(FN(1),FN(2))
   50 K=KL+3
   51 IF(FN(K)) 52,52,53
   52 K=K-1
      IF(K-KL) 54,54,51
   53 K=K-1
      FN(K)=1.
      IF(K-KL) 54,54,53
```

```
SUBROUTINE SPLINE      74/74    OPT=1                                FTN 4.5+414        JN/05/7

      54 K=K+1
         IF(K-N) 55,55,56
      55 IF(XN(K+1)-XN(K)-1.5*(XN(K)-XN(K-1))) 56,56,56
      56 KU=K
         FN(K-2)=AMAX1(FN(K-2),FN(K-1))
      57 KKU=K
      58 K=K-1
         IF(K-KL) 59,59,60
      59 IF(XN(K)-XN(K-1)-1.5*(XN(K+1)-XN(K))) 59,58,61
      61 FN(K+1)=AMAX1(FN(K),FN(K+1))
      60 KL=K
         K7=0
         IF(FN(K)) 62,62,63
      63 K=K+1
         IF(K-KKU) 64,65,65
      64 IF(FN(K)) 65,65,63
      65 K7=1
      62 K7=K7+1
         K=K+1
         IF(K-KKU) 62,65,65
      67 IF(FN(K)) 62,62,68
      68 IF(K2-7) 69,69,70
      69 J=K-K7
      71 FN(J)=1.
         J=J+1
         IF(J-K) 71,63,63
      70 IF(K+1-KKU) 72,65,65
      72 K=K+1
         FN(K)=1.
         GO TO 63
      66 IF(KL-KKL) 75,74,74
      75 FN(KKL-2)=AMAX1(FN(KKL-2),FN(KKL+1))
         FN(KKL-1)=AMAX1(FN(KKL-1),FN(KKL+3))
      73 K=KKL-4
      74 IF(FN(K)) 76,76,77
      76 K=K+1
         IF(K-KKL) 74,79,79
      77 FN(K)=1.
         K=K+1
         IF(K-KKL) 77,79,79
      73 IF (IK .EQ. 1) GO TO 87
         IF (IK .EQ. 2) GO TO 80
      74 IF(KU-N) 81,82,82
      81 KL=KU
         FN(KL+1)=AMAX1(FN(KL+1),FN(KL-1))
         FN(KL)=AMAX1(FN(KL),FN(KL-1))
         GO TO
      87  IK = 2
         KKL=N
         GO TO

C     INSERT EXTRA KNOTS FOR NEW APPROXIMATION

      80 DO 83 J=1,N
      83 SN(J)=XN(J)
         JN=1
         DO 84 J=2,N
```

```
ROUTINE SPLIN1      74/74    OPT=1                          FTN 4.5+414          14/15/7

      IF(FN(J-1)) [illegible]
   [illegible] NN=NN+1
      XN(NN)=0.5*(GN(J-1)+GN(J))
   [illegible] NN=NN+1
      XN(NN)=GN(J)
   [illegible] CONTINUE
      N=[illegible]
      IW=[illegible]
      DO [illegible] J=1,JW
      I=[illegible]+J
   [illegible] W(I)=[illegible](J)
      GO TO 11
C
C     RESTORE DATA WITH ZERO WEIGHTS
C
   [illegible] IF([illegible]) [illegible]
   [illegible] IF(IP[illegible]INT) [illegible]
   [illegible] J=[illegible]
      K=[illegible]
   [illegible] J=J+[illegible]
      K=K+1
      W(J)=XO(K)
      W(J+1)=YO(K)
      W(J+2)=WO(K)
      IF(K-[illegible]) [illegible]
   [illegible] I=INT([illegible]J+2)+0.1)
   [illegible] IF(K-I) [illegible]
   [illegible] XO(K)=XO([illegible])
      YO(K)=YO([illegible])
      WO(K)=WO([illegible])
      K=K-1
      [illegible]=[illegible]-1
      GO TO [illegible]
   [illegible] XO(K)=W(J)
      YO(K)=W(J+1)
      WO(K)=[illegible]
      K=K-[illegible]
      J=J-[illegible]
      IF(J) [illegible]
   [illegible] CALL SPLINT([illegible],XO,YO,WO,[illegible],XN,FN,GN,[illegible],THETA,W,IA[illegible]S(IPSINT))
   [illegible] RETURN
      END
```

```
FUNCTION SPLIN2     74/76   OPT=1                    FTN 4.6+414        08/06/7
      FUNCTION SPLIN2(X,I,XN,FN,GN,ITYP)
C  *  *  *  *  *  *  *  *  *  *  *  *  *  *  *  *  *  *  *  *  *  *  *  *  *
C
C  - - A FUNCTION UTILITY TO BE USED IN CONJUNCTION WITH THE SPLINE
C     ROUTINE S SPLINE OR SPLINI.
C
C          X   IS  VALUE  OF THE INDEPENDENT VARIABLE AT WHICH THE SPLINE
C              OR ITS DERIVATIVE ARE TO BE EVALUATED. X MUST BE BETWEEN
C              XN(1) AND XN(N) FOR CORRECT RESULTS.
C          N = THE NUMBER OF KNOTS (RETURNED BY SPLINING ROUTINES)
C         XN = ARRAY OF KNOT POSITIONS (RETURNED BY SPLINE ROUTINES)
C         FN = ARRAY OF SPLINE VALUES (RETURNED BY SPLINE ROUTINES)
C         GN = ARRAY OF DERIVATIVE VALUES (RETURNED BY SPLINE ROUTINES)
C      ITYP  = 1 RETURNS SPLINE VALUE AT X
C              2 RETURNS THE DERIVATIVE VALUE AT X
C
C  *  *  *  *  *  *  *  *  *  *  *  *  *  *  *  *  *  *  *  *  *  *  *  *  *
C
      DIMENSION XN(1),FN(1),GN(1)
      IF(X .LT. XN(1)) GO TO 100
      IF(X .GT. XN(N)) GO TO 110
       DO 5 K=1,N
       IF(X .LE. XN(K)) GO TO 6
       KK = K
       GO TO 120
    5  CONTINUE
    6  DO 10 K=2,N
       IF(X .GT. XN(K)) GO TO 10
       JK=K
       GO TO 20
   10  CONTINUE
   20  HH=XN(JK)-XN(JK-1)
       HH3=HH**3
       T1=HH*GN(JK-1)+FN(JK-1)-FN(JK)
       T2=HH*GN(JK)+FN(JK-1)-FN(JK)
       T3=XN(JK)-X
       T4=X-XN(JK-1)
       IF (ITYP .EQ. 2) GO TO 201
       SPLIN2=(T3*FN(JK-1)+T4*FN(JK))/HH+T3*T4*(T3*T1-T4*T2)/HH3
       RETURN
  201  SPLIN2=(FN(JK)-FN(JK-1))/HH-T3*T4*(HH*(GN(JK-1)+GN(JK))+2.*(FN(JK-
     1        1)-FN(JK)))/HH3+(XN(JK-1)+XN(JK)-2.*X)*(T3*T1-T4*T2)/HH3
       RETURN
  100  JK=1
       GO TO 20
  110  JK=N
       GO TO 20
  120  IF (ITYP .EQ. 2) GO TO 301
       SPLIN2=FN(KK)
       RETURN
  301  SPLIN2=GN(KK)
       RETURN
       END
```

```
SUBROUTINE SPLINE  V2.0   OPT=1                    FTN 4.5+416        04/15/77

      SUBROUTINE SPLINE(I,J,X,Y,W,D,S,XN,FN,GN,DN,THETA,M,IPOINT)

      DIMENSION W(1),X(1),Y(1),WT(1),SS(1),XN(1),FN(1),G(1),DN(1),
     1          S(1),THETA(1)

C     SPLINE KNOTS TO M. AND INSERT EXTRA KNOTS AT ENDS OF RANGE

      XN(N)=AMAX1(XN(N),X(I))
      DO 1 I=1,J
    1 W(I+3)=X(I)
      DO 2 J=1,3
      K=M-J
      W(K)=W(K+1)+W(K+1)-W(K+2)
      K=J+N
    2 W(K+2)=W(K+2)+W(K+2)-W(K+1)

C     SET UP THE LEAST SQUARES EQUATIONS IN W

      I=1
      J=2
      K=N+12
      AA=1.0/((W(3)-W(1))*(W(3)-W(5))*(W(3)-W(6))*(W(3)-W(7)))
      JJ=1.0/((W(2)-W(1))*(W(2)-W(5))*(W(2)-W(5))*(W(2)-W(6)))
    3 A=AA
      AA=1.0/((W(J+2)-W(J+3))*(W(J+2)-W(J+4))*(W(J+2)-W(J+3))*
     1   (W(J+2)-W(J+6)))
      B=(1.0*(W(J+2)-W(J+6))/(W(J+2)-W(J+1))
      JJ=2
      B=1.0/((W(J+4)-W(J))*(W(J+4)-W(J+1))*(W(J+4)-W(J+2))*
     1  (W(J+4)-W(J+3)))
      C=(1.0*(W(J+2)-W(J-1))/(W(J+2)-W(J+4))
      FN(J-1)=S-7
      IF(J-2) 4,4,5
    4 W(K-6)=-J)
      W(K-5)=-C-D
      W(K-4)=A+B
      W(K-3)=AA
      W(K-2)=0.
      IF(I-M) 6,6,7
    5 W(K-1)=1.
      W(K)=0.
      GO TO 8
    6 W(K-4)=AA*(W(K-4)+3.0)
      W(K-3)=AA*3
      W(K-2)=AA*AA
    8 K=K+7
      IF(I-M) 9,9,12
    9 IF(W(J+3)-XD(I)) 11,10,10
   11 W(K-6)=WT(I)*(W(J+3)-XD(I))**3
      W(K-5)=WT(I)*(C*(W(J+2)-XD(I))**3+D*(W(J+4)-XD(I))**3)
      W(K-4)=WT(I)*(A*(XD(I)-W(J+1))**3+B*(XD(I)-W(J+2))**3)
      W(K-3)=WT(I)*AA*(XD(I)-W(J+2))**3
      W(K-2)=WT(I)*XD(I)
      W(K-1)=1.
      W(K)=0.
      I=I+1
      GO TO 3
```

```
ROUTINE SPLINS      74/74    OPT=1                                    FTN 4.5+414          09/05/7

      10 IF(J-N) 11,4,4
      11 J=J+1
         AW=6.*THETA(J-1)
         W(K-6)=AW*DD
         W(K-5)=AW*2
         W(K-4)=A+3
         GO TO 7
       7 W(K-1)=0.
         W(K)=1.
         FN(J)=K
C
C        APPLY HOUSEHOLDER ORTHOGONAL TRANSFORMATIONS TO OBTAIN AN UPPER
C        TRIANGULAR LEAST SQUARES MATRIX
C
         KUMAX=K
         I=1
         IPR=N-1
         NPINIT=7
      13 I=I+1
         IPR=IPR+7
         NP=NPINIT
         J=I+NP
         KL=MAX0(IPR+5,IFIX(FN(J-8)+1.5))
         KU=IFIX(FN(J-7)+0.5)
         IF(NP-3) 14,14,15
      14 W(IPR+1)=0.
         W(IPR+2)=0.
         W(IPR+3)=0.
         W(IPR+4)=0.
      15 IF(KU-KL) 25,25,17
      17 NPINIT=MAX0(3,NPINIT-1)
         GO TO 18
      18 NP=NP+1
         J=IPR+NP
         W(J)=W(J-1)
         W(J-1)=W(J-2)
         W(J-2)=W(J-3)
         W(J-3)=0.
         KL=KU+1
         J=I+NP
         KU=IFIX(FN(J-7)+0.5)
      18 DO 19 J=1,NP
         JP=IPR+J
      19 S(J)=W(IPR+1)*W(JP)
         KPIV=0
         PIVMAX=ABS(W(IPR+1))
         DO 20 K=KL,KU,7
         DO 21 J=1,NP
         JJ=K+J
      21 S(J)=S(J)+W(JJ-1)*W(K)
         IF(PIVMAX-ABS(W(K))) 70,20,20
      70 PIVMAX=ABS(W(K))
         KPIV=K
      20 CONTINUE
         IF(KPIV) 71,71,72
      72 DO 73 J=1,NP
         JJ=IPR+J
```

```
ROUTINE SPLINE      74/74    OPT=1                          FTN 4.5+414          09/05/7

      A=W(JJ)
      W(JJ)=W(KPIV)
      W(KPIV)=A
      KPIV=KPIV+1
   73 CONTINUE
   71 AA=SIGN(SQRT(S(1)),W(IPR+1))
      B=W(IPR+1)+AA
      A=1.0/(AA*B)
      DO 22 J=2,NP
      JP=IPR+J
      S(J)=A*(S(J)+AA*W(JP))
   22 W(JP)=W(JP)-B*S(J)
      W(IPR+1)=-AA
      DO 23 K=KL,KU,7
      A=W(K)
      DO 24 J=2,NP
      JJ=K+J
      W(JJ-2)=W(JJ-1)-A*S(J)
   24 CONTINUE
   23 CONTINUE
      IF(KU-KUMAX) 25,26,26
   25 IF(NP-2) 16,27,27
   27 GN(I)=SQRT(W(IPR+1)**2+W(KU+1)**2)
      A=W(IPR+1)/GN(I)
      B=W(KU+1)/GN(I)
      C=W(KU+5)
      DO 28 J=1,7
      JP=IPR+J
      JJ=KU+J
      W(JP)=A*W(JP+1)+B*W(JJ+1)
      W(JJ)=A*W(JJ+1)-B*W(JP+1)
      W(JJ+4)=-B*W(JP+4)
   28 W(JP+4)=A*W(JP+4)
      W(IPR+4)=B*C
      W(KU+4)=A*C
      GO TO 10
   26 IF(NP-4) 29,29,15

      BACK-SUBSTITUTION TO OBTAIN MULTIPLIERS OF FUNDAMENTAL SPLINES

   29 K=KUMAX
      DO 31 J=1,4
      K=K-7
      JJ=IPR+J
      DO 31 I=1,5
      KK=K+I
      JK=JJ+I
      W(KK)=W(JK)
      L=IPR+1
      LK=KK
   32 IF(L-JJ) 33,34,34
   33 L=L+1
      LK=LK+7
      W(KK)=W(KK)-W(LK)*W(L)
      GO TO 32
   34 W(KK)=W(KK)/W(IPR+1)
   31 CONTINUE
```

```
SUBJTINE SPLIN2      76/76    OPT=1                    FTN 4.3+414        09/05/7

            IF=IP-7
         33 DO 34 I=1,3
            L=1
         35 IF(IPR-N) 36,36,37
         37 K=K-7
            L=L-1
            DO 34 I=1,3
            KK=K+I
            JJ=IPR+I
         34 W(KK)=(W(JJ+4)-W(IPR+1)*W(KK+3)-W(IPR+2)*W(KK+6)-W(IPR+3)*W(KK+9)
           1       -W(IPR+4)*W(KK+12))/GN(L)
            IPR=IPR-7
            GO TO 35
         36 KRES=K
C
C     CALCULATE SPLINE VALUES AT THE DATA POINTS, AND SCALAR PRODUCTS
C
            KSDATA=KRES-3*N
            I=1
            J=1
            DO 42 L=1,5
         43 S(L)=0.
            KK=KSDATA
            AA=1./((W(3)-W(4))*(W(3)-W(5))*(W(3)-W(6))*(W(3)-W(7)))
            B=1./((W(3)-W(1))*(W(3)-W(2))*(W(3)-W(3))*(W(3)-W(4)))
         39 J=J+1
            K=K+3
            A=AA
            AA=1./((W(J+2)-W(J+3))*(W(J+2)-W(J+4))*(W(J+2)-W(J+5))*
           1   (W(J+2)-W(J+6)))
            B=AA*(W(J+2)-W(J+6))/(W(J+2)-W(J+1))
            DD=0
            D=1./((W(J+4)-W(J))*(W(J+4)-W(J+1))*(W(J+4)-W(J+2))*
           1  (W(J+4)-W(J+3)))
            C=DD*(W(J+3)-W(J-1))/(W(J+3)-W(J+4))
         40 IF(XD(I)-XM(J)) 41,41,39
         41 DO 42 L=1,3
            LK=L+K
            KU=L+KK
         42 W(KU)=A*W(LK+3)*(XD(I)-W(J+1))**3+(B*W(LK+3)+AA*W(LK+6))*
           1       (XD(I)-W(J+2))**3+(C*W(LK)+DD*W(LK-3))*(W(J+7)-XD(I))**3
           2       +D*W(LK)*(W(J+4)-XD(I))**3
            XD(I)=YD(I)-W(KK+1)
            AS=WD(I)*XD(I)
            BS=WD(I)*W(KK+2)
            CS=WD(I)*W(KK+3)
            S(1)=S(1)+BS*BS
            S(2)=S(2)+BS*CS
            S(3)=S(3)+CS*CS
            S(4)=S(4)+AS*BS
            S(5)=S(5)+AS*CS
            I=I+1
            KK=KK+7
            IF(I-N) 43,40,4
C
C     CALCULATE THE RESIDUALS AND PARAMETERS OF THE REQUIRED SPLINE
C
```

```
ROUTINE SPLIN3      74/74    OPT=1                          FTN 4.3+414          08/05/7

   44 DET=S(1)*S(3)-S(2)*S(2)
      A=(S(3)*S(4)-S(2)*S(5))/DET
      B=(S(1)*S(5)-S(2)*S(4))/DET
      K=KSDATA
      DO 45 I=1,M
      K=K+3
   45 RD(I)=RD(I)-A*W(K-1)-B*W(K)
      KL=KRES+1
      DO 46 K=KL,KUMAX,3
   46 W(K)=W(K)+A*W(K+1)+B*W(K+2)
C
C     COMPUTE ELEMENTS OF FN,GN AND DN
C
      K=KRES
      AA=1.0/((W(2)-W(3))*(W(2)-W(4))*(W(2)-W(5))*(W(2)-W(6)))
      DN(1)=0.
      DO 47 J=1,N
      A=AA*W(K+4)*(XN(J)-W(J+1))**2
      AA=1.0/((W(J+2)-W(J+3))*(W(J+2)-W(J+4))*(W(J+2)-W(J+5))*
     1    (W(J+2)-W(J+6)))
      B=AA*(W(K+7)+W(K+4)*(W(J+2)-W(J+6))/(W(J+2)-W(J+1)))*
     1   (XN(J)-W(J+2))**2
      DD=W(K+1)*(W(J+4)-XN(J))/((W(J+4)-W(J))*(W(J+4)-W(J+1))*
     1    (W(J+4)-W(J+2)))
      FN(J)=A*(XN(J)-W(J+1))+B*(XN(J)-W(J+2))+DD*(W(J+4)-XN(J))
      GN(J)=3.0*(A+B-DD)
      IF(J-1) 48,48,49
   49 DN(J)=6.0*(GN(J-1)+GN(J)+2.0*(FN(J-1)-FN(J))/(XN(J)-XN(J-1)))/
     1(XN(J)-XN(J-1))**2
      DN(J-1)=DN(J)-DN(J-1)
   48 K=K+3
   47 CONTINUE
C
C     PROVIDE PRINT IF REQUESTED
C
      IF(IPRINT) 50,50,51
   50 RETURN
C
   51 PRINT 52
   52 FORMAT(1H1,35X,*SPLINE APPROXIMATION OBTAINED BY SPLIN3*//4X,1HI,
     19X,5HXN(I),18X,5HFN(I),18X,5HGN(I),13X,16H3RD DERIV CHANGE,11X,
     25HTHETA(I)//)
      I=11
      PRINT 63,I,XN(I),FN(I),GN(I)
   54 I=I+1
      IF(I-N) 55,56,56
   55 PRINT 63,I,XN(I),FN(I),GN(I),DN(I),THETA(I)
      GO TO 54
   56 PRINT 63,I,XN(I),FN(I),GN(I)
      PRINT 57
   57 FORMAT(///4X,1HI,9X,5HXD(I),18X,5HYD(I),18X,5HWD(I),13X,7HFIT,
     118X,8HRESIDUAL//)
      J=2
      DO 58 I=1,M
   59 IF(XD(I)-XN(J)) 60,60,61
   61 PRINT 62
   62 FORMAT(5X)
```

```
ROUTINE SPLIN3      74/74   OPT=1                          FTN 4.5+414        08/05/7

            J=J+1
            GO TO 59
         60  YDRO = YO(I)-RO(I)
            PRINT 63,I,XO(I),YO(I),RO(I),YDRO        ,RO(I)
         63 FORMAT(I5,5E23.14)
         59 CONTINUE
            GO TO 50
            END
```

```
ROUTINE DIFF        74/74   OPT=1                          FTN 4.5+414        08/05/7

            SUBROUTINE DIFF (PMC,DEL)
            COMMON /INTP/ YINT(101,2)
            COMMON /PLOTER/ XRAY(900),YRAY(900),INUM
            COMMON /DIFY/ YDIF(101),DY(100)
            COMMON X(80,2),Y(80,2),NPTS(2),XPL(101),DUM6(6),ISET
      C
      C --- COMPUTE DIFFERENCES & DIVIDE BY PMC
      C
            DO 20 K=1,101
            YDIF(K) = (YINT(K,1) - YINT(K,2))/PMC
         20 CONTINUE
      C
      C --- COMPUTE DERIVATIVES
      C
            DO 40 K=2,101
            DY(K-1) = (YDIF(K) - YDIF(K-1))/DEL
            INUM = INUM+1
            XRAY(INUM) = XPL(K)
            YRAY(INUM) = DY(K-1)
         40 CONTINUE
            RETURN
            END
```

```
ROUTINE PLOTR      74/74   OPT=1                    FTN 4.5+414        08/05/7

      SUBROUTINE PLOTR (IC,ISET)
      COMMON /STNAM/ ISTNM(9),IST
      COMMON/PLOTER/X(900),Y(900),II
      DIMENSION R1(8),R2(8),R3(8),R4(4)
      DATA R1/10.,8.,10.,8.,2.,8.,2.,8./,R2/20.,8.,2.,8.,2.,8./
      DATA R3/60.,7.,3.,7.,3.,7.,3.,7./,R4/10.,8.,2.,4./
C
      CALL BGNPL(1)
      CALL PHYSOR(1.0,0.7)
      CALL BASALF ("STANDARD")
      CALL MIXALF ("L/CSTD")
      CALL TRIPLX
C
      CALL TITLE (1H ,-1,"DISTANCE FROM HOLE ((IN.))$",100,
     $  "COMPRESSIVE STRAIN$",100,9.,7.)
      CALL GRAF (-.05,.05,.4,-.01,.01,.06)
C
      CALL MESSAG ("HOLE NO. 3",100,1.2,6.)
      CALL MESSAG (ISET,10,"ABUT","ABUT")
C
      CALL HEIGHT (0.12)
      CALL MESSAG ("LEGEND",6.7,7.7,6.6)
      A = XMESS("LEGEND",6)
      CALL HEIGHT (0.09)
      CALL VECTOR (7.7,6.56,7.7+A,6.56,0)
      HTD = 6.45
      CALL RESET ("TRIPLX")
C
      DO 30 I=1,IC
      IF (I.EQ.2) CALL DOT
      IF (I.EQ.3) CALL CHNDOT
      IF (I.EQ.4) CALL DASH
      IF (I.EQ.5) CALL CHNDSH
      IF (I.EQ.6) CALL MRSCOD(0.6,8,R1)
      IF (I.EQ.7) CALL MRSCOD(0.48,6,R2)
      IF (I.EQ.8) CALL MRSCOD(0.475,8,R3)
      IF (I.EQ.9) CALL MRSCOD(0.28,4,R4)
C
      J = (I-1)*100 + 1
      CALL CURVE (X(J),Y(J),100,0)
      HTD = HTD-0.135
      CALL VECTOR (7.0,HTD,7.9,HTD,0)
      CALL MESSAG (ISTNM(I),10,8.1,HTD-0.045)
   30 CONTINUE
C
      HTD = HTD-0.165
      CALL BLNK1 (6.88,9.12,HTD,6.84,3)
C
      CALL DOT
      CALL RLVEC (-.05,0.0,0.4,0.0,0)
      CALL RLVEC (0.,-0.01,0.0,0.06,0)
C
      CALL ENDPL(0)
      RETURN
      END
```

Appendix C-2

Comments on Input Required

Input deck required for summary data analysis program is basically the same as for the detailed data analysis and plotting routine (Appendix B). The only difference is that an extra initial card is required to give the information which will be used to label the single output graph.

Data card 1: Enter ISET, which is hole number plus other identifying information. Format A10

example: C7 RI = 6.6M

Cards 2 → N same deck as used for detailed analysis of first set of data for the hole (see Appendix B-2).

Cards N + 1 → M Same deck as used for detailed analysis of second set of data for the hole.

And so on to a maximum of 9 sets of data which are to be plotted on this one summary plot.

Note that variable named ISET in detailed plot routine (Appendix B) appears as ISTNM = (setname) in composite plot routine (Appendix C). As used in the detailed plots, ISET is the set number. This same set number appears as a label identifying a particular plot in the composite. The new ISET in the composite routine is an identifying title for the whole composite graph.

APPENDIX D

STATISTICAL SUMMARY PLOTS

Appendix D-1

Typical Computer Program

```
76/03/19   IMPERIAL  COLLEGE  FORTRAN  COMPILER        KRONOS  2.1.X  PSR2+    77/02/28. 15.22.31.
              HNF(B)
                  C
                  C      PROGRAM 'DATA PLOT'      AUTHOR G.L. CLOUD
                  C-----------------------------------------------------------
                  C
                  C    INPUT
                  C      INPUT DATA REQUIRED ARE AS FOLLOWS -- ALL IN FREE FORMAT---
                  C
                  C       X- AND Y- VALUES ARE SCALED IN INCHES FROM EXISTING GRAPHS
                  C
                  C      L= INTEGER NO. OF CURVES TO BE PLOTTED ON ONE COMPOSITE OUTPUT.
                  C         L MAY BE USED TO GENERATE SEVERAL DIFFERENT PLOTS IN MICROFILM
                  C         VERSION OF THIS PROGRAM
                  C      SETNAM1= HOLE NUMBER TO LABEL PLOT-- 3 CHARACTERS
                  C      SETNAM2= INTERFERENCE LEVEL--3 CHARACTERS
                  C      M= INTEGER NUMBER OF X-POINTS USED IN READING DATA GRAPHS.
                  C       XINCH(I)= ARRAY OF X-VALUES IN INCHES AS SCALED FROM DATA
                  C          GRAPHS. M VALUES REQ'D. MUST BE IN ORDER.
                  C      N= INTEGER NO. OF DATA CURVES TO BE AVERAGED = NO OF Y-VALUES
                  C         FOR EACH X-VALUE
                  C      Y(I,J) = ARRAY OF N VALUES OF Y SCALED FROM DATA GRAPHS IN INCHES
                  C          AT EACH VALUE OF X.
                  C
                  C      CHECK PROGRAM FOR ORDER OF DATA CARDS AS PROGRAM INPUT STRUCTURE
                  C      DIFFERS FOR MICROFILM, SINGLE PLOT, AND COMPOSITE PLOT VERSIONS.
                  C    OUTPUT
                  C       OUTPUT IS LISTINGS OF SCALED INPUT, STATISTICAL MEANS AND
                  C       STANDARD DEVIATIONS OF INPUT Y-VALUES. THESE STATISTICAL
                  C       RESULTS ARE PLOTTED IN ONE OF THREE DIFFERENT WAYS.
                  C
                  C
0000008        1.       PROGRAM GLC (INPUT,TAPE5=INPUT,OUTPUT,TAPE6=OUTPUT,TAPE 62)
```

```
0060608        2.        DIMENSION X(25), Y(25,15), YSUM(25), YAV(25), S(25,15)
0060608        3.        DIMENSION SUM(25), YSIG(25),XINCR(25)
0060608        4.        DIMENSION XP(25), YP(25)
0060608        5.        CALL START(2)
C-------------------------------------------------------------------
0077508        6.        READ(5, ) L
C-------------------------------------------------------------------
C
C  PUT '4  CONTINUE' CARD HERE FOR MULTIPLE SINGLE PLOTS
C
C  MOVE ORIGIN ON PAPER
C-------------------------------------------------------------------
0077548        7.        CALL PLOT(2.0,1.5,-3)
C
C  WRITE CAPTION
C-------------------------------------------------------------------
0077568        9.        CALL SYMBOL(-.5,-.7,.14,6HFIG.     RESIDUAL SURFACE RADIAL STRAIN
     &  NEAR COLDWORKED HOLE,0.0,60)
C
C  DRAW AND LABEL AXES--ALSO FIXES ORIGIN FOR ALL LATER SUBROUTINE CALLS
C-------------------------------------------------------------------
0077608        9.        CALL AXIS(0.0,0.0,24HDISTANCE FROM HOLE (IN.),-24,0.0,0.0,0.0,.05)
0077628       10.        CALL AXIS(0.0,0.0,36HRESIDUAL RADIAL STRAIN (COMPRESSION),36,
     &  6.0,90.0,0.0,0.2)
C-------------------------------------------------------------------
0077648       11.        READ (5,1) SETNAM1, SETNAM2
C-------------------------------------------------------------------
0077728       12.     1  FORMAT(2A3)
C
C  WRITE IDENTIFIERS ON GRAPH---CHANGE 'H' FIELD TO FIT PLOT--
C  CAN DELETE SETNAM LABELS AS DESIRED
C-------------------------------------------------------------------
0077728       13.        CALL SYMBOL(1.0,5.0,0.21,10HHOLE NO.  ,0.0,10)
0077748       14.        CALL SYMBOL(3.1,5.0,0.21,SETNAM1,0.0,3)
SEG    14. CAUTION - ARGUMENT 4 IS OF DIFFERENT TYPE IN CALL OF - SYMBOL
```

```
                                                
```

```
0101446          SUM(I) = SUM(I) + S(I,J)
0101468          YSIG(I) = SQRT(SUM(I)/FLOAT(N))
0101548       66 CONTINUE
0101578       44 CONTINUE
0101628          WRITE(6,105)
0101658      105 FORMAT(1X//2X,'INPUT DATA SCALED TO INCHES AND STRAIN ARE---'//)
0101668          WRITE (6,100) SETNAM1, SETNAM2
0101748      100 FORMAT(2X, 'HOLE NO.', 2X, A3, 5X,'RADIAL INTERFERENCE=',2X,A3,
                 & X,'MILS'//)
0101748          WRITE (6,101)
0102008      101 FORMAT(4X,'DISTANCE FROM HOLE', 5X,'COMPRESSIVE STRAINS'/ )
0102008          DO 77 I=1,M
0102028          WRITE(6,102) X(I), (Y(I,J), J=1,N)
0102228      102 FORMAT(5X, F9.5, 5X, 13F9.5)
0102228       77 CONTINUE
0102248          WRITE(6,106)
0102308      106 FORMAT(1X///2X,'COMPUTED STATISTICAL VALUES ARE---'///)
0102308          WRITE (6,100) SETNAM1, SETNAM2
0102368          WRITE(6,103)
0102428      103 FORMAT(1X,/2X,'DISTANCE FROM HOLE',2X,'AVERAGE STRAIN',3X,
                 &'STD. DEV.'/)
0102428          DO99 I=1,M
0102448          WRITE(6,104) X(I), YAV(I), YSIG(I)
0102578      104 FORMAT(5X,F 10.8,10X,F10.8,10X,E12.5)
0102578       99 CONTINUE
                C
                C  PLOT DATA POINTS--DELETE NEXT 7 CARDS FOR COMPOSITE PLOT
                C-----------------------------------------------------------
                C
0102618          DO222 I=1,M
0102628          CX= X(I)/.05
0102638          CY= YAV(I)/.01
0102658          CSIG= YSIG(I)/.01
0102668          CALL SYMBOL(CX,CY,.07,5,0.0,-1)
SEQ     70. CAUTION - ARGUMENT 4 IS OF DIFFERENT TYPE IN CALL OF - SYMBOL
0102728          CALL SYMBOL(CX,CY,CSIG,13,0.0,-1)
SEQ     71. CAUTION - ARGUMENT 4 IS OF DIFFERENT TYPE IN CALL OF - SYMBOL
0102748      222 CONTINUE
                C
                C  ARKIST DRAWS SMOOTH CURVE THRU DATA POINTS IN X(I) AND Y(I) ARRAYS
                C-----------------------------------------------------------
0102768          I=1
0102778          CALL ARKIST(X(I),YAV(I), 1,M,20,20.0,100.0,0.0,0.0,2,1)
                C
                C  WRITE LEGEND - DELETE NEXT 7 CARDS FOR COMPOSITE PLOT
                C-----------------------------------------------------------
                C
```

```
0103038          75.        CALL SYMBOL(2.0,4.07,.14,5,0.0,-1)
SEG     75. CAUTION - ARGUMENT 4 IS OF DIFFERENT TYPE IN CALL OF - SYMBOL
0103058          76.        CALL SYMBOL(2.3,4.0,.14,20HIS AVERAGE OF SAMPLE,0.0,20)
SEG     76. CAUTION - ARGUMENT 4 IS OF DIFFERENT TYPE IN CALL OF - SYMBOL
0103078          77.        CALL SYMBOL(2.0,3.82,.14,13,0.0,-1)
0103118          78.        CALL SYMBOL(2.3,3.75,.14,20HIS STD DEV OF SAMPLE,0.0,20)
0103138          79.        FPN=FLOAT(N)
0103148          80.        CALL NUMBER(1.93,3.5,0.14,FPN,0.0,-1)
0103168          81.        CALL SYMBOL(2.3,3.5,.14,21HVALUES IN THIS SAMPLE,0.0,21)
                      C
                      C   DRAW METRIC X-AXIS
                      C-----------------------------------------------------------------
                      C
0103208          82.        IF(L.NE.1) GO TO   889
0103218          83.        DO88 I=1,21
0103238          84.        YP(I)=6.0
0103238          85.        XP(I)=FLOAT(I-1) * 10.0
0103268          86.     88 CONTINUE
0103308          87.        YP(22)=0.0
0103308          88.        YP(23)=1.0
0103318          89.        XP(22)=0.0
0103328          90.        XP(23)=25.4
0103348          91.        I=1
0103358          92.        CALL LINE(XP(I),YP(I),21,1,1,13)
0103428          93.        CALL SYMBOL(2.31,6.25,.14,24HDISTANCE FROM HOLE (MM.),0.0,24)
0103448          94.        DO 888 K=1,11
0103458          95.        FDN=FLOAT(K-1)
0103468          96.        DX=FDN / (25.4*.05)
0103478          97.        CALL NUMBER(DX,6.1,.1,FDN,0.0,-1)
0103538          98.    888 CONTINUE
                      C
0103558          99.    889 L=L-1
0103578         100.        IF(L) 999,999,4
0103608         101.    999 CALL ENPLOT(9.0)
0103638         102.        STOP
0103658         103.        END
```

Appendix D-2

Typical Input Deck for Statistical Summary Program

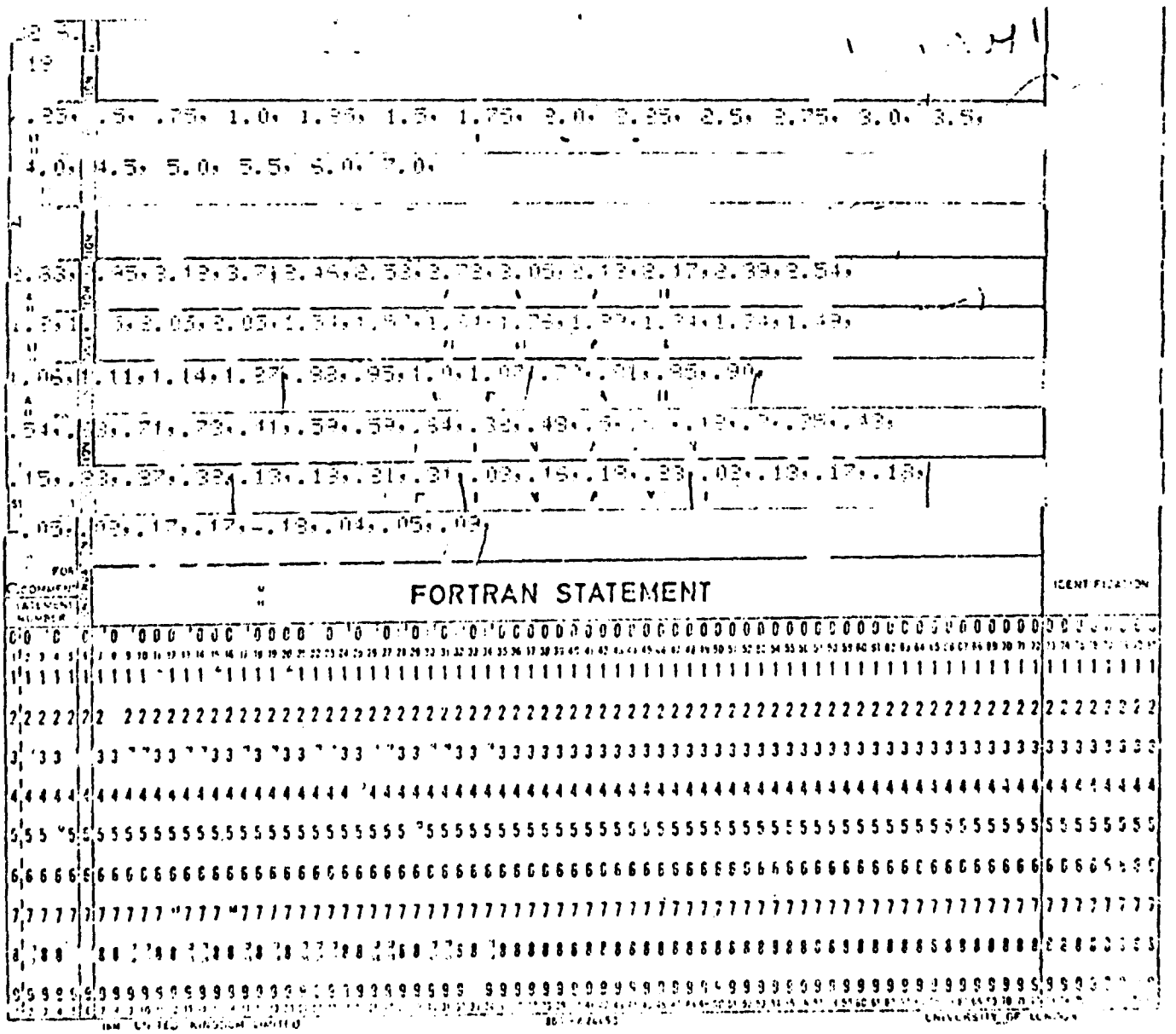

Best Available Copy

Appendix D-3

Typical Printed Output

.25	.50	.75	1.00	1.25	1.50	1.75	2.00	2.25	2.50	2.75	3.00	3.50	4.00	4.50	5.00	5.50	6.00	7.00
2.83		2.95		3.12		3.70												
2.46		2.52		2.72		3.05												
2.13		2.17		2.39		2.54												
1.80		1.85		2.05		2.05												
1.54		1.57		1.64		1.76												
1.29		1.34		1.34		1.49												
1.06		1.11		1.14		1.27												
.88		.95		1.00		1.07												
.73		.81		.85		.90												
.54		.68		.71		.73												
.41		.59		.59		.64												
.32		.48		.50		.55												
.18		.3		.35		.43												
.15		.23		.27		.38												
.13		.18		.21		.31												
.06		.16		.18		.23												
.02		.13		.17		.18												
-.05		.02		.17		.17												
-.18		.04		.05		.09												

INPUT DATA SCALED TO INCHES AND STRAIN ARE---

HOLE NO. C2 RADIAL INTERFERENCE= 6.[illegible] MILS

DISTANCE FROM HOLE	COMPRESSIVE STRAINS			
.01250	.02830	.02950	.03120	.03700
.02500	.02460	.02520	.02720	.03050
.03750	.02130	.02170	.02390	.02540
.05000	.01800	.01850	.02050	.02050
.06250	.01540	.01570	.01640	.01760
.07500	.01290	.01340	.01340	.01490
.08750	.01060	.01110	.01140	.01270
.10000	.00880	.00950	.01000	.01070
.11250	.00700	.00810	.00850	.00900
.12500	.00540	.00680	.00710	.00730
.13750	.00410	.00580	.00590	.00640
.15000	.00320	.00480	.00500	.00550
.17500	.00180	.00300	.00350	.00430
.20000	.00150	.00230	.00270	.00380
.22500	.00130	.00180	.00240	.00310
.25000	.00080	.00160	.00180	.00230
.27500	.00020	.00140	.00170	.00180
.30000	-.00050	.00020	.00170	.00170
.35000	-.00180	.00040	.00050	.00090

COMPUTED STATISTICAL VALUES ARE---

HOLE NO. C2 RADIAL INTERFERENCE= 6.0 MILS

DISTANCE FROM HOLE	AVERAGE STRAIN	STD. DEV.
.01250000	.03150000	.333845E-02
.02500000	.02687500	.23037E-02
.03750000	.02307500	.16679E-02
.05000000	.01937500	.11388E-02
.06250000	.01627500	.84668E-03
.07500000	.01365000	.75000E-03
.08750000	.01145000	.77621E-03
.10000000	.00975000	.69462E-03
.11250000	.00815000	.73655E-03
.12500000	.00665000	.74338E-03
.13750000	.00557500	.87571E-03
.15000000	.00462500	.86132E-03
.17500000	.00315000	.90692E-03
.20000000	.00257500	.82878E-03
.22500000	.00207500	.65717E-03
.25000000	.00162500	.54125E-03
.27500000	.00125000	.53443E-03
.30000000	.00077500	.35754E-03
.35000000	.00000000	.10559E-02

*U.S.Government Printing Office: 1979 - 657-002/524